



INTERNATIONAL CONFERENCE ON
HYDROPOWER

A VITAL SOURCE OF SUSTAINABLE ENERGY FOR PAKISTAN

ICHP-2017

LAHORE-PAKISTAN, DECEMBER 19-20, 2017

CONFERENCE PROCEEDING

ORGANIZED BY:

CENTER OF EXCELLENCE IN WATER RESOURCES ENGINEERING
UNIVERSITY OF ENGINEERING AND TECHNOLOGY, LAHORE-PAKISTAN





International Conference on

HYDROPOWER

A VITAL SOURCE OF SUSTAINABLE ENERGY FOR PAKISTAN

ICHP-2017

Lahore-Pakistan, December 19-20, 2017

Conference Proceeding

CENTRE OF EXCELLENCE IN WATER RESOURCES ENGINEERING

University of Engineering and Technology, Lahore-Pakistan

Co-Sponsored by:



Suggested citation:

AUTHOR, A. (2017), Title of the Paper. In: International Conference on HYDROPOWER-A Vital Source of Sustainable Energy for Pakistan 2017. Centre of Excellence in Water Resources Engineering: UET Lahore-Pakistan, pp. xx-xx. ISBN: 978-969-8670-06-01

© 2017 Centre of Excellence in Water Resources Engineering, UET Lahore-Pakistan.

All rights reserved. Published 2018.
Printed in Pakistan.

ISBN: 978-969-8670-06-01

The views expressed in this publication are those of the authors and do not necessarily reflect the views and policies of the Centre of Excellence in Water Resources Engineering (CEWRE), its Board of Governors, or any official.

CEWRE does not guarantee the accuracy of the data included in this publication and accepts no responsibility for any consequence of their use.

CEWRE encourages printing or copying information exclusively for personal and noncommercial use with proper acknowledgment of CEWRE. Users are restricted from reselling, redistributing, or creating derivative works for commercial purposes without the express, written consent of CEWRE.

Conference Secretary

- Engr. M. Kaleem Sarwar

Editors


- Dr. Ijaz Ahmad
- Engr. M. Kaleem Sarwar

Compiled By

- Dr. Ijaz Ahmad
- Engr. Rana Zain Nabi Khan

Centre of Excellence on Water Resources
Engineering
UET, G.T. Rd, Lahore- Pakistan. 54890
Tel: +92 42 99250257
Fax: +92-42-99250259
Email: cewre@cewre.edu.pk
www.cewre.edu.pk

For orders, please contact:
Conference Organizing Committee
Tel: +92 42 99250257
Email: cewre.media@gmail.com

 Printed on recycled paper.

FOREWORD



The CEWRE was established with the objectives of high level goal-oriented capacity building of professionals, teaching and research in water resources sector in the country. These objectives are being achieved by imparting post graduate degrees, conducting specialized research, dissemination of the knowledge through short courses, seminars, training workshops and International Conferences etc. Centre provides the healthy research facilities to the students as well as faculty members. Many national and international organizations collaborate with Centre to carryout research activities in term of financing, data collection, analysis and finalization of research reports.

Hydropower is clean renewable energy source that doesn't pollute environment. It is very efficient energy source because some turbines can achieve efficiency as high as of 95% and more. It provides about 20 % of the world's electricity and is the main energy source for more than 30 countries. Hydropower's advantage over other renewable energy sources is the fact that average rainfall is highly predictable and therefore output is reliable and river flow doesn't fluctuate from minute to minute like is the case with wind energy.

Hydropower development has been recognized as one of the key drivers in optimally utilizing the available water resources towards achieving the objective of energy security and green growth. Despite Pakistan having a hydropower potential of 60,000 MW, it could develop so far only 7,320 MW. Further, due to the recent incidences of hydro-meteorological disasters and concerns raised about social and environmental aspects from many quarters, the development of hydropower potential has not made much of headway. Therefore, there is a huge opportunity to further optimally harness the hydropower potential towards acquiring energy security and green growth. There is a need of serious relooking of the existing status, policy, environmental, financial, social and technical barriers in implementation.

To provide forum for exchange of experiences on technological innovations, best practices and scope of hydropower development as a clean, green and sustainable source of development, Centre of Excellence in Water Resources Engineering (CEWRE), University of Engineering and Technology, Lahore organized an International Conference on "Hydropower – A Vital Source of Sustainable Energy for Pakistan" at CEWRE, UET, Lahore during December 19-20, 2017.

Director

CHIEF GUEST



Prof. Dr. Fazal Ahmad Khalid S.I

Vice Chancellor

University of Engineering & Technology, Lahore

I take this opportunity to welcome you all at this 2 days International Conference on Hydropower - A Vital Source of Sustainable Energy for Pakistan being held in CEWRE UET Lahore. Hydropower offers a wide range of benefits-especially for developing countries. The resource is environmentally responsible and has substantial economic advantages.

There is an urgent need to develop this promising sector of renewable energy in all developing countries as only a fraction of available potential has been harnessed so far. To further boost the developing of this sector, a need was felt to share the views in this field through organizing International Conference covering the advances made in the planning, technologies selection and implementation of hydropower projects. With all the varied efforts underway to promote the development of small hydropower, a need has developed to share information on what has worked, and what has not.

I wish a meaningful discussion and a great success for the intended purpose in this conference with pragmatic and positive approach that incorporates sustainability requirements in the decision-making process for growth and prosperity of all.

Thank you!

GUEST OF HONOR



Prof. Dr. Niaz Ahmad Akhtar
Vice Chancellor
University of Engineering & Technology,
Taxila

“

First of all, I feel honored and humble for being invited in this conference on Hydropower- A vital Source of Sustainable Energy for Pakistan.

It is my great pleasure to congratulate the team of CEWRE which effectively organized this conference and provided an opportunity for the likeminded and concerned individuals to gather and discuss the issues which Pakistan is facing regarding water and power generation. A well planned and well managed hydropower plant is a real long asset of any country which results in spin off benefits in many areas like agriculture, industry, drinking water, tourism and cultural.

I would also like to pay my gratitude to all the honorable speakers and participants. Moreover, it is my utmost desire that the decisions and the discussion taken place today among the professionals in this field find its rightful place in the policy circles of our society and bring about meaningful change in how we look and work on these issues.

Thank you!

”

ACKNOWLEDGEMENT

The Centre of Excellence in Water Resources Engineering would like to acknowledge the excellent work of our conference organizing committee which comprised of the following:

Gratitude is also extended to all of our distinguished research presenters and to our keynote speakers. We would also like to acknowledge the important contributions of all of our conference participants and in particular those who use their services for sharing with us their personal insights and aspirations.



Prof. Dr. Habib Ur Rehman

Conference Chairman

Centre of Excellence in Water Resources Engineering
UET Lahore



Prof. Dr. Noor Muhammad Khan

Conference Coordinator

Department of Civil Engineering, UET Lahore



Engr. M. Kaleem Sarwar

Conference Secretary

Centre of Excellence in Water Resources Engineering
UET Lahore

ORGANIZING COMMITTEE



Engr. M. Kaleem Sarwar

Centre of Excellence in Water Resources Engineering
UET Lahore



Dr. Ghulam Nabi

Centre of Excellence in Water Resources Engineering
UET Lahore



Engr. Mohammad Masood

Centre of Excellence in Water Resources Engineering
UET Lahore



Dr. Ijaz Ahmad

Centre of Excellence in Water Resources Engineering
UET Lahore



Dr. Muhammad Waseem

Centre of Excellence in Water Resources Engineering
UET Lahore



Engr. Rana Zain Nabi Khan

Centre of Excellence in Water Resources Engineering
UET Lahore

PROGRAM

December 19, 2017 (Tuesday)		
09:15	10:00	Registration of Delegates
Inaugural Session		
10:00	10:15	Guests to be seated & arrival of Chief Guest
10:15	10:25	Recitation from the Holy Quran & National Anthem
10:25	10:35	Welcome Address: Director CEWRE, UET Lahore
10:35	10:55	Opening Address: Vice Chancellor, UET Lahore
10:55	11:15	Address by the Chief Guest
11:15	11:35	Presentation of Shield to Chief Guest and Group Photo
11:35	12:00	Coffee/Tea Break

December 19, 2017 Technical Session-I (12:00 to 14:30) Venue: Seminar Hall CEWRE			
Session Chairman (PROF. DR. ABDUL SATTAR SHAKIR, DEAN FACULTY OF CIVIL ENGINEERING)			
12:00	12:20	Keynote Lecture	Engr. Haji M. Farooq Former GM Wapda
12:20	12:40	Keynote Lecture	Engr. Munwar Iqbal Director (Hydel) PPIB
12:40	13:00	Hydraulic Transient Analysis for Proposed Penstock of Jari Tunnel	Engr. Javed Munir GM Nespak
13:00	13:15	Application of Computational Flow Dynamics (CFD) Analysis for Surge Inception and Propagation in Low Head Hydropower Projects	Engr. Mohsin Munir Nespak
13:15	13:25	Q & A Session and Concluding Remarks by The Session Chairman	
13:25	13:30	Distribution of Shields/Certificates	
13:30	14:30	Lunch/Prayer Break	

December 19, 2017 Technical Session-II (14:30 to 16:30) Venue: Seminar Hall CEWRE			
Session Chairman (PROF. DR. HABIB-UR-REHMAN DIRECTOR CEWRE)			
14:30	14:50	Keynote Lecture	Prof. Dr. Khamaruzaman UTP Malaysia
14:50	15:10	Statistical Analysis of Inflows of River Indus At Tarbela In the Wake of Climate Change	Dr. Khurram Shahzad Inst. Of Southern Punjab
15:10	15:25	Scientific Evaluation of Water Footprint Methods for Hydropower Generation	Dr. Atiq-Ur-Rehman Tariq CUST, Islamabad
15:25	15:40	Evaluation of Suitable Design Flood Frequency Approaches for the Mountainous Watershed (A Case Study of Upper Indus Basin)	Dr. M. Yasin PU, Lahore
15:40	15:55	Impacts of Hydro Climatic Variables Trends on Water Resources of Yihe River Basin During the Past 50 Years	Dr. M. Saifullah China
15:55	16:10	Q & A Session and Concluding Remarks by The Session Chairman	
16:10	16:30	Distribution of Shields/Certificates	

PROGRAM

December 20,2017 Technical Session-III (09:00 to 11:30) Venue: Seminar Hall CEWRE			
Session Chairman: Prof. Dr. Khamaruzman, UTP Malaysia			
9:00	9:10	RECITATION FROM THE HOLY QURAN & National Anthem	
09:10	09:30	Keynote Lecture	Javed Rashid Hydropower Economist
9:30	9:50	Keynote Lecture	Dr. Raza-Ul-Mustafa UTP, Malaysia
9:50	10:05	Risk Involved on Hydropower Projects in Pakistan	Raheel Ahmad Rana CEWRE UET Lahore
10:05	10:20	Sensitivity Analysis of Hydraulic Parameters for Water Hammer in Penstock Design	Muhammad Yasar Dr. Ghulam Nabi CEWRE UET Lahore
10:20	10:35	Physical Modeling to Control Scouring Under Natural Flow Conditions	Dr. Atiq-Ur-Rehman Tariq CUST, Islamabad.
10:35	10:50	Assessment of Defects, Remedial Measures and Development Prospects of Sick Jaglot Hydropower Projects to Meet Future Demands.	Major Qaiser Karim MES, Rawalpindi
10:50	11:00	Q & A Seccession and Concluding Remarks by The Session Chairman	
11:00	11:10	Distribution of Shields/Certificates	
11:10	11:30	Coffee/Tea Break	
December 20,2017 Technical Session-IV (11:30 to 14:30) Venue: Seminar Hall CEWRE			
Session Chairman (Engr. Tariq Altaf V.P. NESPAK)			
11:30	11:50	Keynote Lecture	Dr. Shams-Ul-Mulk Former Chairman Wapda
11:50	12:10	Keynote Lecture	Dr. M. Nadeem Leads University
12:10	12:25	Modeling of Double Stilling Basin-A Case Study	Engr. Ubaid Ullah Eric J Lesleighter EGC (Pvt.) Pakistan
12:25	12:40	Modeling of Spillway Breach for Attabad Landslide Dam	Engr. Wajid Ijaz Dr. Ata-Ur-Rehman Tariq Muet, Jamshroo
12:40	12:55	Design Of U/S Overflow Cofferdam of Patrind Hydropower Project	Engr. Rizwan Fareed Pes (Pvt.) Lahore
12:55	13:10	Enhancing the Hydropower Potential of Runoff River Type Project Operating in Chitral Pakistan: A Case Study of Chitral Hydel Station on Lutkho River	Engr. Javed Zulfiqar WAPDA
13:10	13:25	Q & A Seccession and Concluding Remarks by The Session Chairman	
13:25	13:30	Distribution of Shields/Certificates	
13:30	14:30	Lunch/Prayer Break	
December 20,2017 Concluding Session (14:30 to 16:30) Venue: Seminar Hall CEWRE			
14:30	14:40	Recitation from the Holy Quran	
14:40	15:00	Presentation of Conclusions and Recommendations of Conference	
15:00	15:20	Address by the Chief Guest of Concluding Session	
15:20	15:40	Distribution of Certificates to Participants, Organizers & Presentation of Shield to Chief Guest	
15:40	15:55	Vote of Thanks by Director CEWRE & Group Photo	
15:55	16:30	Coffee/Tea Break	

TABLE OF CONTENTS

Sr. No.	Title of Paper	Pages
1	Detection and estimation of sediment transport trends in the upper Indus River during the last 50 years Authors: Sardar Ateeq-Ur-Rehman, Minh Duc Bui, Peter Rutschmann	1-6
2	Hydraulic Transient Analysis for Proposed Penstock of Khari Power House at Jari Dam Downstream Authors: Javed Munir, Syed Abbas Ali, Irfan Mahmood	7-12
3	Application of Computational Flow Dynamics (CFD) Analysis for Surge Inception and Propagation in Low Head Hydropower Projects Authors: M. Mohsin Munir, Taimoor Ahmad, Dr. Javed Munir	13-18
4	Statistical Analysis of inflows of River Indus at Tarbela in the Wake of Climate Change Author: Dr. Muhammad Khurram Shahzad	19-27
5	Scientific Evaluation of Water Footprint Methods for Hydropower Generation Authors: F. Seemab, W. Sherani, M. Abbas, M.N. Alam, R. Farooq, Z. Ashfaq, M.A.U.R. Tariq	28-33
6	Evaluation of Suitable Design Flood Frequency Approaches for Hydropower Structures on the Mountainous Rivers (A Case Study of Upper Indus Basin) Authors: Muhammad Yaseen, Ijaz Ahmad, Bilal Nasir, Muhammad Imran Azam, Muhammad Hassan Rehman, Muhammad Afzel	34-41
7	Impacts of hydro climatic variables trends on water resources of Yihe River Basin during the past 50 years Authors: Muhammad Saifullah, Ijaz Ahmad, Muhammad Zaman, Zhijia Li, Abdul Nasir	42-46
8	Sensitivity Analysis of Hydraulic Parameters for Water Hammer in Penstock Design Authors: Muhammad Yasar, Muhammad Waseem, Ghulam Nabi	47-55
9	Physical modeling to control scouring under natural flow conditions Authors: Farooq. R., Ghumman A.R., AlSaleem, S.S., Seemab, F., Tariq. M.A.U.R.	56-63
10	Assessment of Defects, Remedial Measures and Development Prospects of Sick Jaglot Hydropower Project Authors: Muhammad Waseem, Qaiser Karim, Muhammad Kaleem Sarwar	64-70
11	Double-Stillling Basin Modelling, Pakistan – Case Study Authors: Ubaid Ullah, Eric J Lesleighter, Muhammad Iqbal, Umair Mannan	71-76
12	Modeling of spillway breach for Attabad landslide dam Authors: Muhammad Wajid Ijaz, Ata-ur-Rehman Tariq	77-85
13	Design of Upstream Overflow Cofferdam of Patrind Hydropower Project Authors: Rizwan Farid, Ijaz Ahmad, Rana Zain Nabi Khan	86-91

TABLE OF CONTENTS

14	Evaluation of Small Hydropower Scheme Operating in Chitral, Pakistan; a Case Study of Chitral Hydel Station on Lutkho River Authors: Engr. Javed Zulfiqar, Engr. Nazakat Hussain	92-97
15	Impact of Baglihar Hydroelectric Power Plant on Design Flood of Pakistan Authors: Adnan Majeed, Rana Zain Nabi Khan, Neelam Pari, Ahsan Naseem	98-100
16	Risk of Indus Basin Water Transfer in Violation of Indus Basin Treaty Authors: Ahmad Raza, Muhammad Waseem, Navid Tahir, Ijaz Ahmad	101-106
17	Subsurface Flow Analysis of Hydraulic Structures using Bligh's Theory, Lane's Weighted Creep Theory and Modern Khosla's Theory Authors: Hasnain Jillani, Muhammad Haris Asghar Khan, Hammad ur Rehman	107-113
18	Assessing Hydropower Resilience under Changing Climate: Murum-Bakun Cascade in East Malaysia Authors: Khamaruzaman B. Wan Yusof, Mubasher Hussain, Muhammad Raza-ul-Mustafa	114-119
19	Rainfall-Runoff Relationship for Small Watershed in Potohar Area Authors: Moien Ahsan, Sonia Zafar, Ghulam Nabi	120-126
20	Selection of Best Diversion Facility for the Construction of Kohala Hydropower Dam Authors: Muhammad Yaseen, Muhammad Naveed, Muhammad Kaleem Sarwar, Muhammad Hassan Rehman, Muhammad Imran Azam	127-134
21	Hydropower Optimization Station using PSO and GA Techniques Authors: Ijaz Ahmad, Muhammad Zaman, Shouqi Yuan, Liu Junping, Muhammad Saifullah	135-140
22	One Dimensional Numerical Simulation of Scour and Deposition in a Channel using Finite Difference Method Authors: Muhammad Zain Bin Riaz, Muhammad Masood, Rana Zain Nabi Khan	141-147
23	Risks Involved on Hydropower Projects in Pakistan Author: Raheel Ahmed Rana	148-159
24	Analysis of regime behavior of lower Gugera branch canal after rehabilitation/remodeling of the system. Author: Sajid Mehmood, Ghulam Nabi	160-168
25	Impact Analysis of Floods on Fixation of Road Profile Grade Level for Roads in Hilly Terrain Authors: Zafar Iqbal, Kaleem Sarwar, Sajid Mahmood, Muhammad Afzal	169-176
26	Hydraulic Performance Assessment of an Orifice Spillways using CFD Modeling Authors: Zohaib Nisar, Muhammad Kaleem Sarwar, Ghulam Nabi	177-184

Detection and estimation of sediment transport trends in the upper Indus River during the last 50 years

Sardar Ateeq-Ur-Rehman^{1*}, Minh Duc Bui¹, Peter Rutschmann¹

¹Department of Hydraulic and Water Resources Engineering
Technical University of Munich
[*sardar.ateeq@tum.de](mailto:sardar.ateeq@tum.de)

Abstract: The water availability during the spring and summer has changed significantly in the Indus River over the last 50 years. The change in water availability has also affected the sediment load transport capabilities of the river at the upper Indus basin (UIB). To assess the changes in sediment transport patterns, neural network models coupled with discrete wavelet transforms (WA-ANN) were developed. The modelling process used daily discharges and distinct suspended sediment concentration (SSC) samples from the last 50 years. Sediment load trends were obtained using daily sediment loads calculated by WA-ANN. The results showed that sediment load transport patterns in UIB have been shifting from the summer to the spring months due to an increase in effective discharge. The results also showed, at Partab Bridge (an upstream gauge station draining the glacier zone), sediment load and flow volume have been increasing, except in August. Surprisingly, the flow volume at Besham Qila gauge station (downstream of Partab Bridge in precipitation zone) has been decreasing during the summer months and causing an overall reduction of sediment load transport capability of the Indus river in-between Partab Bridge and Besham Qila. As a result of the change in water availability in different zones, the sediment load transport capacity of the river has been increasing in glacial melt zones and decreasing in snowy and precipitation zones. Consequently, it was concluded that sediments are being deposited in-between glacial melt (Partab Bridge) and precipitation (Besham Qila) zones of UIB. The current findings are important to develop the reservoir operational rules and sediment management strategies for the under construction and existing dams under sediment load transport changing scenarios.

Keywords: Sediment load estimation, Sediment pattern, Besham Qila, Partab Bridge

Introduction

Detection and precise estimation of sediment load trends are important for designers and engineers to plan and operate dam and reservoir structures. One of the most popular methods for estimating sediment load is to develop sediment rating curves (SRCs) based on the observed data of suspended sediment concentration (SSC) and water discharges. The SRC method has a limited accuracy for the Indus River due to hysteresis phenomenon in sediment transport in the domain. As it can be seen in Tab. 1, the estimated annual sediment loads for the Indus River vary in a wide range from 200 Mt yr⁻¹ to 675 Mt yr⁻¹ over the last 50 years. Therefore, applying SRC methods to detect and estimate trends of sediment load may cause significant flaws in the results.

Table 1 Estimates published for the Indus river suspended sediment load (SSL) at Besham Qila and Tarbela dam.

SSL	References
480	Holeman (1968)
400	{Peshawar University} (1970)
475	Meybeck (1976)
200	Lowe and Fox (1982)

675	Milliman et al. (1984)
300	Summerfield and Hulton (1994)
200	Collins (1996)
197	Ali (2009)
200	Dasu Hydropower Consultants (2013)

In contrast to many studies of climate degradation impact on river flow patterns in UIB, very few investigations concerning the impact of flow pattern changes on the sediment load carrying capacity of the river have been conducted (Azim et al. 2016).

During recent years, the Artificial Neural Networks (ANNs) have gained warm reception as a new perspective in the fields with non-linear nature. In general, the advantages of ANNs over other conceptual models are: the application of ANNs does not require a prior knowledge of the process. ANNs have the inherent property of nonlinearity since neurons activate a nonlinear filter called an activation function. ANNs can have multiple input with different characteristics, which can make ANNs able to represent the time-space variability. In spite of suitable flexibility of ANNs in modelling time series, sometimes

ANNs have a weakness when signal fluctuations are highly nonstationary and physical hydrological processes operate under a large range of scales, varying from one day to several years. In such a situation, different methods have been proposed among which are wavelet transforms. They have become a useful method for analysing such variations and trends in hydrological time series. A wavelet has been defined as a small wave whose energy is restricted into a short period of time and is an efficient method for signals that are non-stationary, have short-lived transient components, features at different scales, or singularities. A non-stationary signal can be decomposed into a certain number of stationary signals by wavelet transform. Then ANN is combined with wavelet transform (WA-ANN). It is thought that the WA-ANN models are more accurate than the conventional methods since wavelet transforms provide useful decompositions of the original time series, and the wavelet-transformed data improves the performance of the conventional ANN model by capturing useful information on a various resolution levels.

In this paper, we develop WA-ANN models for suspended sediment load (SSL) estimation based on daily observed flow discharges and possible data of SSC samples in the upper Indus River. The designed WA-ANN models can be used to reconstruct the missing daily SSL. Further, a non-parametric Mann-Kendall (MK) test can provide the detailed changes in the trends of SSL without requiring the data to be normally distributed (Zhang et al. 2006). The MK seasonality test shows the trends by removing the cycles from the time series. Given a statistical significance of the trend, the Sen's slope estimator defines the magnitude. The calculated results describe the effect of change in flow patterns on sediment load transport capacity of the Indus River in UIB over the last 50 years.

Study area and data description

Data of river flow and observed SSC at two-gauge stations, Besham Qila and Partab Bridge, are used in this study (Fig. 1).

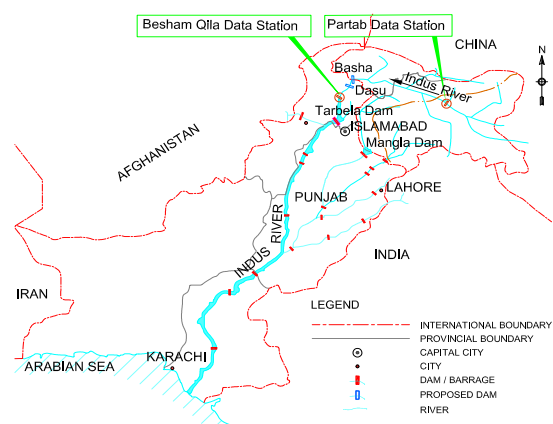


Fig. 1 Location of gauge stations in the study area, developed by Dasu Hydropower Consultants (2013).

The time lengths of the data sets are from 1969 to 2008 at Besham Qila and from 1962 to 2008 at Partab Bridge. Downstream of Besham Qila, the Tarbela dam is located which is the only dam in UIB.

The specific sediment yield from the drainage area at Besham Qila was estimated approximately 1,197 Mt km⁻² yr⁻¹. The high sediment yield in this area is due to the large number of small and relatively steep catchments discharging straight into the Indus river. An amount of 80 to 85% of the annual sediment load was observed at the Tarbela dam in July and August. The contribution of rainfall, glacier and snow melt to the total flow at the Tarbela dam in monsoon is about 33% to 55%. Partab Bridge gauge station is located 300 km upstream from Besham Qila.

The gauge station is located at a river elevation of 1,250 masl with a drainage area of 142,800 km² measures the flow of glacierized areas of the Karakoram and Himalaya (Ali 2009). The contribution in flow at Besham Qila from Partab Bridge is approximately 74%. The SSC sampling frequency at both gauge stations represents an average 22% of a daily sampling in a year at Besham Qila and 14% at Partab Bridge. The sampling is done in such a way that it represents all events in the year. More details of data quality, data collection, period of records for the Indus river can be found in Ali (2009).

Methods

First, based on the information of the observed data in the region, we built a suitable relationship between inputs and SSC (output) by applying a trial-and-error method to optimise the architecture of the conventional ANN approaches. To improve the performance of ANN, we decomposed the raw input data time series (daily flows) into approximation (a_n) and

details (d_1, \dots, d_n) using wavelets (Fig. 2). The approximation consists of high scale and low frequency components of the signal. While the details consist of low scale and high frequency components of the signal which are obtained from low-pass and high-pass filters respectively. These decompositions were fed to input neurons, which in turn pass them on to the hidden layer neurons after multiplying by a given weight. A hidden layer neuron adds up the weighted input received from each input neuron, associates it with a bias, and then passes the result on through a nonlinear activation function. The output neurons do the same operation as that of a hidden neuron. Therefore, a neuron output in a layer depends on the signal received from the previous layer, its defined weight and activation function type. Applying the trial-and-error method again, we chose an optimal architecture of WA-ANN models. More details about ANN and wavelets can be found in Haykin (1999) and Shoab et al. (2016).

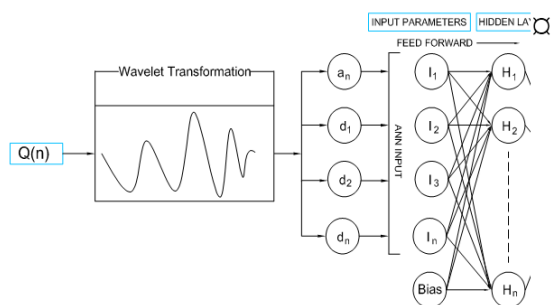


Fig. 2 Schematic diagram of WA-ANN model.

In the present study, we trained the network using 70% of the data for training, 15% for testing and 15% for validation on a random basis. The daily discharges were decomposed up to eight levels using Daubechies (db1) wavelet. The output of WA-ANN was un-decomposed SSC samples. The permutation of logsig, tansig, radbas and purelin transfer functions was used in the hidden and output layers. The Levenberg-Marquardt algorithm, due to its simplicity, was used to calibrate the network. The neurons in the hidden layer were selected based on the criteria described by Fletcher and Goss (1993). The stopping criteria of the model was a maximum of 1000 epoch. The final network was saved for later use to generate the daily missing SSL. Due to different data characteristics of both gauge stations, we developed two separate WA-ANN models.

The performance of WA-ANN models was assessed using absolute (i.e. represented in the units of output) and relative (i.e. dimensionless) statistic parameters. The absolute statistic parameters are root mean square error (RMSE)

and mean absolute error (MAE). While the relative statistic parameters are correlation coefficient (R) and Nash-Sutcliffe coefficient of efficiency (NSE).

After getting the daily SSL time series, we analysed statistical significance of the trends using the MK tests, which have been proposed first by Mann (1945) and later by Kendall (1975) to test statistic distribution. This test is found to be an excellent tool for trend detection without being affected by outliers. Eq. 1 gives MK test for Z statistic.

$$Z = \begin{cases} \frac{S - 1}{\sqrt{Var(S)}}, & S > 0 \\ 0, & S = 0 \\ \frac{S + 1}{\sqrt{Var(S)}}, & S < 0 \end{cases}$$

Whereas S is the sum of positive or negative signs, Var is variance of S. A positive value of Z indicates an upward trend and vice versa. If there is no trend in the time series, the statistic Z has a standard normal distribution. In case of trend, Sen's slope estimator was used to get the magnitude of the trends. The Sen's slope test was originally developed by (Sen 1968) to estimate the true slope using simple a non-parametric procedure. The Sen's test is not affected by outlier and is closely related to MK test. More information about the MK and Sen's slope tests can be found in the books written by Gilbert (1987) and Gibbons et al. (2009).

Results and discussions

The best performed WA-ANN model provided values for correlation coefficient, $R=0.90$ at Besham Qila and $R=0.81$ at Partab Bridge. The NSE was also at 0.81 and 0.66, respectively. The estimated mean annual SSLs at Besham Qila and Partab Bridge were at 160 and 188 Mt yr⁻¹. The value estimated by WA-ANN for Besham Qila is less than the previous estimates ranging from 200 to 675 Mt yr⁻¹ (Tab. 1). Additionally, the SSL trend at Besham Qila shows a decreasing tendency (Fig. 3a), while it has been increasing at Partab Bridge (Fig. 3b).

The Mann-Kendall (MK) test has also shown a decreasing trend in SLL at Besham Qila with a true Sen's slope of 0.634 Mt yr⁻¹ and an increasing trend at Partab Bridge with a slope of 0.20 Mt yr⁻¹ (Tab. 2). At both gauge stations, the sediment load is significantly decreasing in August, which is due to less snowmelt and the cooling effect. At Besham Qila, the sediment load is also decreasing in April, June, July, and August.

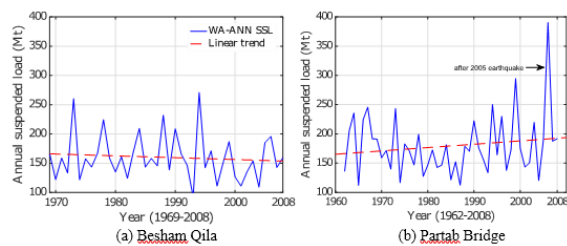


Fig. 3 Annual SSL shows decreasing trend at (a) Besham Qila and increasing trend at (b) Partab Bridge.

The flow in April at Besham Qila is contributed with base flow and rainfall. The decreasing trend of sediment transport in April is due to dryness and less river flow. The increase in SSL in May at Besham Qila is caused by early snowmelt at low altitude, which is causing increase in flow and effective discharge for sediment transport. On the other hand, decreasing trend in discharge during monsoon season in-between Partab Bridge and Besham Qila (Böhner and Lucarini 2015) is causing to decrease the sediment transport capacity of the river. For examples in June, Besham Qila is showing decreasing trend in sediment load, however, it is opposite at Partab Bridge (Tab. 2). Consequently, the increase in sediment load noticed at Partab Bridge is not being transported downstream until Besham Qila, which indicates that sediment load is being deposited in the channel in-between Partab Bridge and Besham Qila. The deposition effect is more prominent in 2006 when 390 Mt SSL was estimated at Partab Bridge, but it did not pass through Besham Qila, even in the subsequent years (Fig. 3).

Nevertheless, changes in both snow and glacier melt regimes all together can result a sophisticated alteration of the hydrological

regimes of UIB , which require certain changes in the operating curve of the existing reservoirs operational rules for future. These changes may be the use of additional water for power generation (Hussain et al. 2017) during low flows in winter months or for irrigation or flushing operation in May when more water with less SSC is available. Flushing in May will not only erode the deposits from the dam due to less SSC in incoming flow but will also provide the opportunity to re-fill the reservoirs in the proceeding high flow months, e.g. June or July.

Conclusion

The results predicted by the designed WA-ANN models along-with the Mann-Kendall test, Sen's slope estimator and linear regression show a shifting trend of sediment load from summer to spring in the upper Indus River over the last 50 years. The annual sediment load share in May has increased by more than 100%, which is very significant. In contrast, it has decreased by 13% in August. While annual sediment load has been increasing in glacial melt zones, i.e. at Partab Bridge gauge station, the contribution of early snowmelt has caused a particularly pronounced increase in the spring. As a result of early snow melt, the sediment load transport capacity of the Indus River has been decreasing during the summer at Besham Qila. The decrease in transport capacity led to a long-term decrease in sediment load, in contrast to a long-term increase in flow volume in snow and precipitation zones of the Indus River. For future water and food security along the Indus River command area, it is necessary to estimate the impact of long-term sediment load variations on water resources capacities located on the Indus River.

Table 2 Annual and monthly sediment load trends at Besham Qila and Partab Bridge.

Annual/Month	Mann-Kendall test			Sen's slope (Mt yr ⁻¹)		
	statistic Z	trend type	confidence interval	true slope	lower limit	upper limit
Besham Qila						
Annual	-1.21	downward	89%	-0.634	-1.397	0
January	2.74	upward	95%	0.00111	0.00062	0.00212
February	2.76	upward	95%	0.00158	0.00060	0.00237
March	1.08	upward	84%	0.00200	0.00000	0.00431
April	-1.14	downward	87%	-0.00280	-0.00528	0.00000
May	2.66	upward	95%	0.07692	0.00000	0.13333
June	-0.35	downward	64%	-0.05263	-0.05013	-0.05013
July	-0.82	downward	79%	-0.18182	-0.32738	0.00000
August	-1	downward	84%	-0.24138	-0.46863	0.00000
September	0.61	upward	73%	0.03704	0.03704	0.03704
October	0.51	upward	69%	0.00161	0.00168	0.00168
November	2.16	upward	95%	0.00125	0.00015	0.00227

December	1.05	upward	85%	0.00040	0.00000	0.00104
Partab Bridge						
Annual	0.38	upward	65%	0.20	-0.42	0.82
January	0.2.17	upward	95%	0.00040	0.00000	0.00090
February	0.71	upward	76%	0.00000	0.00000	0.00023
March	1.51	upward	93%	0.00034	0.00000	0.00060
April	3.09	upward	95%	0.00300	0.00125	0.00455
May	3.98	upward	95%	0.05882	0.03078	0.08452
June	2.14	upward	95%	0.33333	0.07418	0.50000
July	0.41	upward	66%	0.05556	-0.06559	0.25000
August	-1.28	downward	90%	-0.26829	-0.40000	-0.11538
September	1.35	upward	91%	0.11111	0.01250	0.18750
October	2.87	upward	95%	0.00816	0.00438	0.01348
November	3.58	upward	95%	0.00222	0.00125	0.00311
December	2.13	upward	95%	0.00080	0.00034	0.00118

Acknowledgements

This work was jointly funded by the German Academic Exchange Service (DAAD) and Higher Education Commission (HEC) of Pakistan. Hydrological data was provided by the Water and Power Development Authority, Pakistan and Dasu Hydropower Consultants. Their help is greatly appreciated.

References

- Peshawar University, 1970. "The sediment load and measurements for their control in rivers of West Pakistan." Department of Water Resources, Peshawar.
- Ali, K. F., 2009. "Construction of Sediment Budgets in Large Scale Drainage Basins: The case of the upper Indus River." PhD thesis, Department of Geography and Planning, University of Saskatchewan, Saskatoon.
- Azim, F., Shakir, A. S. and Kanwal, A., 2016. "Impact of climate change on sediment yield for Naran watershed, Pakistan." *Int. J. Sediment. Res.*
- Böhner, J. and Lucarini, V., 2015. "Prevailing climatic trends and runoff response from Hindukush-Karakoram-Himalaya, upper Indus basin." *arXiv preprint arXiv:1503.06708*.
- Collins, D. N., 1996. "Sediment transport from glacierized basins in the Karakoram mountains, Erosion and sediment yield: Global and regional perspectives " *IAHS(236)*.
- Dasu Hydropower Consultants, 2013. "Detailed Engineering Design Report, Part A; Engineering Design." 7.
- Fletcher, D. and Goss, E., 1993. "Forecasting with neural networks: an application using bankruptcy data." *Information & Management*, 24(3), 159-167.
- Gibbons, R. D., Bhaumik, D. K. and Aryal, S., 2009. *Statistical Methods for Groundwater Monitoring: Second Edition*.
- Gilbert, R. O., 1987. *Statistical methods for environmental pollution monitoring*, John Wiley & Sons.
- Haykin, S., 1999. "Multilayer perceptrons." *Neural networks: a comprehensive foundation*, 2, 156-255.
- Holeman, J. N., 1968. "The sediment yield of major rivers of the world." *Water Resour. Res.*, 4(4), 737-.
- Hussain, M., Nadya, S., Yusof, K. and Mustafa, M., 2017. "Potential impact of climate change on river inflows to the Batang Ai hydro plant,." *The International Journal on Hydropower & Dams(01)*, 44-48.
- Kendall, M., 1975. "Rank Correlation Methods (4th edn.) Charles Griffin." *San Francisco, CA*, 8.
- Lowe, J. and Fox, I., "Sedimentation in Tarbela reservoir." *Proc., Commission Internationale des Grandes Barrages. Quatorzieme Congres des Grands Barrages, Rio de Janeiro*.
- Mann, H., 1945. "Nonparametric tests against trend." *Econometrica*, 13(3), 245-259.
- Meybeck, M., 1976. "Total mineral dissolved transport by world major rivers/Transport en sels dissous des plus grands fleuves mondiaux." *Hydrolog. Sci. J.*, 21(2), 265-284.
- Milliman, J., Quraishee, G. and Beg, M., 1984. "Sediment discharge from the Indus River to the ocean: past, present and future." *Marine Geology and Oceanography of Arabian Sea and Coastal Pakistan*, 65-70.
- Sen, P. K., 1968. "Estimates of the regression coefficient based on Kendall's tau." *J. Am. Stat. Assoc.*, 63(324), 1379-1389.

- Shoaib, M., Shamseldin, A. Y., Melville, B. W. and Khan, M. M., 2016. "Hybrid Wavelet Neural Network Approach." *Artificial Neural Network Modelling*, Springer, 127-143.
- Summerfield, M. A. and Hulton, N. J., 1994. "Natural controls of fluvial denudation rates in major world drainage basins." *J. Geophys. Res-Sol. EA.*, 99(B7), 13871-13883.
- Zhang, Q., Xu, C.-y., Becker, S. and Jiang, T., 2006. "Sediment and runoff changes in the Yangtze River basin during past 50 years." *J. Hydrol.*, 331(3), 511-523.

Hydraulic Transient Analysis for Proposed Penstock of Khari Power House at Jari Dam Downstream

Javed Munir^{1*}, Syed Abbas Ali², Irfan Mahmood³

^{1*}General Manager, Water Resources Division, NESPAK

²Senior Engineer, Water Resources Division, NESPAK

³Senior Engineer, Water Resources Division, NESPAK

*jm786@hotmail.com

Abstract: Jari pond separates from main Mangla reservoir below EL. 1102 ft asl, creating trapped water storage. The technical feasibility of enhancing power generation capacity of existing Khari powerhouse has been evaluated in the study. Additionally, the option of a new powerhouse capable of generating 3.5MW power has also been analyzed and penstock proposed accordingly. The total head loss in the penstock for all options have been considered. The most feasible option has been assessed for safety against the development of water hammer or hydraulic transient pressures in case of sudden gate/valve closure. Conclusions to the study have been proposed at the end.

Keywords: Transient analysis; Penstock; Khari powerhouse

Introduction

Jari dam is constructed across a saddle along the rim of Mangla reservoir away from the main dam as shown in Fig. 1. Jari dam is 4495.8 m long, with a height of 92.66m above river bed. Another ridge in the reservoir separates the Jari pocket from the main Mangla reservoir. This ridge is cut to EL. 335.89. Jari pocket separates from main reservoir when water level in the reservoir drops below EL. 335.89 m. Jari pocket becomes a part of the main reservoir when water level in the reservoir rises above EL. 335.89 m. A 2.13m (7 ft) diameter tunnel was constructed to drain trapped water in Jari pocket with tunnel invert at EL. 320.04m. An intake gate 2.74m (9 ft) wide x 1.52m (5 ft) high has been provided for flow regulation.

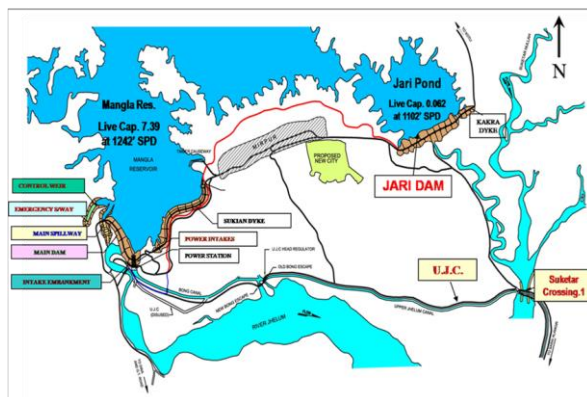


Fig. 1 Location Map

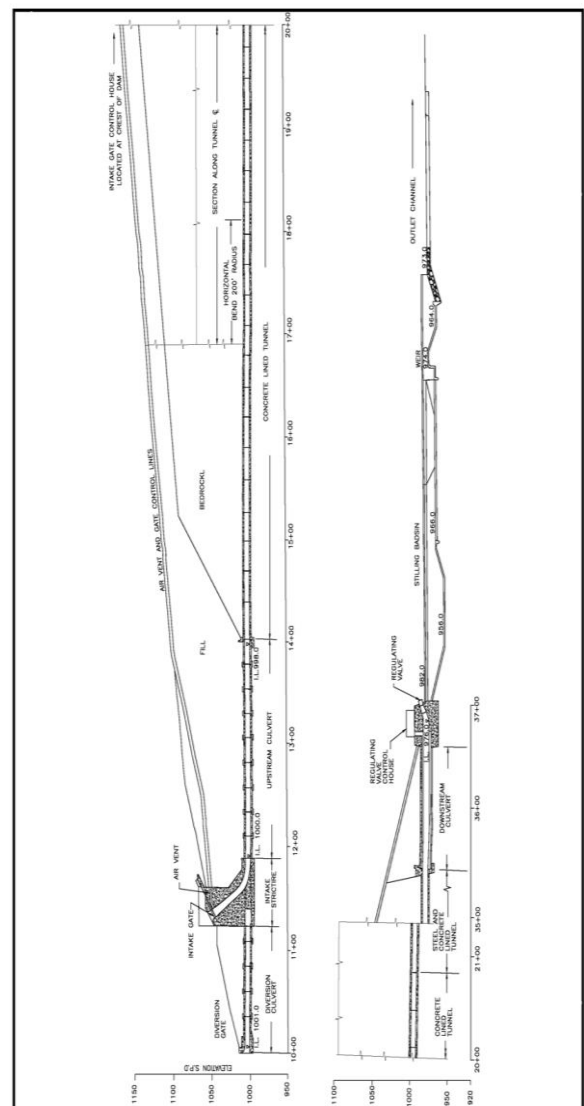


Fig. 2 Longitudinal Section of Jari Tunnel

Scope of Hydraulic Studies:

The scope under this study is as below:

- i) to check if 3.5MW can be generated by passing 4.25m³/s through existing Khari powerhouse tapping
- ii) to propose a new penstock for 3.5MW power generation with for a new powerhouse at different location by bifurcating and enlarging the existing tapping, keeping the existing powerhouse as it is
- iii) to perform hydraulic transient analysis for the technically feasible option

Hydraulic Analyses

The performed hydraulic analyses involved calculation of head losses, power generation, water hammer analysis, etc. Head loss determination at main tunnel and respective tappings under consideration included calculation of major loss due to friction and other minor losses. Friction losses were calculated using Darcy Weisbach equation as given below:

$$h_f = \frac{\lambda L V^2}{D 2g}$$

where,

h_f = head loss

L = conduit length

D = conduit diameter

V = flow velocity in conduit

g = acceleration due to gravity

λ = Darcy Weisbach friction factor; calculated using Colebrook White formula

$$\frac{1}{\lambda^{0.5}} = -2 \log \left[\frac{e}{3.7 D} + \frac{2.51}{Re \lambda^{0.5}} \right]$$

where,

Re = Reynolds number

e = absolute roughness in mm

Trash rack, intake, transition, bend, gradual expansion, gradual contraction, bifurcation, exit and wicket gate/valve losses collectively fall under minor loss category and each has been calculated using the following equation:

$$h_l = K \frac{V^2}{2g}$$

where,

K = coefficient of minor loss (taken from Design of Small Dams, USBR)

Power has been calculated using the following equation,

$$P = \rho g \eta Q H_n$$

where,

P = power in Watts

η = overall efficiency = $\eta_t \eta_g \eta_{tr}$

η_t = turbine efficiency
(taken as 92.0%)

η_g = generator efficiency (taken as 97.5%)

η_{tr} = transformer efficiency (taken as 98%)

Q = discharge

H_n = net head = total head – head losses

Water Hammer Analysis

The closure of a wicket gate/valve at the end of a conduit results in head rise at u/s side of gate/valve called water hammer. As a result of this head rise, a pressure wave is generated that travels in the upstream direction and gets reflected from the free surface reservoir at the upstream end of the conduit travelling back towards the gate/valve. The wave motion results in the development of negative pressures in the conduit. This to and fro movement of positive and negative pressure wave is gradually dissipated to zero by friction of the conduit. The pressure wave velocity is calculated by using following equation,

$$a = \frac{1}{\sqrt{\rho \left(\frac{1}{K_w} + \frac{D C_1}{t E} \right)}}$$

where,

a = pressure wave velocity

ρ = density of water

K_w = volume modulus of water

D = diameter of conduit

C_1 = factor for anchorage and support of conduit

t = thickness of lining of Tunnel or thickness of pipe/penstock

E = Young's modulus of elasticity of the lining or pipe material

The maximum head rise just at the upstream side of the gate/valve is calculated from the Allievi's chart. To determine the maximum pressure rise from Allievi's chart, two constants given below are to be calculated.

$$\text{Pipeline Constant } K = \frac{a V}{2 g H_o}$$

$$\text{Time Constant } N = \frac{a T}{2 L}$$

where,

H_o = total head = reservoir level – elevation at centerline of wicket gate/valve

T = closure time of gate/valve

L = total length of the conduit up to gate/valve

For conduit with varying cross sections, different type of lining or pipe material and anchorage/support, the weighted average of pressure wave and flow velocities is calculated for each section of the conduit. The weighted average values are used to calculate the pipeline and time constants for determining maximum pressure rise from Allievi's chart.

Analysis of Existing 1m Dia Tapping for 1MW Khari Powerhouse

The description of length and alignment for concrete and steel lined section of Jari tunnel and existing Khari powerhouse tapping are given below:

Jari Tunnel

Six trash rack units 1.02m x 2.0m
 Rectangular entrance 1.52m x 2.74m
 Transition from rectangular to circular tunnel
 2.13m diameter tunnel
 Length of 2.13m dia concrete lined tunnel
 332m
 Vertical bend in concrete lined tunnel 53°
 Horizontal bend in concrete lined tunnel
 36°
 Length of 2.13m dia steel lined tunnel 445m
 Free standing 2.13m dia steel lined tunnel
 28.5m

Existing Steel Penstock

Diameters of conical off-take 1120
 mm/800mm
 Length of 800mm pipe 2.33m
 Vertical bend after cone 90°
 Butterfly valve diameter 800mm
 Transition after butterfly valve 800mm to
 1000mm
 Horizontal bend after butterfly valve 15°
 Length of 1.0m penstock 11m

The maximum tail water level in the stilling basin considered was at El. 298.86m. The raising of Mangla Dam was taken into account and the maximum conservation level of El. 378.56m was considered. The power calculations were performed by varying the reservoir level from maximum conservation level of El. 378.56m down to El. 323.09m.

The power calculations were carried out by passing 4.25m³/sec discharge through the existing penstock with aforementioned setting. The calculated power versus reservoir level curve is shown in Fig. 4.

The results of the analysis show that maximum power of 2.64MW can be achieved at reservoir level of El. 378.56m. *Therefore, it is not possible to produce the desired power of 3.5MW by passing 4.25m³/sec through the existing Khari Powerhouse tapping.*

The hydraulic analysis also shows that flow velocity in the 1000mm diameter penstock is 5.41m/s which marginally exceeds the generally acceptable velocity limit of 5.0m/s, but the velocity in 800mm diameter pipe at the start of penstock is 8.45m/s which greatly exceed the acceptable velocity limit of 5.0m/s.

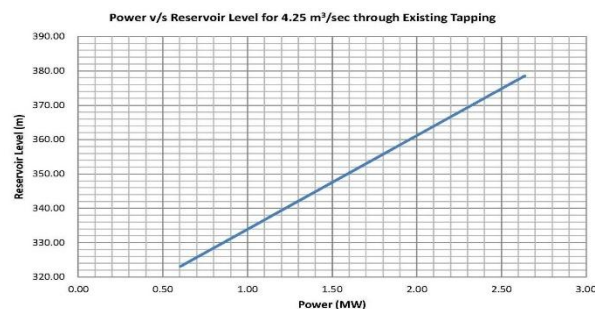


Fig. 4 Power v/s Reservoir Level for 4.25 m³/sec through Existing Tapping

In order to achieve the target of 3.5MW through the existing Khari powerhouse tapping, calculations were carried out by passing 5.76m³/sec through the existing tapping. The power versus reservoir level is shown in Fig. 5.

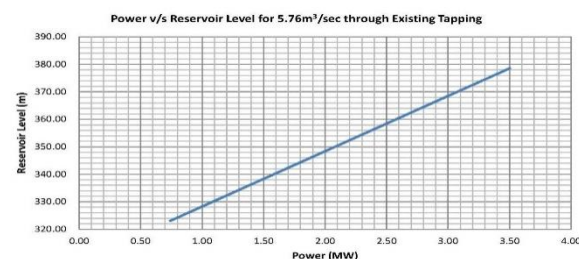


Fig. 5 Power v/s Reservoir Level for 5.76m³/sec through Existing Tapping

The calculation results show that 3.5MW can be achieved by passing 5.76m³/sec through the existing tapping at reservoir level of El. 378.56m. The flow velocities through the 1000mm diameter penstock and 800mm diameter pipe at start of penstock are 7.34m/s and 11.46m/s respectively. These velocities greatly exceed the limiting velocity of 5.0m/s. The velocity in 800mm diameter pipe exceeds limiting velocity for abrasion i.e. 9.14m/s (30.0ft/s).

Therefore, it was concluded that the existing Khari powerhouse tapping was not technically viable for the generation of 3.5 MW power.

Proposed Enlargement of Tapping (1219mm) for 3.5 MW Powerhouse

As discussed previously it was not possible to generate 3.5MW from the existing Khari powerhouse by increasing the discharge to 4.25m³/sec. The increase in discharge from 4.25m³/sec to 5.76m³/sec to generate 3.5MW power resulted in increased flow velocities exceeding the maximum permissible limit. This induced the possibility of abrasion in 800mm pipe of the penstock.

Therefore, it was proposed to provide the 3.5MW powerhouse at separate location while keeping 1MW powerhouse intact. The layout plan of proposed scheme is shown in Fig. 6 and

longitudinal section of proposed penstock in Fig. 7. It was also proposed to use the tapping of existing Khari powerhouse for the proposed scheme and enlarge an entire length to 1.2m diameter. The tapping will bifurcate after 90° bend to branch towards the proposed powerhouse

while keeping the existing 1MW penstock intact. The tapping proposed will pass 5.66m³/sec to produce 3.5MW power at reservoir level of El. 378.56m. The flow velocity in entire penstock will remain within 5.0m/s not exceeding the permissible velocity limit.

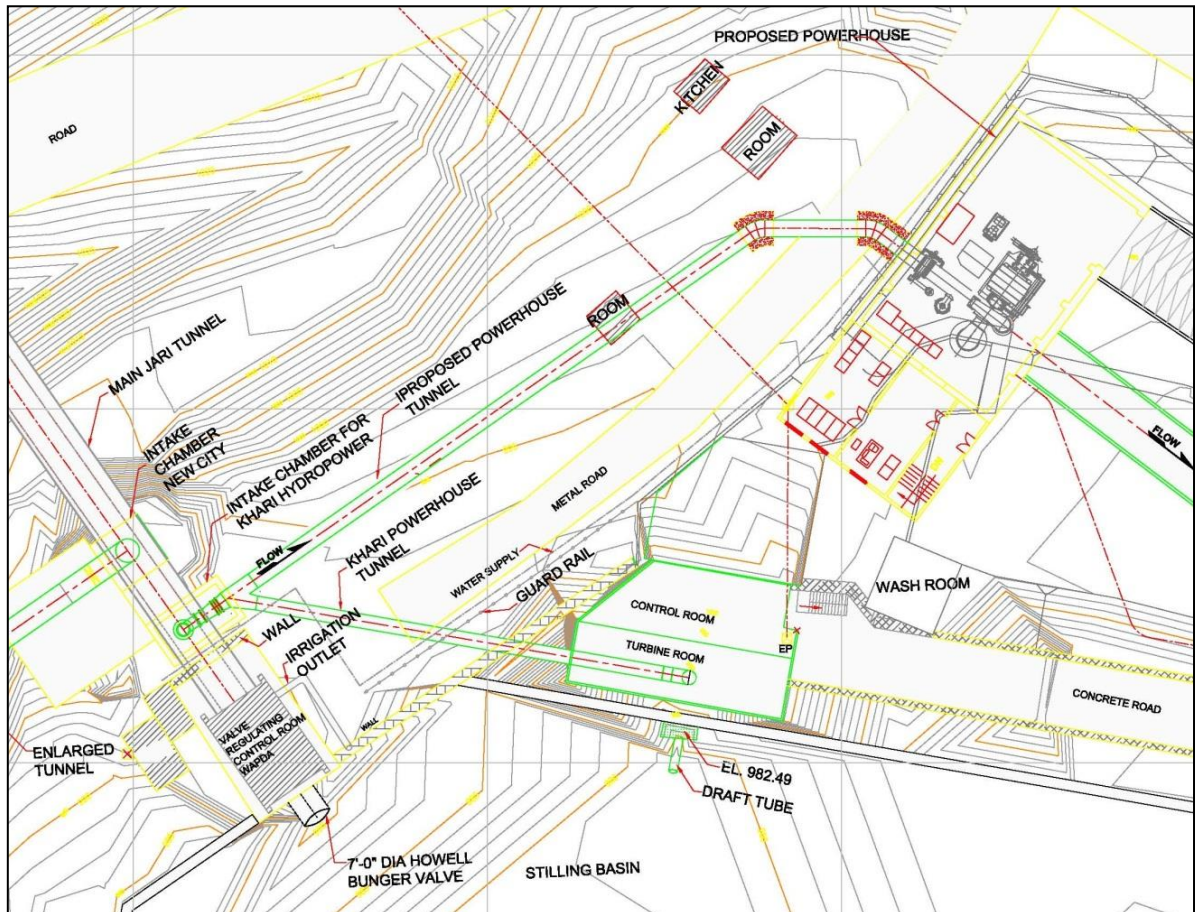


Fig. 6 Layout Plan of Proposed Powerhouse

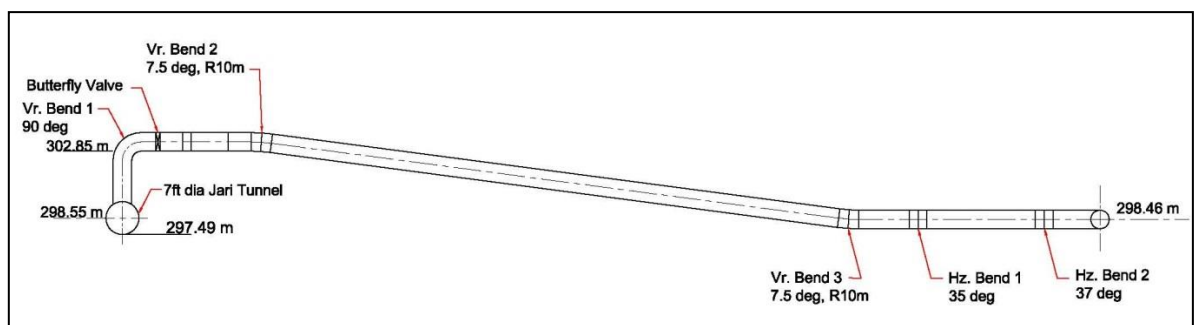


Fig. 7 Longitudinal Section of Proposed Penstock for 3.5 MW Powerhouse

The description of tapping is given below:
 First vertical bend after tapping 90 degrees
 Power tunnel length between tapping and bifurcation 7.74 m
 Butterfly valve diameter 1.2 m (48 inch)
 Bifurcation diameter 1.2 m
 First horizontal bend 35 degrees
 Second horizontal bend 37 degrees
 Second vertical bend after bifurcation 7.5 degrees

Third vertical bend after bifurcation 7.5 degrees
 1.2m diameter penstock from bifurcation to powerhouse 57.64 m
 The power versus reservoir level developed after hydraulic analyses for the proposed scheme is shown in Fig. 8. The results show that 3.5MW power is achieved for the proposed configuration with reservoir level at El. 378.56m by passing 5.66m³/sec discharge through the penstock. The

power will reduce as the reservoir level is lowered. Power generation equal to 3.0MW can be achieved at reservoir level of El 367.5m. So far the reservoir level of El. 378.56m has not been achieved. Normally the reservoir is filled up to the normal pond level by the end of the monsoon season if adequate flows are available. After the monsoon season low flow season starts and the reservoir starts depleting.

The hydraulic analysis shows that the proposed scheme is technically viable and 3.5MW power can be produced from the proposed powerhouse. However, when reservoir level is low and it is not possible to produce power from this facility, the existing 1MW unit can be operated.

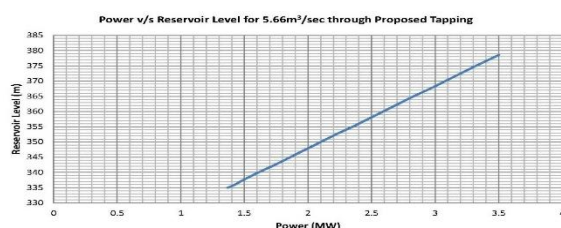


Fig. 8 Power v/s Res. Level for 5.66m³/sec through Proposed Penstock of 3.5MW Power Unit

Table 5 Summary of Water Hammer Calculations for Proposed 3.5MW Powerhouse

Location	Diameter	Flow Velocity	Distance from Intake	Tunnel Centerline Elevation	Res. Elv.	Static Head	Head Rise	Total Head
	(m)	(m/s)	(m)	(m)	(m)	(m)	(m)	(m)
Wicket Gates Closure Time = 6 sec								
At start of steel lining	2.13	4.44	332.00	305.26	378.56	73.30	39.59	112.89
At tunnel start in culvert	2.13	4.44	778.00	303.43	378.56	75.13	92.77	167.91
At tapping for Khari PH	2.13	4.44	806.50	298.55	378.56	80.01	96.17	176.18
At Turbine	1.20	5.01	873.25	298.52	378.56	80.04	104.13	184.17
Wicket Gates Closure Time = 10 sec								
At start of steel lining	2.13	4.44	332.00	305.26	378.56	73.30	20.56	93.86
At tunnel start in culvert	2.13	4.44	778.00	303.43	378.56	75.13	48.17	123.30
At tapping for Khari PH	2.13	4.44	806.50	298.55	378.56	80.01	49.94	129.95
At Turbine	1.20	5.01	873.25	298.52	378.56	80.04	54.07	134.11

The calculations show a total head rise of 184.17m at the turbine and 176.18m in the free-standing tunnel in the culvert for six (6) second wicket gates closure time. For ten (10) second wicket gates closure time, the total head rise is

Water Hammer Analysis for 3.5 MW Powerhouse Tapping

Water hammer analysis was carried out to determine the maximum pressures in Jari tunnel and penstock for the case when full load rejection takes place and wicket gate/valve at the turbine are closed in a short period of time. The maximum pressures have been calculated for six (6) and ten (10) second wicket gate closure times separately.

As explained above, the weighted average of pressure wave velocity and flow velocity has been used for the determination of maximum pressure at wicket gates from Allievi's chart. The pressure at other locations in the tunnel has been determined by considering linear decrease of head rise up to the reservoir.

Head losses in the penstock and Jari tunnel have been neglected for the determination of water hammer pressure. The summary of the results of water hammer analysis is given in Table 5.

134.11m at the turbine and 129.95m in free standing tunnel in the culvert.

The tunnel must be safe against the total head developed due to full load rejection in both cases i.e., wicket gate closure time of 6 and 10 seconds.

The penstock for additional power has been proposed accordingly. It is suggested that a relief valve may be provided at the turbine which automatically opens when load rejection takes place to protect Jari tunnel from water hammer pressures.

Conclusions

The carried-out water hammer analysis shows that the existing Khari powerhouse penstock cannot be used for generation of 3.5MW and therefore, a new penstock has been proposed for 3.5MW generation. The proposed penstock must be safe against the total head developed due to full load rejection at wicket gate closure time of 6 and 10 seconds; the penstock for additional power has been proposed accordingly.

The proposed penstock is hydraulically safe against developed water hammer pressures or

hydraulic transients. It is suggested that a relief valve may be provided at the turbine which automatically opens when load rejection takes place to protect Jari tunnel from water hammer pressures.

References

- [1] Creager W.P. and Justin J.D., 1950, Hydroelectric Handbook, 2nd Edition, John Wiley and Sons, London
- [2] Gulliver J.S. and Arndt R., 1991, Hydropower Engineering Handbook, McGraw Hill, USA
- [3] Mosonyi E., 1987, Low Head Hydropower Plants,
- [4] US Bureau of Reclamation (USBR), 1987, Design of Small Dams, 3rd Edition
- [5] Warnick C.C., 1984, Hydropower Engineering

Application of Computational Flow Dynamics (CFD) Analysis for Surge Inception and Propagation in Low Head Hydropower Projects

M. Mohsin Munir^{1*}, Taimoor Ahmad², Dr. Javed Munir³

^{1*}National Engineering Services, Pakistan, Pvt, Ltd

²National Engineering Services, Pakistan, Pvt, Ltd

³National Engineering Services, Pakistan, Pvt, Ltd

[*mohsin_uett@yahoo.com](mailto:mohsin_uett@yahoo.com)

Abstract: Determination of maximum elevation of a flowing fluid due to sudden rejection of load in a hydropower facility is of great interest to hydraulic engineers to ensure safety of the hydraulic structures. Several mathematical models exist that employ one-dimensional modeling for the determination of surge but none of these perfectly simulate real-time circumstances. The paper envisages investigation of surge inception and propagation for a Low-Head Hydropower project using Computational Fluid Dynamics (CFD) analysis in FLOW-3D software. The fluid dynamic model utilizes its analysis for surge by employing Reynolds' Averaged Navier-Stokes Equations (RANSE). The CFD model is designed for a case study at Taunsa Hydropower Project in Pakistan. Various scenarios have run through the model keeping in view upstream boundary conditions. The prototype results were compared with the physical model testing results and proved quite accurate coherence with the physical model testing and offers insight into phenomenon which are not apparent in physical model and shall be adopted in future for the similar low head projects limiting delays and cost incurred in the physical model testing.

Keywords: Surge, FLOW-3D, Numerical Model, Taunsa, RANSE

Introduction

Maximum elevation that the flow will achieve due to a sudden rejection of load in a hydropower facility is an important parameter to hydraulic engineers. The information is required in setting the maximum height of sidewalls to prevent overflow in the headrace channel as well as to understand the surge propagation upstream in headrace channel to schedule the opening of gates of the main barrage and balance the discharge through the barrage and power channel.

In Pakistan, physical model studies are the only practical medium available to understand and analyze the three dimensional and time-dependent complexities of the fluid flow phenomenon. Physical models can only be setup at the final design stage and their execution is expensive. However, the avant-garde computational flow dynamics has emerged not only as an alternative analysis and design tool but can also be employed to analyze phenomenon that are not possible to assess with physical testing.

Literature Review

A monoclinal wave exhibiting a rapidly varying flow may result in a hydropower project due to sudden closure or opening of the powerhouse control structure such as the sluice gates or wicket gates. This hydraulic transient analysis is

of immense importance especially during the design phase of the hydropower project. The rising wave can easily overtop the banks of the fore-bay or the headrace channel and damage appurtenant structures of the hydropower facility. Moreover, studying the propagation of wave through the headrace channel and into the reservoir is required to assess the effect of rapidly varying flow in the headrace on the reservoir water levels.

Several mathematical methods exist for one-dimensional determination of surge for different conditions i.e. for straight channels, for propagation of surge on a gradient, analysis of reflected surges and the Johnson method. The first three methods are simplifications of the original problem and are based on several assumptions. These methods do not truly represent the original problem and these conditions are rarely met in practice. Similarly, the Johnson method can be arduous as the computation proceeds since numerous surges will be produced and propagated. Hence it becomes inaccurate and difficult to assess the surge using these methods.

Other time dependent analysis increases the complexities of the problem by introducing additional independent variable of time since the resulting equations become partial differential equations instead of ordinary differential equations. Method of Characteristics and Implicit

and Explicit Finite-Difference Methods have better accuracy and rigor but are time-consuming and cannot be applied fully to original conditions. In special cases, such as analysis of hydropower projects comprising of open headrace channel with tailrace tunnel (Closed conduit), implicit methods are preferred for the closed conduit. Such complexities can only be modelled using a powerful software package like FLOW-3D, based on numerical solution schemes that can accurately predict fluid flow using the concept of fluid volume tracking.

FLOW-3D was developed at the Los Alamos National Laboratory in the 1960s and 1970s as a general purpose computational fluid dynamics simulation package. FLOW-3D uses an Eulerian framework in which volume tracking technique models the free surface. This method, based on fluid volume fraction analyses the amount of fluid in each cell and is robust enough to handle the breakup and coalescence of fluid masses.

FLOW-3D uses several models to numerically simulate turbulent flows. For this case study, the Renormalization group (RNG) k-epsilon turbulence model was used with a no slip or partial slip wall shear boundary condition. The RNG turbulence model uses statistical models to solve the turbulent kinetic energy (k) and the turbulent kinetic energy dissipation rate (ϵ), renormalizing the Navier Stokes Equations to use cater for the effects caused by smaller scale motion.

FLOW-3D employs the Volume-of-Fluid (VOF) technique developed by Hirt and Nichols in 1981 to deal with interfaces between two fluids and to model. VOF depends on the volume fraction which is assigned value of either 1 or 0 depending the cell is occupied by the fluid or not. It is governed by the following convection transport equation:

$$\frac{\partial F}{\partial t} + \frac{\partial F u_j}{\partial x_j} = 0$$

A detail on VOF method related issues can be found in Bombardelli et al. (2001) while its development can be referred to C.W. Hirt et al (1981). The free surface is not only unknown in 3-D computations, but it also acts a boundary for the problem. A sharp representation of interface is necessary to be maintained apart from locating the free surface in a 3-D Eulerian grid, doing it effectively in terms of computational time.

Case Study of 135MW Taunsa Hydropower Project

Taunsa Hydropower Project has been sited along right bank of Taunsa Barrage across Indus River

in Pakistan. It is a run of the river, low head hydropower scheme envisaged to provide power to the national grid. Table 1 summarizes the salient features of the project.

Table 1 Salient Features of 135MW Taunsa HPP

Type of Turbine	Horizontal Bulb
Mode of Operation	Run of the River
Installed Capacity	135 MW
Gross Head	6.0m
Rated Head	5.8m
Design Discharge	3,155.5 m ³ /sec
Turbine Units	9 Units
Headrace Width	203m
Headrace Length	1100m
Vertical Gate Height	16m

FLOW-3D analysis are often limited by computation power available. For numerical simplicity in this case, the three-dimensional model was setup based on only one hydropower unit and not the complete power-station. FLOW-3D can effectively use the symmetry conditions of the project layout without affecting the accuracy of the surge analysis. A 3D model was used since flow has three-dimensional characteristics.

Model Preparation

The model for Taunsa hydropower project was prepared in AutoCAD and imported in stereolithographic format which is used for rapid prototyping, 3D printing and computer-aided manufacturing. Three dimensional models were prepared for the headrace, transitions, powerhouse and tailrace. Fig. 1 illustrates the 9-unit powerhouse with gates open. Fig. 2 shows the detail of transitions of a single unit with bulb turbine housed inside.

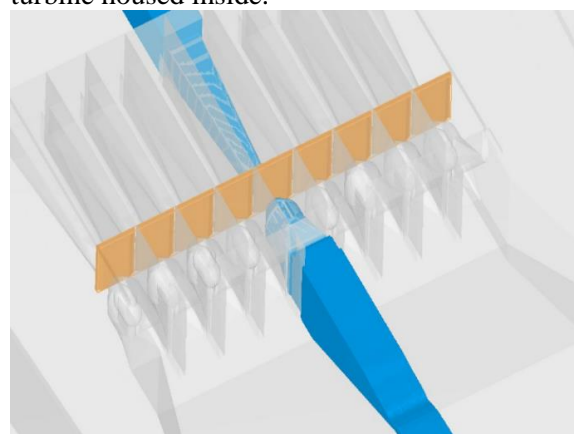


Fig. 1 Isometric View of Taunsa HPP Model

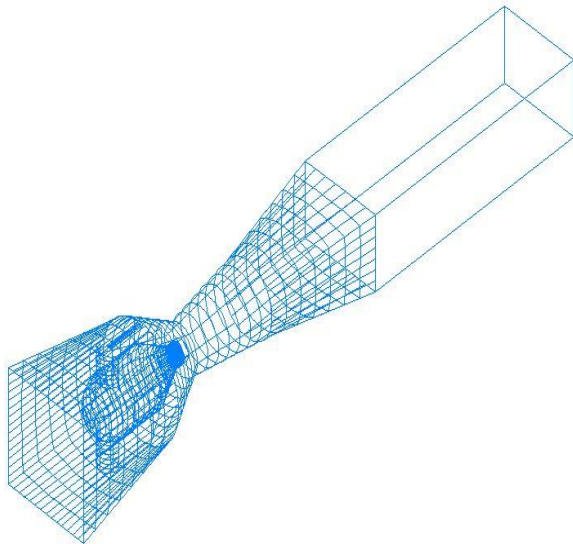


Fig. 2 Wireframe of a single in-take and draft tube with bulb turbine

Meshing

Meshing is a consequential part of the analysis process which not only determines the numerical accuracy of the model but also the memory and time required for the simulation. Meshing was done and refined in FLOW-3D model setup options. FLOW-3D has an advantage of FAVOR; Fractional Area/Volume Obstacle Representation Method which allows modeling of complex geometries based on equations formulated as functions of the area and volume porosity.

As specified before, for simplicity as well as increased accuracy, meshing was done for one unit. This is a common practice since for large models, no of total active cells are limited by computer memory. For Taunsa Hydropower Project, the extents, no of cells and cell sizes are tabulated in Table 2.

Table 2 Summary of meshing in FLOW-3D

Total active cells	2320000		
Dimension	Extent (m)	No of cells	Cell size (m)
X	400	400	1.00
Y	18.5	50	0.37
Z	29	116	0.25

Cell sizes for the mesh were selected based on two factors. First consideration in this regard is the model accuracy. In case of surge analysis, height of surge (z-direction) is the most important. Hence, smallest cell size has been selected for z axis. Second consideration is CPU

memory and computation time. Increasing the number of cells requires greater computation power and longer simulation time. Average simulation time in for Taunsa HPP was 15 hours. Keeping in view the two factors, minimum cell size was selected so that full computation power was being employed.

Boundary Conditions

Boundary conditions have a huge impact on the final results of the simulation. It is necessary to assess the boundary conditions that best replicate the real-time conditions and actual simulation. Boundary conditions applied for the problem are specified below:

X minimum	Specified Pressure Boundary
X maximum	Outflow Boundary
Y minimum	Symmetry Boundary
Y maximum	Symmetry Boundary
Z minimum	Wall Boundary
Z maximum	Symmetry Boundary

The upstream boundary condition consisted of a specified pressure to maintain a prescribed reservoir elevation. The downstream boundary utilized the FLOW-3D outflow boundary condition. A symmetry boundary condition was applied along right and left side of the mesh section to take advantage of the inherent symmetry in the problem and thereby decrease computational time while maximizing spatial resolution. Boundary conditions used have been explained below:

Symmetry Boundary: There is no mass flux (flow) through a symmetry boundary. There is also no shear stress or heat transfer applied at this boundary type. It is useful for reducing the size of a simulation when symmetry exists by cutting the simulation at the symmetry plane.

Wall Boundary: The wall boundary is similar to the symmetry boundary in that mass flux across the boundary is not allowed. However, with a wall boundary, heating and viscous stresses can be applied.

Specified Pressure Boundary: This boundary type sets a pressure condition. The pressure can be constant by setting a value in the dialog box, or time dependent by selecting the pressure button.

Outflow Boundary: This boundary type is useful for surface waves because they are able to leave the flow region without reflecting back into the domain. This boundary type looks at flow conditions just inside the mesh and matches them

to allow fluid to freely dissipate through the mesh extent.

Case Study Scenarios

Two flow scenarios have been analyzed for the case study as tabulated in Table 3. During normal flow operation, initial water level elevation of 135.94m will be maintained in the headrace channel and 130.25m in the tailrace channel during full operation of 9 units. The model is allowed to operate freely for 30 seconds after which the gates are shut at 1.4m/s to close the orifice in 5 seconds in order to replicate sudden closure conditions. Type B surge or the rejection surge occurs as a result of sudden decrease in power output. Similarly, during flood flow operation, initial water level elevation of 136.25m will be maintained in the headrace channel and 133.26m in the tailrace channel. Other conditions are kept same as in normal flow conditions.

Table 3

Flow Condition	U/S water level (m)	D/S water level (m)
Normal Flow	135.94	130.25
Flood Flow	136.25	133.26
Normal Flow	135.94	130.25
Flood Flow	136.25	133.26

Results

The rejection surge occurs as a result of sudden decrease in power output. Fig. 3, 4 and 5 illustrate the surge inception and propagation at different times after load rejection in the extent just upstream of the gates. The points of flow direction reversal can easily be tracked for the upstream advancing surge. This is a feature that is only possible with computational flow dynamics analysis since it is not possible to observe these phenomenon in physical model testing.

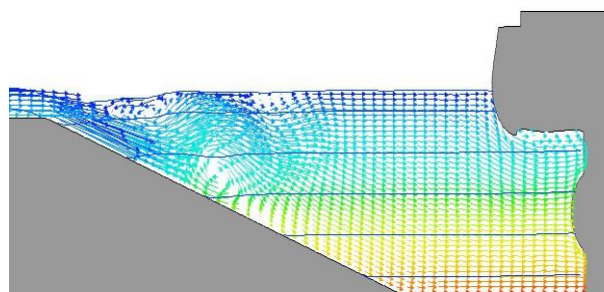


Fig. 3 Flow through the power unit at full operation

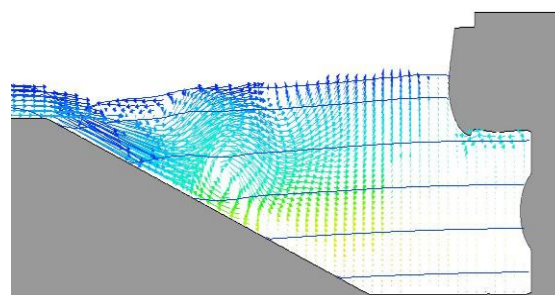


Fig. 4 Surge inception at time of load rejection

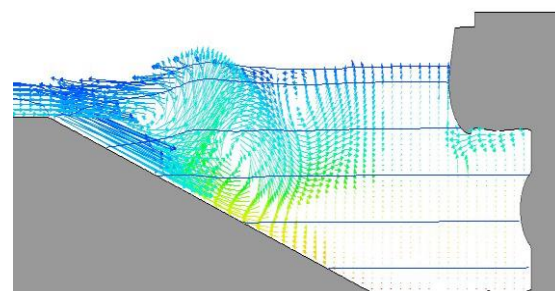


Fig. 5 Flow reversal after 10 seconds of load rejection

In Fig. 3, flow vectors at full flow conditions are illustrated by arrows. This shows an uninterrupted movement of fluid. After load rejection, a *region of fluid immobility* starts to develop as observed from Fig. 4. This region acts a cushion against incoming discharge and reverses its direction which results in surge inception. Fig. 5 shows the region of fluid immobility develops upstream with time as surge wave begins to achieve greater elevation. The phenomenon holds true for both normal flow conditions and flood flow conditions.

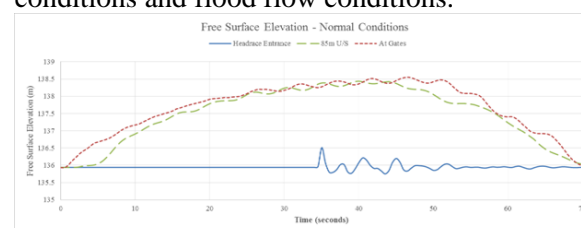


Fig. 6 Change in water elevation vs time after load rejection for Normal Flow Conditions Taunsa

Normal Flow Conditions

As the surge moves upstream, change in flow depth will ensue. FLOW-3D can track the change in elevation of free surface efficiently for any spatial location of the model. Changes in surface elevation with time were observed for three locations i.e. at turbine unit entrance, 85m upstream of the entrance and at headrace entrance.

The temporal and spatial change in free surface elevation at 3 locations have been shown in Fig. 6. Table 4 shows the summary of results which

depict a maximum surge of 2.25m at unit entrance. Time of arrival of first wave has also been tabulated. The surge is expected to reach the headrace entrance in 260 seconds after gate closure with an average velocity of 4.84m/s. As the surge wave moves upstream, the height of wave dampens.

Table 3 Summary for Normal Conditions

Location	Max Surge	Surge Elevation	Time (sec)
Unit Entrance	2.25m	138.19m	7
85m U/S	2.21m	138.15m	14
Headrace Entrance	0.53m	136.47m	260

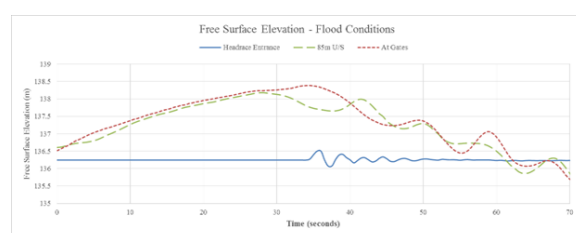


Fig. 7 Change in water elevation vs time after load reject Flow Conditions Taunsa Headrace

In case of flood flows in Taunsa hydropower, an upstream water level of 136.25m is maintained in the headrace with a corresponding tail-water level of 133.26m in tail-race. Other conditions are kept same as in normal flow conditions. The surge is expected to reach the headrace entrance in 206 seconds with an average surge velocity of 6.7 m/s. Maximum surge elevation of 138.4m (2.21m) is observed at the power unit entrance. The results have been tabulated in Table 5. Fig. 7 shows the change in free surface elevation at the three selected locations vs time after load rejection from the power unit.

Table 4 Summary for Flood Conditions

Location	Max Surge	Surge Elevation	Time (sec)
Unit Entrance	2.21m	138.39m	6
85m U/S	2.00m	138.20m	12
Headrace Entrance	0.32m	136.52m	206

Flood Flow Conditions

It is observed that the surge travels faster and achieves a lower maximum free surface elevation for the flood flow conditions compared to the Normal Flow Conditions.

Conclusion

Observations of the surge inception and propagation are in line with the theory and assumptions specified by VenTe Chow and other authors. For upstream advancing surge, when the surge wave reaches any point in the headrace, the water elevation behind the wave approximately equals the maximum elevation of the surge wave. The simulation results were compared with the mathematical formulae mentioned above as well as the physical testing model carried out at Irrigation Research Institute, Nandipur, Punjab. The results of the physical model testing were within $\pm 2\%$ of the results achieved with simulations in FLOW-3D. This has built greater confidence in modelling using computational flow dynamics especially for modelling in field of power generation.

Applications of computational flow dynamics have been increasing in engineering applications over recent times. The computer numerical models are a cost-effective alternative to physical modeling techniques offering more flexibility during design and analysis and can offer insights into phenomenon that are not apparent in physical model testing. However, CFD analyses limited by computational power. The present 3D detailed analysis of a single unit required more than 24 hours of computation per simulation to examine a 70-second time-history. A longer time-history is often more desirable.

The analysis of Taunsa hydropower headrace channel using computational flow dynamics is a step-forward in supplementing the results from mathematical modelling and conventional physical model testing in Pakistan. It is not only a robust analysis software solution but can be employed as efficacious tool in the design process of hydraulic structures where it can offer extensive flexibility to assess and compare different proposed designs and their efficiencies. This design support can save a lot of time and money by the optimization process before final designs are physically tested at Irrigation Research Institute, Nandipur.

References

1. VenTe Chow (1959). *Open Channel Hydraulics*. United States of America: McGraw-Hill Book Company Inc. 561-565
2. Rich, G.R. (1951) *Hydraulic Transients*, 2nd ed., Dover Publications, New York, NY, U.S.A
3. M. Hanif Chaudhry (2014). *Applied Hydraulic Transients*. 3rd ed. London: Springer. 450-474

4. Yakhot, V.; Orszag, S. A.; Thangam, S.; Gatski, T. B.; Speziale, C. G. (1992). Development of Turbulence Models for Shear Flows by a Double Expansion Technique. *Physics of Fluids A*. 4 (7), 1510-1520
5. Flow Science Inc. Los Alamos New Mexico, USA. 1997. *FLOW-3D® User's Manual Version 9.3*
6. Flow Science Inc. Los Alamos New Mexico, USA. 1997. *FLOW-3D® User's Manual Version 10 Chapter 2: Tutorial*
7. C.W. Hirt and B.D Nichols. 1981. Volume of Fluid (VOF) Method for the Dynamics of Free Boundaries, *J. Computational Phys.*
8. Teklemariam, E., Korbaylo, B. W., Groeneveld J.L., Fuchs, D.M. 2002. Computational Fluid Dynamics: Diverse Applications in Hydropower Project's Design and Analysis, *CWRA 55th Annual Conference June 11-14*.
9. D.T. Souders and C.W. Hirt, Modeling Roughness Effects in Open Channel Flows
10. Bombardelli, F. A., Hirt, C. W. and García, M. H.: 2001, 'Discussion on 'Computations of Curve Free Surface Water Flow on Spiral Concentrators' ' by B. W. Matthews, C. A. J. Fletcher, A. C. Partridge and S. Vasquez, *J. Hydr. Eng. ASCE 127(7)*, 629–630.
11. Rodi, W.: 1984, *Turbulence Models and their Application in Hydraulics*, IAHR Monograph, Delft.
12. Vošnjak, S., "Verification of the Flow-3D mathematical model by a physical hydraulic model of a small hydropower plant", *presentation, European FLOW-3D User Meeting 2006*, CFD Consultants, Tübingen

DECLARATION

I, the corresponding author, confirm that the authors listed on the manuscript are aware of their authorship status and qualify to be authors on the manuscript according to the guidelines above. I confirm that all of the content, Fig.s (drawings, charts, photographs, etc.), and tables in the submitted work are either original work created by the authors listed on the manuscript or work for which permission to reuse has been obtained from the creator. The submitted work has not been published elsewhere. In case the article is accepted for publication in 'Proceedings of the Pakistan Academy of Sciences', its copyright will be assigned to Pakistan Academy of Sciences. Authors must obtain permission to reproduce copyrighted material from other sources and ensure that no copyrights are infringed upon.

Statistical Analysis of inflows of River Indus at Tarbela in the Wake of Climate Change

Dr. Muhammad Khurram Shahzad^{1*}

^{1*}Department of Civil Engineering, Institute of Southern Punjab, Multan; Email:
[*shahzadmuhammadhurram@gmail.com](mailto:shahzadmuhammadhurram@gmail.com)

Abstract: Pakistan, after signing Indus Basin Treaty with India in 1970, mainly relies upon the discharges from the three western rivers of Indus Basin i.e. Indus, Jhelum and Chenab along with the inflow of River Kabul that enters Pakistan from Afghanistan near Nowshera. The major portion of these Western rivers' inflow is contributed by River Indus. The effect of climate change on the glacial melt of Himalayan-Karakorum-Hindu Kush (HKH) region and the regional precipitation of Upper Indus Basin (UIB) is widely reported. However, the impacts of changing climate could be only verified if its foot prints are reflected in the discharges of the river Indus that drains the basin. Pakistan holds restricted capability to withstand the impacts of climate change on pushing the flows towards extreme, excess and otherwise, due to its limited water storage capacity. Similarly, the limited capacity of conveyance system, natural passages and the regulatory structures, inhibits the high flows to be routed through the system without flooding. Therefore, the climate change induced scenarios of long term positive / negative trend and / or increased fluctuations in intra-year and inter-year discharges, both adversely affect the water regulation of the country. Consequently, this study is focused on the investigation of temporal variation of flows of Indus at Tarbela. The seasonal and yearly trend is investigated by applying statistical techniques including Mann-Kendall Test. The 10-daily discharge data of Indus at Tarbela from 1961 to 2010 is used to conduct the analysis. A less significant decreasing trend is observed in the Kharif season and yearly discharges of Indus, whereas, significant increasing trend is observed in the Rabi flows.

Keywords: Statistical analysis, River inflows, Tarbela dam

Introduction

The phenomenon of global climate change is an outcome of natural processes and anthropogenic activities. The natural processes include natural variability, solar activity, volcano eruption, land & ocean change, where the major anthropogenic activities affecting the climate are urbanization, land use change, aerosols and the emission of greenhouse gases (Rasul, G. et. al., 2011). The effect of climate change on various meteorological parameters like temperature, precipitation, humidity etc. has been widely reported. In general, there is a consensus of the experts, on global warming mainly due to the emission of GHG; however, its impact on the hydro-meteorological processes is not uniform in different geographical regions. Initially, the 3rd assessment report of Intergovernmental Panel on Climate Change (IPCC) has captured the impacts of climate change on water resources. The variations in magnitude and frequency of precipitation have been predicted. It was predicted that global warming will result in the diminishing of glaciers due to additional melt, that may cause increased discharges consequently flooding in few future years but after that the flows will sharply decrease because

some of the contributing glaciers will completely disappear.

The upstream snow and ice reserves of South and South East Asian River basins; Indus, Ganges, Brahmaputra, Yellow, and Yangtze, fed the water demand of over 1.4 billion people. The people are likely to be affected under different scenarios of climate change (Imerzeel, W.W. et al., 2010). However, there is a conflict of expert opinion in the case of glacial melt of Karakorum-Hindu Kush (HKH) region. Initially, more runoff yield was predicted in this region because of increase in global temperature under different climate change scenarios (Akhtar, M, et. al., 2008). However, many studies that have analyzed the meteorological processors of this region came to different conclusions (Gosain, A.K., 2006 et. al.) from the pattern of retreat and thinning of the glaciers of Eastern Himalaya. In fact, the anomaly of thickening of Karakorum glaciers was reported (Julie, G. et. al., 2012). It is predicted that Indus and Brahmaputra are more prone to the reduction of discharges under the influence of climate change that may affect around 60 million people (Imerzeel, W.W. et al., 2010). In a study by Fowler, H.J. and Archer, D.R. (2005) the historical analysis of temperature trends indicated that the winter and summer

temperatures of UIB are increasing and decreasing respectively. Where, the verification of trend in meteorological parameters could be verified by analyzing the catchment response that occurs in the form of runoff. This study focused on the investigation of historical discharges of main stem of Indus River that drains the major part of Upper Indus Basin. Descriptive statistical checks are applied to estimate the mean and deviation from the mean on seasons of different time intervals. A long-term trend in the inflow data is explored by applying various statistical techniques.

Characteristics of Upper Indus Basin (UIB)

The Indus River emerges from the Tibetan Plateau and travels initially east to west and then north to south descending from above 5500 m to the mean sea level before emptying into Arabian Sea. The Indus basin mainly fall in the category of semi-arid to arid region, where, the excess moisture is available in the UIB located in the region of northern Pakistan ranging up to China in the east and Afghanistan in the West. The HKH range runs from west to east in an arc with Hindu Kush in the west and the main Himalayan chain in the south east. Where, the central Karakorum region, hosting much of the glaciers, is contributing the major portion of Indus flows (Young, G.J. and Hewitt, K., 1988). In UIB, the Indus River is mainly contributed by the flows from two set of sub-basins; 1) the northern sub-basins includes Hunza River that travel south-west, whereas, the Gilgit River moves in from the North-Western side and merge into Hunza River near Gilgit city, 2) the eastern sub-basins comprises of Shyok River which combines with River Indus, in which Shigar River add its share of flow before Katchura gaging site, after which this confluence move towards north-west and is joined by the consolidated flow coming from the northern sub-basins between the gaging sites of Partab Bridge and Alam Bridge. This combined discharge in Indus River from the northern and eastern sub-basins is later joined by the contributions from the Astore River and Gorband River from its left and right side respectively, before entering into the Tarbela storage. Where, the flow from the Siran River directly enters into the Siran Pocket in the Tarbela Reservoir.

Indus River accounts for approximately 90% food production and 13 GW of hydroelectricity generation in Pakistan (Cook, E.R., et al., 2013). Due to high altitude, most of the precipitation occurs as a snow in this region. The outcome is extensive glaciation in the Indus basin with total covered area of 16,300 km² (Faran Ali and De Boer, 2003), where, around 13000 km² of this

glaciated area is located within Pakistan (Mercer, 1975). More than 80% of total flow of the UIB is contributed from less than 20% of its total area. This area mainly includes heavy snowfall zone and glaciated basins above 3500 m elevation (Hewitt, K. et al., 2017). There are thousands of glaciers in the Karakorum region with 23 bigger glaciers accounting for about 60% of total glacier areas (Young, G.J. and Hewitt, K., 1988). It is one of the largest glaciated areas outside the polar ice belt. The glaciers of Himalayan-Karakoram region contain huge amount of frozen water storage. The temperature rises in the late spring to early summer initialized the melting of snow in the mountains that reaches to the maximum in mid-summer months. The salient features of distinct hydrological regimes of UIB has been investigated by Archer (2003) and presented three kinds of controls that are responsible for Indus flow; summer temperatures, winter & spring precipitation, and summer monsoon rainfall. Young, G.J. and Hewitt, K. (1988) reported that snow and ice melt is responsible for about 80% of flow for the main stem of Indus above Tarbela. Where, in the years of heavy winter snowfall followed by cool summer, the glaciers grow in size and vice versa.

The Tarbela dam, commissioned in 1976 with gross storage capacity of 11.62 MAF, is situated at the main stem of Indus River at a distance of 1126 km from its source. The historical record indicates that it received the annual runoff of 45 MAF to 82 MAF in dry to wet year with an average of 61 MAF from the drainage area of 169645 km². The installed hydro-electric power generation capacity of 3478 MW will be increased to 6928 MW after the completion of fourth and fifth extension projects. Where, the one third of live storage capacity of the Tarbela reservoir has been lost due to siltation. The operational rule curves of releases from the Tarbela are based on future water availability estimates and the crop water demand of the Irrigation system in combination with auxiliary demand for hydroelectric power generation.

Descriptive Statistics and Trend Analysis of Indus flows at Tarbela

The inflows of Indus River at Tarbela are normally calculated on the basis of volumetric mass balance of inflow, outflow & change in storage with the help of rating curve of Tarbela that is updated from time to time. Where, the data before the Tarbela dam may have been obtained from the nearby gage to compile one monolithic data series. The historical daily discharge data of Indus at Tarbela from 1961-62 to 2010-11 from Water and Power Development Authority

(WAPDA) is used in the descriptive statistical analysis of univariate time series. The 50-year data is organized into volumetric discharges of following time intervals: 10-daily, seasonally (Rabi Season: Oct-Mar and Kharif: Apr-Sep), annually (hydrologic year: Apr-Mar) and 10-yearly in order to investigate the characteristics of flow for shorter, mid-term and longer duration. In the statistical analysis of the discharges the center (mean and median), terminal limits (maxima, minima) variability from the mean (standard deviation and Coefficient of Variance) and the trend is determined. Conventional non-parametric Mann Kendall (MK) Test is used to check the trend in data. Before applying the test, the data is checked for the presence of serial correlation by computing sample Pearson correlation coefficient (r) by using Eq-1:

$$r = \frac{\sum(q_i - \bar{q}_i)(q_{i+1} - \bar{q}_{i+1})}{\sqrt{\sum(q_i - \bar{q}_i)^2 \sum(q_{i+1} - \bar{q}_{i+1})^2}} \quad (1)$$

The presence of serial correlation can be tested for any confidence interval, say 95% in this case by using two tailed tests as under:

$$r(95\%) = \frac{-1 \mp 1.96\sqrt{(n-2)}}{(n-1)} \quad (2)$$

If the serial correlation coefficient for the discharge data series fall within the interval computed by Eq-2, than the data is serially correlated, hence, the pre-whitening has to be conducted before applying the MK test.

Where, the Mann Kendall Test assumes that variable under consideration is function of time as under:

$$q_i = f(t)_i + \epsilon_i \quad (3)$$

In the Eq-3, q is any variable, discharge in this case, of i th time that is dependent upon time with a residual, ϵ_i .

As per basic concept of statistics, two hypotheses are considered, Null (H_0) and Alternate (H_1). Where, the Null hypothesis states that there is no trend in data and alternate hypothesis indicates otherwise. The S and Z statistics of MK Test indicate the trend and significance level of the trend in the data.

The MK test is applied by using the procedure illustrated in various studies (Kendall, M.G., 1975; Ahmad, I. et. al., 2014; Salmi, T. et. al. 2002). The S value computations are based on pairing the first data point in the series with all the subsequent data points and the process is repeated for the next data point pairing with all subsequent points in the series. The signs,

positive and negative, are the results of each difference of pair that are summed separately. The process is repeated in a special array as per sequence given in Eq-4. Refer to Eq-4 & 5; the net result of all the positive and negative numbers counts indicates whether there is negative or positive trend in the data. The positive S and Z value indicate positive trend and vice versa.

The S value in MK can be computed as:

$$S = \sum_{i=1}^{n-1} \sum_{j=i+1}^n \text{sig}(q_j - q_i) \quad (4)$$

$$\text{Sgn}(q_j - q_i) = \begin{cases} +1 & \text{if } (q_j - q_i) > 0 \\ 0 & \text{if } (q_j - q_i) = 0 \\ -1 & \text{if } (q_j - q_i) < 0 \end{cases} \quad (5)$$

Where, q_i and q_j are the discharge data values in year i and j , and $j > i$. And n shows the total number of values in the dataset. As the n values in this case were greater than 10, therefore normal approximation test is used. But prior to that the Variance of S is computed to take into account the effect of tied (equal) values in the data series as they reduce validity of normal approximation

The variance S of data series is computed by Eq-6

$$\text{Var}(S) = \frac{1}{18} [n(n-1)(2n+5) - \sum_{p=1}^m t_p(t_p-1)(2t_p+5)] \quad (6)$$

Where, m is number of tied groups and t_p is the number of ties for p^{th} values. The Z statistics can be computed as:

$$Z = \begin{cases} \frac{s-1}{\sqrt{\text{Var}(S)}} & \text{if } S > 0 \\ 0 & \text{if } S = 0 \\ \frac{s+1}{\sqrt{\text{Var}(S)}} & \text{if } S < 0 \end{cases} \quad (7)$$

In order to test the trend, the following two tailed tests is applied:

$$H_0 \text{ is rejected if } |z| > |Z_{1-\alpha/2}| \quad (8)$$

$$H_0 \text{ is accepted if } |z| < |Z_{1-\alpha/2}| \quad (9)$$

Where, α indicates the significance level. The trends in the discharge data series of different time intervals is tested with α ranging from 0.1 to 0.001.

After trend analysis the best fit linear line is plotted with least squared error optimization in

the scatter plot of discharge time series and their respective time dependent equations are developed. The equation of straight line is used to plot the trend line:

$$q_i = \beta(t_i) + C + \epsilon_i \quad (10)$$

The coefficient of determination (R^2) is used as an objective function to reach the best fit regression line as under:

$$R^2 = 1 - \frac{SS_{res}}{SS_{tot}} = 1 - \frac{(q_i - \hat{q}_f)^2}{(q_i - \bar{q})^2} \quad (11)$$

Where,

q_i = observed discharges

\hat{q}_f = discharge estimates by the best fit linear regression line

Where, the residual ϵ_i is not further treated and the deterministic part of Eq-10 is used to estimate the discharges.

Further, the Weibul distribution (Eq. 12) is used to calculate the exceedance probability of discharges against the percent of time for plotting the flow duration curves of 1st and the last decade of available data series.

$$P = \left[\frac{M}{(n+1)} \right] * 100 \quad (12)$$

Where,

P = the probability that a discharge will be equaled or exceeded (% of time)

M = the ranked position

n = the number of events

Results and Discussion

The mean and median plot of 10-daily discharges of Indus at Tarbela, as shown in Fig-1, indicates

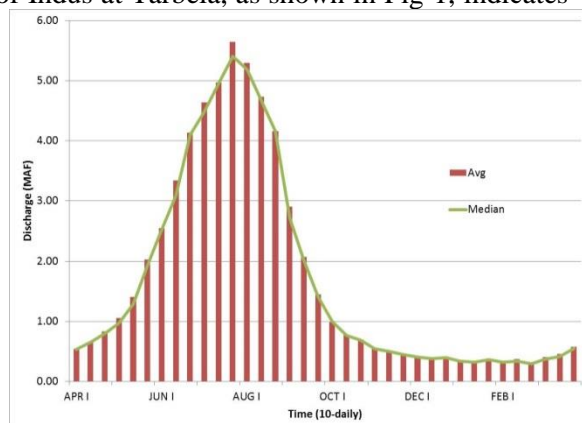


Fig. 1 Mean and Median of 10-daily flows of Indus at Tarbela

However, the flow range widened in the Kharif months and reaches to maximum width in the late June and remains wide till 2nd 10-daily of August but after that it starts shrinking till end of

that the flows start rising in the month of March, possibly due to early snow melt, and reach the peak by end of July by which time the summer rainfall add into snow melt from the glaciers of UIB. After hitting the peak, the discharges recede gradually till end of August. From September onwards, the receding in flows increases sharply, because the summer monsoonal rainfall dries up and temperature in the high altitude start decreasing, till they hit the base flows in November. The base flow period remains steady till the end of February. The mean and median, both are the indicator of data center, the perfect overlapping of these values reflect un-biasness in the data, however, the outlier or occurrence of extreme values lead mean-median mismatch as it can be seen in peak flow months of July and August.

In general, the discharges of snow-fed rivers show strong seasonality with high flows in hot summer months and low flows to no flows in cold winter months. The seasonal flow variations from year to year are the outcome of variations in inter-annual meteorological forcing especially the degree day temperature or radiation etc. Whereas, in the mixed fed rivers, the occurrences of rainfall result in additional variability in the flow pattern. The plot of minimum, average and maximum flows on 10-daily basis from the available record of 50 years starting from year 1961-62 in Fig-2 shows that there is quite narrow range between minimum and maximum flows in the Rabi season.

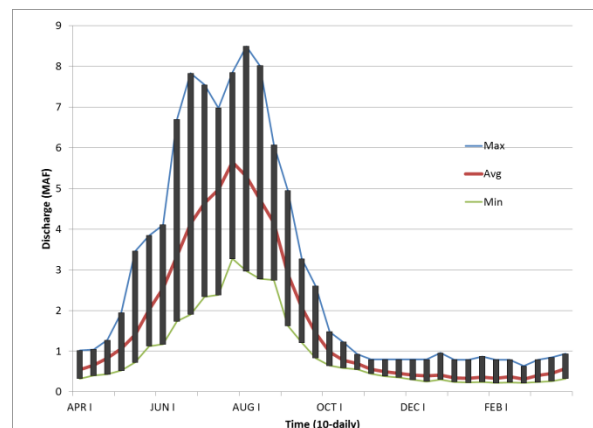


Fig. 2 Minimum and maximum 10-daily flows of Indus at Tarbela

October. The huge fluctuations of flow in June, July and August could be attributed to several reasons, albedo affect in the late snow and glacial melt coupled with the variability in rainfall

received in the monsoon months. The low snow melt together with scarce rainfalls ends up in low flows and vice versa. However, the top and bottom range are based on historical minimum and maximum 10-dailies and that does not necessarily mean that they occur in the same year. The flows in any one 10-daily can be strongly affected by short term weather conditions. Consequently, it is quite possible that one 10-daily receive less than average inflow and the subsequent one more than average flows and vice versa.

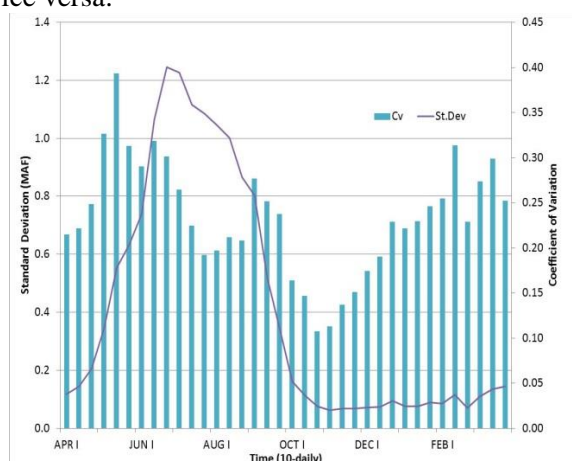


Fig. 3 Standard deviation and coefficient of variation of 10-daily Indus flow at Tarbela

The variation of discharges around the mean is best captured by the standard deviation. However, since the standard deviation is dependent upon the magnitude of the mean, therefore, the data with high mean values ends up in large standard deviation magnitudes and vice versa. Whereas, the coefficient of variation is a unit-less quantity which indicate the deviation in relation to the magnitude of mean values. As anticipated, the shape of standard deviation curve of mean 10-daily discharges of Tarbela, as presented in Fig-3, is similar to the shape of mean discharges curve as shown in Fig. 1. However, the coefficient of variation is better representing the variations in flows with respect to mean discharges. Unlike, the curve of mean and standard deviation, the plot of Cv is multimodal with at-least three defined peaks occurring in the month of May, September and February-March. Where, the highest coefficient of variation is 40%

of the mean value that occurred in September. The peak Cv in May, September and February may be attributed to the fluctuations in late snow and glacial melt, occurrences of summer rainfall and early snowmelt respectively.

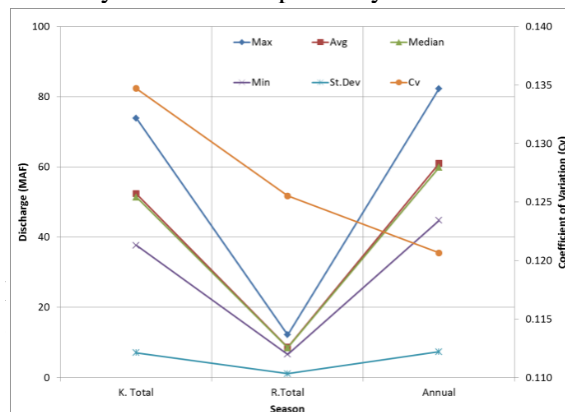


Fig 4. volumetric discharges and its fluctuations

Fig. 4 Normally, the volumetric discharges of long time durations show less fluctuations, however, it is different in the case of Indus. Historical Rabi, Kharif and annual flow characteristics of Indus at Tarbela are plotted in The maximum recorded Kharif Season and annual flows are double than the corresponding minimum flows. Whereas, the minimum recorded flows in Rabi season are 2/3rd of the maximum recorded flows of Rabi. However, the coefficient of variation is less in the annual data series in comparison to Kharif and Rabi flows that is in according to the general principle of less variation in the averages or sums of longer time intervals.

The MK tests are applied separately for individual 10-dailies and on seasonal and annual basis. The results are given in Table-1. The Z-statistics indicate the direction of trend. The significance of trend is mentioned in the separate column, where the notations like +, *, **, *** indicates significance level at 90%, 95%, 99% and 99.9% respectively. In the Kharif season, a significant positive (rising) trend is noted in the month of May, whereas, a non-significant negative (falling) trend is observed from June to September. MK test of overall Kharif season resulted in non-significant negative trend.

Table 1 Results of Mann Kendall (MK) Test

Time series	Test Z	Significance	Time series	Test Z	Significance
APR I	2.5	*	OCT I	0.4	
APR II	0.8		OCT II	1.0	
APR III	1.0		OCT III	0.8	

MAY I	2.7	**	NOV I	2.2	*
MAY II	3.8	***	NOV II	3.6	***
MAY III	2.7	**	NOV III	4.2	***
JUN I	-0.6		DEC I	3.0	**
JUN II	-1.2		DEC II	2.4	*
JUN III	-1.1		DEC III	3.2	**
JUL I	-1.0		JAN I	2.0	*
JUL II	-1.5		JAN II	2.0	*
JUL III	-1.0		JAN III	2.0	*
AUG I	-0.5		FEB I	3.4	***
AUG II	-1.0		FEB II	2.5	*
AUG III	-1.3		FEB III	3.4	***
SEP I	-0.7		MAR I	2.9	**
SEP II	-1.0		MAR II	1.7	+
SEP III	0.8		MAR III	2.6	**
Kharif Season	-0.8		Rabi Season	3.6	***
Annual	-0.2				

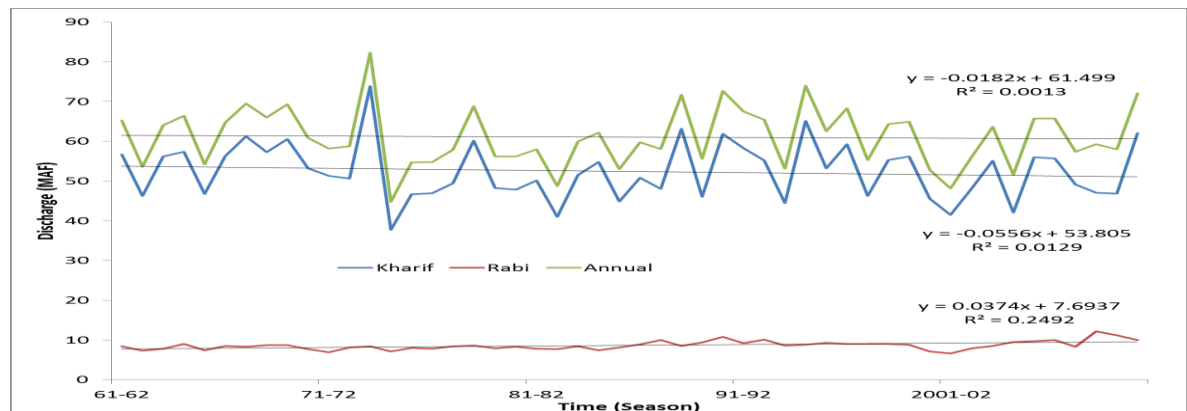


Fig. 5 Fitting best fit trend line in seasonal flows Indus at Tarbela

The analysis revealed a positive trend in all the 10-dailies of Rabi season. A very significant positive trend is noted in the months of November, December and February. Where, the months of January and March also show increasing trend with reasonable significance level. The outcome of MK test indicates overall significantly positive trend is in the bulk Rabi season flows. Where, the annual series has shown slightly negative trend.

Fig-5 presents the Rabi, Kharif and annual volumetric discharge of Indus from year 1961-62 to year 2010-11. The trend line and respective straight-line equation show slight negative trend in annual and Kharif season flows, whereas, a visible positive trend can be observed in the Rabi season flows.

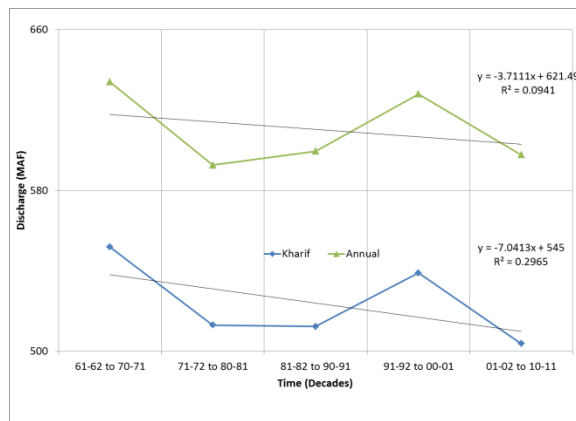


Fig. 6a Trend of decadal accumulative volumetric discharges of Indus at Tarbela for annual values and Kharif season.

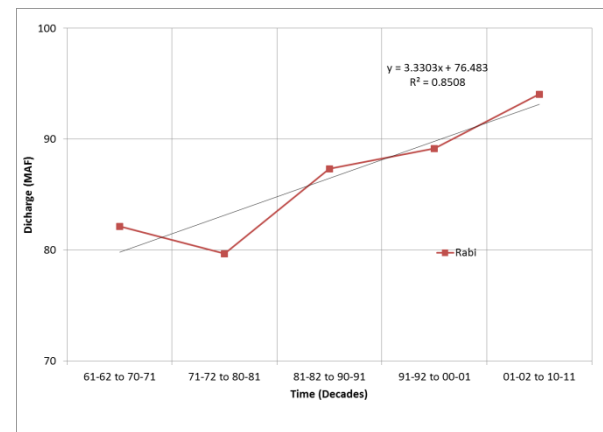


Fig. 6b Trend of decadal accumulative volumetric discharges of Indus for Rabi season

In order to further investigate the seasonal and annual trends, the seasonal discharge volumes are added per decade in chronological order to smoothen the yearly variations in the seasonal volumes. Plot of 10-yearly sum of Kharif and annual discharge volumes of 5 decades is given in Fig-6a. The trend line indicates strong downwards trend in Kharif flows with coefficient of determination of 0.3. However, the coefficient of determination of trend line for 10-yearly accumulative discharge volumes is relatively small, i.e. 0.01. The plot of 10-yearly accumulative volumetric discharges for Rabi season, as presented in Fig-6b, shows very strong rising trend with a significant high R^2 value, i.e. 0.85. This rising trend of winter flows of Indus at Tarbela endorses the findings of the study by Fowler, H.J. and Archer, D.R. (2005) in which it is stated that winter temperatures of UIB are rising which lead to increase flows in winter. Similarly, the sinking of mean summer temperature in UIB as reported Fowler, H.J. and Archer, D.R. (2005) are in harmony with the results of current study as the estimated decreasing summer temperature consequently results in reduced flows in Kharif due to less

snow melt, which is the finding of this study. These results further agree with the findings of study conducted for swat basin, a sub-basin of UIB, by Ahamd, I. et. al. (2014). The impact of decade wise reduction in flows is further explored by comparing the flow duration curves of yearly discharges of 1st (1961 to 1970) and the last decade (2001- to 2010) in the available data series as shown in Fig-7. The log-scale of y-axis indicates the sharp reduction of discharge from 1st to last decade against almost all the exceedence probabilities.

Conclusion

The descriptive statistical analysis of 10-daily discharge data series of 50 years from 1961 to 2011 revealed that on the average discharges varies from 09 to 52 MAF in yearly cycle from Rabi to Kharif season respectively. The means are slightly higher than median discharges, especially, during the peak season which indicates the occurrence of high magnitude peaks.

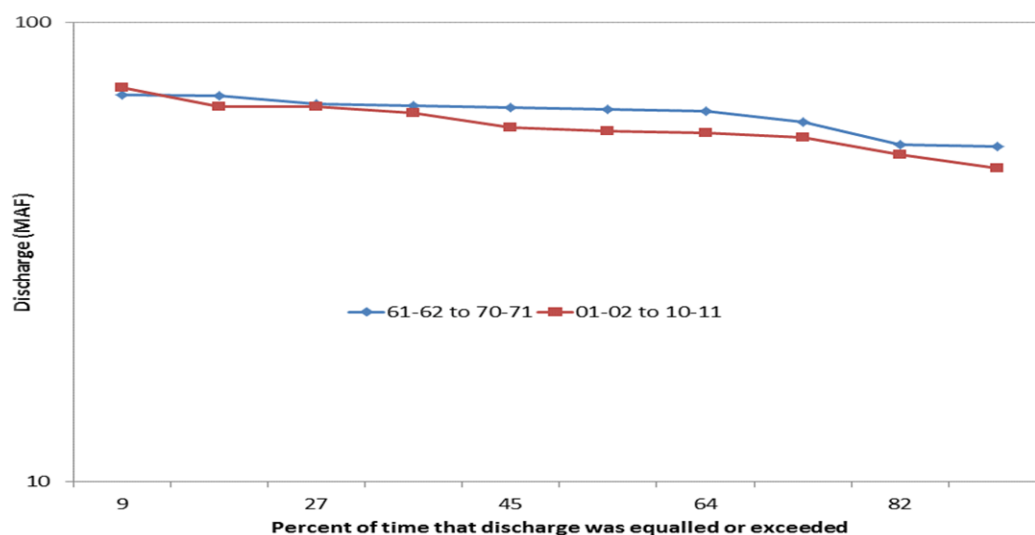


Fig. 7 Flow duration curve for the decade: a) 1961 to 1970, b) 2001 to 2010

The coefficient of variations of 10-daily data indicated, three peaks in the yearly cycle, that occurred in the months of May (0.39), September (0.28) and Feb-Mar (0.31). High Cv in these months owes to the variations in the performance of local meteorological processors responsible for early snowmelt, late glacial melt and end summer season rainfalls in UIB.

High inter-annual variations are apparent from the fact that maximum recorded flows are twice as much the minimum flows. Same pattern is observed in the Kharif flows. However, there is slightly less variation in Rabi flows with the minimum flows are 30 % lesser than the maximum flows. The implications of occurrence of dry year with total annual flows reducing down to 45 MAF may strictly constraints the ability of the system to meet the annual water demand especially in the absence of carry over dam.

The test results of MK verified the upward trend in Rabi flows and downward trend in Kharif and consequently annual discharges which may results in continuous reduction in the capacity of the system to meet annual water demand. Where, the magnitude of reduction has been estimated by running the trend line in the seasonal and annual discharge series. However, low coefficient of determination (R^2) caused by the yearly scatter deter the author to use the trend lines equations for predicting the seasonal and annual flows. Therefore, the analysis was repeated on 10-yearly accumulated discharges. Evidently, the scatter reduced in the plot of accumulated discharges in large temporal increments. High R^2 (0.85) is observed in the equation developed for the linear trend line of Rabi flows, however, the coefficients of determinations for the equations

of accumulated Kharif and annual flows are comparatively small (0.3 & 0.01 respectively). Extrapolating the best fit trend line for the estimation of future discharges indicated that the flows of Rabi increase by 3 MAF (4%), whereas, the Kharif and annual flows decrease by 7 MAF (1.3%) & 4 MAF (0.6%) per decade respectively. The interesting fact is that around 50% reduction in the flows of summer is compensated by the increased winter flows. Since, no major anthropogenic activity has been seen in UIB that could affect the flow pattern; therefore, the trend in discharges could be attributed to the impacts of climate change.

The analysis of flow duration curves for 1st and last decade of discharges in the available data verify the reduction of discharge availability against various exceedance probabilities of time. The implication of these curves are important with respect to future operational rule curves of Tarbela, especially considering the matter in the context of continuous reduction of live storage of the reservoir and increased water demand from the reservoir for hydroelectric power generation at the completion of 4th and 5th extensions of Tarbela.

Acknowledgement

The Water and Power Development Authority, Pakistan is hereby acknowledged for the discharge data

References

- Archer, D., 2003: Contrasting hydrological regimes in the upper Indus basin, *Journal of hydrology*, 274, 198-210
- Akhtar, M., Ahmad, N. and Booij, M.J., 2008: The impact of climate change on the water

- resources of Hindukush-Karakorum-Himalaya region under different glacier coverage scenarios, *Journal of Hydrology*, 355, 148-163
- Ali, K.F. and Boer, D.H.D., 2003: Construction of sediment budget in large-scale drainage basins: the case of upper Indus River, Erosion prediction in un-gauged basins: Integrated methods and techniques (proceedings of symposium), IAHS Publ. Nr. 279, 206-215
- Ahmad, I., Tang, D., Wang, T., Wang, M. and Wagan, B., 2014: Precipitation trend over time using Mann-Kendall and Spearman's rho tests in Swat River basin, Pakistan, *Advances in Meteorology*, 2015, 1-15
- Cook, E.R., Palmer, J.G., Ahmad, M., Woodhouse, C.A., Fenwick, P., Zafar, M.U., Wahab and M. Khan, N., 2013: Five centuries of upper Indus river flow from tree rings, *Journal of hydrology*, 486, 365-375
- Fowler, H.J. and Archer, D.R., 2005: Conflicting signals of climate change in the Upper Indus Basin, *Journal of Climate*, 19, 4276-4292
- Gosain, A.K., Rao, S. and Basuray, D., 2006: Climate change impact assessment on hydrology of Indian river basins, *Current Science*, 90, 346-353
- Hewitt, K., Wake, C.P., Young, G.J. and David, C., 2017: Hydrological investigations at Biafo glaciers, Karakorum range, Himalaya; an important source of water for the Indus river, *Annals of glaciology*, 13, 103-108
- Immerzeel, W.W., Beek, L.P.H. V and Bierkens, M.F.P., 2010: Climate change will affect the Asian towers, *Science*, 328, 1382-1385
- Julie, G., Etienne, B. and Yves, A., 2012: Slight mass gain of karakoram glaciers in the early twenty-first century, *Nature geoscience*, 5, 322-325
- Khattak, M.S., Babel, M.S and Sharif, M., 2011: Hydro-meteorological trend in Upper Indus River basin in Pakistan, 46, 103-119
- Kendall, M. G., 1975: Rank Correlation Methods, Griffin, London, UK
- Mercer, J.H., 1975: Glaciers of the Karakorum, Mountain glaciers of the northern hemisphere, 1, 371-409
- Rasul, G., Chaudhry, Q. Z., Mahmood, A, Hyder, K. W., Dahe Q., 2011: Glaciers and Glacial Lakes under Changing Climate in Pakistan, *Pakistan Journal of Meteorology*, 8, 1-8
- Salmi, T., Maata, A., Anttila, P. Rouho-Airola, T. and Amnell, T., 2002: Detecting trends of annual values of atmospheric pollutants by the Mann-Kendall Test and Sen's Slope estimates – The excel template application Makesens, Finnish Meteorological Institute, 31, 1-35
- Young, G.J. and Hewitt, K., 1988: Hydrology research in the upper Indus basin, Karakorum Himalaya, Pakistan, Hydrology of Mountainous Areas, Proceedings of the Strbske Pleso workshop, IAHS Nr. 190, 139-152.

Scientific Evaluation of Water Footprint Methods for Hydropower Generation

F. Seemab¹, W. Sherani¹, M. Abbas¹, M.N. Alam¹, R. Farooq¹, Z. Ashfaq¹, M.A.U.R. Tariq^{1*}

^{1*}Capital University of Science and Technology, Islamabad

*atiq.tariq@yahoo.com

Abstract: *The water footprint has attracted interest as a standard that indicates the use of freshwater resources and its impacts. Although hydropower is most economical and environmental friendly, it also has a large water footprint per unit energy as compared to other sources. The methodology to quantify the water footprints of hydropower is in its preliminary stages. Currently, there are three developed methods namely WF1, WF2, and WF3. These methods have their own limitations but are widely used to calculate water footprint for different hydropower plants. The aim of this paper is to evaluate and perform a detailed systematic assessment of these water footprint methods for hydropower generation. The task includes the assessment of complexity and sensitivity of the involved factors, practical implications, as well as the accuracy and reliability along with the limitations that the method inherits. First two methods are based on the consumptive use, while the third considers input and output of the reservoirs. WF1 is a single parameter simple, and easy to measure method with reliable and consistent results. However, it grossly ignores the water losses due to evapotranspiration that might occur in the absence of reservoir, which is considered in WF2. The practical implications in measurement of evapotranspiration and the demarcation of the system boundary are the two biggest challenges for the WF2 that may arise the issues of accuracy, reliability and consistency of the results. WF3 accounts the net water balance by considering the water leaving and entering the surface of reservoir, namely the evaporation as output and precipitation as input. WF1 and WF2 results have always a positive value whereas WF3 can give negative value if the input is greater than the output which means the net water is surplus. The negative value of WF3 still requires physical based interpretation of WF of a hydropower project.*

Keywords: Water footprint methods, hydropower generation

Introduction

Water footprint is an indicator of use of water that measures the volume of water used to produce a product. It is mainly divided into two components i.e. water consumed during production and water polluted during production process. Water consumption refers to the water that is lost from the reservoir or from the available catchment area due to evaporation and evapotranspiration processes whereas water footprint refers to the water which is used for production of goods which are used by people. Water footprint is divided into three parts i.e. blue, green, and grey. The blue water footprint is an indicator of consumptive use of fresh surface water or groundwater. The term 'consumptive water use' refers to one these four cases: 1) Water evaporation, 2) Water incorporation into the product, 3) Water not returning to the same catchment area e.g. it is returned to sea 4) water not returning in the same period i.e. withdrawn in a scarce period and returned in a wet period. The blue water footprint measures the amount of water available in a certain period that is consumed (in other words, not immediately returned within the same catchment). The green water footprint is an indicator of the human use

of so-called green water. Green water indicates the precipitation on land that does not run off or recharge the groundwater but is stored in the soil or temporarily stays on top of the soil or vegetation. This footprint is the volume of rainwater consumed during the production process. It is mostly used in agriculture and forestry. The grey water footprint refers to the volume of water that is required to assimilate waste, quantified as the volume of water needed to dilute pollutants to such an extent that the quality of the ambient waste remains above agreed water quality standards. (Herath, Deurer, Horne, Singh, & Clothier, 2011) WFs can be assessed for different entities, for example, products, consumers, businesses, nations, or humanity.

Water is vital and essential for energy production. It is a hidden input for almost all types of power plants. It is used to grow biomass for bioenergy and in the extraction, processing, and transport of fuels for energy production. Energy and water are two critical and important necessities for modern world. Thermal power plants require a huge amount of cooling water and hydropower plants results in evaporative loss from large surface areas of the reservoirs (Lee, Han, Elgowainy, & Wang, 2017). The WF of

electricity refers to the water volumes consumed and polluted in the different stages of the supply chain of electricity. It is distinguished in three major stages in the production of electricity i.e. fuel supply, construction, and operation. The first stage is relevant only for fuel-based electricity (when electricity is based on coal, lignite, oil, gas, uranium, or biomass). In the other cases (hydro, solar, wind and geo-electricity), we only consider two production stages: construction and operation. There are three methods adopted for the calculation of water footprint of hydropower generation i.e. WF1, WF2, and WF3. (Herath et al., 2011)

WF-1: (consumptive water use)

In this method the water footprint can be calculated as the evaporative water loss from the surface of the reservoir divided by the energy produced by that hydropower plant (Herath et al., 2011)

$$WF1 = \frac{E_o}{P}$$

Here, E_o is the annual open-water evaporative loss from the reservoir (m^3) and P is the energy production of the power plant (GJ).

WF-2 (net consumptive approach)

The second approach also considers consumptive water use, but it compares the consequences of land use changes created by the dam. Building of a dam results in the replacement of vegetation by a free-water surface. Thus, evapotranspiration from the vegetation is replaced by open-water evaporation from the reservoir. Taking this into account, the WF-2 (m^3/GJ) considers the net evaporative water loss from the area occupied by the reservoir (Herath et al., 2011).

$$WF2 = \left(\frac{E_o - ET_c}{P} \right)$$

ET_c is the amount of water lost by evapotranspiration.

WF-3 (net water balance)

This moves beyond the simply consumptive use definition of the water footprint. A simple water balance was used to estimate the water footprint considering supply side of hydrology. WF3 accounts the net water balance by considering the water leaving and entering the surface of reservoir. The net water balance is calculated as:

Output – Input = Evaporation – Rainfall
So, WF3 is calculated as:

$$WF3 = \left(\frac{E_o - RF}{P} \right)$$

Where RF is the annual volume of rainfall falling on the reservoir (m^3) (Herath et al., 2011)

Problem statement

There is no well documented and accepted methodology to quantify the WF of hydroelectricity (Herath et al., 2011). However, there are three developed formulae to measure the water footprint. There is no consensus as to which method should be adopted as a standard (Coelho et al., 2017). These methods have their own limitations but are widely used to calculate water footprint for different hydropower plants. The aim of this paper is to investigate the detailed systematic assessment of these water footprint methods for hydropower generation.

Literature review

Hoekstra introduced the concept of water footprint in 2007. The three adopted methodologies of WF calculation have been used widely throughout the world for WF estimation. Gleick evaluated the gross consumption by plants in USA in the 90's. This method was conceptualized by Hoekstra in 2007 and is now known as WF1. WF2 was introduced because WF1 does not consider the situation before the dam. (Herath et al., 2011) worked on the case study of New Zealand and proposed WF3 stating that regional climatic conditions are not considered in the first two methods. Since, the introduction of WF3 it has been rarely used and thus has been used so far for only three model cases i.e. Brazil, Norway and New Zealand. WF1 and WF2 have been used widely by all the scientists. Hoekstra has used these two methods on 35 plants out of which 7 are in Brazil and 12 are in remaining Latin America. Furthermore, many others have used these two methods in different case studies of Austria, Egypt, China, Norway, New Zealand and many others (Coelho et al., 2017).

The parameters of evaporation, evapotranspiration, and rainfall will be taken from the nearest meteorological station to the reservoir. WF1 yields high values as compared to WF2 whereas WF3 can yield negative values if the amount of rainfall occurred on a reservoir is greater than the evaporation rate.

Methodology

The three methods normally used in WF calculation yields three different results. The aim is to evaluate scientifically that which method out of these is the most accurate, reliable, and easy to measure based on scientific parameters.

Theoretical legitimacy

WF1 follows the definition of water footprint given by Hoekstra and Chapagain (2007). Furthermore, it also follows the definition used by (Gerbens-Leenes, Hoekstra, & van der Meer, 2009) to estimate the WF of hydropower on global average basis. This method was suggested by (Mekonnen & Hoekstra, 2012) who used this method to estimate water consumption of hydropower plants. The method accounts the water consumed in the process under consideration. The second approach also considers consumptive water use, but it compares the consequences of land use changes created by the dam. A similar approach has recently been discussed in WF assessment of beer, and this was termed “net green water” loss (SABMiller, 2009). In the third method, the focus moved beyond the consumptive use. WF3 was developed to assess the hydrologically rational water footprint to quantify the influences of regional climatic conditions (Herath et al., 2011). WF1 and WF2 measure the consumptive use but pay no attention to supply side of hydrology which is accounted in WF3.

WF1 is controversial as it appears to be too simple by not considering the water lost by evapotranspiration before reservoir impoundment. WF3 was also criticized stating that the method simply indicates if the evaporation is greater than the precipitation on the reservoir surface divided by the power production. WF3 was further elaborated that this method is important for weighing the advantages and disadvantages of building a dam in a certain region (Bakken, Killingtveit, Engeland, Alfredsen, & Harby, 2013). Based on theory WF2 seems the most legitimate as it estimates the WF based on the condition before and after the construction of the reservoir.

Results comparison

WF1 results in larger values as compared to WF2 whereas WF3 also yields negative values when input is greater than the output. The negative value suggests that a reservoir has received more water as rainfall than they lost through evaporation. With reference to the results WF1 and WF2 are reliable and WF3 results seems unrealistic because negative value is unreliable and unacceptable (Herath et al., 2011).

Variability based on change in temperature throughout the year

The values of WF1 vary with respect to the evaporation and power production. The highest value of WF1 will be observed for the month/period in which evaporative loss is maximum,

and power production is minimum. WF1 will yield lower values for the opposite scenario. WF2 values can come close to WF1 if a period occurs where evapotranspiration before the construction of the dam was not significant. WF3 can yield negative values for the month in which there is large amount of rainfall (Coelho et al., 2017).

Sensitivity to Area

WF1 is most sensitive to reservoir area. The surface area of reservoir accounts for 38.6% percent variability of WF1. WF2 is not significantly sensitive to the reservoir area but WF3 is also sensitive to this parameter because it relates to the effectiveness of dam to collect rainfall. The major part of variability of WF1 and WF3 is due to local climate and reservoir area. But still there is an unexplained variability which may be due to the difference in efficiency of power generation (Herath et al., 2011).

Comparison between dams for Water efficiency

In the case of comparison between multiple dams, if the WF1 values of a dam results in lower values as compared to other dams than it demonstrates that it has higher water efficiency as compares to others. Similarly, in case of WF2 if the values are lower a dam in comparison to others than it has high water efficiency as compared to the others.

Sensitivity based on Region

For tropical regions, WF1 is not suitable for explaining the consumption because evapotranspiration values are high even before the construction of the dam. Thus, this method allocates excessive water consumption to hydropower generation that already existed before its implementation. This effect is minimized when applied to temperate regions where evaporation rates are low before construction of the dam. WF2 is more accurate than WF1 because it considers evapotranspiration into consideration which has a significant value for tropical regions as compared to temperate regions. The accuracy of WF2 is more than WF3 because the latter method does not consider the real consumption of water and also does not considers the evapotranspiration before the construction of the reservoir (Coelho et al., 2017).

Scientific Innovation

The study focuses on the criticality of each parameter involved in the evaluation of water footprint. Furthermore, complexity, the ease of measure, accuracy and reliability of results

obtained by these methods lies in the scope of this paper.

Limitation

This study ignores economic perspective and is focused only on water consumption. Among all methods, the deleterious impacts that the dam might have on the local ecosystem i.e. water scarcity is ignored because all three methods are focused purely on water quantity.

Result/Output

A scientific evaluation of the results obtained from the past studies are considered and compared to check the complexity, ease of measure, accuracy, and reliability of the methods and to devise the most appropriate method to be used for future calculations of WF. WF1 is too simplistic and follows the definition of Hoekstra but yields large values that appear to be unrealistic and unreliable whereas WF3 has not been backed by scientists and is found out to be region sensitive, because of these factors WF3 has not been widely used till now. WF2 appears to be the most accurate method because it compares the situation before and after construction of reservoir. This method is being theoretically and scientifically backed by many scientists like Bakken. Moreover, the method is not sensitive to the area and gives reliable results based on region.

Discussion

From water footprint perspective, it is advantageous to locate hydroelectric dams in wet regions where evaporation rate is low. Furthermore, the WF is also an indicator of water efficiency which will indicate the power generation capacity of a dam. Theoretically, WF2 is the soundest method because it compares the situation before and after construction. The values obtained by WF2 are reasonable and justifiable as both evaporation and evapotranspiration are obtained from meteorological stations and can be incorporated to evaluate water footprint. WF1 on the other hand yields large values which shows over estimation whereas WF3 can yield negative value which altogether seems absurd and inappropriate. The values of these three water footprints vary with temperature and change of climate throughout the year. In the case of dry climate, the values of WF1 are highest as compared to WF2 because the gross evaporation is greater than the net evaporation. The values of WF2 and WF1 can sometimes be approximately same for the months in which the evapotranspiration is almost negligible. For WF3 the values can appear

negative for those months in which the rainfall is greater than evaporation while it yields positive values during summer time as evaporation rate is very high in contrast to the precipitation.

WF1 and WF3 are sensitive to the reservoir area. If reservoir area increases then the rate of evaporation also rises. Hence evaporation increases which results in increase in water scarcity. This scarcity is found out by evaluating the water scarcity index. Water efficiency is the most important factor for evaluating the hydropower capacity of a reservoir. By evaluating the hydropower capacity of multiple dams, if it is found out that WF1 values of one dam is lower as compared to the remaining dams than this dam has greater water efficiency which means that evaporation rate is lower, or the power generation capacity of this particular dam is high. The power generation capacity is also dependent on the speed of spinning of the turbine.

The water footprint methods are region sensitive which means that in a region where evaporation is lower, and rainfall is higher, than in that region the WF3 values will appear negative but for tropical region the WF3 values will be unreliable as the evapotranspiration plays a significant role in such region. Similarly, for the case of temperate region where evapotranspiration is not that high as compared to other region, then in this case WF3 will yield reliable results but in this case results obtained by WF2 are also reliable.

Conclusion

WF1 and WF2 only considers the consumptive water use but not the supply side of hydrology which is accounted in WF3. WF1 and WF2 are inadequate to understand the impact of hydroelectric power generation on freshwater resource availability. Water related issues are highly local and WF3 shows sensitivity to it. The study also shows the effect of local climate differences and the surface area of the reservoirs on the water footprint calculated using different methods. The methods are still under development and needs further research and understanding of the concept to refine the evaluation techniques. All methods have their pros and cons, but detailed systematic assessment will help in proposing the most efficient method for hydropower evaluation. Based on theoretical understanding, complexity evaluation and reliability and ease consideration, WF2 seems to be the most reliable for the time being but still this method needs to be studied further to incorporate the precipitation in this method.

Recommendation

WF2 method does not include rainfall on the

reservoir and it needs research in future to incorporate precipitation in this formulation. Still there is no study to incorporate seepage losses in these methods. Detailed analysis is needed in future to incorporate seepage and ecosystem effects in all three methods.

References

- Bakken, T. H., Killingtveit, Å., Engeland, K., Alfredsen, K., & Harby, A. (2013). Water consumption from hydropower plants—review of published estimates and an assessment of the concept. *Hydrology and Earth System Sciences*, *17*(10), 3983-4000.
- Bakken, T. H., Modahl, I. S., Engeland, K., Raadal, H. L., & Arnøy, S. (2016). The life-cycle water footprint of two hydropower projects in Norway. *Journal of Cleaner Production*, *113*(Supplement C), 241-250. doi: <https://doi.org/10.1016/j.jclepro.2015.12.036>
- Bakken, T. H., Killingtveit, Å., & Alfredsen, K. (2017). The Water Footprint of Hydropower Production—State of the Art and Methodological Challenges. *Global Challenges*.
- Bueno, E. d. O., Mello, C. R. d., & Alves, G. J. (2016). Evaporation from Camargos hydropower plant reservoir: water footprint characterization. *RBRH*, *21*(3), 570-575.
- Coelho, C. D., da Silva, D. D., Sedyama, G. C., Moreira, M. C., Pereira, S. B., & Lana, Â. M. Q. (2017). Comparison of the water footprint of two hydropower plants in the Tocantins River Basin of Brazil. *Journal of Cleaner Production*, *153*, 164-175.
- Costa, L., & Neto, J. A. (2017). Proposal for a water resource management strategy model using the water footprint concept. *Brazilian Journal of Operations & Production Management*, *14*(3), 371-380.
- Egan, M. (2011). The Water Footprint Assessment Manual. Setting the Global Standard. *Social and Environmental Accountability Journal*, *31*(2), 181-182. doi: 10.1080/0969160X.2011.593864
- Gerbens-Leenes, W., Hoekstra, A. Y., & van der Meer, T. H. (2009). The water footprint of bioenergy. *Proceedings of the National Academy of Sciences*, *106*(25), 10219-10223.
- Herath, I., Deurer, M., Horne, D., Singh, R., & Clothier, B. (2011). The water footprint of hydroelectricity: a methodological comparison from a case study in New Zealand. *Journal of Cleaner Production*, *19*(14), 1582-1589.
- Lee, U., Han, J., Elgowainy, A., & Wang, M. (2017). Regional water consumption for hydro and thermal electricity generation in the United States. *Applied Energy*.
- Mekonnen, M., & Hoekstra, A. (2012). The blue water footprint of electricity from hydropower. *Hydrology and Earth System Sciences*, *16*, 179-187.
- Oel, P., & Hoekstra, A. (2010). The green and blue water footprint of paper products: Methodological considerations and quantification.
- Pahlow, M., Snowball, J., & Fraser, G. (2015). Water footprint assessment to inform water management and policy making in South Africa. *Water SA*, *41*(3), 300-313.
- Papadopoulou, M., Charchousi, D., Tsoukala, V., Giannakopoulos, C., & Petrakis, M. (2016). Water footprint assessment considering climate change effects on future agricultural production in Mediterranean region. *Desalination and Water Treatment*, *57*(5), 2232-2242.
- Scherer, L., & Pfister, S. (2015). Water scarcity footprint of selected hydropower reservoirs.
- Scherer, L., & Pfister, S. (2016). Global water footprint assessment of hydropower. *Renewable Energy*, *99*(Supplement C), 711-720. doi: <https://doi.org/10.1016/j.renene.2016.07.021>
- SABMiller, W. (2009). Water footprinting: identifying & addressing water risks in the value chain. *SABMiller, Woking, UK, and WWF-UK, Goldalming, UK*.
- Chavez-Rodriguez, Mauro F., Silvia, A.N., 2010. Assessing GHQ emissions, ecological footprint, and water linkage for different fuels. *Environmental Science and Technology* *44*, 9252-9257.
- Zhou, Y., Hejazi, M., Smith, S., Edmonds, J., Li, H., Clarke, L., Calvin, K. and Thomson, A., 2015. A comprehensive view of global potential for hydro-generated electricity. *Energy & Environmental Science*, *8*(9), pp.2622-2633.
- Abbasi, S.A. and Abbasi, N., 2000. The likely adverse environmental impacts of renewable energy sources. *Applied Energy*, *65*(1), pp.121-144.
- Yu, B. and Xu, L., 2016. Review of ecological compensation in hydropower development. *Renewable and Sustainable Energy Reviews*, *55*, pp.729-738.
- Van der Ent, R.J., Savenije, H.H., Schaeffli, B. and Steele-Dunne, S.C., 2010. Origin and fate of atmospheric moisture over continents. *Water Resources Research*, *46*(9).

- Fthenakis, V. and Kim, H.C., 2010. Life-cycle uses of water in US electricity generation. *Renewable and Sustainable Energy Reviews*, 14(7), pp.2039-2048.
- Hammond, G.P., 2006, February. 'People, planet and prosperity': The determinants of humanity's environmental footprint. In *Natural Resources Forum* (Vol. 30, No. 1, pp. 27-36). Blackwell Publishing Ltd.
- Hertwich, E.G. and Peters, G.P., 2009. Carbon footprint of nations: A global, trade-linked analysis. *Environmental science & technology*, 43(16), pp.6414-6420.
- Torcellini, P.A., Long, N. and Judkoff, R., 2003. Consumptive water use for US power production.
- Döll, P., Fiedler, K. and Zhang, J., 2009. Global-scale analysis of river flow alterations due to water withdrawals and reservoirs. *Hydrology and Earth System Sciences*, 13(12), pp.2413-2432.
- Postel, S.L., 2000. Entering an era of water scarcity: the challenges ahead. *Ecological applications*, 10(4), pp.941-948.
- Matthews, H.S., Hendrickson, C.T. and Weber, C.L., 2008. The importance of carbon footprint estimation boundaries.
- Druckman, A. and Jackson, T., 2009. The carbon footprint of UK households 1990–2004: a socio-economically disaggregated, quasi-multi-regional input–output model. *Ecological economics*, 68(7), pp.2066-2077.

Evaluation of Suitable Design Flood Frequency Approaches for Hydropower Structures on the Mountainous Rivers (A Case Study of Upper Indus Basin)

Muhammad Yaseen^{1*}, Ijaz Ahmad², Bilal Nasir¹, Muhammad Imran Azam³, Muhammad Hassan Rehman², Muhammad Afzel²

¹Centre for Integrated Mountain Research, University of the Punjab, Lahore, Pakistan

³Centre of Excellence in Water Resources Engineering, University of Engineering and Technology, Lahore 54890, Pakistan

²College of Hydraulic and Environmental Engineering, China, Three Gorges University, Yichang 443002, China

*yaseen.cimr@pu.edu.pk

Abstract: The proper assessment of design flood is a major concern for many hydrological and hydraulic applications in mountainous watersheds. A number of statistical approaches can be used; however, each method has its own limitations and assumptions being applied to the real world. The aim of this study is to evaluate the most suitable design flood frequency approaches in the mountainous watersheds of Upper Indus Basin (UIB), Pakistan. Different flood frequency approaches i.e. Gumbel, Weibull, Normal, Lognormal, Lognormal Type 3, Pearson Type 3 and Log Pearson Type 3 were applied at 33 stream gauges of 21 watersheds in UIB. These approaches were evaluated by the chi-square test. Log Pearson-III frequency distribution showed good results with minimum chi-square test value on 30 stream gauging stations as compare to Gumbel distribution.

Keywords: Flood frequency analysis, Indus River basin, distributions

Introduction

Reliable estimates of extreme flood events are required for the design and operation of vital infrastructures and also for more general flood risk management and planning. This information is generally obtained through the use of flood frequency estimation techniques. These techniques are based upon the principle of statistical analyses of series of observed flood events, providing estimates of the likely magnitude of future extreme events through extrapolation.

The Indus River is the main river tributary in which most of the smaller streams originating from mountainous areas of Himalayas of Baltistan, Pakistan. The Indus River provides a major source of water for agriculture and hydropower. Due to lot of human activities in the inundation plain, it becomes important for the protection of floods. Some of the structures are constructed by human to control floods are levees, reservoir and channel improvement. For an economic and efficient design of these measures, flood has been estimated with particular level of accuracy. Maximum or peak flood can be estimated which may occur in a particular site; an ideal solution can then be proffered by a hydraulic Engineer (Haan, 1977).

The flood discharge adopted for the design of hydraulic structures while putting economic and hydrological factor into consideration is known as design flood and as it (design flood increases), the cost of the structure decreases but there will be a reduction in the probability of yearly damage. It is of great importance to select a design flood, which is unlikely to occur during the design life of a hydraulic structure and difference between the design return period and the estimated life of the structure should be quite large. Large return period of hydraulic structure (spillway of dams) is taken to reduce hazard of failure (Izinyon and Igbino, 2011).

Frequency analysis is a procedure for estimating the frequency of occurrence or probability of occurrence of the past or future events. A number of approaches can be used including statistical approach and the continuous simulation and design storm methods. However, each method has its own limitations and assumptions being applied to the real world. Statistical approaches (Gumbel, Weibull, Normal, Lognormal, Lognormal Type 3, Pearson Type 3 and Log Pearson Type 3) were used to determine the inaccuracy of data as well as design flood for particular site. Reliable flood frequency estimates are essential for flood plain management, protection of public infrastructure,

cost reduction of food related matters to government and private enterprises, for assessing hazards related to the development of flood plains and epidemic control (Tumbere, 2000). In order to ensure safety and economic hydrologic design in the catchment area, the Gumbel distribution, a stochastic generating structure that produce random outcomes was used to model the annual peak discharge data of Indus basin. Not only the river has its prime importance in the river basins of Pakistan but also has the gratitude among the biggest rivers in the world. In addition, the country has an agro based economy with arid or semi-arid climatic conditions. Therefore, accurate estimates of flood magnitudes become an important part of the design and operation of water resource systems, land use planning and management, flood insurance assessment and protection of inhabited areas, etc.

The paper presents results of flood frequency analysis of annual maximum peak (AMP) flows observed at 33 stream gauges of 21 watersheds in UIB. Present study estimates the occurrence exploration of Indus basin gauging stations. On the basis of our analysis, we find out flood quantity on any return period.

Description of study area

Present study was carried in the Upper Indus Basin (UIB). The catchment of this basin falls in range 33° 40' to 37° 12' N latitude and 70° 30' to 77° 30' E, longitude. The Upper Indus basin boundary was derived from Digital Elevation Model (DEM) just upstream of Massan as shown in Fig.1. Most of area of this catchment is lies in China and India. Due to unavailability of data from China and India, the study area was confined to the catchment falling within Pakistan boundary as shown in Fig.1. The elevation varies from 254 m to 8570 m above mean sea level. There are so many rivers which contribute water to main Indus River.

The important sub basins are Chitral, Swat, Kabul, Hunza, Gilgit, Astore, Shigar, Shyok, Kunhar, Neelum, Kanshi, Poonch, Soan, Siran, Sil, Haro etc. Indus River originates from the north side of the Himalayas at Kaillias Parbat in Tibet having altitude of 18000 feet.

Material and Methods

Stream flows measurement of UIB is carried out by the Water and Power Development Authority—Surface Water Hydrology Project (WAPDA-SWHP) with the earliest records commencing in 1960. The stream gauges have a wide range of drainage area from 262 km² to

286,000 km² (see Figure 2). The study area contained three major basins namely Jhelum, Indus and Kabul. There were 21 sub-basins in all these three basins. The stream flow gauges are installed at all the sub-basins of Upper Indus Basin on different locations are shown in Fig.1. The flow data of these sites will be collected from Surface water Hydrology Project (SWHP), WAPDA for the period 1961-2012. The geographical distribution of these stations is shown in Fig. 1. Characteristics of these selected gauging sites are given in Table 1.

Determination of the frequency of occurrence of extreme hydrologic events is very important in water resources planning and management. Frequency analysis was done by using HyfranPlus tool with applying the Gumbel, Weibull, Normal, Lognormal, Lognormal Type 3, Pearson Type 3 and Log Pearson Type 3 distribution. One of the most commonly used tests for goodness of fit of empirical data to specified theoretical frequency distributions is the Chi-Square Test. This test makes a comparison between the actual number of observations and the expected number of observations (expected according to the distribution under test) that fall in the class intervals. Expected numbers of observations are calculated by multiplying the expected relative frequency by the total number of observations. The chi-square test value was calculated by the following equation.

$$X_C = (O - E)^2 / E$$

Where

O=observed Values

E=Expected Values

The expected frequencies are computed on the basis of a hypothesis. If under the hypothesis the computed value of X_C is greater than some critical value. This test is called Chi-square test of hypothesis. If chi-square results well enough for all distribution than we select distribution having least chi-square value.

Results and discussions

Table 2 presents the summary of chi-square test results values for different distributions applied at different gauging stations of Upper Indus Basin. The chi-square test value helps in selection of suitable frequency distribution, the chi-square test value should be less than 12 (C.T.Haan). However, if the values of Chi-square test for more distributions remain below or equal to 12 then the distribution with relatively lowest value of test is selected. Table representing the chi-square Test results for Gumbel and Log Pearson-III

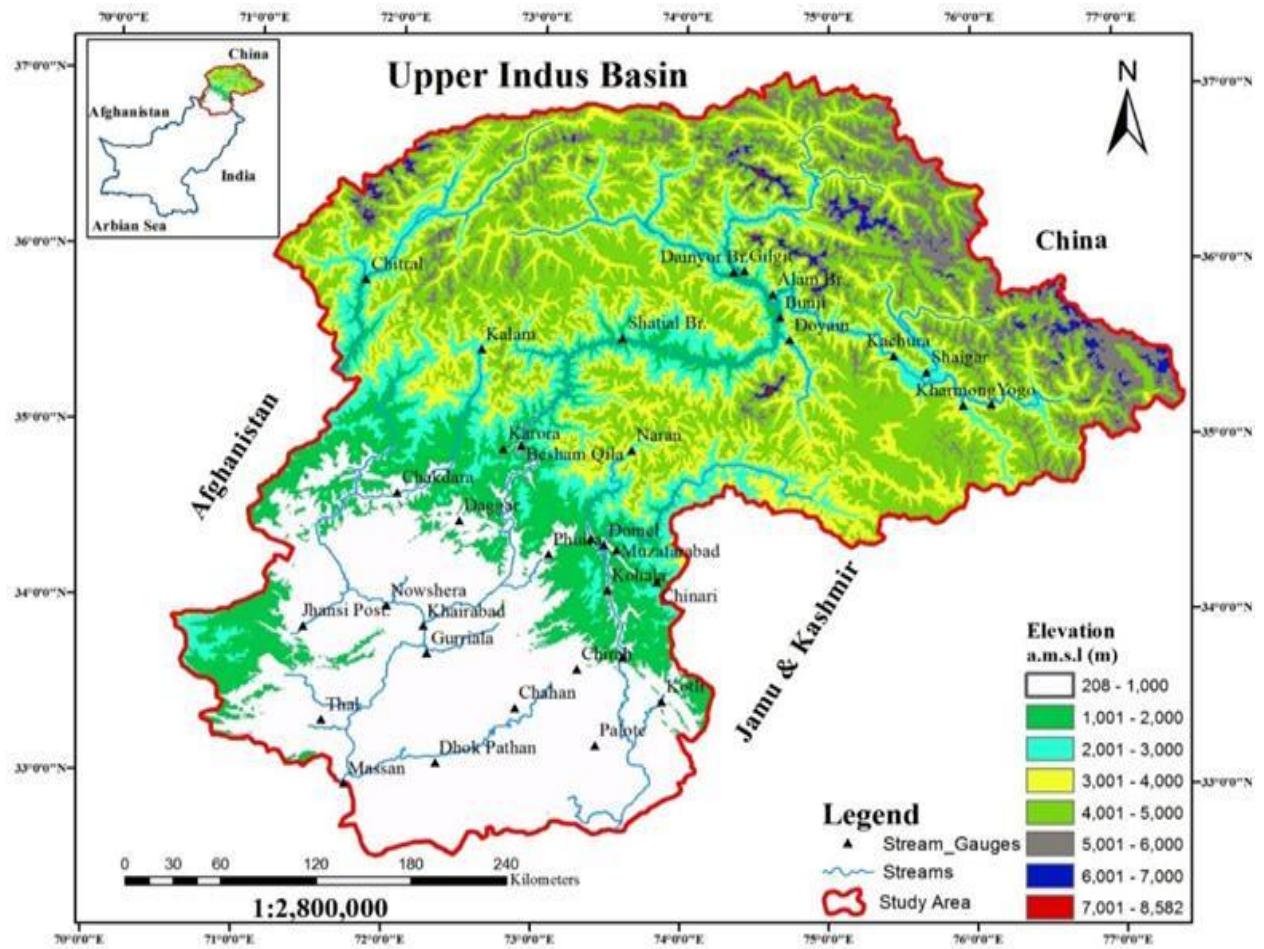


Fig. 1: The Upper Indus Basin confined in Pakistan boundary showing rivers, stream gauges and elevation.

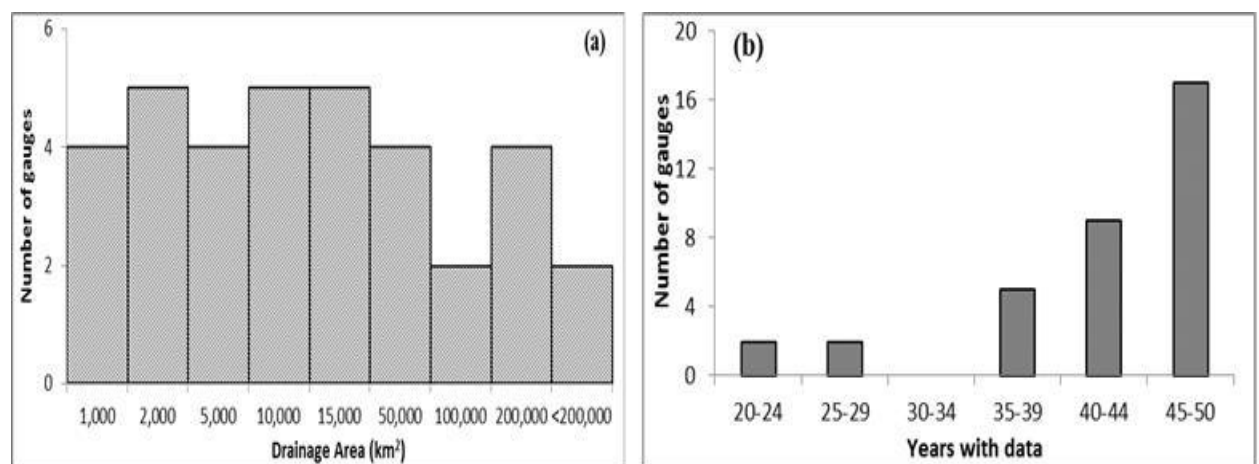


Fig. 3: (a) Number of gauges by drainage basin area. (b) Number of gauges with different length of discharge records.

distributions of different stream gauging stations of Upper Indus Basin. At Garhi Habibullah stream gauging station of Mangla (Sub-Basin) Log-Pearson Type-III representing the good results with lowest value of Chi-Square as compare to Gumbel Distribution. In Mangla River basin, Log-Pearson Type-III for six stream gauges (out of 8) has the most suitable results. At

the point of Yogo stream gauging station of Shyok River both distributions representing the data adequately, but the value of Chi-Square Test for Log-Pearson III is 3.15 as compare to Gumbel Method. Similarly, at the point of Khairabad both distributions representing the data adequate with low values of chi-square test, but Gumbel is more fit on the data as compare to Log-pearson III with

lowest value of chi-square test. Generally, Log Pearson III is suitable as compare to Gumbel with lowest value of Chi-Square Test on Upper Indus Basin.

Table 1 List of stream gauges used in the present study and their characteristics.

S. N.	Station	Lat (dd)	Lon (dd)	River	Basin	Area (Km ²)	No of Years	Mean Annual Streamflows (cumec)
1	Naran	34.9	73.7	Kunhar	Jhelum	1036	43	227.84
2	G. Habibullah	34.4	73.4	Kunhar	Jhelum	2355	43	432.18
3	Muzaffarabad	34.4	73.5	Neelum	Jhelum	7275	43	1373.69
4	Chinari	34.2	73.8	Jhelum	Jhelum	13598	43	922.91
5	Domel	34.4	73.5	Jhelum	Jhelum	14504	38	1106.11
6	Kohala	34.1	73.5	Jhelum	Jhelum	24890	43	2706.49
7	Azad Pattan	33.7	73.6	Jhelum	Jhelum	26485	43	2946.63
8	Kotli	33.5	73.9	Poonch	Jhelum	3238	43	1724.24
9	Palote	33.2	73.4	Kanshi	Jhelum	1111	43	295.87
10	Kharmong	35.2	75.9	Indus	Indus	67858	31	1871.07
11	Yogo	35.2	76.1	Shyok	Indus	33670	41	2252.5
12	Shigar	35.4	75.7	Shigar	Indus	6610	18	1107.72
13	Kachura	35.5	75.4	Indus	Indus	112665	43	4970.11
14	Gilgit	35.9	74.3	Gilgit	Indus	12095	43	1350.42
15	Dainyor Br.	35.9	74.4	Hunza	Indus	13157	43	1571.25
16	Alam Br.	35.8	74.6	Gilgit	Indus	26159	43	2760.36
17	Bunji	35.7	74.6	Indus	Indus	142709	12	2053.94
18	Doyain	35.5	74.7	Astore	Indus	4040	40	626.12
19	Shatial Br.	35.5	73.6	Indus	Indus	150220	30	9425.71
20	Karora	34.9	72.8	Gorband	Indus	635	36	186.19
21	BeshamQila	34.9	72.9	Indus	Indus	162393	43	10605.37
22	Daggar	34.5	72.5	Brandu	Indus	598	43	90.13
23	Phulra	34.3	73.1	Siran	Indus	1057	43	242.74
24	Kalam	35.5	72.6	Swat	Kabul	2020	43	361.33
25	Chakdara	34.6	72	Swat	Kabul	5776	43	757.32
26	Chitral	35.9	71.8	Chitral	Kabul	11396	43	1067.31
27	Jhansi Post	33.9	71.4	Bara	Kabul	1847	43	64.87
28	Nowshera	34	72	Kabul	Kabul	88578	43	3303.74
29	Gurriala	33.7	72.3	Haro	Indus	3056	43	611.26
30	Khairabad	33.9	72.2	Indus	Indus	252525	26	11702.71
31	Thal	33.4	71.5	Kurram	Indus	5543	43	213.92
32	Chirah	33.7	73.3	Soan	Indus	326	43	224.12
33	Chahan	33.4	72.9	Sil	Indus	241	43	74.8
34	DhokPathan	33.1	72.3	Soan	Indus	6475	43	1302.7
35	Massan	33	71.7	Indus	Indus	286000	42	14320.91

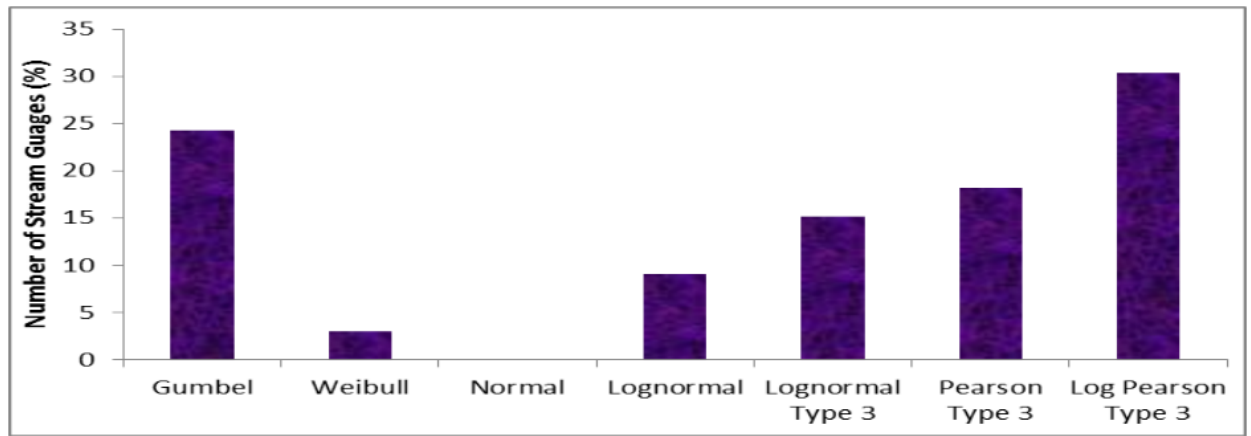
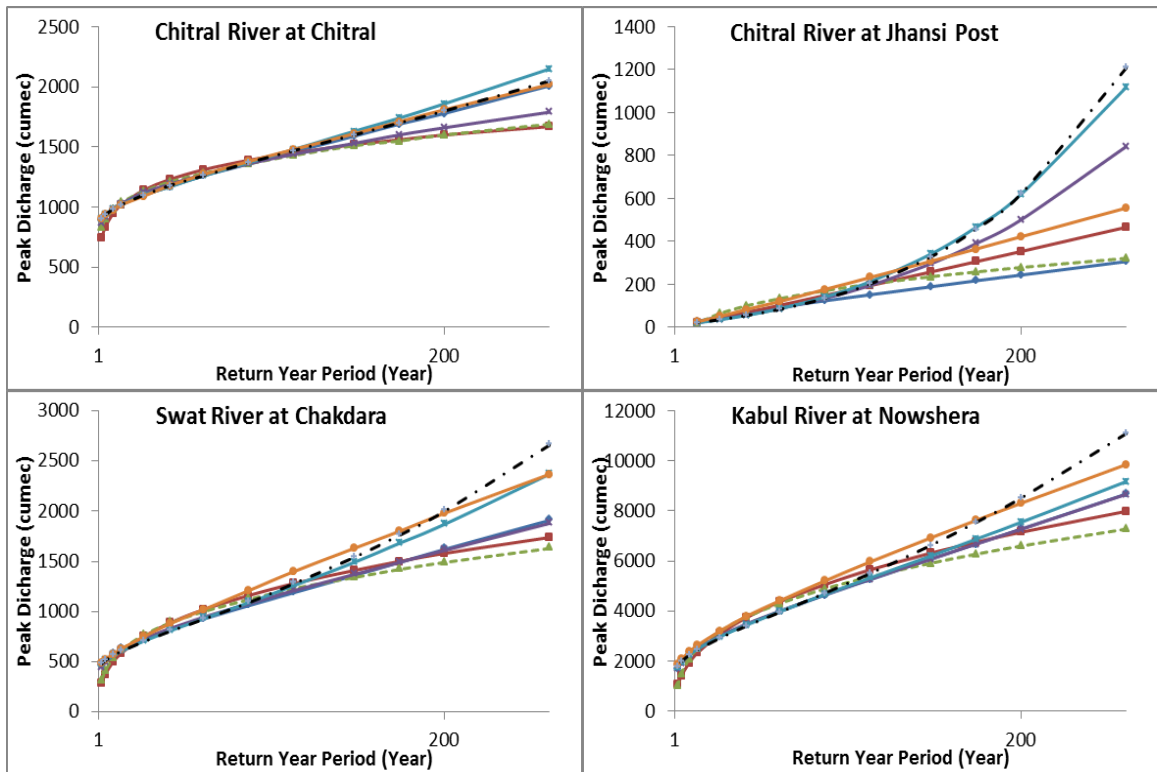


Fig. 3 Comparison of most suitable flood frequency distributions.

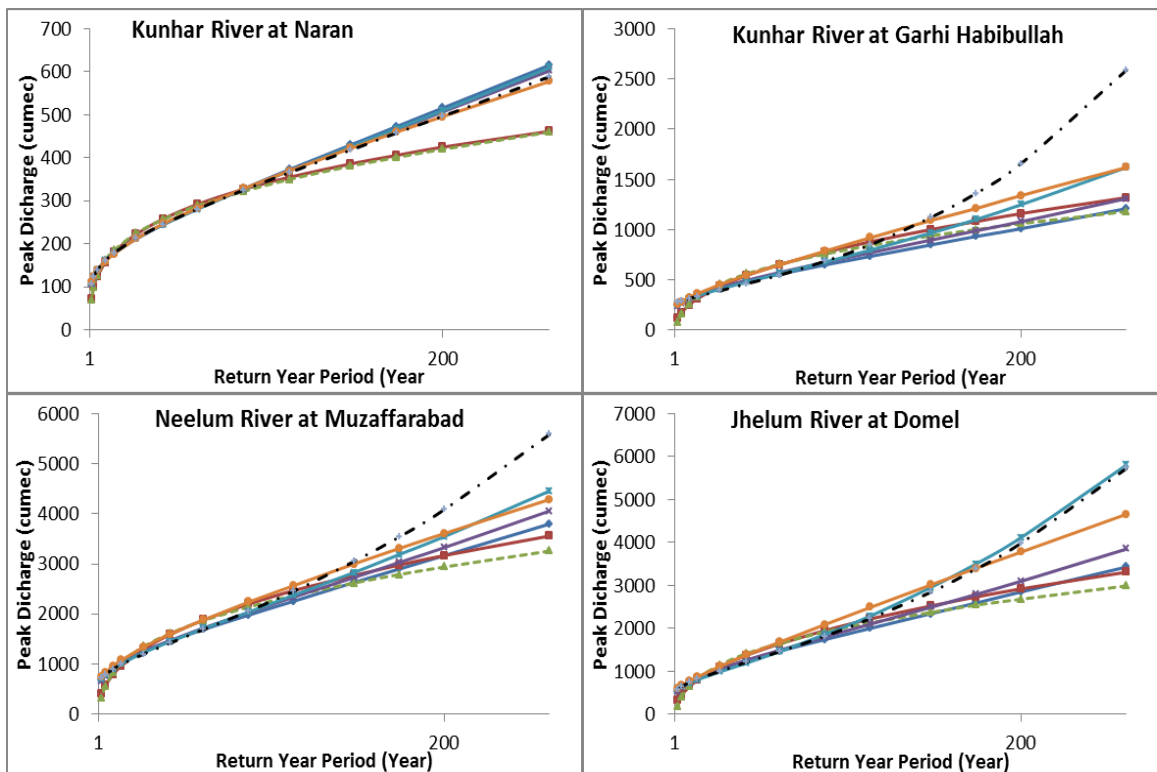
Table 2 Chi-Square Test Results of Upper Indus Basin(UIB)

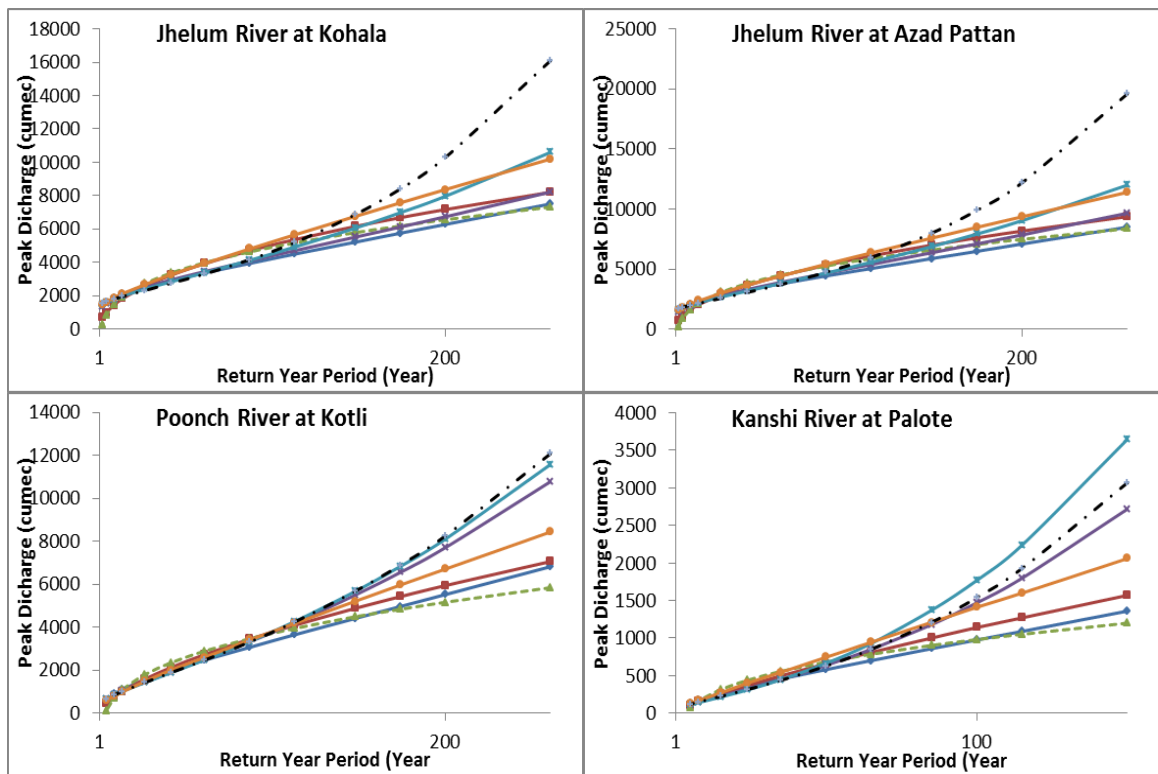
Sr. No.	Station	Chi Square Test Value							Most Suitable Method
		Gumbel	Weibull	Normal	Lognormal	Lognormal Type 3	Pearson Type 3	Log Pearson Type 3	
1	Naran	7.9	7.0	7.9	7.9	7.9	6.2	4.9	Log Pearson Type 3
2	Garhi Habibullah	12.5	26.7	47.6	15.8	10.8	230.6	7.9	Log Pearson Type 3
3	Muzaffarabad	10.0	21.3	23.4	12.5	14.1	105.8	10.0	Log Pearson Type 3
4	Domel	11.3	12.5	15.1	7.9	7.1	73.2	7.1	Log Pearson Type 3
5	Kohala	3.3	24.6	27.5	4.5	4.1	153.5	6.2	Gumbel
6	Azad Pattan	11.6	35.5	30.5	13.3	10.4	166.1	12.1	Lognormal Type 3
7	Kotli	10.0	10.8	22.5	6.2	6.6	6.6	6.6	Lognormal
8	Palote	12.1	6.2	28.0	9.1	9.5	17.9	9.5	Weibull
9	Kharmong	4.0	5.0	3.0	3.0	2.0	3.0	2.5	Log Pearson Type 3
10	Yogo	6.0	8.8	3.7	4.5	6.4	5.2	8.0	Lognormal
11	Shigar	5.3	5.3	6.0	7.3	6.0	90.0	8.7	Gumbel
12	Kachura	4.9	4.9	7.9	5.8	3.7	7.4	4.9	Lognormal Type 3
13	Gilgit	14.6	30.5	22.1	12.5	10.4	219.7	6.6	Log Pearson Type 3
14	Dainyor Br.	6.6	13.7	12.9	7.9	6.6	6.6	7.4	Gumbel
15	Alam Br.	7.9	12.1	6.6	5.8	4.9	5.8	4.1	Log Pearson Type 3
16	Bunji	1.3	0.5	0.5	1.3	0.5	0.5	0.5	Log Pearson Type 3
17	Doyain	1.2	4.4	2.0	1.2	3.2	4.4	3.2	Gumbel
18	Shatial Br.	8.7	12.0	8.3	9.7	8.3	5.0	6.4	Pearson Type 3
19	Karora	5.3	6.2	16.9	8.9	8.9	7.6	14.7	Gumbel
20	Besham Qila	5.4	16.7	12.9	9.1	5.4	5.8	5.8	Gumbel
21	Daggar	6.2	6.2	7.9	3.3	3.7	4.5	6.6	Lognormal
22	Phulra	7.4	10.0	10.4	7.0	5.8	5.8	5.4	Log Pearson Type 3
23	Chakdara	6.2	15.4	20.8	7.0	7.9	230.6	7.9	Gumbel
24	Chitral	4.1	13.7	10.4	3.3	2.4	2.0	2.4	Pearson Type 3
25	Jhansi Post	26.7	11.2	63.1	6.6	5.4	8.3	7.0	Lognormal Type 3
26	Nowshera	2.8	12.5	8.3	3.3	2.0	153.5	3.3	Lognormal Type 3
27	Gurriala	9.5	20.8	52.2	10.4	10.8	4.1	11.6	Pearson Type 3
28	Khairabad	2.5	0.9	0.4	2.5	4.2	0.9	2.5	Pearson Type 3
29	Thal	7.0	7.4	10.4	7.0	4.9	1.2	3.3	Pearson Type 3
30	Chirah	4.9	10.4	23.4	13.3	10.8	8.7	13.3	Gumbel
31	Chahan	17.9	5.8	54.3	5.4	4.1	7.4	7.4	Lognormal Type 3
32	Dhok Pathan	10.0	6.6	16.7	16.7	8.7	15.0	5.4	Log Pearson Type 3
33	Massan	3.0	4.5	9.1	3.0	3.0	2.2	2.6	Pearson Type 3



— Gumbel — Weibull - - - Normal — Lognormal — Lognormal Type 3 — Pearson Type 3 - - - Log Pearson Type 3

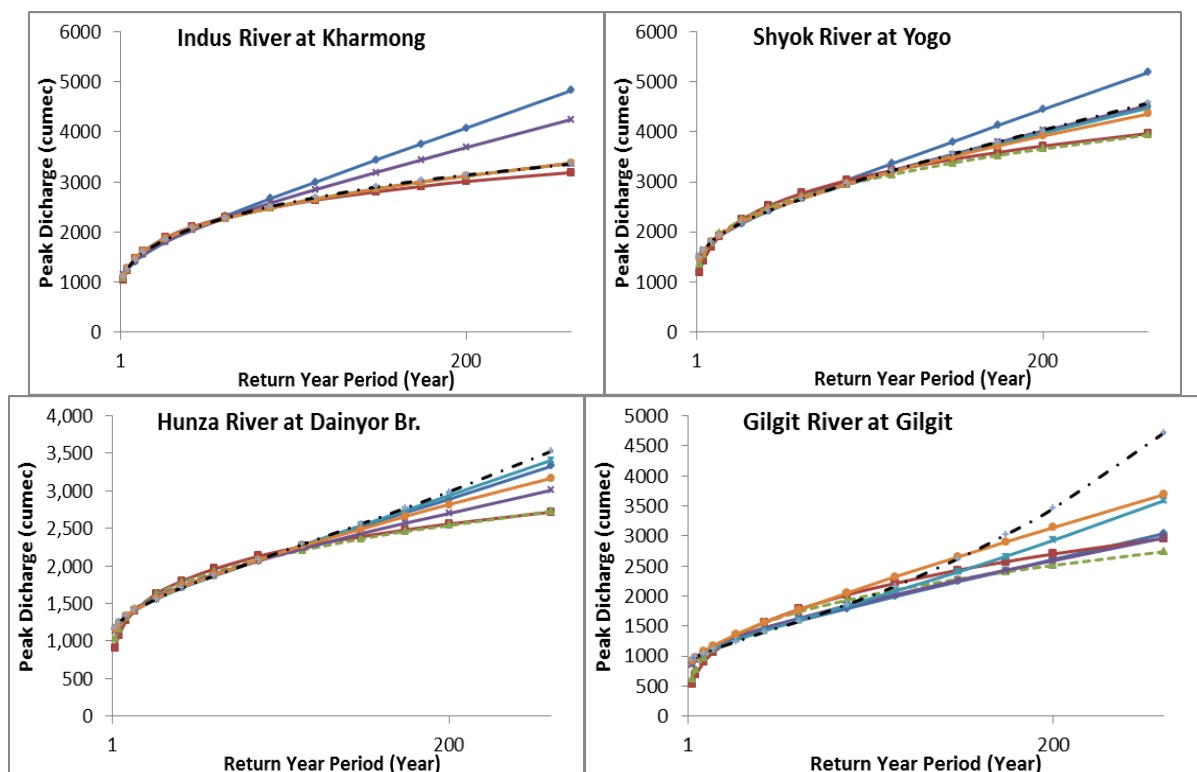
Fig. 3 Comparison of design flood magnitude from different flood frequency method in different rivers of Kabul River Basin.

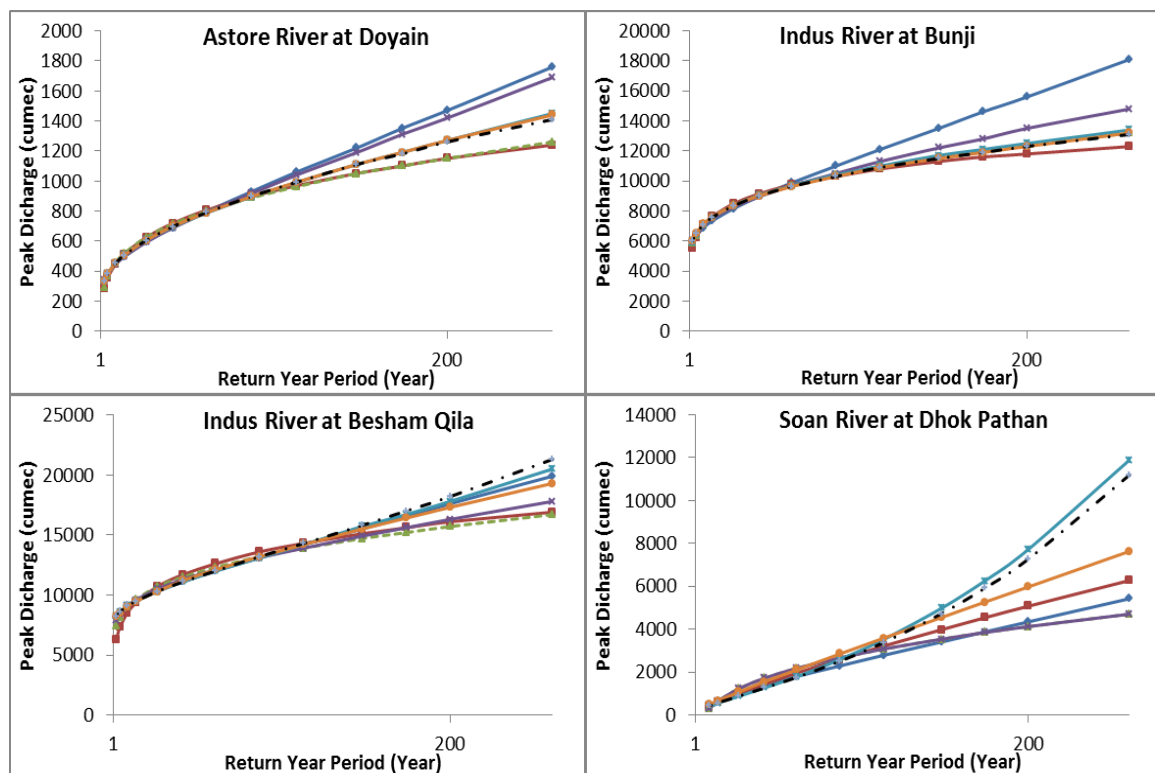




— Gumbel — Weibull — Normal — Lognormal — Lognormal Type 3 — Pearson Type 3 — Log Pearson Type 3

Fig. 4 Comparison of design flood magnitude from different flood frequency method in different rivers of Jhelum River Basin.





— Gumbel — Weibull — Normal — Lognormal — Lognormal Type 3 — Pearson Type 3 — Log Pearson Type 3

Fig. 5 Comparison of design flood magnitude from different flood frequency method in different rivers of Indus River Basin.

Conclusions

- Identification of hydrological similarities was carried out for un-gauged and gauged sites for flood frequency analysis. There are the following conclusions.
- Flood Frequency analysis showed that Log Pearson Type-III distribution providing suitable flood magnitudes on mostly areas of Upper Indus Basin with minimum values of Chi-square test.

From the Previous discussion and Analysis of results it may be worthwhile recommending the following. The study area was within geographical region. Consequently, there are limits on the accuracy with which flow characteristics were estimated from the rationalization techniques.

References

Reddy, D. V. Kumar, D. Saha, Dipankar Mandal, M. K. 2008 “The 18 August 2008

Kosi river breach: an evaluation” CURRENT SCIENCE, VOL. 95, NO. 12, 25 DECEMBER 2008.

Haan, C.T. 1977 “Statistical Hydrology” McGraw Hill Book Company, Singapore.

Solomon, O. and Prince, O 2013 “Flood Frequency Analysis of Osse River Using Gumbel’s Distribution” Civil and Environmental Research ISSN 2224-5790, Vol.3, No.10.

Pegram, G. and Parak, M. 2004 “A review of the regional maximum flood and rational formula using geomorphological information and observed floods” ISSN 0378-4738 = Water SA Vol. 30, No. 3.

Tumbare, M. J. (2000), “Mitigating Flood in South Africa”, paper presented at the 1st WARSFA/water Net Symposium: sustainable use of water Resources, 1-2 November, Maputo.

Impacts of hydro climatic variables trends on water resources of Yihe River Basin during the past 50 years

Muhammad Saifullah^{1,4*}, Ijaz Ahmad², Muhammad Zaman³, Zhijia Li⁴, Abdul Nasir¹

^{1*} Department of Structure and Environmental Engineering, University of Agriculture, Faisalabad, Pakistan

² Center of Excellence in Water Resources Engineering, University of Engineering and Technology, Lahore 54890, Pakistan

³ Department of Irrigation and Drainage, University of Agriculture, Faisalabad, Pakistan

⁴ College of Hydrology and Water Resources, Hohai University, Nanjing 210098, China

* saif_2146@yahoo.com

Abstract: For sustainable water resources, the hydro climatic variables are important and influence on the availability of water resources. In this study, Sen innovative method, Spearman's rho test was used to analyze the trends of hydro climatic variables of Yihe river basin during 1961-2011. Results indicated that precipitation, streamflow and evapotranspiration showed decreasing trend in the Yihe river basin. The trend patterns of hydro climatic variables matched by spearman's rho test which showed good agreement in the most cases. The findings of this study can be used as a reference for the planning and management of water resources of the river system

Keywords: climate change, Innovative trend pattern, Spearman's rho test, Streamflow

Introduction

A lack of water resources has become one of the critical factors forcing the development of the societies and economics of many countries of the world (Jia et al. 2015). Water resources are influenced by climate change. Recent hydrologic regime changes attributable to climate variability impacts which brought into focus the search for trend analysis. A lot of scientist investigated systematic trends of key climate variables attribute to climate change. It is well known that climate change is expected to have significant impacts on the water resources attributable to positive or negative trends in hydro climatic time series (flood, drought, etc.). The variation in rainfall runoff process may be alter the availability and quality of water resources and change the spatiotemporal characteristics of watershed, such as timing of flood events, and the frequency and severity of flood and droughts. These variations cannot be considered to be constant, which leads that future predictions are no more statistically indistinguishable from his historical records.

Nowadays, there are different statistical methods for analyzing hydro climatic variables such as t-test; regression analysis, Pearson correlation coefficient, the spearman's Rho, Sen's slope, auto correlation and most commonly used Mann-Kendall method. Trend analyses have been extensively used for detecting variability in climate and hydrologic works. Consequently, the

numerous scientists investigated the impact of climate change on water resources of different rivers of the world at various spatiotemporal scales (Zhang et al. 2014; Kormann et al. 2015). Similar studies have also investigated for Chinese river (Amo-Boateng et al. 2014; He et al 2013; Zhao et al. 2015). Zhang et al. (2011) estimated water resources variations across China and identified that mean annual streamflow reduced in arid and semi-arid region of North and increased in South of China. Although previous studies have found the decline trend in water resources of the Yihe River, it is still unclear whether the water resources will continue to decline in future, and to what extent hydro climate variables are responsible for the decline. Thus, the objective of the study analyzed these variables through spearman's rho test and auto correlation. Also, Sen's innovative method (Sen 2012) is used to analyze the trend pattern of hydro climatic variables at different time scale. Hence this study will be helpful to identify the regime of water resources of Yihe river basin.

Materials and Methods

Study Area Description

One of the large tributaries of Yellow River is Yihe River and major upper tributary sub-basin of the Yihe River is Dongwan basin as (Fig. 1), which exists in the semi-arid climate zone. The Dongwan watershed is situated in Henan

Province, China, between longitudes 111° to 112° E and latitudes 33.5° to 34.5° N, with a drainage area of 2856 km². It drains the area of rising mountains Fuiwu located in the Qinling Mountain. There is a massive area of forest land in the upstream region and soil erosion is not a serious problem.

Innovative trend analysis technique

Sen (2012) divided the time series into subsection and plotted the time series on Cartesian coordinate system which is independent of the trend in time series, pre-assigned significance level, magnitude of trend, sample size and the amount of variation within time series. This plot draws triangle and trend free line draws at 45°. The upper and lower part exhibited as increasing and decreasing trend respectively. If all the observations lie on 1:1 line, it means that there is trend free time series. The scatter points above or below the 1:1 line indicate increasing or decreasing monotonic trends, respectively in innovative trend analysis technique. The trends of hydro climatic variables can be analyzed through this simple but still powerful innovative trend analysis methodology. The Monte Carlo simulation was applied to validate this method and then applied for two annual stream flow data sets and one precipitation time series from Turkey (Sen 2012).

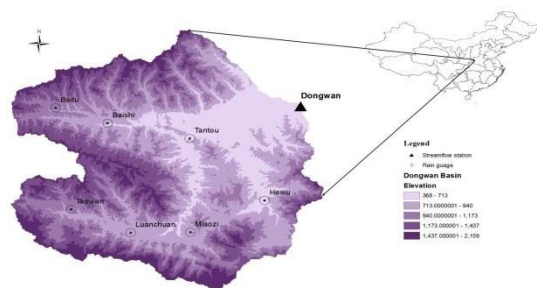


Fig. 1 Location of the study area

Autocorrelation

All the hydro climatic variables were first tested through autocorrelation. The lag one autocorrelation coefficient is calculated as:

$$r = \frac{[\sum_{i=1}^{n-1} (x_i - \bar{x})(x_{i+1} - \bar{x})]}{[\sum_{i=1}^{n-1} (x_i - \bar{x})^2]} \quad (1)$$

The time series data come from random process, the expected value and variance of r_1 are:

$$E(r_1) = -\frac{1}{n} \quad (2)$$

$$Var(r_1) = \frac{(n^3 - 3n^2 + 4)}{[n^2(n^2 - 1)]} \quad (3)$$

$$z = \frac{|r_1 - E(r_1)|}{Var(r_1)^{0.5}} \quad (4)$$

where z is test static of test, n is number of observations.

Spearman's rho Test.

Spearman's rho (Lehmen 1975; Sneyers 1990) test is another rank-based nonparametric method used for trend analysis and the innovative trend technique validated through this test. In this method, the time series data assumes independent and identically distributed, the null hypothesis identify no trend over time; the alternate hypothesis (H_1) estimate that a trend exists and that data increase or decrease with i . The test statistics R_{sp} and standardized statistics Z_{sp} are defined as:

$$R_{SP} = 1 - \frac{6 \sum_{i=1}^n (D_i - i)}{n(n^2 - 1)} \quad (5)$$

$$Z_{sp} = R_{sp} \sqrt{\frac{n-2}{1-R_{sp}^2}} \quad (6)$$

Where n is number of observations, D_i is rank of observation, R_{sp} is rho coefficient and Z_{sp} test statics respectively.

Results and Discussion Innovative pattern of hydro climatic variables

A simple qualitative method was introduced by Sen in 2012 which estimated the trends of total time series. This trend pattern was used for annual time series of hydro climatic variables in the present research in which the findings confirm from other methods. As other researcher also investigated the trend of hydro climatic variables using this innovative pattern (Sen 2012; Nourani et al. 2015).

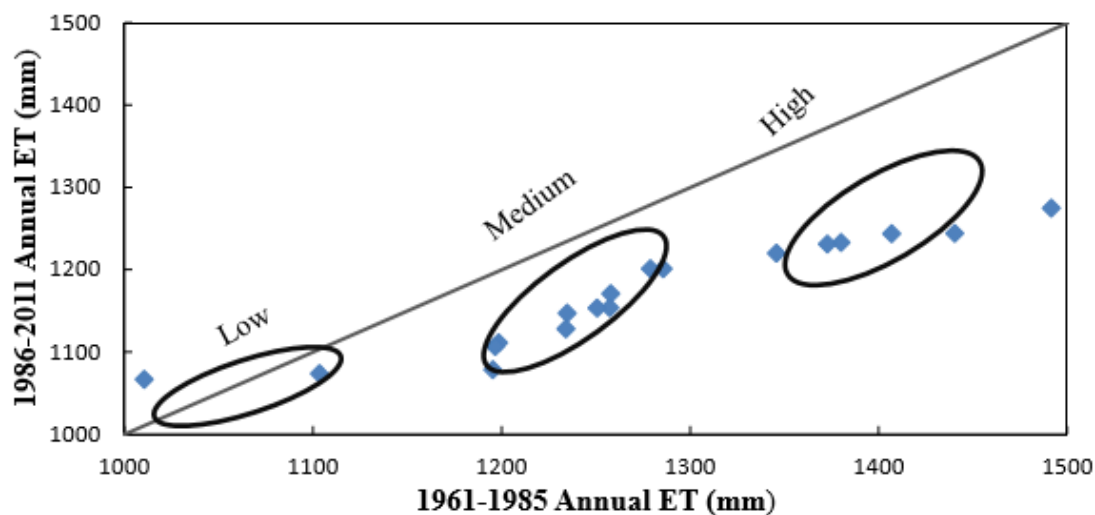


Fig. 2 Result of Innovative trend pattern of evapotranspiration

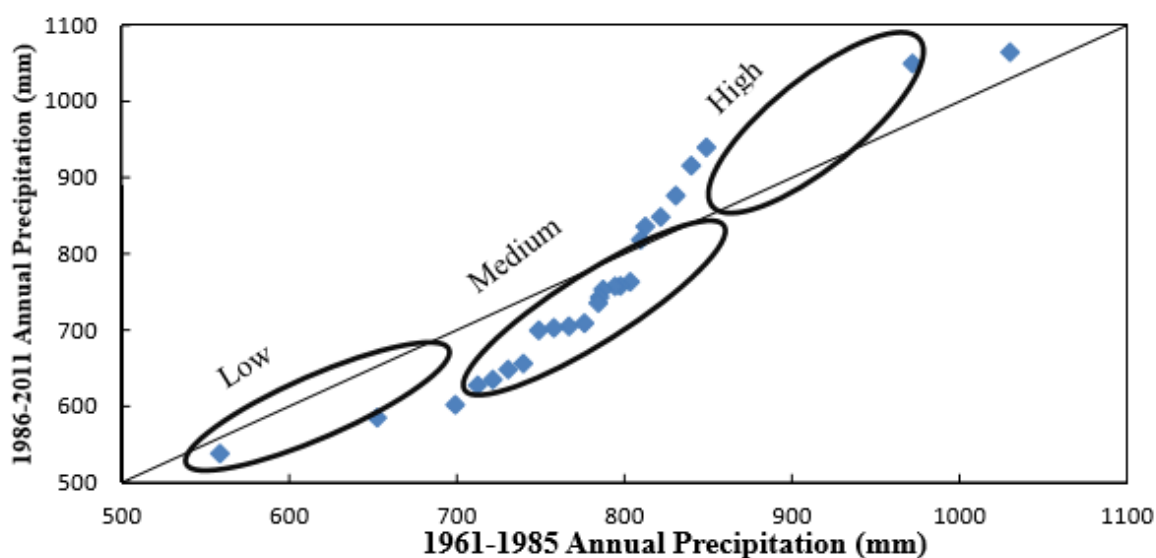


Fig. 3 Result of Innovative trend pattern of precipitation

For this purpose, the time series of hydro climatic variables were divided into two parts with respect to time and arranged in ascending order. Based on scatter diagram plot by time series of hydro climatic variables from 1961-2011, the trend analysis via Sen's method justified good agreement with obtained results of Spearman's rho test in the most cases. The result of Sen's scatter diagram justifies the same result as determine from the rho's test. The scatter diagram divided into low, medium and high cluster. The low and medium clusters of hydro

climatic variables show decreasing trend and high value of precipitation show increasing trend. The streamflow and evapotranspiration identified as decreasing trend as previous studies (He et al. 2013; Xing-Jie et al. 2012). The time series possess serial correlation, but proposed idea estimate the trend of hydro climatic variables as (Table.1). The annual time series of hydro climatic variables plot as scatter diagram as (Fig. 2-4).

Table 1: Result of auto correlation and Spearman's rho test

Months	Precipitation		Evapotranspiration		Streamflow	
	Correlation	rho static	Correlation	rho static	Correlation	rho static
Jan	0.07	-0.65	0.9	-2.39**	0.70	-1.68***
Feb	2.03**	1.36	-0.10	-2.01**	1.16	-2.08**

Mar	2.62*	-1.33	3.09*	-2.48**	2.28*	-1.60
April	1.54	-3.70*	0.76	-1.39	0.70	-3.89
May	-0.55	0.04	1.38	-2.50**	2.19**	-3.83*
June	-0.02	-0.18	2.69*	-4.45*	-0.91	-1.70***
July	1.36	2.00**	4.56*	-5.24*	-0.64	-2.73*
Aug	-1.51	-1.07	3.42*	-4.52*	-0.69	-1.00
Sept	2.14**	-0.64	3.44*	-3.44*	1.59	-2.40**
Oct	-0.90	-2.23**	3.30*	-3.76*	1.64	-3.26*
Nov	-0.20	-1.97**	-0.41	-1.27***	0.98	-3.10*
Dec	0.52	0.27	-0.05	-2.22**	2.54**	-2.18**
Annual	0.98	-0.67	4.96*	-5.26*	1.00	-0.71

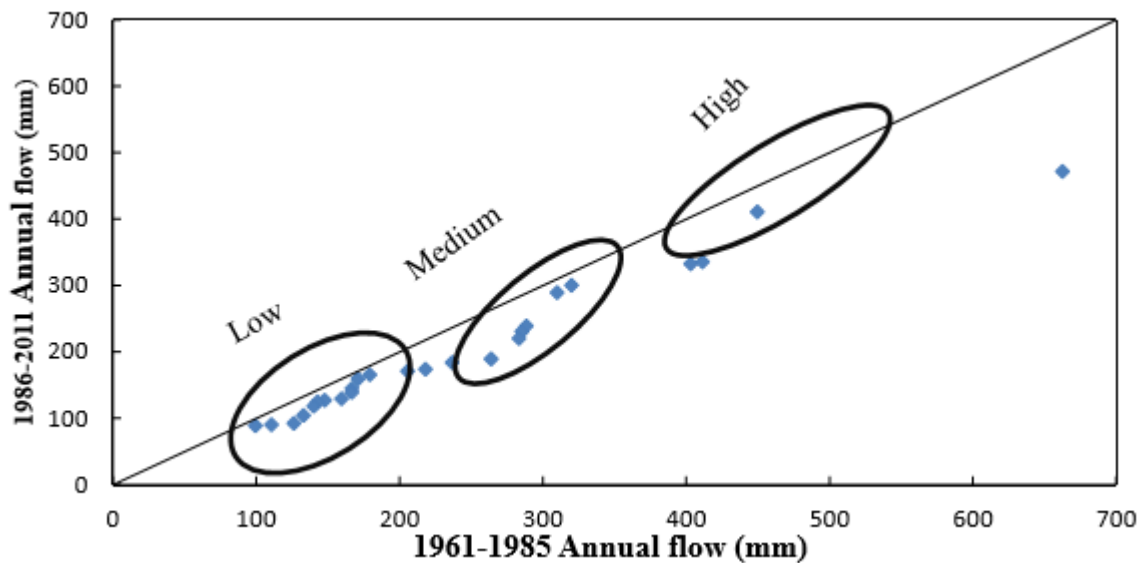


Fig. 4 Result of Innovative trend pattern of runoff

Note: ***, Significant trend at 90% significance level, ** Significant trend at 95 % and * significant trend at 99% respectively.

The trend of hydro climatic variables found to be similar as innovative trend pattern. The potential evapotranspiration showed decreasing pattern during low, medium and high cluster values. The high cluster of precipitation show slighter increasing trend which show good match with spearman's rho test as in Table 1. The streamflow shows decreasing trend as innovative trend patter. The result of all month of hydro climatic variables and innovative pattern found to be similar.

Conclusion

In this study, Sen's innovative method was used to analyze the hydro climatic variables in which findings were in accordance with Spearman's rho test results and confirmed the existence of decreasing trend in precipitation, evapotranspiration and streamflow. The PET show decreasing trend using innovative trend pattern and spearman's rho test. The

precipitation and streamflow are highly dependent and sensitive to each other. Finally, the result showed the changes in the water resources of Yihe river basin. Overall, we believe that this study provides an elaborate view of hydro climatic variables trends in Yihe River basin, using nonparametric tests in conjunction with accumulated deviation curve and Parde coefficient which should be useful for further investigation. This study provides an idea regarding the effect of natural forces on water resources. More importantly, this study opens new horizon for additional research that can address human activities on the water resources of the region.

References

- Amo-Boateng M., Z. Li. and Yiging G. 2014 Inter-annual variation of streamflow, precipitation and evaporation in a small humid watershed (Chengcun Basin, China). Chinese Journal of Oceanology and Limnology 32(2): 455-468.

- He B., C. Miao. and Shi W. 2013 Trend, abrupt change, and periodicity of streamflow in the mainstream of Yellow River." *Environ Monit Assess* 185(7): 6187-6199.
- Jia X., C. Li. Cai Y. Wang X. and Sun L. 2015 An improved method for integrated water security assessment in the Yellow River basin, China. *Stochastic Environmental Research and Risk Assessment* (Online Published). doi 10.1007/s00477-014-1012-2
- Kormann C., Francke T. and Bronstert A. 2015 Detection of regional climate change effects on alpine hydrology by daily resolution trend analysis in Tyrol, Austria. *Journal of Water and Climate Change*, 6(1), 124-143. doi: 10.2166/wcc
- Lehmann E. L. 1975 *Nonparametrics, Statistical Methods Based on Ranks*. Holden-Day, San Francisco, Calif, USA.
- Nourani V., Nezamdoost N., Samadi M. and Vousoughi F.D. 2015 Wavelet-based trend analysis of hydrological processes at different timescales. *Water and Climate Change* (in press)
- Sen Z. 2012 Innovative trend analysis methodology. *Hydrologic Engineering*, Technical note, 17(9), 1042-1046.
- Sneyers, R. 1990 On the statistical analysis of series of observations. World Meteorological Organization, Technical Note 143, WMO no. 415.
- Xing-Jie J., Ji-Jun W., Wan-Long G., Ye-Yu Z. and Feng-Xiu L. 2012 Trends in Annual and Seasonal Pan Evaporation in the Lower Yellow River Basin from 1961 to 2010. *Advances in Climate Change Research*, 3(4), 195-204. doi: 10.3724/sp.j.1248.2012.00195
- Zhang Q., Peng J., Singh V. P., Li J. and Chen, Y. D. 2014 Spatio-temporal variations of precipitation in arid and semiarid regions of China: The Yellow River basin as a case study. *Global and Planetary Change*, 114, 38-49. doi: 10.1016/j.gloplacha.2014.01.005
- Zhang Z.X., Chen X., Xu C.Y., Yuan L.F., Yong B. and Yan S.F. 2011 Evaluating the nonstationary relationship between precipitation and streamflow in nine major basins of China during the past 50 years. *J Hydrology*, 409:81–93.

Sensitivity Analysis of Hydraulic Parameters for Water Hammer in Penstock Design

Muhammad Yasar^{1*}, Muhammad Waseem¹, Ghulam Nabi¹

¹Centre of Excellence in Water Resources Engineering, University of Engineering and Technology, Lahore 54890, Pakistan

*yasar.joyia@gmail.com

Abstract: Water hammer is a transient flow which is produced as a result of sudden velocity changes in penstock of hydropower plant. This phenomenon may lead to initiate strong pressure wave in penstock. If the pressure wave exceeds the design pressure of penstock, the result would be collapse of pipe. Sensitivity analysis is an analysis that finds out how sensitive an output is to any change in specific input while keeping other inputs constant. In hydropower system, it refers to an analysis of how each of the input variables (such as diameter, length, wave velocity, etc.) affects the fluctuation of pressure wave in penstock. In this study, governing equations of water hammer i.e. continuity and momentum equations are numerically solved and simulated by developing a computer program in "Visual Basic" environment. The fluctuations in positive and negative pressures were calculated by varying hydraulic design parameters one by one considering the rest of parameters as constant. The program employs method of characteristic (MOC) for numerical solution. Depending upon the sensitivity of the water hammer phenomenon, it is obligatory to prepare adequate and cost-effective design of penstock to avoid any cavitation. In addition, it shows, by reducing the penstock pipe diameter and wave velocity and increasing pipe length, the maximum pressure head increased, and the minimum pressure head decreased. The software developed in this study was also applied to hydropower project in northern area of Pakistan i.e. Kyal Khwar hydropower plant. The developed program showed good agreement with the original data prepared by the commercial software used by the consultant of Kyal Khwar hydropower plant.

Keywords: Water hammer, Transient flow, Valve, Surge Wave, Penstock pipe, VISUAL BASIC

Introduction

Water hammer is a transient flow phenomenon which initiates due to suddenly change in the flow pattern the velocity and pressure varies abruptly. This phenomenon may lead to propagate severe wave in the pressurized pipe; the intensity of such wave is so high which oscillate very high to very low value, it poses to penstock to danger at higher pressure and may collapse the penstock and other conveyance facilitates if the system is not equipped with proper protection devices. Hydraulic transient phenomenon occurs due to flow changes rapidly in pressurized conduits for several reasons such as, sudden valve closure, pump stop, and load failure and changing elevation in reservoir. Wylie and Streeter (1978); White (1979). The peak magnitude of the transient pressure depends on pipe length, profile, wave velocity, friction coefficient and diameter. Wylie and Streeter (1978). Due to the strong pressure wave, the pressure head changes rapidly which may cause severe damages to the pipe (Parmakian, 1963). Abuaziah et al. (2013) showed that the hydraulic transient analysis is an effective and reliable tool to determine the needs for surge protection systems against transient phenomenon. They

found to reduce the water hammer effect and to prevent water column separations and fatigue failures, surge tank recommended as good engineering practices. Furthermore, water hammer effects were also reduced by increase the valve closure time. Araki and Kuwabara (1975) proposed a differential equation for elastic theory of water hammer. Moreover, they introduced a relation for considering head loss simplification by using finite difference method, with the help of a special computer program. A special computer program known as (WHAMO), developed by US Army Corps of Engineers, was being used to solve the equation, by inserting appropriate boundary conditions. Wylie and Streeter (1979) presented similar equation for analyzing water hammer phenomenon in a simple pipeline, with an open reservoir on the upstream side and a valve on the downstream side. They have used the method of characteristics to develop a basic computer program scripted in Fortran Computer Language. Nemet (1974) presented a theory on water hammer and developed a computer program to analyse the pressure increases due to water hammer effect. In addition, he also provided the format for the computer system data input for

developed program. Mansuri et al. (2014a, b) studied, fundamental equation of water hammer solved numerically by method of characteristics by using MATLAB software, the study showed the sensitivity analysis in the pressure variations by changing some parameters of pipe line i.e. diameter, length and wave velocity, the study also shows by increasing these parameters, the pressure changes decrease & vice versa. They also found that by increasing pipe roughness, negative and positive pressure range decrease, while increase in reservoir water level cause severe change in the pressure wave in the pipe. Bernard (2013) showed that the thickness of penstock, Length, initial velocity and bend angle has a significant impact on the fluctuation of pressure wave and structural response. He also observed, in the presence of soil have a substantial benefit for decreasing the von-mises stresses. Norazline and Amin (2015) studied and showed that profile of pressure wave and amplitude depends on the valve operation, time of closure of valve and type of closing laws and showed that the pressure wave profile varies from square to triangular and trapezoidal shape depending on the closing laws and the frequency of the pressure decreases as the closing time is decrease and number of segment increases. Jalil and Solemani (2011) showed that the most sensitive parameters for which maximum hammer developed are the (a) moment of inertia of pump and electrometer, (b) diameter of the pipe, (c) material of the pipe (d) thickness of pipe (e) water temperature and by increasing these parameters, the maximum water hammer decrease and vice versa. Wuyi and Hnang (2013) showed that the compensation strainer should do effect on pressure wave either it is positive pressure wave or negative pressure wave. The study also proves if suitable strainer was selected for pressure vessel, due this water hammer effect and severe pressure fluctuation should be decreases up to some extent. Algirdas et al. (2009) studied that the flow energy loss coefficient in pipe just d/s of the valve is the most important parameter and play vital role on the variance estimate pressure peak. It also showed that the pipe wall roughness and pressure at the pumping head were also play a role on pressure wave fluctuation. Cooper and Johnston (2010) investigated the system boundaries on transient wave, when the system contains a fully closed valve, a partially closed valve and a reservoir. They found negligible effect on the nature and magnitude of the pressure wave after interaction with these boundaries i.e. fully closed valve and reservoir with no flow. The experimental results obtained from the reservoir with flow and

partially closed valve were inconclusive, because of limitations related to the design of the experiment. Their research demonstrates the assumption that a water hammer wave interacts with a boundary and no losses is valid for situations with no flow in the pipeline system. In addition, it provides a foundation on which further research can be undertaken. Various methods of analysis were developed for the problem of transient flow in pipes such as: (a) approximate analytical approaches where are nonlinear friction part in the momentum equation is either neglected or linearized (b) numerical solutions of the nonlinear system or method of Characteristics (Wylie and Streeter, 1978). Among these two methods, method of characteristics (MOC) is the most popular approach for handling hydraulic transient flow. Its importance lies in its ability to convert the two partial differential equations (PDEs) of continuity and momentum into four ordinary differential equations that are solved numerically using finite difference techniques (Gray 1953, Streeter and Lai 1962).

In this study, the numerical modeling method for method of characteristics (MOC) has been presented for sensitivity analysis of water hammer problems by varying pipe parameters such as: diameter length and velocity. For this purpose; a program in Visual Basic environment has been developed. To test the software, fluctuations of surge wave by changing of pipe diameter, length and velocity, are investigated. Engineers and researches working in this area can benefit from the software detailed. The study sensitivity analysis of numerical model by changing parameters helps to understand well about hammer phenomenon and design aspects for improved design of penstock.

Material and Method

$$\frac{\partial H}{\partial t} + \frac{a^2 \partial Q}{gA \partial x} = 0$$

$$\frac{\partial Q}{\partial t} + gA \frac{\partial H}{\partial x} + \frac{fQ|Q|}{2DA} = 0$$

The study consists of sensitivity analysis of hydraulic parameters for water hammer problems in penstock design by changing penstock pipe diameter, length and wave velocity. The full elastic water hammer in one-dimensional unsteady pressure flow equations given by (Wylie and Streeter, 1978)

Where, H is the head of reservoir (m), Q is the discharge (m³/sec), D is internal diameter of pipe (m) and “a” is the celerity of wave (m/sec). The

fundamental equation of water hammer is depending upon the momentum and continuity equation of flow. Eq (3) shows the dynamic equation for non-compressible fluids.

$$\frac{\partial V}{\partial t} + V \frac{\partial V}{\partial x} + \frac{1}{\rho} \frac{\partial P}{\partial x} + \frac{\int V}{2D} + g \cdot \sin \alpha = 0 \quad (3)$$

The continuity equation for a segment of pipe length as shown in Eq. (4) (Mansuri et al. 2014)

$$\frac{\partial V}{\partial x} a^2 + \frac{1}{\rho} \frac{\partial P}{\partial t} + \frac{1}{\rho} V \frac{\partial P}{\partial x} = 0 \quad (4)$$

To the analysis of water hammer phenomenon Eqs. (3 and 4) are solved simultaneously.

Method for Numerical Solution Method of Characteristics (MOC):

There are many methods and technologies are available for the solution of the governing equations of water hammer (momentum & continuity) among them method of characteristic (MOC) is one of the best method to be considered with some minor losses and modify for different boundary conditions. This method has ability to convert the two- partial differential equation (momentum & continuity) into normal differential equation, which were solved numerically using finite difference techniques (Streeter 1967).

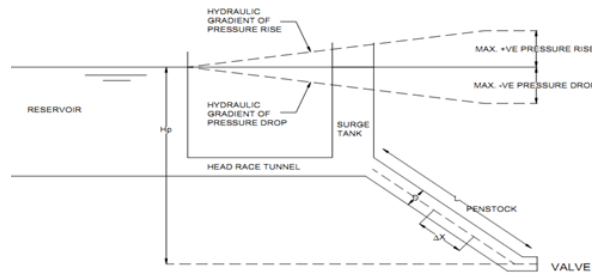


Fig. 1 (x, t) grid for solving simple pipe problem by Characteristic lines Wylie and Streeter (1967).

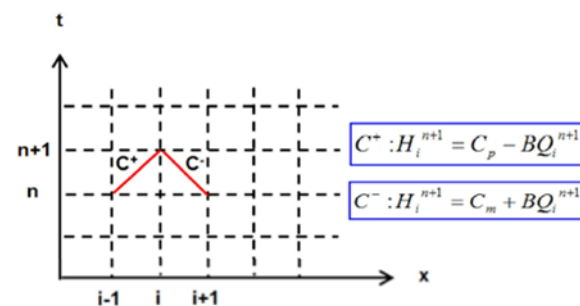


Fig. 3 Schematic diagram of pipe connecting reservoir U/S and D/S a valve.

Applying some mathematical operations in Eqs. (3 and 4), the two-normal differential equations Are deduced as shown in Eqs. (5 and 6)

$$\frac{\partial H}{\partial t} + \frac{a}{gA} \frac{\partial Q}{\partial t} + \frac{af}{2gD} V|V| - \frac{Q}{A} \sin \alpha = 0 \quad (5)$$

$$\frac{\partial H}{\partial t} - \frac{a}{gA} \frac{\partial Q}{\partial t} + \frac{af}{2gD} V|V| - \frac{Q}{A} \sin \alpha = 0 \quad (6)$$

In order to solve the Eqs. (5 and 6) by characteristic line method, a grid of characteristic, now established, the two characteristics C⁺ and C⁻ initiate from node A & B respectively and intersect at nodel point “P” (as shown in fig. 2), at nodes A & B, here value of (Q , H), where the conditions are known, and at node “P”. The conditions are unknown where the value of (Q , H) are calculated. Using liner finite difference scheme between node A & P and between node B & P, deduced the two linear equations as shown in Eqs.(7 and 8) (Streeter, 1967).

$$H_p - H_A + \frac{a}{gA} (Q_p - Q_A) + \frac{f \Delta x}{2gDA^2} Q_A |Q_A| = 0 \quad (7)$$

$$H_p - H_B - \frac{a}{gA} (Q_p - Q_B) - \frac{f \Delta x}{2gDA^2} Q_B |Q_B| = 0 \quad (8)$$

$$C_p = H_{i-1} + BQ_{i-1} - RQ_{i-1}|Q_{i-1}| = 0 \quad (9)$$

$$C_m = H_{i+1} + BQ_{i+1} + RQ_{i+1}|Q_{i+1}| = 0 \quad (10)$$

$$H_{pi} = (C_p + C_m)/2$$

$$Q_{pi} = (H_{pi} - C_m)/B$$

$$\text{Where } B = \frac{a}{gA} \text{ and } R = \frac{f \Delta x}{2gDA^2}$$

In Eqs. (9 and 10) C_m and C_p are known coefficients based on value of H and Q in known time step. By solving these two linear equations, two unknown values H_{pi} and Q_{pi} in the next time step has been found.

Boundary Conditions

The H and Q values at the ends of the pipe were determined by using boundary conditions. These conditions are, Chaudhry (1979).

U/S Boundary Condition (Constant Head Reservoir)

At the U/S end there is constant head reservoir, the H-value remains constant for all time. Thus,

for $i = 1$

$$Q_{pi} = (H_{pi} - (H_{i+1} - BQ_{i+1} + RQ_{i+1}|Q_{i+1}|))$$

$$H_{pi} = H_{res.}$$

D/S Boundary Condition (Valve at end)

At the D/S end there is valve, the $\tau - t$ relationship for valve closure is given by

$$\tau = (1 - \frac{t}{tc})^{E_f}$$

Where, t is current time of analysis (sec), tc is time of valve closure (sec) and E_f is modulus of elasticity of fluid flow (Gpa). For slow closure of valve, closure time (tc) is normally greater than reflection time (tr) and for rapid closure of valve, closure time (tc) is less than reflection time (tr).

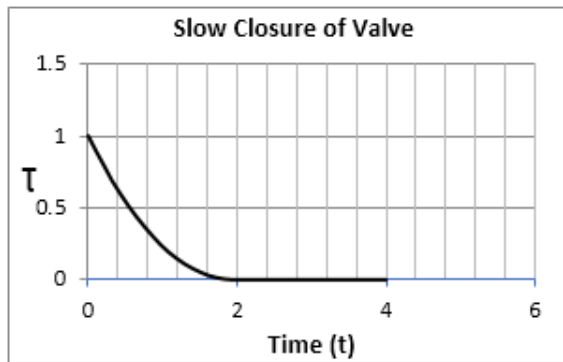


Fig. 4 $\tau - t$, relationship due to Slow valve closure

The governing equations of water hammer (momentum and continuity of flow), are solved numerically by method of characteristics (MOC), a computer program in visual basic (VB) environment has prepared. The prepared module solves the water hammer equations numerically by considering constant head reservoir at u/s end and a valve at d/s end of the penstock. Through value operation and determine the value of C_{DA} for each time step as shown in Eq. (13)

$$Qp = C_D A \sqrt{2gHp} \quad (13)$$

C_D is discharge coefficient, H_p is Head of reservoir (m) and A is the area of orifice (m^2). The behaviour of water hammer phenomenon on a system including a pipe within variable diameter, length and wave velocity within constant head of reservoir is assessed. In order to analyse the transient phenomenon a penstock pipe length (L) is divided into $N = 5$, segments (pipe's full length, pipe's 4/5 length, pipe's 3/5 length, pipe's 2/5 length and pipe's 1/5 length) for the calculation of pressure wave. The datum level for hydraulic are considered for the

geometrical axis of the pipe. The program in each time steps calculates the value of C_{DA} using linear interpolation. Simultaneously, the value of H_{pi} and Q_{pi} in valve was calculated.

Results and discussion

General

In the current study, Table 1 shows the parameters, to test the model and perform sensitivity analysis to understand the behavior of water hammer phenomenon.

Table 1 General hydraulic data of pipe for testing the model and analysis of water Hammer (Wylie and Streeter, 1978)

Description of data	Data
Length of pipe (L)	600 m
Head of reservoir (H_p)	150 m
Diameter of pipe (D)	0.5 m
Celerity of wave (a)	1200 m/sec
Friction coefficient (f)	0.018
$(C_D A)_0$	0.009

Fluctuation of Pressure Wave Due to Valve Closure

The hydraulic transient analysis performed for the pipe parameters listed in table 1. In this analysis, slow valve closure condition has been assumed. Moreover, analysis has been performed for method of characteristics (MOC) (as shown in Fig. 5) and maximum (H_{max}) and minimum (H_{min}) pressure head values are computed. For example, H_{max} and H_{min} values are 268.53m and 116.66m, respectively. Moreover, the maximum and minimum pressure head values are occurring at normalized length (X/L) of 1.

Sensitivity Analysis of Hydraulic Parameters In Penstock

Penstock Diameter (D) as Variable

Fluctuations of pressure head for the change of penstock diameter calculated using computer software. Both MOC and MOI have been used to study hydraulic transient analysis due to valve closure ($T_c > T_r$).

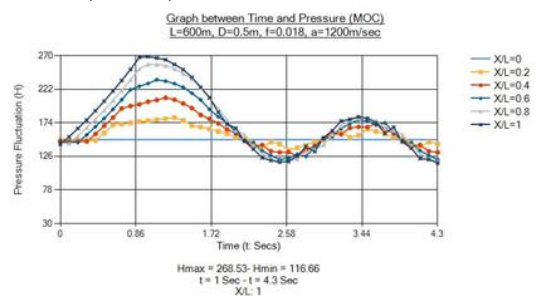


Fig. 5 Pressure fluctuation for slow valve closure by method of characteristics(MOC)

Standard pipe diameter of penstock pipe has been selected as 0.5 meters. The diameter of the penstock pipe has been increased and decreased to study its effect on pressure head, while keeping other parameters (listed in table 1) as constant. Fig. (7) Shows maximum and minimum pressure heads vary rapidly for diameters below standard diameter, while the pressure variation for diameters above the standard diameter start converging and the change in values of pressure head is very small. For minimum pressure head values (-64.99m & -365.32m), which were below the vapour pressure of water (<10.3 m), cavitation may occur.

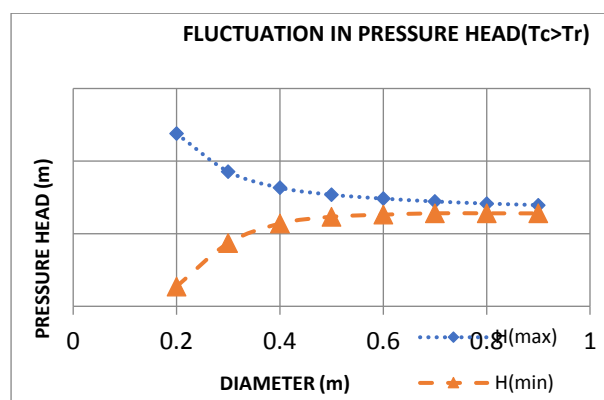


Fig. 6 pressure variation with changing diameter

Those results reached above indicate that the water hammer magnitude is sensitive with respect to the penstock diameter. The reason for this sensitiveness was the variation in the transient-pressure amplitude due to change in standard diameter (0.5m). Study shows that the decreasing exponential trends of water hammer pressure with respect to diameter as shown in Fig (6). Hence, it was evident that when pressure-amplitude increases (268.53m to 688.93m), it poses greater vulnerability to the fluid- structure. It has also been concluded that the frequency of pressure wave is dependent upon the shifts in pipe-diameter.

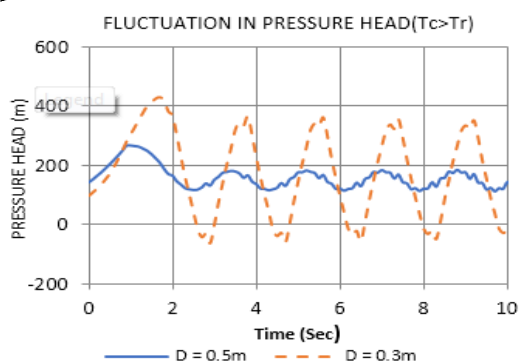


Fig. 7 pressure variation w.r.t. time by changing diameter

Study depicted, when the penstock-diameter was

reduced (0.5m to 0.3m), the number of water thrusts on valve increases for the same time period and magnitude of these thrusts also increases (268.53m to 427.97m) as shown in Fig (7). Therefore, valve life decreases due to water hammer effect. Thus, number of cycles should be considered in sensitivity analyses of water hammer effect in pressure conduits. For diminishing water hammer effect, theoretically pipes of exorbitant diameters should be used. However, considering economic aspects this is not a viable solution therefore optimum pipe diameter should be determined after performing several iterations. In the prevailing scenarios, a good criterion to establish a systematic design and/or develop maintenance-task should include the readiness to employ optimum internal penstock-diameter (and accessories) and lesser rigid pipe materials.

Different scenario analysis presented in this section conclude that the sensitive amplitude of pressure wave occurs at the end of pipe ($X/L = 1$), hence end of pipe must be considered as critical zone and should be designed accordingly.

Hydraulic Transient Analysis for Penstock Length (L) as variable

In the next phase fluctuations of pressure head for the change of penstock length calculated using prepared computer module. the penstock pipe length increases from 600 m to 1200 m, the corresponding increase in the values of maximum pressure head is 8.61% (291.66m) to 52.77% (410.23m); and the corresponding decrease in the values of minimum pressure head is 28.89% (82.96m) to 176.97% (-89.79m) as shown in Fig (11). On the other hand, with the decrease of penstock pipe length below the standard length (600m), the maximum pressure head value decreases while the minimum pressure head value increases. Present study indicates, as the penstock pipe length decreases from 600m to 100m, the corresponding decrease in the values of maximum pressure head is 8.54% (245.61m) to 38.26% (165.79m); and the corresponding increase in the values of minimum pressure head is 15.29% (134.5m) to 17.89% (137.53m) as shown in Fig (8)

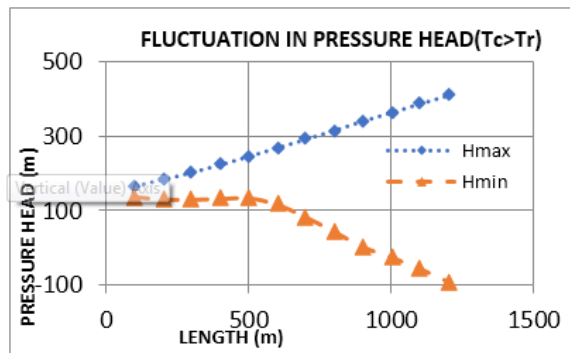


Fig. 8 pressure variation with changing pipe length

Present study showed that the Pipe length has control the reflection time ($T_r=2L/a=1\text{sec}$) and the inertia of water inside the pipe. The longer the pipe is (1200m), the longer the reflection time (2 sec), in addition, the longer the pipe, the larger the mass of water that has been affected on the moment of inertia of the water column, so that the pipe length is greater than 600 m in length (1200m), the risk of sub pressures exists ($-89.79\text{m} < 10.30\text{m}$) which may lead to produced cavitations as shown in Fig (8).

Hydraulic transient analysis by Wave velocity in penstock (a) as variable

In this study celerity of wave (a) is varied, while keeping other parameters (listed in table 1) as constant for the analysis of water hammer phenomenon in penstock, first assumed pipe wave velocity ($a = 1200 \text{ m/sec}$) as standard one and thereby incremental in celerity of wave by same proportions to the standard one, which results increased or decreased in the pressure head. by increasing the celerity of wave by 8% (1300 m/sec), to 33% (1500 m/sec); resulted in the maximum value of pressure head is decreased up to 4.01% (257.75m) and also the minimum value has increased up to 4.81% (122.27m). In second case when pressure wave is reduced by 8% (1100 m/sec) to 58% (600 m/sec) resulted the minimum value was decreased up to 75.89% (28.13m) and maximum value was increased 6.19% (285.16m) as shown in Fig 9.

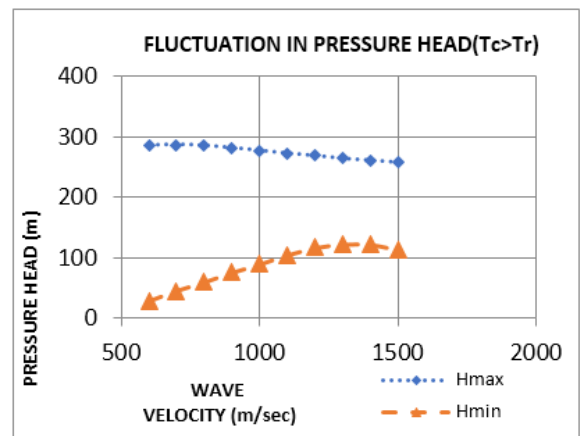


Fig. 9 pressure variation with varying wave velocity

The study showed, wave velocity also controls the reflection time ($T_r = 2L/a = 1\text{sec}$), higher wave velocity lesser the reflection time and vice versa. To avoid cavitations and pipe rupture, used higher wave velocity which was less than velocity of sound (1420 m/sec) i.e. $1000 > a <= 1200\text{m/sec}$, the reason is that in higher wave velocity lesser the reflection time so due this wave's sweep occurs more and rapid and this could encounter waves in opposite direction. It could be seen that increasing wave velocity would results in more increasing transiency.

Model Application

Keyal Khwar Hydropower Project:

The power conduit system of the Keyal Khwar HPP consists of between power intake and Underground powerhouse of a headrace tunnel of about 7.2 km length, a surge tunnel and a pressure shaft/tunnel of about 900 m length as the major components. The powerhouse accommodates two 5-nozzle Pelton turbines with vertical axis with a spherical valve as turbine inlet valve. The elevation of the needles of the Pelton turbine is at 685.0 m. At the rated turbine discharge of $10 \text{ m}^3/\text{s}$ the rated power is 63 MW. With the objective to assure a high degree of flexibility of plant operation, and to protect the headrace tunnel from excessive internal pressure fluctuations, a surge shaft has been provided by means of an inclined surge tunnel. Transient analyses were performed in order to assess the maximum and minimum heads in the pressure shaft/tunnel. The schematic system as applied to Keyal Khwar HPP is shown in Fig. 14.(WAPDA 2011)

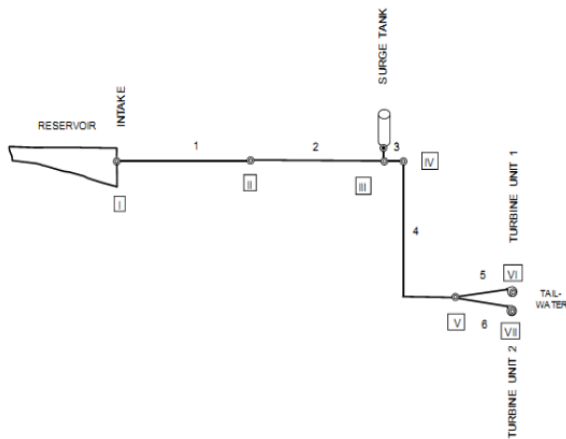


Fig. 10 Schematic Layout of Keyal Khwar HPP

At first a transient analysis was performed for regular load rejection subsequent to full load operation, i.e. with closure of the needles of the Pelton turbines. The results of the corresponding transient analysis are shown in the Fig. 15.

Table 2 Input Hydraulic data for Keyal Khwar Hydropower Project

Description of data	Data
Water level of reservoir	1422.5 m
Inlet level of valve	685.0 m
Diameter of Pressure Shaft(D)	2.2 m
Length of Pressure shaft (L)	900 m
Length of Surge Shaft	900 m
Discharge (Q_0)	20 m ³ /sec
Friction coefficient conc. lined in situ steel	0.002
Closure time of valve	30 sec
Maximum Pressure Head	1460.50 m

The corresponding maximum heads for the closure of the needles of the Pelton turbines in 30 s at FSL = 1422.5 m are: (WAPDA 2011)
 Maximum head at Power House = 1479.00 m
 Maximum head at beginning of pressure shaft = 1460.50 m

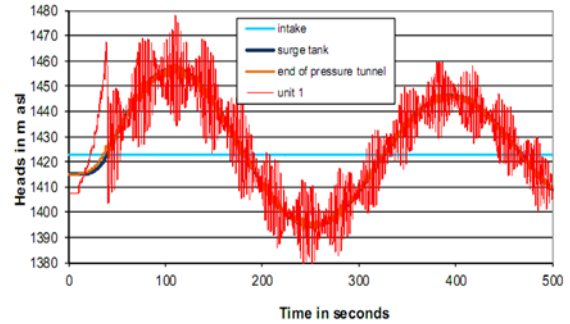


Fig. 11 pressure fluctuation due to slow valve closure by consultant computer program

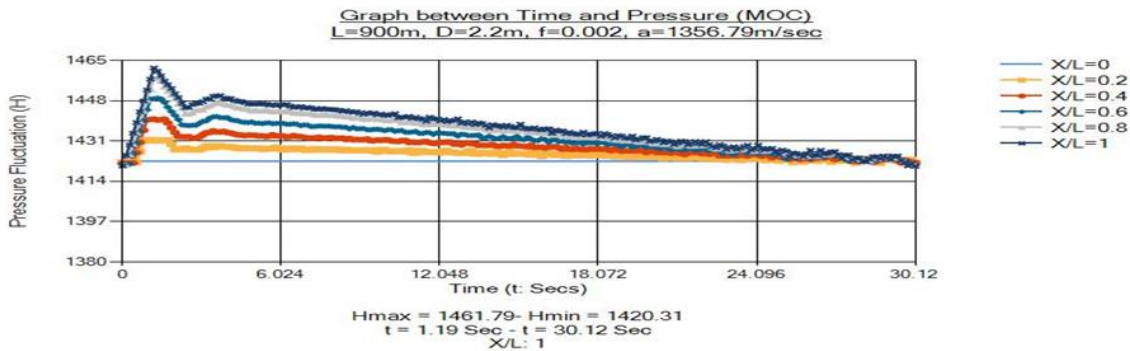


Fig. 12 Fluctuation of Pressure Head of Keyal Khwar HPP due to slow valve closure

Transient analysis in penstock with NMSAWHP.exe Penstock Diameter (D) as a Sensitive Variable

In this scenario increased the pipe diameter from 2.2m to 3.0m, the maximum value of pressure head (H_{max}) was decreased from 0.19% (1458.97m) to 0.92% (1448.37m) and the minimum value (H_{min}) was increased up to 0.08% (1421.46m), and decreased the pipe diameter by same proportion the maximum value of pressure head is increased up to 4%

(1521.61m) and minimum value is decreased up to 4% (1362.50m) respectively.

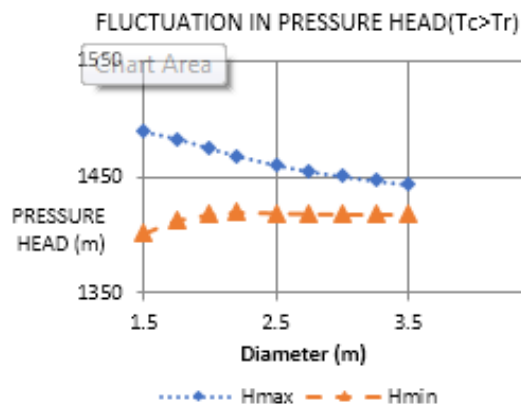


Fig. 13 pressure fluctuation by chaining diameter due to slow valve closure by MOC

Fig (13) also shows at 2.2m diameter of pipe, the pressure head, Hmax, and Hmin are 1461.79 m and 1420.31m respectively which were nearly equal to the value computed with CHARNETS software(1460.5m), which validate the developed program. Moreover, the maximum and minimum pressure head values are occurring at normalized length (X/L) of 1. This must be equipped with proper protection devices and design accordingly.

Conclusions

Those results reached above indicate that the water hammer magnitude is sensitive with respect to the penstock diameter. Study shows the decreasing exponential trends of water hammer pressure with respect to penstock diameter. Hence, it is evident that when pressure-amplitude increases, it poses greater vulnerability to the fluid-structure. Study also depicted, when the penstock-diameter is reduced, the number of water thrusts on valve increases for the same time period and magnitude of these thrusts also increases. Therefore, valve life decreases due to water hammer effect. Thus, number of cycles should be considered in sensitivity analyses of water hammer effect in pressure conduits. Study also depicted, that the Pipe length has control the reflection time and the inertia of water inside the penstock pipe. Generally, the pipe length is greater than 600 m in length, the risk of sub pressures exists which may lead to produced cavitation. Results indicated by high velocities i.e. above 1000 m/se, the pressure fluctuation range has decreased by multiple of 8% that may avoid cavitation and high-pressure problems.

Recommendations

The followings recommendations are made for

further study.

- I. No valve should be closed in less than 10 seconds, 30 seconds or more is preferable i.e. t_c (closure time) greater than or equal to t_r (reflection time = $2L/a$), to avoid any damage
- II. Use optimum diameter (i.e. 2.2m & 1.5 m) of penstock pipe in Keyal Khawar and Satpara Hydropower system respectively, to avoid any misshape due critical amplitude of transient wave.
- III. Study the pipe line profile along with pressure head line, if the distance between them is small, and then provide protective measure to minimize the effect of water hammer phenomenon.
- IV. The critical amplitude of transient wave occurred at along the normalized length (X/L= 1) of penstock pipe, so end of pipe considered being the most critical zone. It is required to provide protective remedial measure at normalized length (X/L= 1) of penstock pipe.

References

1. Abuaziah, A. Oulhaj, K. Sebari , A. A. Saber , D. Ouazar And N. Shakameh (2013). Modeling and controlling flow transient in pipeline systems. *Mar. Sci. Agron.* 3(1). PP. 12-18
2. Akan A. O. (2006). Open channel Hydraulics, Elsevier ltd, Jordan Hill, Oxford. PP. 315-330
3. Algirdas K., V. Kopustinskas and M. vaisnoras (2009). Water hammer model sensitivity study by the FAST method. *ENERGETIKA*, 55(1): PP. 13-19
4. Allievi L. (1925). Theory of Water Hammer, *E. Halmes, trans., Proceedings, American Society of mechanical Engineers.*
5. Araki. M. and T. Kuwabara (1975), Analysis of Pump-Turbine System Including Pipelines, *Hitachi Review*, 24(5).
6. Bernard. D (2013). Numerical modeling of water hammer effects in penstocks. M.Sc. Thesis, Department of Civil Engineering, University of Ottawa, Canada. PP. 1-226.
7. Chaudhry M.H. (1968). Boundary Conditions for Analysis of Water hammer in Pipe System. M.Sc. Thesis, Civil Engineering Department, the University of British Columbia. PP. 1-149.
8. Chaudhry M.H. (1979). Applied Hydraulic Transient. Van Nostrand Reinhold Company, Litton Educational, New York. PP. 45-64
9. Chao W. and J. D. Yang (2015). Water hammer simulation using explicit-implicit coupling methods. *Journal of Hydraulic*

- Engineering, ASCE, 4(141): PP. 04014086-96
10. Cooper and H.R. Johnston (2010). The effect of boundaries on water hammer waves. Final Year project, Civil and Natural Resource Engineering (NRE), University of Canterbury. PP. 1-10
 11. Fiszera ul. J. (2010). Mathematical model and numerical computations of transient pipe flows with fluid-structure interaction. Hydraulic machinery Department, the Szewalski institute of fluid flow, Gdansk, Poland. (14): PP. 77-94
 12. Jalil E. and A. Solemani (2011). Maximum water hammer sensitivity analysis. International scholarly and scientific research and innovation, 5(1): PP. 1-04
 13. Mansuri B., F. Salmasi and B. Oghati (2014). Sensitivity analysis of water hammer problem in pipelines. International Journal of energy and environment, University of Tebraiz, Tabriz. 5(2): PP. 124-131
 14. Mansuri B., F. Salmasi and B. Oghati (2014). Effects of pipe's roughness and reservoir head levels on pressure waves in water hammer. Journal of Civil Engineering and urbanization, Tabriz university, Tabriz. 4(1): PP. 36-40.
 15. Mosonyi .E and H.B.S. Seth (1975). The surge tank a device for controlling water hammers. Water power and Dam construction. 27(2,3)
 16. Norazlina S. and N. Amin (2015). Analysis of water hammer with different closing valve laws on transient flow of hydrogen-natural gas mixture. Department of mathematical science, University Technology Malaysia (UMT). PP. 1-12.
 17. Nemet A. (1974). Mathematical Models of Hydraulic Plants. *Escher Wyss News. No. 1*
 18. Parmakian J. (1955, 1963). Water hammers Analysis. Englewood Cliffs, N.J.: Prentice-Hall inc.
 19. WAPDA 2011. Detailed design report of Keyal Khawar hydropower project, Lahore.
 20. White F.M. (1979). Fluid Mechanics, McGraw-Hill inc., New York: various pages
 21. Wylie E. B. and V.L. Streeter (1967, 1978). Fluid Transient, McGraw-Hill inc., USA: 2(1), PP. 31-63
 22. Wuyi W., W. Huang and C. Li (2013). Sensitivity analysis for the resistance on the performance of a pressure vessel for water hammer protection, 136(1)

Physical modeling to control scouring under natural flow conditions

Farooq. R.¹, Ghumman A.R.^{2,3}, AlSaleem, S.S.³, Seemab, F.¹, Tariq. M.A.U.R.^{1*}

¹Capital University of Science and Technology, Islamabad

²University of Engineering and Technology Taxila

³Qassim University Saudia Arabia

*atiq.tariq@yahoo.com

Abstract: The most common reason for the failure of hydraulic structures is the scour phenomena at their supports. If the scouring is reduced/controlled 90% of failures can be avoided. Numerous mathematical models have been developed for sediment transport. However, scouring around the pier in case of cohesive soil has not been addressed satisfactorily. This lead to perform physical modeling under various recommended flow alteration techniques found in the literature. Many remedial techniques have been applied to control local scour. Mainly, there are two kinds of techniques to reduce erosion process near pier base i.e., bed armoring technique and flow alteration technique. Applying modifications in a pier is an effective technique to control scour. A number of methods have been employed to emasculate scouring process in order to assist the bridge designs. Present study aims to reduce the stagnation of the flow and vortex formation in front of the bridge pier by providing a collar, a cable and openings in combinations around a pier. The scour depth around octagonal pier was tested for various combinations of above modifications. Combination of a collar with cable around the octagonal pier reduced more scour depth than that for other two configurations. Similarly, the scour depth around the octagonal pier with collar and openings was less than that of octagonal pier with cable and openings. Providing a collar, a cable and openings together on the octagonal pier, found to be the best combination in reducing scour depth. It was found 49.4% less than that for the octagonal pier without any modifications. A plain octagonal and circular pier was also tested for maximum erosion depth which was found 14% less for the former pier.

Keywords: Erosion, bridge pier, collar, cable, openings

Introduction

Bridge plays vital role in transportation. Incidence of bridge failures due to scour at their supports is a common occurrence. The erosive process around pier starts due to the downward flow and resulting vortices system. The pier blocks the approaching water as a result velocity at the front face of pier reaches to zero causing an increase in pressure. Thus water level on upstream side of pier increases. As the flow velocity decreases from surface to the bed, the dynamic pressure on the pier face also reduces downwards. The downward flow creates a hole in front of the base of pier, rolls up and by interaction with the coming flow forms a complex vortex system.

Local scour around a bridge pier is the primary result of the downwards flow effect especially towards upstream face of pier. Actually, the downward flow initiates the formation of horseshoe vortex towards pier base that would ultimately increase the scouring process (Kumar et al. 1999), as shown in Fig. 1.

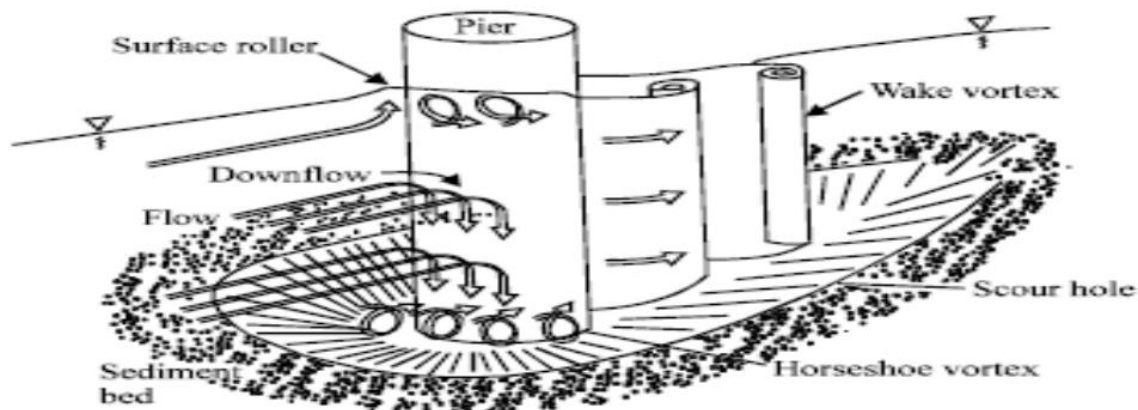


Fig. 1 Demonstration of flow and scour process around pier

Literature review

Local scour at circular bridge piers has been investigated by many researchers. In the river hydraulics, the local sediment scour at the bridge piers has resulted to be one of main reasons for the structure failure (Melville and Coleman, 2000). Whitehouse (1998), and Sumer and Fredsoe (2002) described scour around the bridge pier or pile in a steady current. They studied comprehensively the process of scouring at bridge piers from various aspects, including local scour mechanism & flow characteristics and anticipation of maximum probable scour depth.

Many studies are available in the literature encompassing various features of bridge pier scour in non-cohesive sediment beds including shape effects (Breusers and Raudkivi, 1991; Richardson et al., 1993; Melville, 1997; and many others). On the contrary, studies on local scour around piers on cohesive sediment beds are rather inadequate (Ansari et al., 2002; Debnath and Chaudhuri, 2010). Also, the above studies on bridge pier scour in cohesive sediment beds were carried out on circular piers. B.W. Melville (1975) explained that the downward flow behaves as vertical jet and moves the bed material. He also pointed out that downward flow initially erodes to develop the horseshoe vortex thus increasing the size of scour hole.

It was found in the literature that the shape of the pier can intensively affect the flow pattern around it. Tseng et al. (2000) and Richardson and Davis (2001) stated that the strength of the downward flow, horseshoe and wake vortices are greater in the case of square piers as compared to circular piers in non-cohesive sediment bed.

Many remedial techniques have been applied to control local scour around bridge piers. There are two kinds of techniques to reduce erosion process near pier base.

1. Bed armoring technique
2. Flow alteration technique

Zarrati et al. (2006) examined the application of riprap at the base of collared pier and found a significant reduction in sediment movement around the pier. They concluded that two collared piers in a line parallel to the flow direction with riprap at the bed, decreased erosion up to 60%.

A number of other pier modification techniques were also employed to dissipate effect of downward flow thus minimizing horseshoe vortex consequently reducing local scour. The present research is aimed at investigating the erosion around bridge piers by using pier modification techniques. One of the pier modification techniques that often used to minimize pier scour, is the provision of a collar. Fotherby et al. defined collar as a device built

around the pier base in order to block the removal of sediments at the pier. Collars of different shapes and varying thickness are practiced around the bridge piers as protective plates against the sediment removal (Melville and Coleman, 2000) and (Fotherby and Jones, 1993). The thickness of collar could be increased up to certain limit otherwise it would cause high turbulence in the flow resulting in excessive scour (Whitehouse, 1998). Zarrati et al. (2004) studied the effect of width of a collar on the local scour around pier and found that the optimum width of collar is thrice to that of pier in controlling erosion. Thus, in present study the width of collar equal to three times to that of pier, was kept for all the experiments. The provision of a collar initiates the scour on the downstream of the pier and forms a wake vortex there. This wake vortex progresses toward upstream to create horseshoe vortex. This horseshoe vortex enhances scouring thereby dissipating the effect of collar (Mashahir and Zarrati, 2002).

Entesar EL-Ghorab (2013) suggested a technique to provide openings on upstream side of a pier. These openings starting from upstream face of pier continue transversely to lateral sides and straight to the downstream side. In his experiments, he varied discharge, depth, size and vertical spacing of openings. He used opening size equal to 10%, 15% and 20% at vertical spacing of 0.5, 1.0 and 1.5 times the pier width respectively. He found that the opening size equal to 20% with vertical spacing 1.0 times the pier width was the best in decreasing flow pressure thereby reducing the scour.

Dey et al. (2006) and Elham and Manouchehr (2012) examined the provision of threading or cable around a vertical pier at different angles, i.e., 15°, 30° and 45°. They suggested that the cable wrapped at 15° with a cable-pier ratio of 0.15, was the most effective to countermeasure and weaken the downward flow effect causing horseshoe and wake vortices. The provision of threading around a vertical pier is an economical technique to minimize local scour.

Thus, in addition to a collar, other methods could also be adopted to countermeasure local scouring around bridge piers. These procedures include combination of a cable and openings around the pier. The main objective of this experimental investigation is to develop techniques whose application would make bridge piers safer and more strengthened against scouring action by stream flow and flood. These measures are providing protections to bridge piers, in the form of different combinations of collar, cable and openings.

Experimental procedure

Pier Alteration

Pier alteration is very essential as this component of bridge is directly affected by the scour action during normal and flood seasons. When the upstream flow collides with the pier, the water moves downward, all around the pier. This flow

acts on the bed resulting in the formation of horseshoe and wake vortices. In all the experiments, bridge pier models made of wood were used. The maximum width of both octagonal and circular piers equal to 7 cm was used. All other dimensions of pier and collar are shown in the Fig. 2.

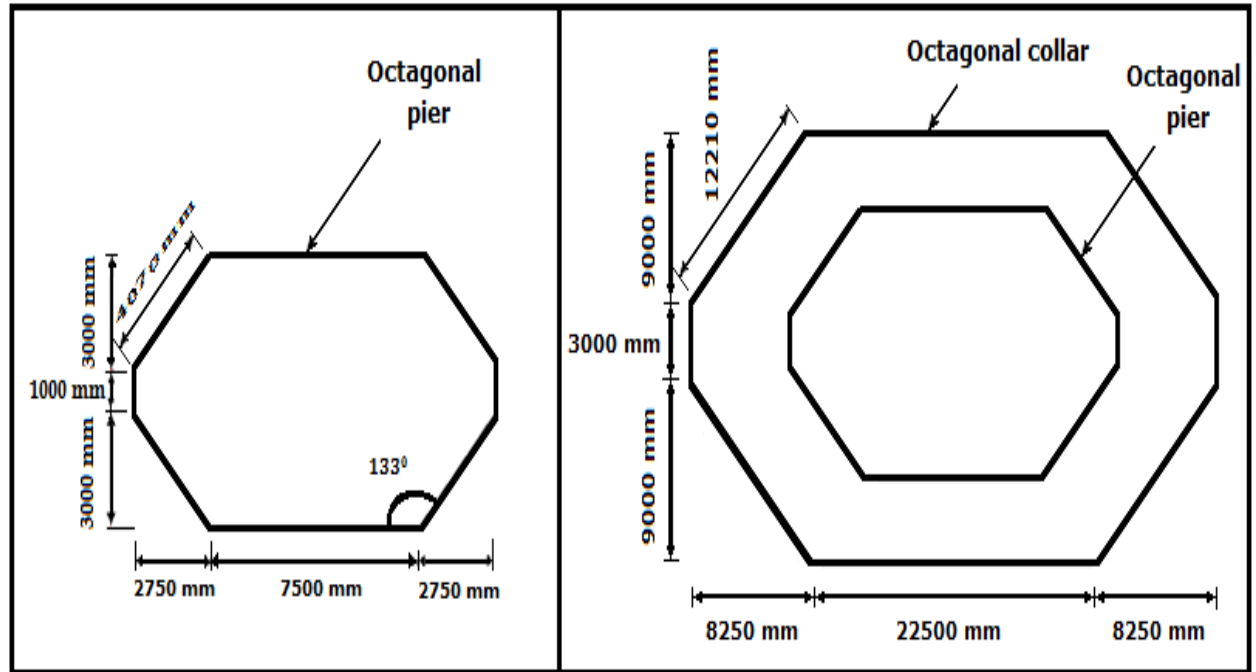


Fig. 2 Detail of pier

& collar dimensions

M.M. Abdel-Motaleb (1997) studied the provision of openings in the pier. In his experiments he used openings, each having a diameter equal to 10% of the pier width. R.J. Garde and U.C. Kothyari (1998) carried out experiments on pier models by providing a slot in the direction of flow. He found that the maximum scour depth reduced up to 30%. The upstream to downstream openings provided another path to divert the flow. This reduced the effect of downward flow velocity along the pier causing less scour.

Following are the details of the pier configurations as shown in Fig. 3.

1. In all collar-pier experiments, the width of collar equal to thrice to that of pier was maintained.
2. In all cable-pier experiments, the cable of thickness 10.5mm was wrapped around the pier. The vertical spacing between the cable loops was equal to width of the pier; in fact, each cable is parallel to the other.
3. In all openings-pier experiments, the diameter and vertical spacing of openings was 20% and 100% of the pier width, respectively.

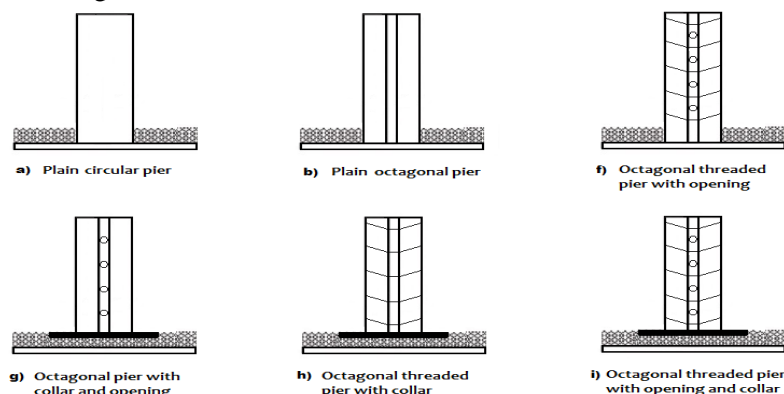


Fig. 3 Details of pier modification

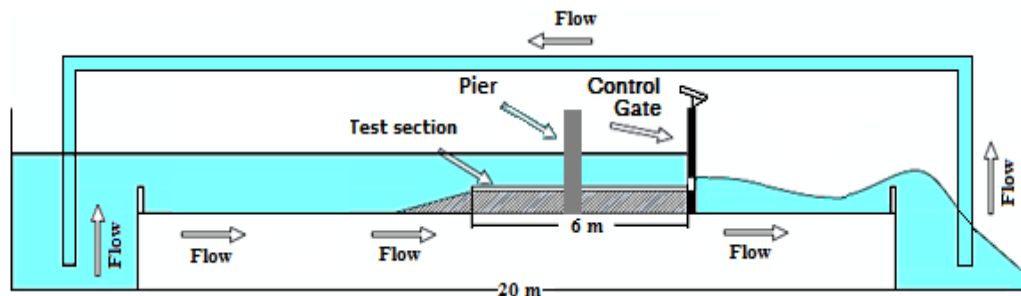


Fig. 4 (a) Cross section of Experimental channel

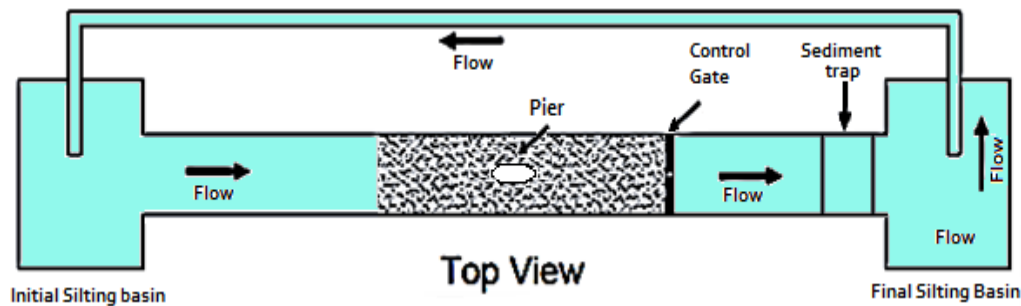


Fig. 4 (b) Top view of Experimental channel

Experimental Set-up and Materials

All the experiments were performed in a smooth rectangular flume (2000 cm length, 100 cm width and 75 cm depth) equipped with recirculating water facility. The flume is located in the Hydraulics Laboratory of Civil Engineering Department at University of Engineering & Technology, Taxila, Pakistan. The flume base is built of concrete and side walls are made of 12 mm thick glass sheet. For all experiments same flow conditions was maintained. Fig. 4a and Fig. 4b show a sketch of experimental setup.

The flume has a straight entrance with working segment consists of 600 cm long and 30 cm deep layer of non-cohesive uniformly graded fine sand material in which wooden pier is centered. The fine sand with grain size, i.e., $D_{50} = 0.28$ mm is used. The sediment used in the experiments is considered as uniform having specific gravity 2.79 and geometric standard deviation (σ_g) = $(d_{84}/d_{16}) = 1.21$; where d_{16} = diameter for which 16% by mass of sediments are finer; and d_{84} = diameter for which 84% by mass of sediments are finer. The standard deviation of grain sizes was $\sigma_g = 1.21 < 1.30$ to terminate the impact of non-uniformity of the bed material on scour depth (Zarrati et al., 2010). Particle size analysis of the fine sand is shown in Fig. 5.

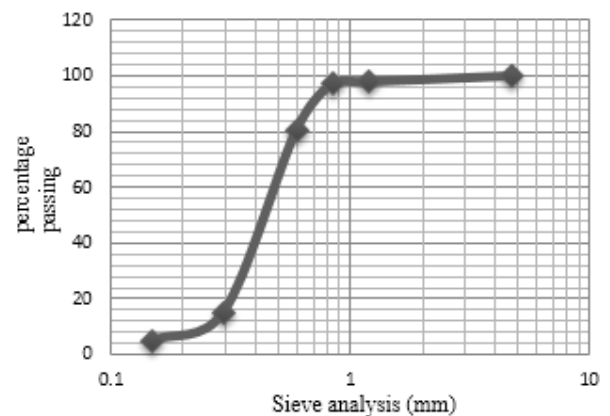


Fig. 5 Gradation curve for fine sand.

The experimental process was made out under clear water condition. At the end of the channel, there is a circular gated weir which control and measure the discharge. To measure flow velocity at different locations in the channel and also near stream bed digital velocity sensor is used. Similarly, due to scouring phenomenon, the scouring depth around vertical pier is measured by means of digital point gauge with an accuracy of ± 0.01 mm.

Testing Procedure

A series of twenty-one experiments on five different pier configurations, all under clear-water scour condition, were performed. For each experiment, the initial plane bed level was measured precisely. As the flow continues, the scour progresses at the bed until the equilibrium depth is reached. Same flow depth and discharge was maintained for all the experiments. In order

to monitor the eroded profile of scour hole, a meter rod attached with a small flat circular tip was used.

At the end of each experiment, water was drained off from the flume carefully to keep scour pattern unaffected from the draw down flushing. The scour holes and scour pattern profiles around octagonal pier were then accurately measured with the help of depth gauge. Finally, temporal development of scour for all pier configurations was plotted. Fig. 6 shows the description of experimental tests.

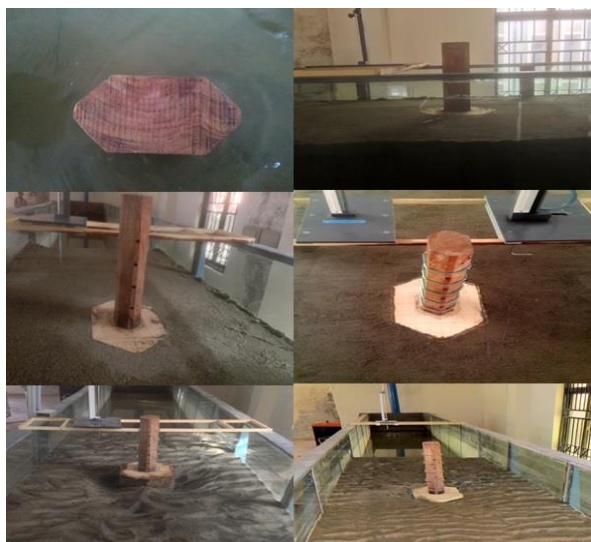


Fig. 6 Detailed experimental setup of bridge pier

Test Duration Effect

The equilibrium clear water scour depth is achieved asymptotically with time thereby it takes a very long time for the equilibrium scour hole to evolve. Several researchers have looked temporal development of scour depth experimentally under both clear water and live bed conditions. Due to clear water conditions, scour depth progresses slowly with time towards the equilibrium state. However, under live bed conditions, the scour depth reaches to equilibrium state rapidly (Chabert and Engeldinger 1956, Raudkivi 1976, Melville and Chiew 1999). The equilibrium scour depth under clear water is 10% more than that under live-bed conditions (Graf 1996). Based on their experimental work, a number of researchers have suggested time duration for scour depth to reach equilibrium state. Kumar et al. (1999) halted their experiments, as the scour depth did not vary over a period of 3 hours by more than 1 mm. Similarly, Mia and Nago (2003) stopped their experiments as the scour depth did not increase by 1mm over a period of 1hour. They also concluded that almost major scouring takes place after the first 3 to 4 hours. Melville and Chiew (1999) specified

the equilibrium time, when the scour depth did not vary by more than 5% of the pier diameter in the succeeding 24 hours and developed the following equation for the prediction of the equilibrium time for the clear-water condition.

$$\frac{ds}{dse} = \exp\{-0.03 \left| \frac{u}{Uc} \ln \frac{t}{te} \right|^{1/6}\} \quad (1)$$

Here 'ds' is the scour depth, 'dse' is the equilibrium scour depth, 'u' represent local velocity, 'Uc' is the critical velocity, 't' is the time and 'te' is the equilibrium time.

In the current study, a long-time experiment was performed for 12 hours according to the Melville and Chiew (1999) criteria. The results suggested that, depth of scour increases with time and there is a good correspondence between experimental results and equation (1) for the equilibrium time. It was observed that 90% of the equilibrium scour depth was achieved in the initial 3 to 4 hours. Since the peak flood flow may not last long enough to develop equilibrium scour depth, the duration for further experiments was maintained as 8 hours.

Results and discussion

In the current study, experiments were conducted to determine the effectiveness of pier modification on scouring action. In order to minimize scour around pier, different pier configurations were used. Initially, to examine the response of pier geometry on scour dynamics, two pier shapes, i.e., circular and octagonal, were studied under same flow conditions. After getting much satisfactory results from octagonal shaped pier, both in terms of overall spatial distribution and temporal development of scour, as shown in Fig. 7, further modifications and experiments were performed on octagonal pier.

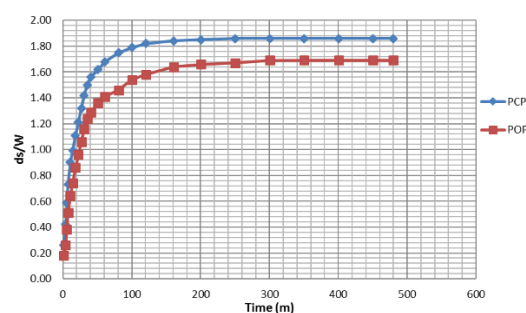


Fig. 7 Temporal evolution of scour at the upstream of pier

Temporal evolution of scour was analyzed specifically at the upstream of the pier for all the experimental runs. From the experimental results, maximum scour depth was observed for plain octagonal pier. The erosive action of downward flow caused horseshow vortex

resulting in maximum scour of octagonal pier as it was unprotected and without any modifications.

Three combinations of different configurations were examined, under same flow conditions, around octagonal pier, i.e., threaded pier with collar, threaded pier with openings and pier with openings and collar. The maximum scour depth for octagonal threaded pier with collar was found to be less than that of other two cases. The reduction in scour depth occurred due to provision of collar in combination with threads causing obstruction to downward flow and resulting horseshoe vortex. Initially scouring action blocked at the upstream of pier. The flow is shifted to downstream of pier forming wake vortex there resulting in small scour pits. These pits expand and progress towards upstream and initiate scour depth there. Due to this delayed process, the equilibrium stage of scouring takes more time. As the scouring action, for collared pier was started with delay, addition of threads makes pier more effective as it further delayed to start scouring due to which equilibrium time is longer than that of other two cases. Maximum scour depth around threaded pier with openings was observed to be less than collared pier with openings. The threads of cable obstructed the downward flow more effectively than the openings in the pier as shown in Fig. 8.

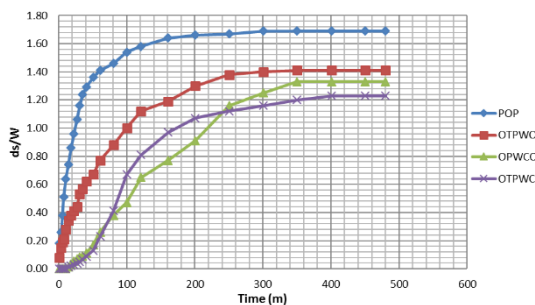


Fig. 8 Temporal evolution of scour at the upstream of pier

Table 1 Summary of Experiments

Sr. no.	pier shape	cab le	openi ng	coll ar	scour depth
1)	circula r	-	-	-	13.02 cm
2)	octago nal	-	-	-	11.83 cm
3)	octago nal	Y	Y		9.87 cm
4)	octago nal	Y		Y	8.61 cm
5)	octago nal		Y	Y	9.31 cm

6)	octago nal	Y	Y	Y	6.93 cm
----	------------	---	---	---	---------

However, the combination of all three modifications, i.e., provision of collar, threads and openings in the pier resulted in the most effective configuration in reducing scour depth produced by downward flow and the formation of horseshow vortex. Comparison of scour depth of plain circular pier (PCP), plain octagonal pier (POP), octagonal pier with opening (OPWO), octagonal threaded pier with collar (OTPWC), octagonal threaded pier with opening (OTPWO) and octagonal threaded pier with collar and opening (OTPWCO) were made as shown in Fig. 9.

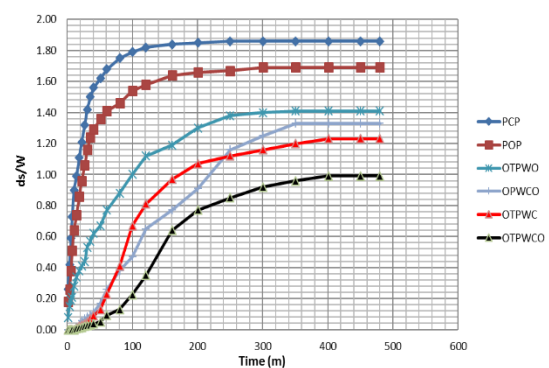


Fig. 9. Temporal evolution of scour at the upstream of pier

Conclusion

This experimental study aimed at assessing the capability of various pier modifications to minimize erosive power of flow acting on the river bed around bridge pier. The main objective of this research is to reduce maximum scour depth using a collar, cables and openings provided in the pier separately and in combination in clear water flow over mobile sand bed. It was concluded,

1. Under same conditions the maximum scour depth around octagonal and circular pier was monitored and found to be 9.1% less around the former pier.
2. The scouring under combination of different configurations was also determined. Octagonal threaded pier along with collar was more effective in reducing scour as compared to the other two cases. i.e., collared pier with openings and threaded pier with openings. For the first case the reduction of scour was 7.5% and 12.8% than that for the second and third case respectively.
3. A combined provision of collar, cable and openings in the pier found to be the most effective configuration for reducing scour.

The resulting scour was 41.4% less than that for the plain octagonal pier.

4. In all experiments of collared pier with different combinations, because scouring action started with delay, the equilibrium time was longer than those without collar.

References

- [1] Ansari, S.A., Kothiyari, U.C., Ranga Raju, K.G. 2002, Influence of cohesion on scour around bridge piers. *Journal of Hydraulic Research*, Vol. 40, NO. 6, pp. 717–729.
- [1] B.W. Melville 1975, local Scour at Bridge Sites, Univ. of Auckland, Auckland, New Zealand.
- [2] Breusers, H.N.C., Raudkivi, A.J. 1991, Scouring. *IAHR Hydraulic Structures Design Manual No. 2*. Balkema, Rotterdam, The Netherlands.
- [3] Chabert, J., and Engeldinger, P. 1956, Etude des affouillements autour des piles des ponts, (scour around bridge piers). *Laboratoire National d'Hydraulique*, Chatou, France.
- [4] Dey S., Sumer B. M., FredsØe J. 2006, Control of scour at vertical circular piles under waves and current. *Journal of Hydraulic Engineering*, ASCE, Vol. 132, No. 3, pp. 270–279.
- [5] Debnath, K., Chaudhury, S. 2010, Cohesive sediment erosion threshold: a review. *ISH Journal of Hydraulic Engineering*, Vol. 16, No. 1, pp. 36–56.
- [6] Entesar A.S. EL-Ghorab. 2013, Reduction of scour around bridge piers using a modified method for vortex reduction, *Alexandria Engineering Journal*, Vol. 52, pp. 467-478.
- [7] E. IZADINIA and Manouchehr H. 2012, Simultaneous use of cable and collar to prevent local scouring around bridge pier, *International Journal of Sediment Research*, Vol. 27, pp. 394-401.
- [8] Fotherby L. and Jones J. S. 1993, The influence of exposed footings on pier scour depths, *Proc. Hydraulic Engineering*, San Francisco, July 25–30, ed. H.-W. Shen, S. T. Su, and F. Wen, pp. 922–927.
- [9] Graf, W.H. 1996. *Fluvial Hydraulics*. John Wiley & Sons, N .Y.
- [10] Kumar V., Ranga Raju K.G. and Vittal N. 1999, Reduction of local scour around bridge piers using slot and collar. *Journal of Hydraulic Engineering*, ASCE, Vol. 125, No. 12, pp. 1302-1305.
- [11] M.M. Abdel-Motaleb, minimizing of scour around bridge piers using a new method for vortex reduction, *Ain Shams Engineering Journal*, (1997) Vol. 32, No.2, pp. 115–125.
- [12] Melville, B.W. 1997, Pier and abutment scour: integrated approach. *Journal of Hydraulic Engineering*, Vol. 123, No. 2, pp. 125–136.
- [13] Melville, B. W., and Chiew, Y. M. 1999, Time Scale for Local Scour at Bridge Piers, *Journal of Hydraulic Engineering*, ASCE, Vol. 125 No. 1, pp. 125-136.
- [14] Melville B. W. and Coleman S. E. 2000, Bridge scour. *Water Resources Publications*, LLC, Colorado, U.S.A., pp. 550.
- [15] Mashair M. B. and Zarrati A. R. 2002, Effect of collar on time development of scouring around rectangular bridge piers. *5th International Conference on Hydrosience and Engineering*, Warsaw, Poland, pp. 9.
- [16] Mia, Md. F., and Nago, H. 2003, Design method of time-dependent local scour at a circular bridge pier. *Journal of Hydraulic Engineering*, Vol. 129, No. 6, pp. 420-427.
- [17] Raudkivi, A.J. 1986, Functional trends of local scour at bridge piers. *Journal of the Hydraulics Division*, ASCE, Vol. 112, No. 1, pp. 1-13.
- [18] Richardson, E.V., Harrison, L.J., Richardson, J.R., Davis, S.R. 1993, Evaluating scour at bridges. *Hydr. Engrg. Circular No. 18 (HEC-18)*, Fed. Hwy. Admin., U.S. Dept. of Transp., Washington, D. C.
- [19] Richardson, E.V., Davis, S.R. 2001, Evaluating scour at bridges. *HEC18 FHWA NHI Federal Highway Administration*, US Department of Transportation, Washington, D. C.

- [20] R.J. Garde, U.C. Kothyari. 1998, Scour around Bridge Piers, PINSA 64, A (4), pp. 569-580.
- [21] Sumer, B.M., Fredsøe, J. 2002, The Mechanics of Scour in the Marine Environment. World Scientific, Singapore.
- [22] Tseng, M.H., Yen, C.L., Song, C.S. 2000, Computation of three-dimensional flow around square and circular piers. International Journal of Numerical Methods in Fluids, Vol. 34, No. 3, 207–227.
- [23] Whitehouse R. J. S. 1998, Scour at marine structures: A manual for practical applications. Thomas Telford publications, Thomas Telford Ltd, 1 Heron Quay, London, United Kingdom. pp. 198.
- [24] Zarrati A. R, Gholami H, and Mashahir M. B. 2004, Application of collar to contro scouring around rectangular bridge piers. Journal of Hydraulic Research, Vol. 42, No. 1, pp. 97–103.
- [25] Zarrati A. M., Nazariha M., and Mashahir M. B. 2006, Reduction of local scour in the vicinity of bridge pier groups using collars and riprap. Journal of Hydraulic Engineering, ASCE, Vol. 132, No. 2, pp. 154-162.
- [26] Zarrati, A.R., Chamani, M.R., Shafaie, A., Latifi, M. 2010, Scour countermeasures for cylindrical piers using riprap and combination of collar and riprap. Int. J. Sediment Res., Vol. 25, pp. 313–322.

Assessment of Defects, Remedial Measures and Development Prospects of Sick Jaglot Hydropower Project

Muhammad Waseem¹, Qaiser Karim^{1*}, Muhammad Kaleem Sarwar¹

¹Centre of Excellence in Water Resources Engineering, University of Engineering and Technology, Lahore, Pakistan

*qaiser.karim@yahoo.com

Abstract: This study was carried out to identify the major causes of failure of the project, suggest remedial measures and to explore the power potential of Sai & Damot nullah. A field survey was carried out to get essential data of civil works for the identification of major causes of failure and to propose the remedial measures. Hydrological, topographical and geological data analysis was conducted to explore power potential of both nullah's (Sai and Danot). Defects in Jaglot hydropower scheme includes wrong design of intake structure, unnecessary lengths of power channel, non-consideration of better/ideal power house site, channel construction on large fills in critical areas and insufficient cross flow structures. Defects in Jaglot hydropower scheme can be rectified by constructing tyrolean weir type intake, cross flow structure, spillway at RD 2.5, desilting base at RD 2.8, repairing of expansion Joint of Penstock and improving the cross section of power channel at same critical locations. Data analysis shows that power potential of Sai nullah can be enhanced from 1 MW to 177 MW by using a discharge of $0.77 \text{ m}^3/\text{s}$ from Damot nullah.

Keywords: Jaglot hydropower project; Assessment of defects; Remedial measures

Introduction

Due to its geo-strategic importance and increase in population, Jaglot was upgraded to tehsil headquarters. Accordingly demand of electricity for the town increased manifolds. Previously the energy requirements of the town were being met by a 100 Kw hydropower station constructed near Jaglot Town. The source of water for power generation was the Sai nullah, a right tributary of Indus River. In order to meet the increasing demand of the town, Public Works Department planned to install a new one-Megawatt capacity hydropower plant. A proper rectangular power channel was constructed to feed the new one-megawatt power plant (2 x 500 KW) through two penstocks. The power plant worked only for six and a half years during which it had a large number of failures due to various reasons. The last major failure occurred two and a half years back because of land sliding in which 800 m long section was washed away. It took almost two years to repair the system in which the section washed away was replaced by 800 m long 36 ϕ steel penstock pipe. During this time period the only permanent source of power supply to the area was the above mentioned 100 KW hydropower plant supplemented with a 250 KVA diesel generator for emergency. Keeping in view increased power demand of the people and strategic importance of the area it is necessary,

firstly, to rectify the one-megawatt power plant after thorough assessment of its defects, and secondly to explore the possible power potential of the Sai nullah and its tributary to meet the future demand of the area. This study was conducted to recognize and point out the main causes of failure of the one-megawatt Jaglot hydropower project, to suggest remedial measures for rehabilitation of the sick project, and to explore power potential of the Sai & Damot nullah's to meet the increasing power demand of the area.



Fig. 1 Layout of Jaglot Hydropower Plant

Defects in jaglot hydropower scheme

To identify the defects in sick Jaglot Hydropower, field survey was carried out and following objects were identified:

Inability to Utilize the Channel Capacity

One of the major problems is wrong design of intake structure. One megawatt plant was installed without any proper intake structure, due to which the limitation in availability of adequate volume of water for the power generation remains a permanent feature. Although adequate discharge in the Nullah is available but same cannot be tapped, due to inappropriate design of intake.

Illegitimate Extension of Power Channel beyond the Requirement

On carryin out physical survey, it was found out that the length of power channel was unnecessarily increased which was not the site requirement due to which the channel extended into a stratum having unstable formation with a very frequent record of land sliding during the raining and snowing season. Because of this reason there were extensive breakages of power channel due to landslides. The worst example is that of due to a land slide, the power plant remained closed for over one and a half year in years 2004 and 2005 causing extensive loss to the scheme and over expenditure of funds for the channel construction.

Non-Consideration of Better/Ideal Power House Sites

There are two power houses sites i.e. site A and site B which are at a reduce distance of 1.775 km and 2.500 km from the inlet gate having an available gross head of 95 and 85 meters respectively. At the site ample space is available for the construction of powerhouse, the proposed foundation of power house and supports of penstock lie on the solid granite rock. The site B allows the construction of the penstock with supports foundation on solid rocks of graduraid formation and the foundation of powerhouse can be laid on solid firm strata. Had these options been considered, the cost of the project would have been reduced to a considerable extent and the problem of land sliding would have been minimized. The maintenance and the operating cost would have been reduced to a mark difference and the project would have been financially conductive project.

Channel Construction on Large Fills in Critical Areas

It has been observed that in gorges of the rocky strata, the head race canal has been constructed on the well compacted fill. No cutting and blasting of the rocks were observed in turn large dry masonry retaining wall having depth upto 15 to 20 feet were observed. The detailed checking revealed that there were a large number of breakages due to rock falling and washing away of channel by flash water current created by storm water.

Insufficient Cross Flow Structure

The power channel has been constructed on the forward slopes the mountain, while constructing the channel due consideration had not been given to the storm/rain drainage of the mountain. The channel linearly crosses all the natural courses of water, but no cross-flow structures had been constructed on the channel. However, later on eight cross flow structures were added but were not properly designed as per the expected loading and flow conditions. As a result, all of them were damaged. Eight cross flow structures against the requirement of twenty are grossly insufficient to cater for the storm drainage of the project area.

Unstable Strata

The power channel passes through a number of unstable strata consisting of sandy gravel and morain. While passing through these stratas no additional reinforcement in bed and beds foundation been provided to safeguard against settlement and seepage.

A number of failures were observed due to the leakage/seepage of water through the foundations/bed. The seepage water saturated the underneath strata causing it to flow under self-weight resulting into failure of water channel.

Reduction in Cross-Sectional Area of Power Channel

Reduction in cross-sectional area of power channel without any valid limitation of slope or depth was observed at a number of places.



Fig. 3 Reduction in cross-sectional area of power canal.

Insufficient Side Wall Height

The height of wall of the head race canal is grossly insufficient to stop any sliding boulder/stone entering the power canal. During rain a lot of water enters the power canal as the shoulders/walls of the power canal is at level or lower than the uphill surrounding area.

Head Loss

During the survey it was observed that without any solid valid technical reasons/limitation a fall of 9 m was created at RD 2.4 km causing a head loss of 9 meters. On enquiring from local villagers, it revealed that the construction of channel started from both intake and powerhouse ends when both ends being constructed closed together a 9 meters elevation difference between channels was observed to counter it a 9 m fall was constructed.



Fig. 4 Head loss due to water fall

Penstocks

Length of Penstock

For utilizing 85 m head for the power generation. The length of penstock laid is over 800 meters which is a very expensive affair as compared to

the construction of same length of water channel and utilizing the previous existing penstock facility.

Splitting of one Penstock into Two

The first 750 m of penstock is a single pipe of 36-inch dia, approximately 50 m short of powerhouse this pipe through a thrust block was split into two pipes of 30 inches dia each. The angles substandard by the downstream and upstream turbine feeding pipe is 90° and 130° respectively.



Fig. 5 Splitting of one penstock into two.

Following were the affects:

- i) As per the operators and own observation: The turbine and generator were giving rated output i.e. 500 KW but the upstream couple was giving an output of 325 to 350 kilo watts against its design capacity of 500 kw.
- ii) When only the upstream generator is operated its output does not go beyond 350 kw.
- iii) The synconsisation of both generators have been disturbed due to which

upstream generator was burnt three times costing repairs bill more than 1 crore 10 lacks.

Failure of Electric Distribution System

The electric distribution system failed due to non-synchronisation of generators. Due to this reason the electric distribution has been affected. The electricity produced by both the generators is being supplied to the consumers through separate transformers and electric lines made a short fall in the supply and demand.

Missing of Desilting/Sediment Control Structures

a) Desilting Sediment Control Structures

In this Micro hydropower scheme besides the other problems previously mentioned, the desilting basin is missing due to which, this scheme is facing a lot of breakage of Mechanical equipment and furthermore the entire length of the power canal has to be desilted manually. Although the running water is generally snow melt clear water having negligible sediments (very less quantity of sand or silt), but as soon as it drizzles, light or medium rain occurs. The quantity of sediments increases many times. As the channel has not been designed on non-scouring non-silting velocity, the bulk of the clay, silt and sand settle down in the bed of the channel due to the low velocity of water in various stretches of power channel. The manual desilting of the entire channel is colossal and it is an inefficient job due to the dimension of the channel and the constant running water conditions. This becomes a major reason of the enhanced operating and maintenance cost of the project/system.

Spillways

In the project no spillway or over flow structure has been incorporated in the design of head race canal. During the rains the rain water of almost 4 km linear length of mountain enter the water channel resulting into its spill over at various sections causing extensive damage to it. The damage is of a much higher degree where the natural course of water is disputed specially in gorges and depression where the channel has been made on fill with the help of retaining structures.

Forebay Intake

There is no properly designed forebay for housing of penstock pipes and any desilting arrangements for the protection and safety of the mechanical equipment is also missing. For this

reason, there is excessive wear and tear of the turbines blades and other mechanical equipment causing repeated break down of the power supply causing unnecessary loss in revenue and excessive maintenance expenditure which otherwise could have been avoided.

Jaglot hydro power plant rectification of defects/ remidial measures

Water Rights

The people should only be allowed to take water from Irrigational channels. Use of water from power channel should be forbidden.

Weir

A Retaining wall type, free over fall weir at Rd 17.4 Km of Sai Nullah should be constructed to maintain a constant water level to ensure that a smooth flow enters the power canal be throughout the year irrespective of low or high flow conditions.

Tyroleon Weir construction

A proper Inlet Structure may be constructed for getting adequate quantity of water during Low flow conditions and for desilting of water. The construction of Tyrolion weir is most appropriate solution

Protective and Safety works

The construction of protective works as per the site requirement such as Raising of Channel side walls, Breast Walls, retaining walls, RCC Chanel in the unstable stratas (deep fill etc), Enroute Over Flow structures for disposal of Mountains Run off water may be constructed as per site requirements.

Cross Flow Structures

The Cross flow structure may be redesigned with steeper slopes (>30*) having wing structures as per site requirement may be constructed .

Spillway

The Spillway may be made on solid rock next to proposed cross flow structure at Rd 2.55.

Desilting Basin

Desilting basin may be made on solid rock at Rd 2.8.

Penstock

Redesigning of main penstock splitting from one 36-inch pipe to two 30-inch pipes be done as a smooth curve transition to avoid Eddies and cavitation and for better Synconisation of Generators. The damaged joints should be repaired and worn out rubber seals may be replaced.

**Proposed future development to enhance the power potential
Power Potential of Sai Nullah**

At present only 1 MW hydropower station has been established on Sai Nullah whose mean average flow is more than 10.4 cumecs. The power channel discharge carrying capacity can be enhanced by removing its deflects and slight modification in its design:

Table 1 Power Canal Design Data

Sr. No.	Design Parameter	Design Value
1	Depth of power canal	1.20 m
2	Width of power canal	1.50 m
3	Depth of flow	0.95 m
4	Bed slope S_o	0.002
5	Stone masonry , n	0.019

As it can be easily observed that the best possible dimensions of rectified channel will be = 1.2 m x 1.50 m with depth of flow 0.85 m. This would give a discharge of 1.86 cumecs. This discharge can be utilized for power generation. With available width of channel as 1.85 m, a discharge of 2.5 m³/sec can be passed through plastered stone masonry rectangular section.

By using the available discharge at new site, the gross available head is 85 m. The additional power potential of Sai Nullah will be as under:

$$P = \eta g H Q$$

$$= (0.85) \times 9.8 \times 2.5 \times 85 = 1.77 \text{ MW}$$

Penstocks

It is recommended that there should be one penstock one having a capacity of 2 cumecs. The dia of the penstocks can be calculated by using the relations as mentioned in methodology for permissible loss of 5% will be as under. The proposed dimensions of the penstocks will be:

$$D = 2.69 \times (n^2 Q^2 L/H)^{0.1875}$$

$$D = 2.69 (2^2 \times 0.012^2 \times 170/80)^{0.1875}$$

$$= 0.765 \text{ m}$$

Say 1.1 m

**Poer potential of damot nullah
Damot Nullah Power Canal**

A hydropower plant may be designed on winter available discharge of the Damot Nullah i.e. 0.77 cumecs. The section recommended for proposed Damot Gah Scheme is of stone masonry well plastered in trouble free areas. RCC section for the suspected area of land sliding and area suspecting free fall debris and boulders. The recommended channel section is as given in the following table:

Table 2Power Canal Design

Sr. No.	Design Parameter	Design Value
1	Channel Depth	0.9 m
2	Depth of flow	0.65 m
3	Channel Width	1.00 m
4	Channel Bed Slope	0.002
5	Discharge, Q	0.77 cumecs

Power Potential of Damot Nullah

By using design flow of 0.77 m³/sec from Damot Nullah the data will be as follows:

Head available, H = 80 m
 Discharge available, Q = 0.77 cumecs
 $P = g H Q \eta$
 Power, P = (0.85) x 9.8 x 0.77 x 80 = 513 KW

Forebay

A rectangular structure with the following dimensions can be made to house the pair of the penstocks.

Length:	15 m
Width	4.5 m
Depth	3.5 m

The structure is located on semi-hard rock formation which is granodiroid having ample space to house the structure. The alignment and the location are shown in the Fig. 6.



Fig. 6 Proposed site of forebay

Penstock

A pair of penstocks of 130 meters of length having 0.70 m internal dia are proposed which will be housed on the supports following the ground profile which has an approximate slope of 75°.

Powerhouse

An external type powerhouse at an elevation 1710 m.a.s.l. is proposed. It will be equipped with 2 units having an input of 80 m heads and using a discharge of 0.38 cumecs each which will give an output of 0.25 MW each.

Tail Race

A tail race of 200 m length having a cross sectional area of 1 m x 1 m can be proposed. The 1st 100 meters will require a digging of 4 m to enhance the head of the scheme.

Conclusions

- The one Mega Watt hydro Power Project on Sai Nullah had neither been thoroughly planned nor had it been executed.
- Standard Engineering practices such as site Investigations, Proper Labourity testing, Site Survey, Topographic Survey, Geological Mapping, Project lay out optimization and Design had not been done.
- The Northern area PWD planned and executed the project with least technical Knowledge, Skills Qualifications and knowhow of construction of hydropower projects
- The planning and Execution had been done by Northern area PWD. The Operation and Maintenance is still not in their responsible hands. Any minor or major repairs still takes considerably long time due to inter departmental tussle. It should be transferred to WAPDA for better Efficiency.
- The length of power canal had been increased without any technical justification

/requirement resulting in a substantial increase in Project and project's O&M costs.

- To avoid future land sliding /power canal failure by employing 800m long 0.92 m dia pipe was not a technically and economically a sound solution.
- Splitting one 0.92 m dia Penstock into two (Y shape) of 0.769 m dia pipes in 15 m length through smooth transition to avoid eddies and hydraulic losses is hydraulically a sound solution.

Recommendations

- All the defects as pointed in previously, essential for the safe and trouble-free operation of scheme may be rectified on priority.
- Missing structure may be constructed on priority.
- At present the channel depth and width is 1 m and 1.75 m respectively. The depth of flow in the channel is 0.8 meter. The depth of the channel should be increased to 1.8 m and depth of flow should be kept as 1.5 m. The site permits such a modification in dimensions. This increase in dimension should only be upto RD 1.775.
- The existing stone masonry channel should be well plastered to reduce the frictional losses and enhance the velocity of water in the channel. With this development the enhanced channel capacity theoretically will enhance as per the manning equation:
- Site A at RD 1.543 km having a power generating potential of over 2 MW provides good site conditions for the construction of a powerhouse with a shortfall of steep gradient

(angle of elevation of penstock will be having a vertical angle of 70° to 75°).

f) Damot Nullah scheme having a power potential of over 0.5 MW may be developed to enhance the power production to meet present and future power demand.

g) The existing small HPP in Northern Areas having problem in generating continuous power may be checked in the field to rectify the problem and to improve power and energy production.

References

- American Society of Civil Engineers. 1989. Civil Engineering guidelines for planning and designing hydroelectric developments. Small scale hydro, Vol. 4.
- C.C., Warnick in collaboration with Howard A Mayo Jr. P.E./James L. Carson/ Lee H. Sheldon, P.E. Hydropower Engineering. Published by Prentice-Hall Inc. Englewood Cliffs, NJ.
- COE, U.S. Army Corps of Engineers, 1979. Hydropower Cost Estimating Manual.
- COE, 1979. Feasibility Studies for Small-Scale Hydropower Additions: A Guide Manual.
- Daughery, R.. and J.B. Franzini. 1977. Fluid mechanics with engineering applications.
- GTZ-WAPDA. 1999. Layout and Sizing; High Head Hydropower.
- GTZ-WAPDA. 2000. Hydropower in General, High Head and Low Head Hydropower.
- GTZ-WAPDA. 2000. Power Plant Components; High Head Hydropower.
- Habib, Zaigham & Miarcel Kuper. 1998. Performance assessment of the water regulation and distribution system in the Chishtian subdivision at the main and secondary canal levels. IIMI-Pakistan National Programme, Report No. R-599.
- Jarle Ravn. 1992. Planning and Implementation of Hydropower Projects; published by Norwegian Institute of Technology Division of Hydraulic Engineering.
- John J. Cassidy. 1984. Site Development and Hydraulic Analysis, published by McGraw-Hills Book Company, London.
- L. Monition M. Le Nir and J. Roux. 1984. Micro Hydroelectric Power Stations; translated by Joan McMullan; A Wiley Interscience Publication
- Layman's guide. 1993. How to develop a small hydro site. European Small Hydropower Association. Mosonyi, E. 1986. Low Head Power Plants.
- McKinney et al. 1983. Micro hydropower Handbook, 2 vols. U.S. Department of Energy. A basic manual for very small hydro applications.
- Noyes, R. 1980. Small and Micro Hydroelectric Power Plants, Technology and Feasibility.
- Peurifoy, R.L. and Ledbetter, W.B. 1985. Construction planning, equipment and methods. McGraw-Hill Co., Fourth Edition.
- Punmia, B.C. and Pande B.B. Lal. 1983. Irrigation and water power engineering.
- Sarwar, K. M. 2005. Application of HPC model for the optimum layout of Bunji Dam Hydropower Project. M.Sc thesis of CEWRE, UET, Lahore.
- William P. Greager and Joel D. Justin. Hydroelectric Handbook, published by John Wiley & Sons, Inc. New York.

Double-Stilling Basin Modelling, Pakistan – Case Study

Ubaid Ullah^{1*}, Eric J Lesleighter², Muhammad Iqbal³, Umair Mannan⁴

¹Principal Hydraulics Engineer, Engineering General Consultants (Pvt. Ltd.), Pakistan

²Lesleighter Consulting Pty Ltd, Sydney Australia,

³Principal Hydraulics Engineer, Associated Consulting Engineers (Pvt. Ltd.), Pakistan

⁴Senior Hydraulics Engineer, Associated Consulting Engineers (Pvt. Ltd.), Pakistan

*ubaid006@gmail.com

Abstract: The Mohmand Dam is a 213m tall concrete-faced rockfill dam (CFRD) under design by a consortium of consultants in Pakistan. The consortium comprises SMEC International (Australia), Nippon Khoe (Japan), National Engineering Services (Pakistan), Associated Consulting Engineers (Pakistan), Engineering General Consultants (Pakistan), and BAK Consulting Engineers (Pakistan). The dam is for construction on the Swat River in Pakistan. A strategic component of the hydraulics studies has been large-scale physical model studies carried out by the Irrigation Research Institute, Pakistan. The paper will discuss in detail the use of, and the hydraulic behavior of a double hydraulic jump stilling basin facility incorporated in a 600m long concrete chute. The upper basin was designed to operate with a maximum head of about 100m, and the lower basin was designed to operate with a maximum head of approximately 120m with respect to tailwater level. The studies considered discharges up to approximately 25,500 m³/s. Detailed pressure transducer measurements of transients as part of the design of the basins, and the chutes incorporated several aerators along the length of the chutes.

Keywords: Dams, spillways, hydraulic jump basins, energy dissipation, turbulence, pressure transients.

Introduction

The Mohmand Dam Hydropower Project (MDHP) is a large power project to be built on the Swat River approximately 200 km northwest of Islamabad. The location of the dam is illustrated in Fig. 1. The project investigation and design passed through several studies with a detailed feasibility study preceding the lengthy study that derived the double-stilling basin spillway arrangement – the subject of the present paper. The work, comprising site and dam selection, detailed hydrology, reservoir sedimentation aspects, power station sizing, diversion detailing, and hydraulics progressed the earlier feasibility studies and all has been carried out on behalf of the Water and Power Development Authority (WAPDA) by a consortium of consultant companies.

The diversion works comprise two 15m diameter tunnels. One is to be developed into a permanent, low level outlet facility for necessary releases to the downstream and for drawdown purposes. The power intake will direct flows into a separate tunnel leading to an 800MW power station on the right bank of the river a short distance downstream of the dam and near the spillway discharge location.

Hydrology

In July 2010, the Swat River experienced extreme flooding with a discharge estimated as 9,909 m³/s and considered to have an Annual Exceedance Probability (AEP) of 1 in 1,000. The return periods for the Project went through a number of studies, updating and finally an accepted series of magnitudes. It was confirmed by WAPDA in January 2016 that the Project design team should adopt a panel of expert's recommendation for the Probable Maximum Flood (PMF) of 27,427 m³/s inflow discharge. The computed peak value for AEP 1 in 1,000 and 1 in 10,000 are 10,669 m³/s and 18,640 m³/s, respectively. Fig. 2 presents the inflow flood hydrographs at Mohmand Dam site.

As will be described below, the energy dissipation arrangement selected a two-stilling basin arrangement. The flood routing yielded a PMF outflow discharge from the reservoir of 25,362 m³/s. For the spillway energy dissipation design the design discharge was selected as 90% of the PMF for the upper stilling basin and the AEP 1 in 10,000 discharges for the lower basin.

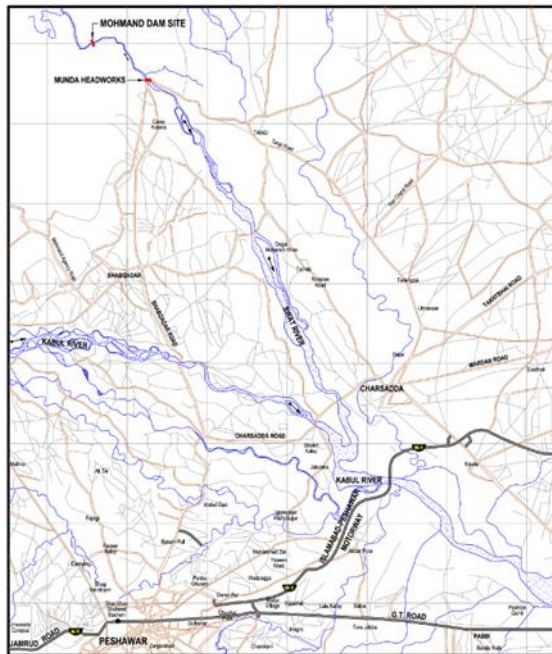


Fig. 1 Location of Mohmand Dam Project, Pakistan

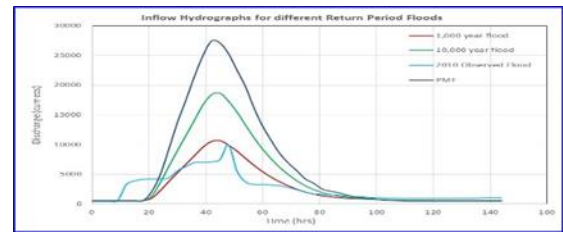


Fig. 2 Inflow flood hydrographs

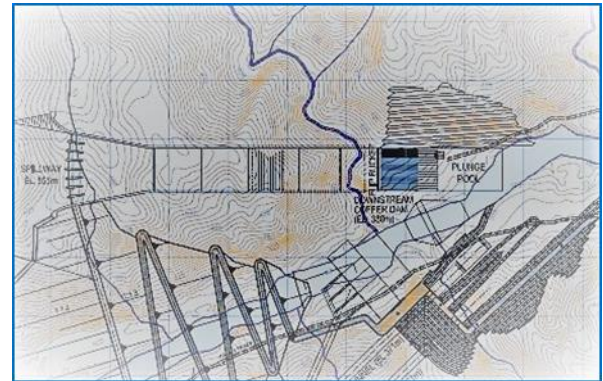


Fig. 3 Early Plunge Pool arrangement

Spillway type and key dimensions

The proposed spillway was to be located on the left abutment of the dam, following the dam-type selection of a concrete-faced rockfill dam (CFRD). The type of spillway received detailed consideration. Originally, the project commenced with the plan to use a flip bucket and plunge pool energy dissipation arrangement, for which the plunge pool pre-excitation would be a large-volume depression on the river's left and against a steep excavation of the hill on the spillway's left. Essential to the provision of an acceptable plunge pool dissipater was the consideration of rock scour and its longitudinal and lateral extent. Even the pre-excitation of the plunge pool would require a large slope excavation on the left side. The site investigations revealed rock largely classified as a foliated schist. Based on the Consultant's experience it was considered very erodible under the action of velocities around 45 m/s.

The main issue with the plunge pool erosion, apart from a likely depth to 60m below river bed level, was its lateral expansion and movement with the result that the entire left hill excavation would be undermined and be subject to collapse. Fig. 3 is a portion-plan of an early plunge pool possibility; it shows the large excavation on the left side of the plunge pool. Such collapse in turn would produce a large volume of scoured and collapsed material to form a huge blockage in the river, affecting the power station, the permanent outlet works and the spillway itself.

The flip bucket-plunge pool arrangement was abandoned, and consideration moved to the application of a hydraulic jump stilling basin alternative as the means of dissipating the energy from the spillway. The dam with a crest level at EL 563, and a parapet wall level at EL 564.5, would provide for a reservoir with a full supply level of EL555m, and a spillway crest level of EL 539m.

Several chutes and stilling basin arrangements were contemplated. The headworks also passed through several alternatives for the number of gates, and whether part of the spillway would remain ungated with the crest at FSL. The result was seven gates, each 15m wide, and piers 5.3m thick, all placed on a curved crest alignment on a 500m radius. The chute was converged from the total gross crest width of approximately 137m to a width of 100m. This led to a unit outflow discharge at PMF of approximately 255 m²/s.

With a reservoir level in the region of EL 560 and the river bed in the dissipation area at EL360, clearly the 200m head placed stringent conditions on the spillway design. Early considerations of a single stilling basin indicated basin inflow velocities around 60m/s, and in due course it was decided to investigate the use of a double stilling basin configuration, somewhat similar to the arrangement used some decades earlier on the Mangla Dam spillway, also in Pakistan. The investigation of the double basin configuration is the thrust of this paper. Detailed physical model studies were carried out at the Irrigation Research Institute (IRI), Nandipur, Pakistan.

Fig. 4 shows a plan view of the spillway and Fig. 5 a profile, depicting the chute from the headworks into the upper basin with an end weir

and discharge into the lower basin with an invert level at EL348.

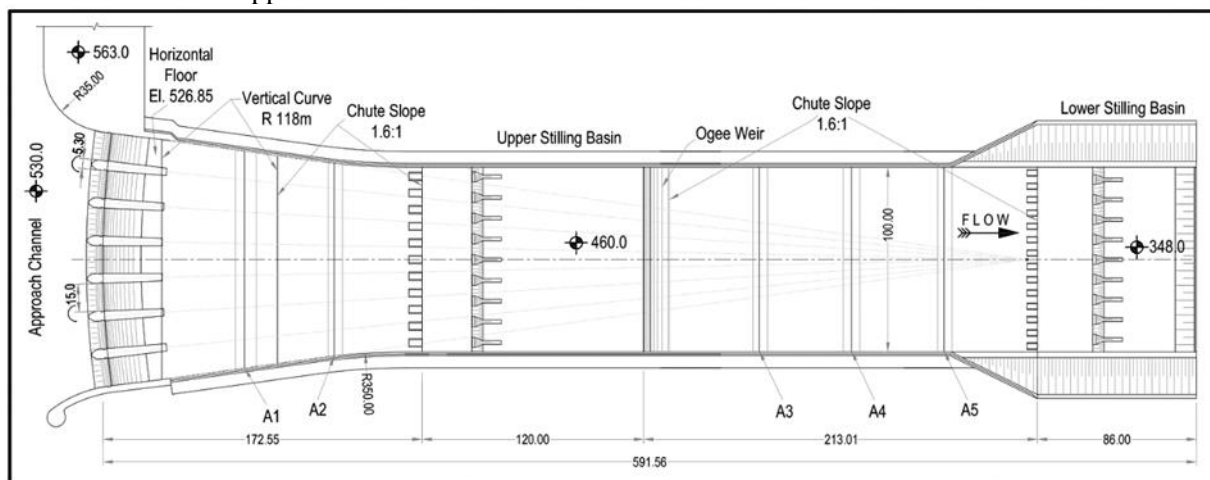


Fig. 4 Plan of the double basin spillway

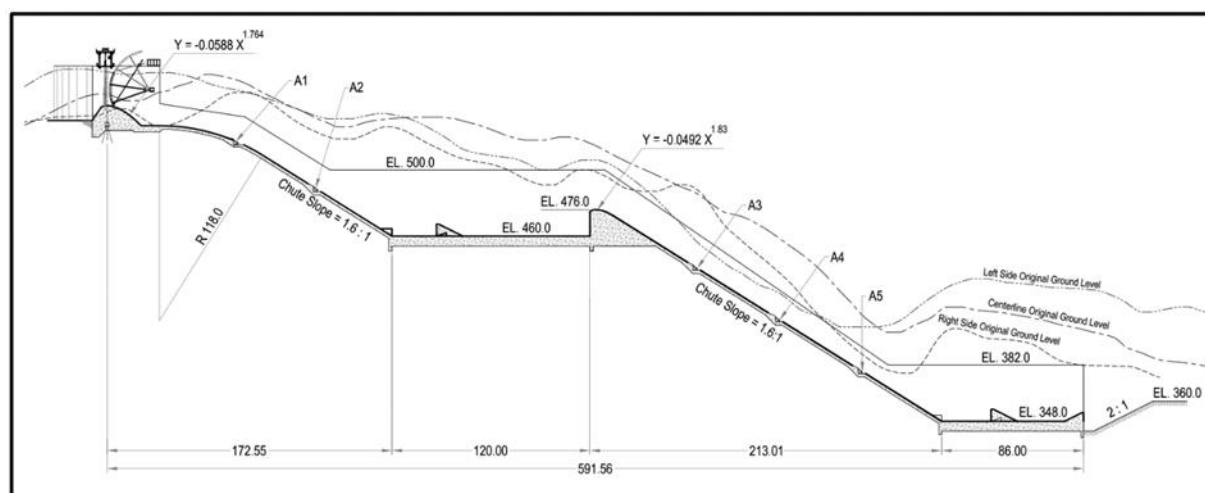


Fig. 5 Profile of the spillway

The upper basin was designed to operate with a maximum head of about 100m, and the lower basin was designed to operate with a maximum head of approximately 120m. The studies considered discharges up to approximately 25,500 m³/s. Detailed pressure transducer measurements of transients in the upper basin were made as part of the design of the basins, and the chutes incorporated several aerators along the length of the chutes, the geometry of which was studied and varied on the hydraulic model.

Hydraulic model description

The model was built and tested with a scale of 1:60. Fig. 6 shows a general arrangement plan of the model boundary. Each stilling basin was designed initially with estimation of spillway losses, and basin length and depths based on the hydraulic jump characteristics, on the basis that a USBR Type III arrangement would be used. The

basins were provided with conventional chute blocks, and baffle blocks were sized according to the jump characteristics and the USBR guidelines on sizes and spacing. The model was constructed in Perspex and instrumented with many piezometers and several locations for pressure transducers. Fig. 7 is a view of the model in operation with a AEP 1 in 10,000 discharge, and Fig. 8 shows the lower basin at AEP 1 in 1,000 discharge.

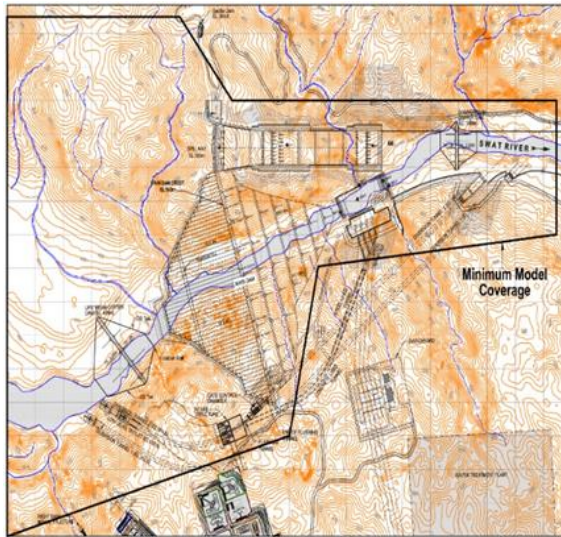


Fig. 6 Coverage of the spillway model

The model studies

Many of the key and major aspects of the hydraulics, leading to a final design arrangement, were studied. First, to obtain satisfactory retention of the hydraulic jumps, by making alterations to the basin lengths and floor levels, and numerous changes to the energy dissipation baffle blocks and aerators. A workable and safe design was achieved through the studies. The second major stage of the studies were the measurements of transient and static pressures in key locations. Several aspects of the model dimensions and details were subject to change:

- Upper basin length from 90m to 120m and end weir height from 14m to 16m
- Aerators reduced from six to five – two on the upper chute and three on the lower chute
- Aerator geometry
- Location, height and number of the baffle blocks in the upper basin, and
- Lower basin lowered from EL 355 to EL348 having regard to the tailwater rating based headworks 5 km downstream.

The baffle block utilized the shape developed by USBR studies of a “supercavitating” block during testing for the Folsom Dam auxiliary spillway (USBR, 2009). The purpose was to “push the limits” for which baffle blocks could be used in a cavitation environment, meanwhile ensuring generous aeration of the lower flow layers in the chute and into the stilling basins.

The aerators on the Mohmand model showed the nappe profiles well. The performance led to the lowering of ramp heights in some cases to reduce **Fig. 8** Lower chute and lower basin entry Q1,000

the length of the aerated zone as well as relocating the aerators to command the chute length sufficiently to provide assurance that the full chute flow would have adequate aeration. There is sufficient experience – model and prototype – to allow confidence in the designs, both in their location and in the air duct areas to meet the demands of the jets from the ramps. Fig. 9 shows the dimensions of the five aerators. Fig. 10 shows the flow profile at the two upstream aerators.

Pressure transients

A key consideration in stilling basin design is the amount of uplift forces due to the combination of under pressures, pressure transients and transmission of pressures through joints. The high-energy conditions in both stilling basins dictated close consideration of the pressure transients in the stilling basins for the slab and anchoring design. Pressure transducers were used on the floor of the basin both upstream and downstream of the baffle blocks, and on the sidewall of the stilling basin. Records of pressures were obtained at a sampling speed of 300Hz for generally up to 5 minutes (model).



Fig. 7 View of the upper basin operation for AEP 1 in 10,000



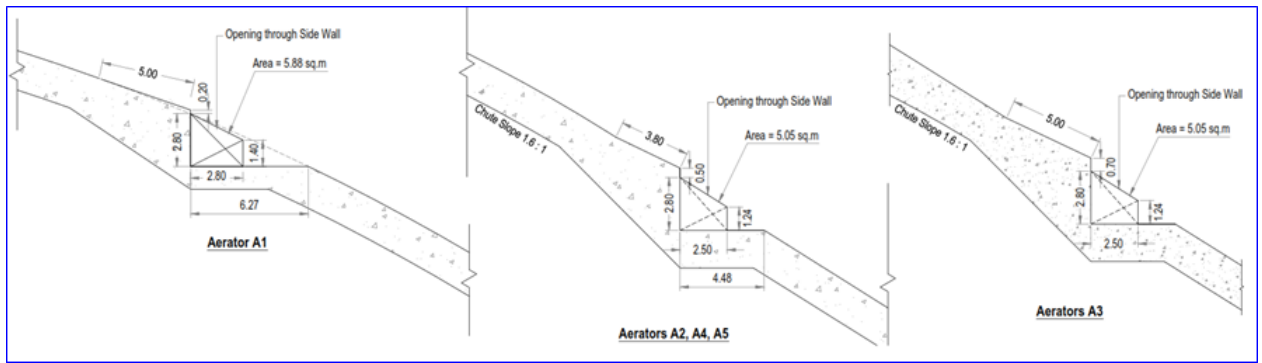


Fig. 9 Final aerator geometry

By way of illustration, Fig. 11 shows the deployment of 8 transducers on the floor of the model upper basin. Fig. 12 shows a small part-sample of the 2,300s (prototype time) total capture of the transients at two of eight transducers in the upper basin. The information, together with cross correlation analysis of signals from pairs of transducers and spectra, provided information for the design of the basin floor thickness as well as anchors.

A sample of the spectral density plots for two transducers for the PMF is shown in Fig. 13. Clearly, the major fluctuations power is around 1 Hz or less, frequencies which are well within the “capability” of the structure floor slabs to respond and therefore relevant for any dynamic analysis of the slab/anchor system.



Fig. 10 Nappe profiles at aerators 1 & 2

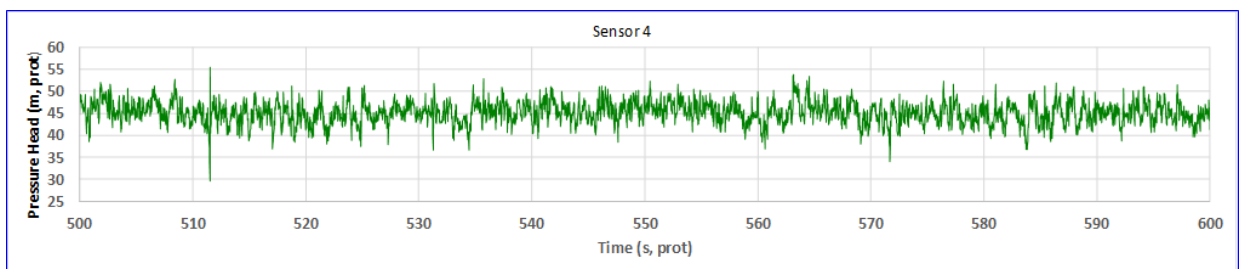


Fig. 11 Transducer locations in the upper basin for one test configuration

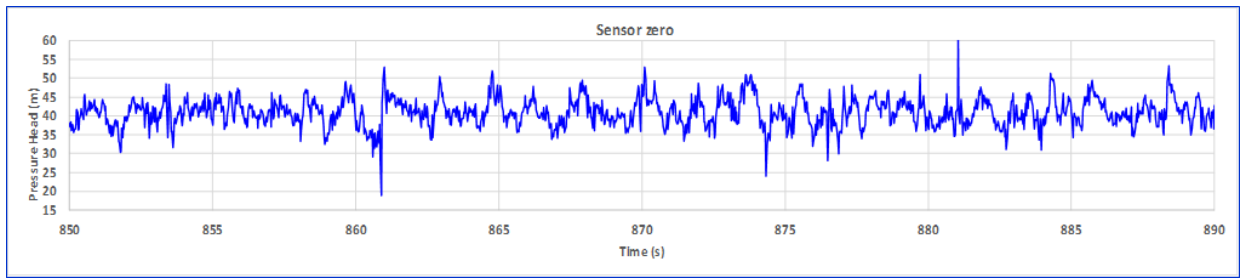


Fig. 12 Sample transient pressures at two transducers, upper basin

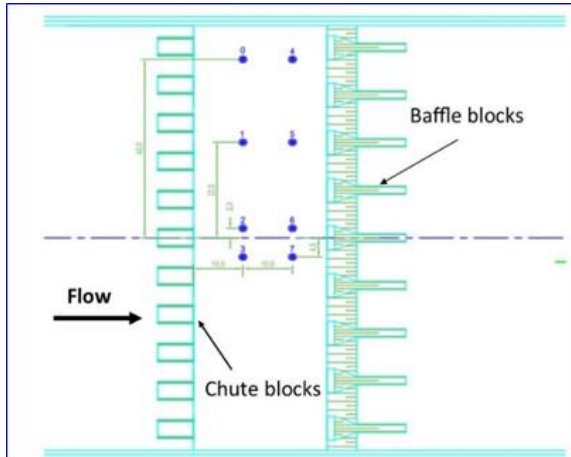
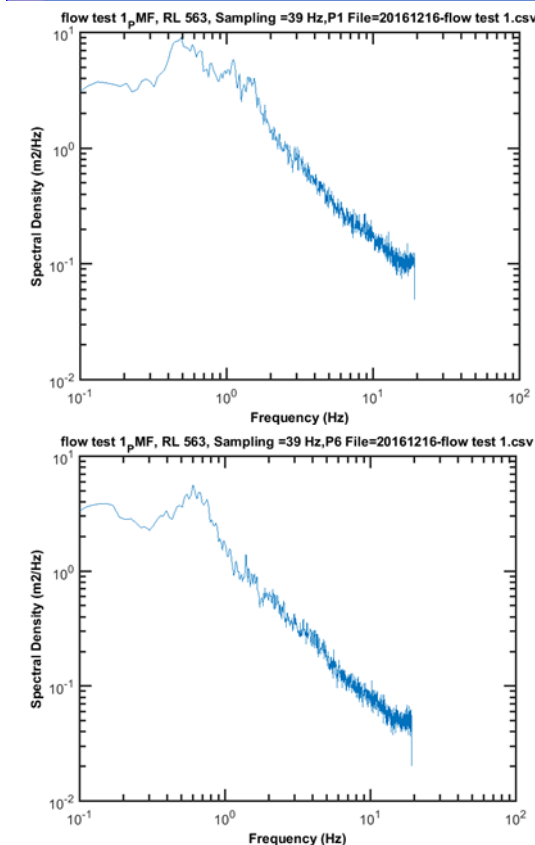


Fig. 13 Sample spectral density plots for transducers 0 and 5 for the PMF



Conclusions

The paper, describing detailed studies on a physical model, shows the value of the exercise in improving significantly on desk-type estimates. Many aspects of the hydraulic structures needed to be addressed by making modifications to the basins, the aerators, and the stilling basin appurtenances. The conditions are major by all comparisons, with high heads and large potential discharges. The double stilling basin presented a workable and desirable option to fit within a narrow corridor with a high mountain (and appreciable excavation) on one side and the dam on the other side. The model results allowed confidence in the detailed design exercise which followed.

Acknowledgments

The authors express their appreciation to the IRI, Nandipur for its skill in building and testing the model, particularly research officers Tariq Anwar and Sana Ullah. Thanks also to Manly Hydraulics Laboratory's (Sydney) assistance in providing instrumentation and advice for the model transient work, and running the pressures analysis.

References

USBR, Denver, Colorado, 2009, Cavitation Potential of the Folsom Auxiliary Stepped Spillway, Hydraulic Laboratory Report HL 2009-07.

Modeling of spillway breach for Attabad landslide dam

Muhammad Wajid Ijaz^{1,2*}, Ata-ur-Rehman Tariq³

¹U.S.-Pakistan Centre for Advanced Studies in Water, Mehran University of Engineering and Technology, Jamshoro, 76062, Sindh, Pakistan

²Environmental Protection Agency, Lahore, 54000, Punjab, Pakistan

³Pakistan Engineering Services, Lahore, 54000, Punjab, Pakistan.

*wajidijaz331@gmail.com

Abstract: Landslides occur due to rock falling on account of slope failure caused by different hydrological, geological and weathering perturbations. A drastic event of landslide occurred on 4th January 2010 at Attabad, Gilgit-Baltistan, Pakistan and a terribly massive landmass choked the Hunza river. It claimed huge losses of living beings and infrastructural damages. There were great suspicions about overtopping of its lake water. In order to avoid the foreseen failure of the dam and extraordinary flooding, an artificial spillway over the saddle of the dam was excavated. After overtopping of water, the predictions did not come true. Keeping it in view, the spillway was modeled in River Analysis System of Hydrologic Engineering Center (HEC-RAS) with synthesized infill gradation and erosion of its bed was simulated in sediment transport module. The results showed that there was very small erosion and the dam was stable against normal overtopping conditions. A hydraulics-oriented scenario of planned breaching of the dam and safe drainage of its lake was tested in the calibrated model. The results demonstrated that by introducing repeatedly check-dam of 15 m height at the mouth of the spillway and its subsequent controlled breaching can effectively lower the spillway invert up to 50 m and remaining part may be accepted or else has to be removed with mechanical or blasting source. For authentic erosion results, additional particle gradation and further measured data should be used in modeling.

Keywords: Natural dam, sediment transport, erosion, Hunza River

Introduction

Landslide dams are created due to falling of landslide mass due to various geological, hydrological, weathering processes etc. across a flowing stream (Liu et al. 2017). Landslide dams are always different in their geomorphology and chemistry (Fort et al. 2014; Stefanelli et al. 2016; Ahmed et al, 2017). Composition and shape of landslide dams primarily depend upon valley characteristics. Landslide dams may be larger than man-made dams in the world. Water stored behind such landslide dams ultimately seep through or over top the landslide dam mass for attaining its natural parent channel path. Stability of these natural dams depends on the volume of landslide mass, tectonic configuration, and rate of flow of runoff from mountainous drainage network. Failure often occurs a short time after formation; 50% of breached landslide dams documented in the world failed within 10 days from the formation (Costa and Schuster, 1988). Karakorum Range of Himalaya traverses the Hunza valley. Sixty historical landslide dam burst events have been reported in the northern part of Pakistan. This gives an average recurrence frequency of about one event every 3 year. Much smaller landslide dam failures took place on the

Gilgit River in 1911 and in Hunza valley in 1977. In recent years there have also been some minor flood events due to the sudden drainage of supra glacial lakes. Dam burst events were relatively common during the period from 1833 to 1933. The most critical glacial lake outburst floods occurred in August 1929, June 1841, August 1885 (landslide), when the massive flood waves resulted in a significant rise in water levels (Calligaris et al. 2010).

In pursuance of the developing situation, Shah et al. (2013) and Iqbal et al. (2014) compiled the background of the incident and present efforts underway. Butt et al. 2013 conducted inundation analysis against different peak values using HEC RAS and geographical information system (GIS). NDMA, (2010) arranged a scenario based dam break analysis from NESPAK who using HEC RAS reported subsequent inundation extents and flooding depth in confluences of Gilgit, Pakistan. Furthermore, Chen et al. (2017) have recently undertaken a dam stability analysis using an empirical model in which likelihood of its failure was quantified and hydrological consequences of dam failure were assessed. All the studies pertaining to Attabad landslide dam were focused majorly over flooding issue and likelihood of

stability, but no results were reported about the use of infill gradation in a scientific way. Thus present study aimed to fill this literature gap and breaching analysis of the spillway was by coupling the lake/river hydrology with the morphological configuration of the landslide dam. This study would help the disaster managers and hydrologists for effective planning and mitigation of such natural calamities in a more rational manner.

Methodology

Study area

In result of October 2005 earth quake in Pakistan, the seismic disturbance generated cracks in Hunza valley near Attabad district Gilgit (Hussain and Awan, 2009). This area has been marked as a fault and high hazard zone by Geological Survey of Pakistan since August 2009. Eventually, it resulted in a massive landslide due to the disintegration of rock from mountain slopes. The landslide mass estimated as 45 million m³ fell in Hunza River (36.307°N, 74.816°E) on 4th January 2010. The slide occurred from the northern wall of Hunza Valley and a landslide dam was created across the Hunza River (Petley, 2010), shown in Fig. 1. Hunza River is considered as a major tributary of Indus River in Pakistan.

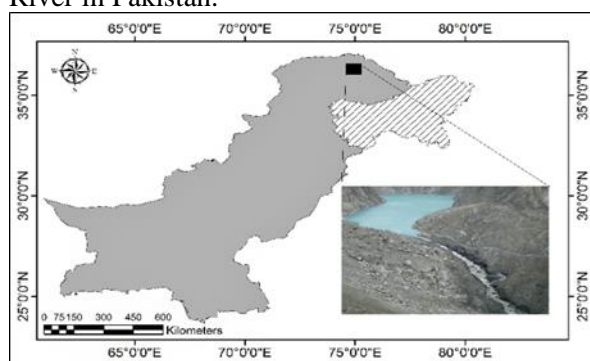


Fig. 1 Attabad landslide site location in Northern Areas of Pakistan

The slide occurred on a steep cliff consisting primarily of diorite and granodiorite of the Cretaceous-Tertiary age Karakoram batholiths. These rocks contain pervasive veins of pegmatite and quartz and are heavily tectonized, with both folding and large-to local-scale faulting being evident. The slope was extensively mantled with glacial tills and colluvium, which was integrated into the slide (Petley et al. 2011).

The crest of the landslide dam is approximately 140 m above the river bed. A spillway as triggering element was formed by massive excavation on the 2 km long crest of landslide

dam in order to mitigate the expected losses due to sudden breached flooding.

Methods

Breaching analysis was performed using River Analysis System developed by Hydrologic Engineering Centre (HEC RAS). Mobile bed analysis of sediment transport module was used to model the lowering of spillway invert. Spillway channel was reproduced in the geometric editor with 15 cross sections measuring reach length 2000 m. Channel shape was trapezoidal with bottom width 1 m, to width 6 m and average depth 16 m (NDMA).

Since 4th January 2010 water was pounding behind the dam and on 29th May 2010 lake water overtopped the spillway invert. Available data up to 14 June 2010 was used in quasi-unsteady flow form in order to calibrate the model. Three soil gradation curves were constructed on the basis of results of mechanical sieve analysis obtained from Royal Material Testing Laboratory, Rawalpindi, Pakistan, and value of Manning roughness coefficient (n) were computed using Strickler formula.

Breaching analysis is carried with the assumption that whole landslide mass could be eroded by the erosive power of overtopping water. So, maximum depth is put equal to the depth of landslide mass from river bed level. Laursen-Copeland sediment transport function was selected for breaching analysis (Copeland & Thomas, 1989). Because the spillway channel and its whole mass were not uniformly settled, so it is treated as nonhomogeneous and graded bed channel. Exner 5 method was selected to simulate the sorting and armoring process. Report 12 was used as fall velocity calculation method.

The average depth of degradation along the spillway channel on the crest of the landslide dam was designated as “Measured Minimum Depth” and an average depth of degradation along downstream shoulder as “Measured Maximum Depth” in a unit of length as shown in Fig. 2. However, calibration was done by making logical variations in the bed gradation during each trial. Measured minimum and maximum depths were used as a reference while the change in bed gradation made possible for closing the modeled results to measured results.

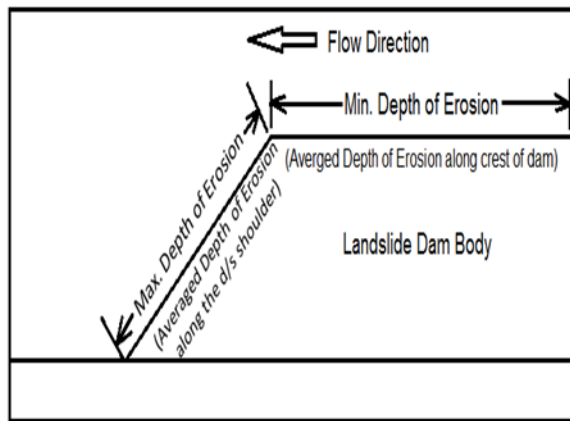


Fig. 2 Schematic diagram of Maximum and Minimum Depth of degradation

Scheme of breaching scenario testing

The inflow rate of Hunza River at the time of spillway overtopping was approaching towards its peak so within 10 days of overtopping a maximum depth of degradation achieved was 38.7 m while the minimum depth of degradation was 4.95 m. After some time, inflow rate of Hunza River and outflow rate through spillway channel were equalized and finer material eroded had been transported. It was hypothesized that exposed material in spillway channel was comparatively coarser and flow rate through spillway was not large enough to continue further erosion with its weak stream power. That is why it was assumed that for the time being an armor layer had been developed. So the dam did not breach as it was expected at the time of spillway excavation because of low flow rates and channel self-stabilization through armoring. It was formulated in order to restart the erosion from the spillway. Scheme of the solution was arranged in such a way that erosive power of overtopping water could be enhanced so that expected armor layer breaks up and erosion is restarted. If the mouth of the spillway is plugged with earth plug / stop log/bulkhead, the water surface elevation would automatically start increasing. After a reasonable time, the plugged mouth of spillway be opened by removing the earth plug by controlled blasting or any other mean. This stored water will be routed and rush through armored spillway channel and its high erosive power should restart the erosion which would ultimately lead towards breaching of that landslide dam; this process was repeated fifteen times until sufficient lake water lowering was achieved. This hypothesized option was implemented in the model with an inline structure as check dam and hydrograph resulted by the simultaneous breaching of this check dam in

unsteady flow module of HEC RAS was routed through spillway channel in order to achieve the high erosive power of flowing water.

Results & Discussion

Following particle size gradation curves were prepared with results of sample 1, 2 and 3. These samples represent finer part of the fill. It is most likely that larger grains could as well as part of the avalanche infill representing gravel, cobbles, and boulders. Gradation of Sample 1, 2 and 3 varies from clay to gravel classes of particle size those are shown in Fig. 3 (a to c).

The spillway erosion results on the basis of the three-sample gradation are shown in Fig. 4 (a to c). There was a large difference among measured and modeled results on using these gradation curves. There is a major difference of magnitudes of the depth of erosion among modeled maximum and a minimum depth of erosion. It was confirmed during sediment transport analysis that particle gradation curves are not a true representative of whole landslide mass.

It is obvious that there is always a large variety of grain classes present in landslide dams. Keeping in view the natural gradation of landslides the theoretical gradation was formulated. Numerous trials were carried out by altering the percentage of passing corresponding to each grain size class during calibration in order to bring modeled erosion results closer to the observed spillway erosion. The adopted gradation curve is shown in Fig. 3 (d).

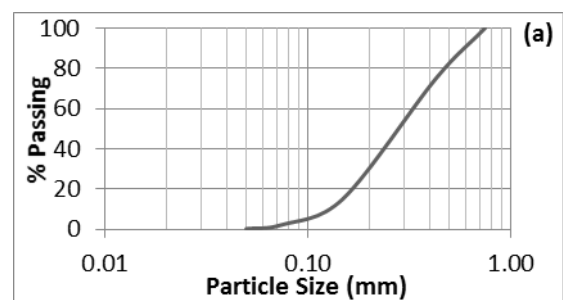


Fig. 3(a) Infill gradation curves (Sample 1)

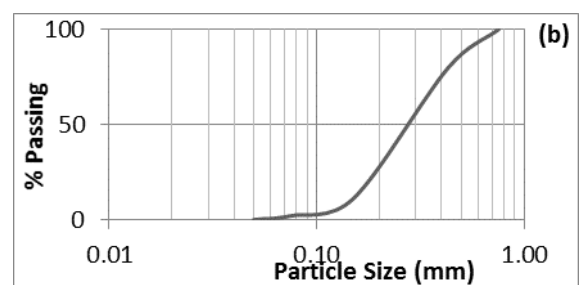


Fig. 3(b) Infill gradation curves (Sample 2)

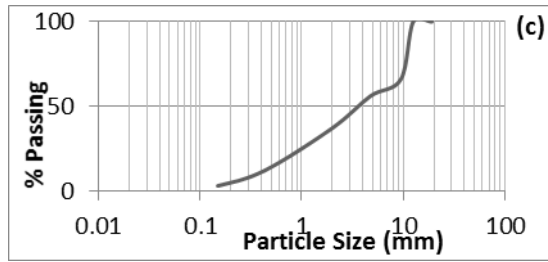


Fig. 3(c) Infill gradation curves (Sample 3)

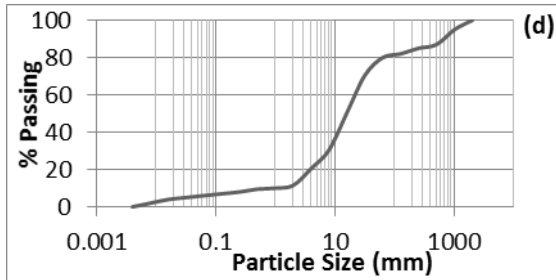


Fig. 3(d) Synthesized gradation

Modeled results were much closer to actual measured results of erosion (Fig. 4 (d)) and thus the theoretical gradation curve was used for further which enables the gradation curve to be used for further analysis. Theoretical gradation encompasses the landslide mass containing all grain size classes (from clay to cobbles/boulders).

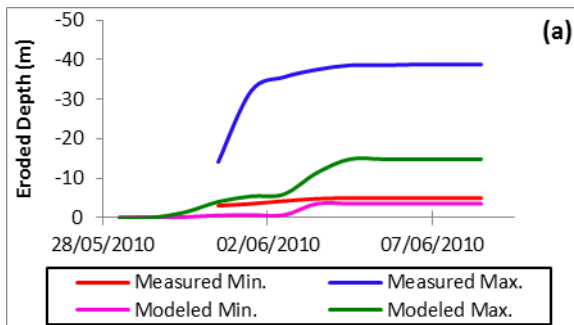


Fig. 4(a) Results of erosion of spillway bed and downstream shoulder of the dam, based on Sample 1

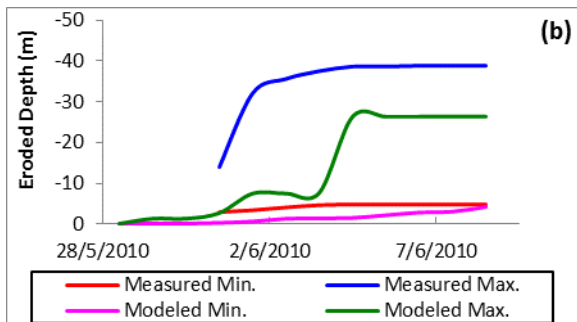


Fig. 4(b) Results of erosion of spillway bed and downstream shoulder of the dam, based on Sample 2

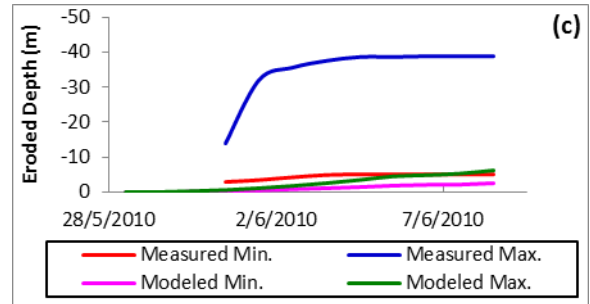


Fig. 4(c) Results of erosion of spillway bed and downstream shoulder of the dam, based on Sample 3

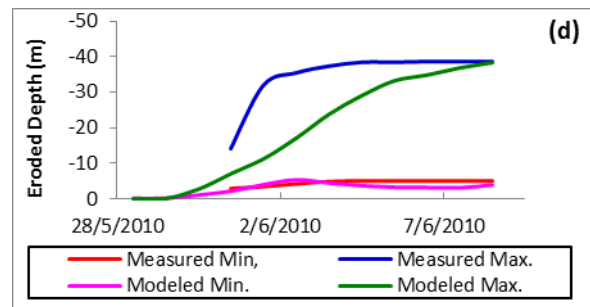


Fig. 4(d) Synthesized gradation

Best efforts were made to train the modeling tool with theoretical gradation. Spillway discharge rate data was available up to the end of June 2010 but data regarding the depth of erosion was available only for first nine days of June 2010. So HEC RAS was precisely calibrated for simulation within a short span of time. Setting up initial and boundary conditions of HEC RAS similar to the calibration portion, analysis of breaching was extended up to the end of June 2010 and erosion results are shown in Fig. 5.

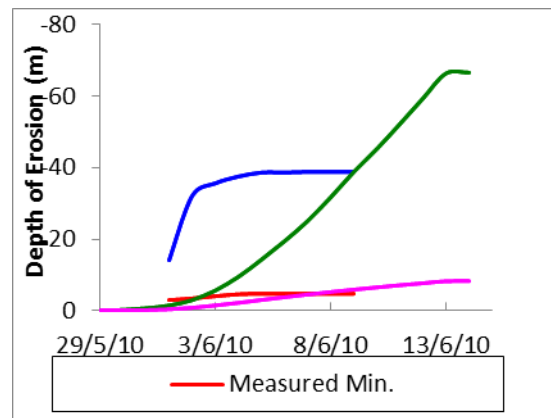


Fig. 5 Results of erosion of spillway bed and downstream shoulder of the dam up to known spillway discharges

Table 1 Actual state of the erosion of Attabad landslide mass

Measured Depths of Erosion Along Spillway Reach		Measured Depths of Erosion Along Downstream Shoulder	
First 3 Days	Further 6 days	First 3 Days	Further 6 days
1.2 m	0.75 m	21.5 m	3.2

In first three days, 21.5 m depth of erosion was measured because all fines were present on upper layers of landslide deposit while in next six days only 3.2 m depth of erosion was experienced which shows that coarser grain sizes are exposing (Table 1).

Successive Case Testing

With the help of trained software, breaching analysis was conducted for two months with successive case testing. On the basis of repeatedly constructing / plugging the spillway mouth, allowing the river flows to store and pond up behind the plug and then later removing the plug to suddenly release the water stored behind the plug. Simulation results are shown in Fig. 6. The simulation has shown that more than 70 m depth of erosion could be lowered from crest of successive erosion with the proposed breaching plan. In result of sediment transport from landslide deposit, the eroded material will be deposited on river bed d/s of landslide dam as depicted in simulation.

1st Breaching

In result of erosion up to period of known flow rates the crest of spillway was lowered 7.7 m under natural condition. Due to non significant progress in spillway degradation the mouth of spillway in u/s side was plugged with 5 m high check dam. For restarting the erosion by breaking up the presumed armor layer check dam was suddenly breached with controlled blasting and hydrograph generated by impounded water was routed through spillway channel as shown in Fig. 6 (a). With this poundage very nominal depth of erosion of 0.6 m was experienced as shown in Fig. 6 (b).

2nd Breaching

Due to very nominal depth of erosion in result of first poundage with 5 m check dam, the spillway bed would mechanically excavated 7.5 m so that spillway mouth may be plugged with 15 m high check dam. Hydrograph generated with such huge poundage is shown in Fig. 6 (c). In result of

this hydrograph routing a 7.29 m degradation of spillway bed was experienced as shown in Fig. 6 (d).

3rd Breaching

After routing of 2nd hydrograph the spillway mouth was once again plugged with 15 m high check dam in order to expedite the erosion of landslide mass. In result of sudden breach of check dam the hydrograph was generated shown in Fig. 6 (e). After routing this hydrograph, the spillway bed got 3.37 m depth of erosion which is depicted in Fig. 6 (f).

4th Breaching

After routing of 3rd hydrograph the spillway mouth was once again plugged with 15 m high check dam in order to expedite the erosion of landslide mass. In result of sudden breach of check dam the hydrograph was generated shown in Fig. 6 (g). After routing this hydrograph the spillway bed got 6 m depth of erosion which is depicted in Fig. 6 (h).

5th Breaching

After routing of 4th hydrograph the spillway mouth was once again plugged with 15 m high check dam in order to expedite the erosion of landslide mass. In result of sudden breach of check dam the hydrograph was generated shown in Fig. 6 (i). After routing this hydrograph the spillway bed got 4.3 m depth of erosion which is depicted in Fig. 6 (j).

6th Breaching

After routing of 5th hydrograph the spillway mouth was once again plugged with 15 m high check dam in order to expedite the erosion of landslide mass. In result of sudden breach of check dam the hydrograph was generated shown in Fig. 6 (k). After routing this hydrograph, the spillway bed got 4.5 m depth of erosion which is depicted in Fig. 6 (l).

7th Breaching

After routing of 6th hydrograph the spillway mouth was once again plugged with 15 m high check dam in order to expedite the erosion of landslide mass. In result of sudden breach of check dam the hydrograph was generated shown in Fig. (m). After routing this hydrograph the spillway bed got 5.3 m depth of erosion which is depicted in Fig. 6 (n).

8th Breaching

After routing of 7th hydrograph the spillway mouth was once again plugged with 15 m high

check dam in order to expedite the erosion of landslide mass.

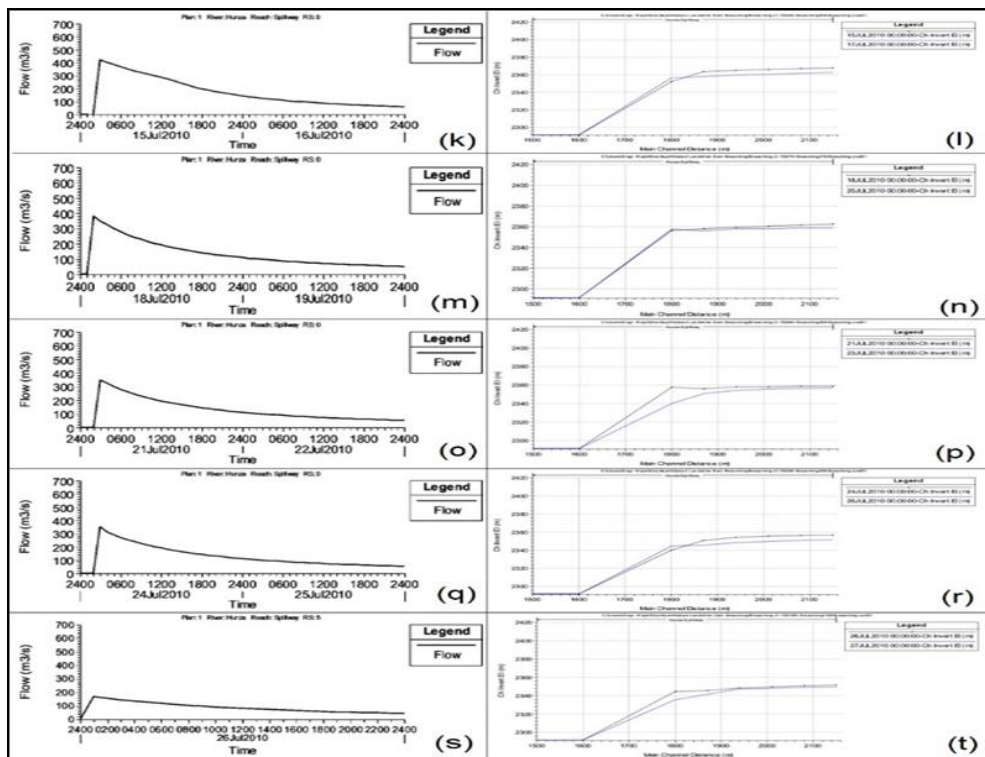


Fig. 6 (k to t)

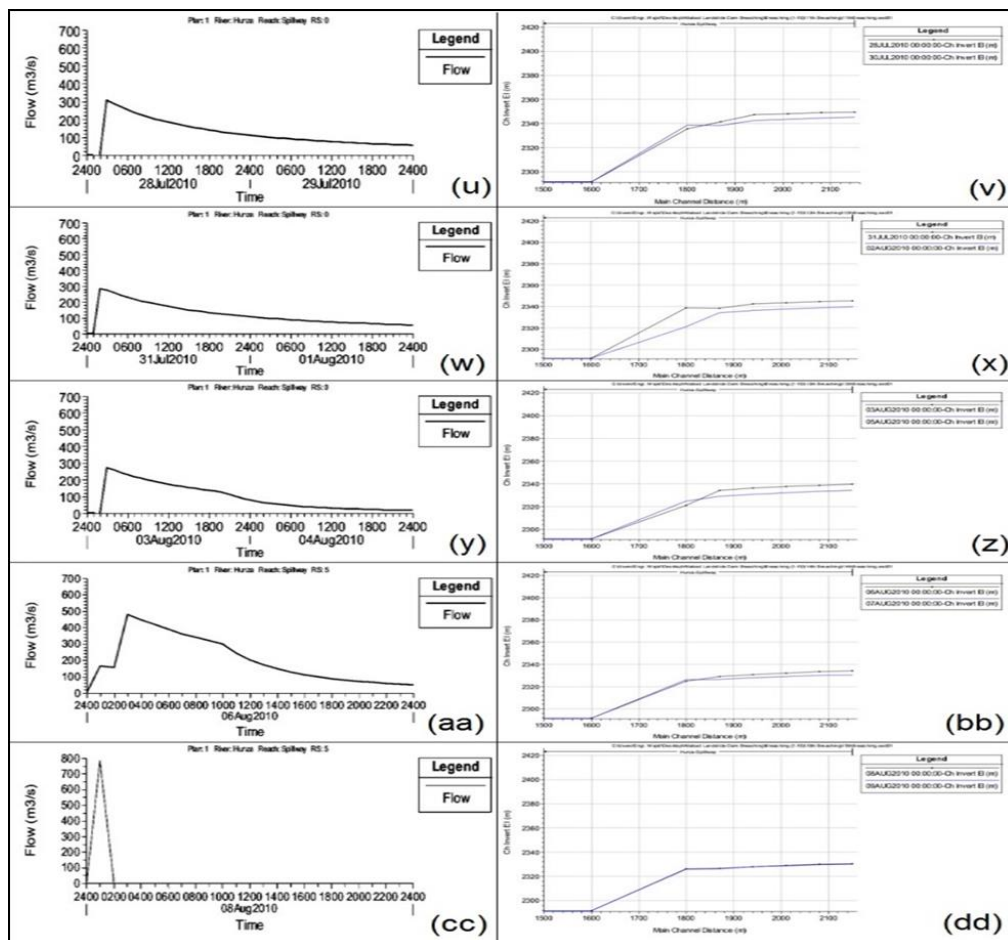


Fig. 6 (u to dd) Fig. 6: Flood hydrograph with instantaneous peak flow (on the left side) generated from removal of check dam and subsequent lowering of spillway invert and d/s shoulder (on the right side) of Attabad landslide dam (a) to (dd) exhibiting breaching scenario 1 to 15, respectively.

In result of sudden breach of check dam the hydrograph was generated shown in Fig. 6 (o). After routing this hydrograph, the spillway bed got 3.5 m depth of erosion which is depicted in Fig. 6 (p).

9th Breaching

After routing of 8th hydrograph the spillway mouth was once again plugged with 15 m high check dam in order to expedite the erosion of landslide mass. In result of sudden breach of check dam the hydrograph was generated shown in Fig. Fig. 6 (q). After routing this hydrograph, the spillway bed got 2.3 m depth of erosion which is depicted in Fig. 6 (r).

10th Breaching

After routing of 9th hydrograph the spillway mouth was once again plugged with 15 m high check dam in order to expedite the erosion of landslide mass. In result of sudden breach of check dam the hydrograph was generated shown in Fig. 6 (s). After routing this hydrograph, the spillway bed got 5 m depth of erosion which is depicted in Fig. 6 (t).

11th Breaching

After routing of 10th hydrograph the spillway mouth was once again plugged with 15 m high check dam in order to expedite the erosion of landslide mass. In result of sudden breach of check dam the hydrograph was generated shown in Fig. 6 (u). After routing this hydrograph the spillway bed got 2.1 m depth of erosion which is depicted in Fig. 6 (v).

12th Breaching

After routing of 11th hydrograph the spillway mouth was once again plugged with 15 m high check dam in order to expedite the erosion of landslide mass. In result of sudden breach of check dam the hydrograph was generated shown in Fig. 6 (w). After routing this hydrograph the spillway bed got 4.3 m depth of erosion which is depicted in Fig. 6 (x).

13 Breaching

After routing of 12th hydrograph the spillway mouth was once again plugged with 15 m high check dam in order to expedite the erosion of landslide mass. In result of sudden breach of check dam the hydrograph was generated shown

in Fig. 6 (y). After routing this hydrograph, the spillway bed got 5.29 m depth of erosion which is depicted in Fig. 6 (z).

14th Breaching

After routing of 13th hydrograph the spillway mouth was once again plugged with 15 m high check dam in order to expedite the erosion of landslide mass. In result of sudden breach of check dam the hydrograph was generated shown in Fig. 6 (aa). After routing this hydrograph, the spillway bed got 5.5 m depth of erosion which is depicted in Fig. 6 (bb).

15th Breaching

After routing of 14th hydrograph the spillway mouth was once again plugged with 15 m high check dam in order to expedite the erosion of landslide mass. In result of sudden breach of check dam the hydrograph was generated shown in Fig. 6 (cc). After routing this hydrograph, the spillway bed got 0.17 m depth of erosion which is depicted in Fig. 6 (dd).

By the results of successive breaching simulation, a total depth of erosion got by spillway bed is 70 m within 2 months.

From results of the model in the above Fig.s, it has been shown that in the start of case testing the crest of dam gets more eroded than in later months. The small decrease in dam crest level is experienced because as dam losses its height similarly lake storage behind the dam gets shorter and thus breaching rate retards consequently.

It may be noted that complete description of landslide infill material (in terms of particle gradation, uniformity of fill over various location and depth, geotechnical parameters of the fill material) was far from being completely accurate. In this context, the results presented herein may be deficient. Further that the proposition of constructing a plug at the mouth spillway, letting river water to store and rise behind the plug and controlled breaching of the plug may have many technical, safety, logistic and social challenges and this should be adopted after all due analysis and considerations.

Impacts of Dam Breaching

Due to planned breaching of this landslide dam following impacts are likely to be observed:

1. As the dam got eroded its crest started lowering. In result of crest lowering the lake water impoundment level will decrease which ultimately leads towards a decrease in lake length according to Fig. 7.

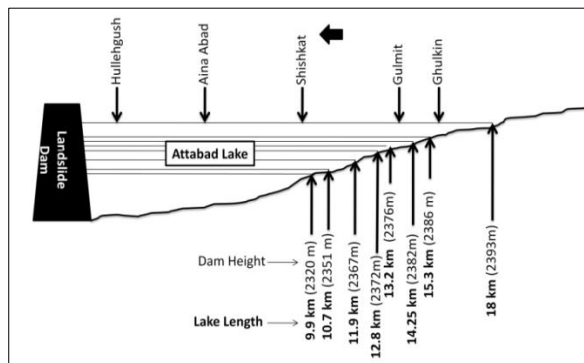


Fig. 7 Change in lake length with respect to dam height after successive breaching

2. Breaching of Attabad Landslide Dam in this manner drains the inundating lake water in a safer mode. Consequently, structures and drowned portion of KKH will once again expose so the danger of catastrophic flooding on downstream side will be minimized.

Summary & Conclusions

In this study flows of Hunza River were used for simulation of lake levels behind Attabad landslide dam and the likelihood of its failure were assessed based on a synthesized infill gradation curve. Following conclusions are drawn:

1. Attabad landslide dam is stable without any external intervention and dam is unlikely to breach under natural flow conditions.
2. Introducing repeatedly check dam and subsequent blasting can effectively lower the dam height up to 70 m. This will considerably rescue the area from inundation effect.
3. The landslide dam of shortened height and a short lake cannot be eliminated by hydraulic erosion and may have to be accepted. Else mechanical excavation or controlled blasting has to be resorted for dam's complete removal.

It is, thus, recommended that for safe drainage of Attabad lake check dam should be introduced and breached subsequently for spillway channel bed erosion by instantaneous high discharges. This should be repeated many times until maximum erosion is achieved. Additional gradation and geotechnical data of landslide mass should be

collected and used in modeling analysis for more reliable and authentic results.

References

- Ahmed, M. F., Rogers, J. D., & Ismail, E. H. (2017). "Correlations between Fluvial Knickpoints and Recurrent Landslide Dams along Upper Indus River". *Environmental & Engineering Geoscience*, 1078-7275.
- Calligaris, C., Comi, M., Tariq, S., Bashir, F., Karim, D., and Khan, H. (2010). "Attabad landslide survey in Hunza, Ev-K2-CNR Committee".
http://www.mtnforum.org/rs/ol/counter_docdo wn.cfm?fID=6241.pdf dated 10-oct-2010)
- Chen, X., Cui, P., You, Y., Cheng, Z., Khan, A., Ye, C., & Zhang, S. (2017). "Dam-break risk analysis of the Attabad landslide dam in Pakistan and emergency countermeasures". *Landslides*, 14(2), 675-683.
- Copeland, R.R. and Thomas, W.A. (1989). "Corte Madera Creek Sedimentation Study. Numerical Model Investigation. US Army Engineer Waterways Experiment Station, Vicksburg" MS. TR-HL-89-6
- Costa, J. E. and Schuster, R. L. (1988). "Formation and failure of natural dams". *Geological Society of America Bulletin*, Vol. 100(7), 1054-1068.
http://www.fsl.orst.edu/wpg/events/S04/Costa_1988.pdf dated 10-oct-2010)
- Fort, M., Braucher, R., Bourlès, D., Guillou, V., Nath Rimal, L., Gribenski, N., & Cossart, E. (2014). "Geomorphic impacts, age and significance of two giant landslide dams in the Nepal Himalayas: Ringmo-Phoksundo (Dolpo District) and Dhampu-Chhoya (Mustang District)". In *EGU General Assembly Conference Abstracts* (Vol. 16).
- Iqbal, M. J., Shah, F. H., Chaudhry, A. U. H., & Baig, M. N. (2014). "Impacts of Attabad lake (Pakistan) and its future outlook". *European Scientific Journal*, ESJ, 10(8).
- NDMA daily report. (2010). "Update on Atta Abad Lake 30th July 2010".
http://ndma.gov.pk/Documents/Hunza_Land slide_2010/One%20Pager%2030%20July.d oc dated 10-oct-2010)
- Liu, A., Zheng, L., Deng, J., & Huang, Y. (2017). "Landslide susceptibility of the Xiangjiaba Reservoir area associated with the Yaziba Fault". *Bulletin of Engineering Geology and the Environment*, 1-11.

- Petley, D. N. (2010). "The Landslide at Attabad in Hunza, Gilgit/Baltistan, NDMA Pakistan". Version 1.01. (Unpublished)
http://ndma.gov.pk/Documents/Hunza_Landslide_Report/Report%20by%20Prof.%20Dr.%20David%20N.%20Petley%20on%20Hunza%20Landslide.pdf dated 10-oct-2010)
- Petley, D. N., Rosser, N. J., Karim, D., Wali, S., Ali, N., Nasab, N., and Shaban, K. (2011). "Non-seismic landslide hazards along the Himalayan Arc". International Landslide Centre, Durham University, United Kingdom
- Shah, F. H., Ali, A., & Baig, M. N. (2013). "Taming the monster—Attabad landslide dam". *Journal of Environmental Treatment Techniques*, 1(1), 46-55.
- Stefanelli, C. T., Segoni, S., Casagli, N., & Catani, F. (2016). "Geomorphological analysis for landslide dams".

Design of Upstream Overflow Cofferdam of Patrind Hydropower Project

Rizwan Farid^{1*}, Ijaz Ahmad², Rana Zain Nabi Khan²

^{1*}Pakistan Engineering Services (Pvt) Ltd. Lahore

²Centre of Excellence in Water Resources Engineering, University of Engineering and Technology,
Lahore 54890, Pakistan

*rizwan.farid@pespk.com

Abstract: An overflow type of cofferdam has been proposed at 150 MW Patrind hydropower project for cost saving of diversion work. The objectives of the study included the design of an overflow type upstream cofferdam; estimate the quantity of spill water over the cofferdam during high flood, evaluating adequacy of low level outlet and the determination of the downstream required protection work for the cofferdam for safety against overspill flood flows. HEC RAS model was used for flood routing. A 16-m high rock fill cofferdam is proposed with upstream membrane of clay and downstream fine filter. The downstream slope of the embankment is proposed to be protected by a stepped chute of gabion along the slope of the embankment. Upstream slope of the embankment is steeper i.e. 2H: 1V while slope of the downstream face is relatively flatter 3H: 1V and 10 m wide crest of cofferdam is proposed. 1 m thick concrete slab is also provided on the crest of the cofferdam to prevent the damage from overflowing water. During high flow season 181 cumecs water is overtopped over the cofferdam with 2.1 m water depth above the cofferdam crest. The pondage is created between cofferdam and diversion weir upto the elevation of 740.8 m amsl, so the main weir should be completed upto the elevation of 741 m amsl before the high flow season. Seepage quantity i.e. 0.001 cumecs is estimated through the cofferdam. The cost of the diversion works with non-overflow type cofferdam is 53% more than the overflow type cofferdam.

Keywords: Overflow, Cofferdam, Hydropower

Introduction

Construction of the hydro-power plant is normally done in the river stream. For creating dry working conditions, the river flow is temporarily diverted by construction of a diversion weir or diversion dam across the main river course. Size and type of the diversion structure depends upon the flood characteristics of the river and topographical conditions at the diversion site. It can be a diversion tunnel if the topography is favorable. A planed diversion scheme can minimize potential flood damage to the work in progress and overall project completion period.

Stream flow records provide dependable information about stream flow characteristics. Depending upon size of the drainage area and its geographical location, floods in a stream may be from snowmelt, rain falling on snow, seasonal rainfall of cloudbursts. Each one of the types of runoff have peak flows and their low flow period dependent on the climatology of the catchment that influences the selection of diversion scheme.

The 10 or 25-year frequency flood is generally selected as the design flood for diversion scheme based on the previous analysis or past experience for sizing the diversion works and risk factor.

Thus, diversion scheme need to be capable of diverting the peak flow of selected frequency flood. Any higher flood is liable to overtop the cofferdam leading to its complete failure / destruction alongwith large damage to the under construction works and delays in project completion.

The choice of diversion through cofferdam, diversion channel or diversion tunnel also depend upon the geological conditions of the area, if the geological conditions are not favorable for off channel diversion, part of the main stream/river can also be used as a diversion channel for phased construction.

Research Methodology

The information relevant to hydrology, hydraulics, topographic survey and the design parameters required for the analysis of the problem in hand were taken from Feasibility Study of Patrind Hydropower Project. Data includes the low and high flow diversion flood, diversion tunnel rating for 7m diameter, Patrind layout plan, Kunhar river x-sections at every 100-m interval and weir site survey of 1 m contour interval. As the nature of this study is analytic, accordingly a compact methodology was adopted to achieve the specific objectives.

Design of Cofferdam

For the design of overflow type cofferdam two seasons low flow and high flow seasons were selected against the 10 years return period. Adequacy of the diversion tunnel was checked during the low flow condition and the quantity of the spill water over the cofferdam was estimated against the high flow seasons. Velocities at different elevation of cofferdam were also estimated and the adequacy of the bottom outlets was also determined against the spill water. For these purposes, the HEC – RAS Model was used.

Formulation of HEC-RAS Model

The geometric data was prepared by assigning the 6-km long reach of Kunhar River. In this reach the diversion weir, cofferdam (Inline structure) and diversion tunnel is provided. The height of the inline weir is 16 m; crest elevation of the weir is 750 m amsl and the bed at 734 m amsl. The diversion tunnel flow was simulated as flow over a lateral weir. The main weir crest elevation of the main weir is 765 m amsl is modeled as a multi barrel culvert. Three low level bottom outlets are provided in the diversion weir having invert level of 735 m amsl and 3 m diameter of each is incorporated as culvert barrels. Unsteady flow conditions were prepared for low and high flow condition. In low and high flow condition, the inflow hydrographs are taken as upstream boundary condition and the normal depth is taken as downstream boundary condition.

The unsteady model was run to check the adequacy of the diversion tunnel i.e the cofferdam cannot be overtopped during low flow condition (QL = 308 cumecs). The model was run for the high flow QH (i.e 1,034 cumecs) through the cofferdam (inline structure) and diversion tunnel (lateral weir) for the estimation of the quantity of spill water (Qs) and depth of the spillage over the cofferdam.

Estimate the Velocities and Check the Adequacy of Bottom Outlets

In order to the get the velocities at every 1 m height of the cofferdam the model was run under for steady mode for Qs without lateral and inline weir. For this purpose, the model was run with or without stepped chute gabion.

In the first scenario the u/s and d/s slopes of the cofferdam were taken as 2H: 1V and 3H:1V respectively and x-sections are taken at 2 m interval. In this model the main weir/dam was taken as the bridge and culvert at R.D 11+010 the

crest elevation of the main weir is 765 m amsl. Three low level bottom outlets are also provided in the main weir having 3 m diameter each and at an invert level of 735 m amsl.

In the second scenario only, the downstream geometry of the cofferdam is defined like a stepped gabion chute with 1 m drop and 3 m tread to dissipate the energy and cross sections are taken at every start and end of the step. The model was run for Qs and the minimum flow to getting the maximum velocities against these discharges. The Manning's roughness coefficients are changed at the downstream of the cofferdam for continuous and stepped gabions. The Manning's "n" for main channel is taken as the 0.055.

Selection of Stone Sizes

For the stability point of view, it is necessary to estimate the rock size which is stable against the maximum velocity along the d/s slope of the cofferdam. For this purpose, Isbash method and Isbash curves was used as a guide for the selection of stable rock sizes / gabion crate size.

Calculation of Scour Depth and Stone Apron

The scour depth at the downstream toe of the cofferdam back slope is calculated by using the Lacey's formula as given below:

$$f_s = 1.76d^{1/2} \quad (2.1)$$

$$R = 0.47 \left(\frac{Q}{f_s} \right)^{1/3} \quad (2.2)$$

Where

R = scour depth in meters

Q = flow in cumecs

d = diameter of particle in mm

fs = silt factor

The diameter of the particle is calculated by using the Isbash Method against the maximum velocity at the downstream toe of the cofferdam and by using this diameter of the particle (d) in relation 2.1 the silt factor is calculated. By using relation 2.2 the scour depth is calculated against the Qs and scour depth is obtained by multiplying with concentration factor 1.27 for straight reach.

Against the calculated scour depth launching stone apron is provided at the toe of the cofferdam. The length of the apron is taken as 1.5 times of the depth of the maximum scour.

The volume of the stone per foot run of an apron would be calculated as;

$$\sqrt{5}xRx2.0 = 4.5R$$

Where

D is the scour depth in ft.

Thickness of the stone apron is calculated by using the following relation;

$$T = V_s / W$$

Where

V_s = volume of stone per unit length (ft²)

W = length of the stone apron (ft)

T = thickness of stone (ft)

Results and Discussion

This section describes the results of Hydraulic analysis and the design of the cofferdam. The hydraulic analysis includes the result of HEC RAS Model for steady and unsteady flow conditions, estimation of rock sizes which is stable against the highest velocity and downstream protection work against scouring.

HEC-RAS Model was used to check the adequacy of the diversion tunnel during low flow (QL) conditions and the simulation proves that the water will not overtop the cofferdam and the diversion tunnel is adequate to pass QL.

HEC-RAS Model is run against the QH to estimate the quantity of spill water over the cofferdam having crest elevation 750 m amsl. The result indicates that the 181 cumecs flood water will spill over the cofferdam with maximum water elevation of 752.1 m amsl during the high flow season. The 853 m³/sec will be diverted through the diversion tunnel due to increased water level.

For the design of the cofferdam velocities are needed along u/s, top and d/s slopes. For this purpose, two simulations are run. In first simulation, the river x-sections are modified to take the shape along the slope of the cofferdam with continuous gabion at the downstream. The model was run for Qs and minimum flow (1 cumecs) without lateral and inline structure. The maximum velocities are obtained against Qs (181 cumecs). The water surface profile at the location of the cofferdam is shown in the Fig. . Velocity and water surface profiles are shown in the Fig. at the upstream and downstream of the cofferdam. The analysis shows the maximum velocity 8.53 m/sec is reached at the river station 15.023 on the downstream side of the cofferdam. The water pondage between cofferdam and the weir is upto the elevation of 740.8 m amsl which is 7.8 m above the river bed. The water level is 2.8 m above the overt of outlet (738 m amsl) so the main weir should be completed upto the elevation of 741 m before the high flow season.

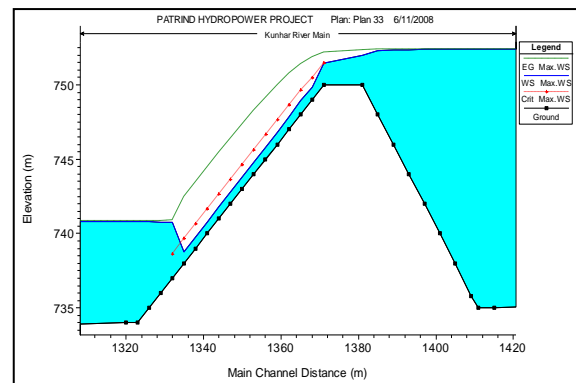


Fig. 1 Water Surface Profile at Cofferdam (with Continuous Gabion)

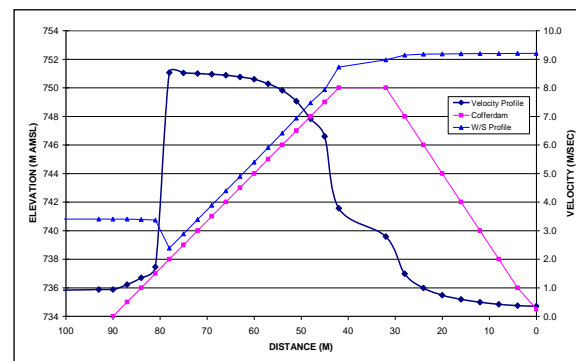


Fig. 2 Velocity and Water Surface Profile at Cofferdam (with Continuous Gabion)

In order to further reduce the velocities at downstream of the cofferdam the model is run with downstream stepped gabion. In this simulation only, the downstream geometry of the cofferdam is replaced by the stepped chute gabion to dissipate the energy. The water surface profile at the location of the cofferdam is shown in the Fig. . The velocity and water surface profiles at the cofferdam are shown in Fig. . The analysis shows that after the stepped chute gabion the velocities are reduced at the downstream of the cofferdam. The maximum 7.95 m/sec velocity is reached at the river station 15.023 on the downstream side of the cofferdam. The downstream slope of the cofferdam is protected against this velocity.

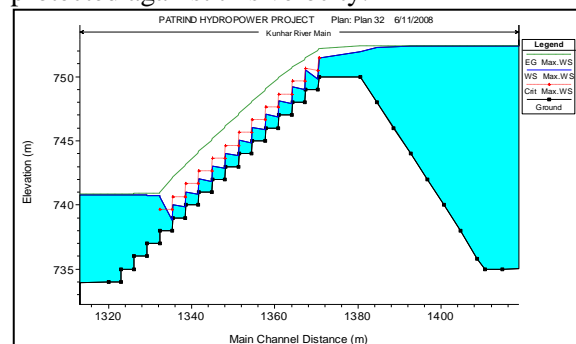


Fig. 3 Water Surface Profile at Cofferdam (with Stepped Gabion)

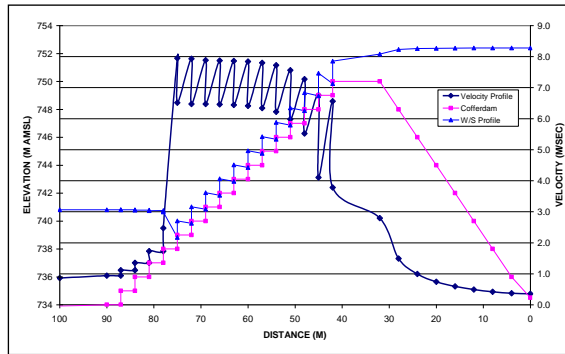


Fig. 4 Velocity and Water Surface Profile at Cofferdam (with Stepped Gabion)

Slope Protection

As the velocities on the downstream side of the cofferdam dam are very high and need to be protected by providing suitable sized stone/gabion. Stone sizes against these velocities are calculated by using the Isbash Method. The maximum 2.5 m size stone is required against the high velocity of 7.95 m/sec. The maximum size of the stone is 2.5 m which is very large and it is very difficult to obtain and place on the site. So, the gabions of minimum 1 m high and 3 m wide are suitable at the downstream side of the cofferdam against this high velocity. The chute type gabions tied with ½ inch (# 4) bars are provided to dissipate the energy. The detail of the gabion and the downstream chute are provided in the design of the cofferdam.

Cofferdam Design Consideration

A rockfill dam is designed for overflow type of cofferdam and utilization of the fill materials available in the vicinity of the weir site. It is the rock fill dam with upstream membrane of clay. At the upstream side, a layer of clay is provided to prevent from seepage and ease of construction during flowing water. The downstream slope of the embankment is proposed to be protected by a stepped chute of gabion and 1 m thick fine filter is provided beneath the gabion to protect against washout of the cofferdam fill material. The foundation seepage is controlled by providing a 6-m deep positive cutoff wall beneath the upper membrane of the rockfill cofferdam. Proposed x-section of the cofferdam is shown in Fig. .

Upstream slope of the embankment is steeper i.e. 2H:1V while slope of the downstream face is relatively flatter 3H:1V as the stability requirements against very high velocities and 10 m wide crest of cofferdam is proposed. A 1 m thick concrete slab is proposed on the crest and on the upstream slope from elevation 747 m upto

the crest level (3 m high) of the cofferdam to prevent damage from overflowing water. The construction of the cofferdam is set in three stages during low flow period. In first stage the excavation of the foundation and filling will be completed. In second stage the fill material (rocks) will be dumped and compacted along the upstream and downstream slope of the cofferdam and in the final stage the fine material (clay) will be dumped over u/s face to reduce the seepage.

Cofferdam Design Consideration

Stepped chute gabions of minimum size 1 m thick and 3 m long are proposed to be provided as protection measure for the downstream slope. These slope is reinforced by a 1 m x 1 m grid of 1/2-inch (# 4) steel bars, anchored backed 3 m into the rockfill embankment. Gabions are also provided at the place where the hydraulic jump is formed.

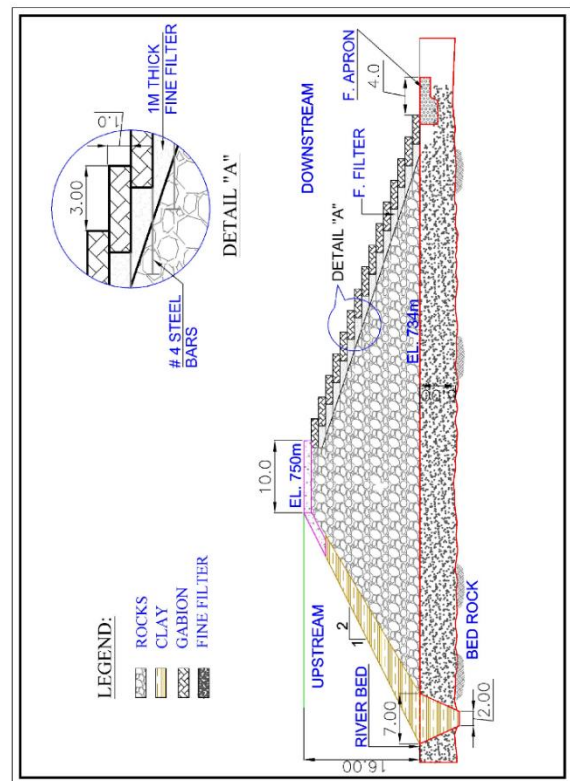


Fig. 5 Proposed Cross Section of Cofferdam

Downstream Floor Scour Protection

The downstream floor is also required to be protected against the scouring. The hydraulic jump is formed at the 10 m above the toe of the cofferdam as shown in the Fig. 4.10 where gabion is already provided. So, a riprap in the form of the launching apron is provided against the scour depth and the layer of geo membrane is also provided behind the launching apron to protect from seepage as shown in the Fig. . The

size of the stone was calculated by using the Isbash method against the maximum velocity of 2.47 m/sec at the toe of the cofferdam.

$$D_{50} = \frac{V^2}{2gC^2 \left(\frac{\gamma_s - \gamma_w}{\gamma_w} \right)}$$

V = 2.47 m/sec (V max)
V = 8.10 ft/sec
 γ_s = 165 lb/ft³
 γ_w = 62.4 lb/ft³
c = 0.86 (for high turbulence)
D₅₀ = 0.84 ft say 1 ft

Determine the silt factor by using Lacey's Formula against the 4.6 mm diameter of the stone

$$f_s = 1.76d^{1/2}$$

F_s = 3.05

Scour depth is calculating against the silt factor 3.05 and discharge 181 cumecs (6391 cusecs) by using the following relation.

$$R = 0.47 \left(\frac{Q}{f_s} \right)^{1/3}$$

R = 6.1 ft say 2 m

Scour depth is calculated by multiplying R with the concentration factor 1.27 for straight reach

D = 1.27 R
D = 2.6 m

Stone apron is designed against the maximum scour depth 2.6 m.

Length of apron (W) = 1.5 x D
= 3.9 m say 4 m

The downstream slope of the cofferdam is 3:1 so the volume of the stone per foot run of an apron is calculated by using slope is given as;

$$\sqrt{10}xRx2.0 = 6.3R$$

The maximum scour depth is 2.6 m and the volume of stone per running meter of an apron is 7.6 m².

Thickness of apron = Vs / W = 2 m

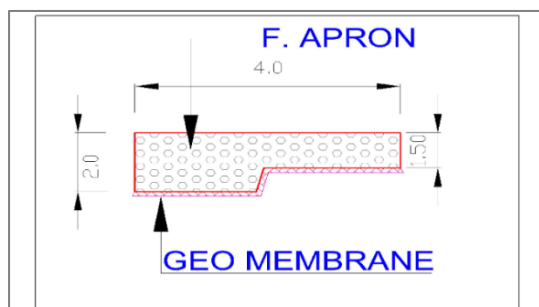


Fig. 6 Detail of Launching Apron

Seepage Analysis

The water losses due to seepage through the cofferdam fill, foundation and abutments are to be kept minimum from the point of view of conservation of water and control of seepage gradients. Detail seepage analysis has been carried out by the Darcy's law, in order to control the exit gradients and limit the overall permissible seepage to a safe and acceptable level. Details of Seepage analysis is given below.

Q = KIA
I = Δh/L
L = 55 m
Δh = 17.5 m
I = 17.5/55 = 0.318
K = 1x10⁻⁵ m/sec
A = 8 m²
Q = (1x 10⁻⁵) x (0.318) x (8) x (40)
Q = 0.001 m³/sec

The seepage through the rockfill cofferdam is very less as compared to the overspill water so the quantity of the seepage is neglected.

Cost Estimate

Cost of the overflow type cofferdam and non-overflow type cofferdam is the important parameters of the study. For cost estimate the unit rates as given in the BOQ of the Feasibility Study were applied.

Overflow Type Cofferdam Cost

The overflow type cofferdam is 16 m high with 2:1 and 3:1 upstream and downstream slope respectively. The quantities and the cost of 16 m high overflow type cofferdam is given in the Table .

Table 1 Cost Estimate of Overflow Cofferdam

Material	Units	Quantity	Unit Rate Rs/Unit	Amount (Rs)
Excavation of Trench	CUM	1020	171.8	175236
Embankment fill, Stone filling	CUM	15995	472.05	7550440
Clay	CUM	3828	521	1994388
Fine Filter	CUM	1495	345	515775
Gabion Fill, Boulders	CUM	1600	600	960000
Welded Steel Mesh: Deformed Bars G-60	TONNES	5.19	85,000	440725
Concrete	CUM	380	3,350	1273000

Stone Apron	CUM	228	532.05	121307
Total Amount (Million Rs.)				13.03

Non-Overflow Type Cofferdam Cost

From the rating curve of the diversion tunnel the QH (1034 cumecs) is passed through the diversion tunnel at an elevation of 753 m amsl. So, the crest of the non-overflow type cofferdam is 755 m amsl with 1 m freeboard (i.e 21 m high). The upstream and downstream slopes of the both overflow and non-overflow cofferdams are same. The quantities and cost of the non-overflow type cofferdam is given in the Table

From the Table and Table it is clear that the cost of the cofferdam increases with the increase in the height of the cofferdam. The non-overflow cofferdam is approximately 46 % expensive than the overflow cofferdam.

Table 2 Cost Estimate of Non-Overflow Cofferdam

Material	Units	Quantity	Unit Rate Rs/Unit	Amount (Rs)
Excavation of Trench	CUM	1020	171.8	175236
Embankment fill, Stone filling	CUM	34240	472.05	16162992
Placement of Clay	CUM	5180	521	2698780
Total Amount (Million Rs.)				19.04

Conclusions

- A 16 m high rockfill cofferdam with upstream membrane of clay is proposed, the upstream and downstream slopes of the cofferdam is 2:1 and 3:1 respectively and 1 m thick reinforced concrete slab provided on the upstream face from elevation 747 to 750 m amsl (3 m) and on the crest of the cofferdam to prevent damage from overflowing water.
- During high flow season the 181 cumecs (Qs) is overtopped over the cofferdam with maximum water flow depth of 2.1 m above the cofferdam.
- The maximum velocity of 7.95 m/sec velocity is obtained against Qs. The stepped chute gabions of 1 m high and 3 m long are provided at the downstream slope of the cofferdam to protect against the high velocities

- Launching apron 2 m deep and 4 m long is provided at the toe of the cofferdam to protect against scouring. The scour depth is calculated against 181 cumecs flow and 2.47 m/sec velocity at the toe of the cofferdam.
- The poundage is created between cofferdam and diversion weir upto the elevation of 740.8 m amsl (7.8 m above the bed level). The water level is 2.8 m above the overt of outlet (738 m amsl), so the main weir should be completed upto the elevation of 741 m before the high flow season.
- 0.001 m³/sec seepage quantity is estimated through the cofferdam, which is very less as compared to overspill quantity, so it is neglected.
- The cost of the non-overflow type cofferdam is 46 % more than the cost of the overflow type cofferdam

References

- USBR. (1987), "Design of Small Dams", Water Resources Technical Publication, Third Edition, SSOP, Washington, D.C, p 491-496
- Pakistan Engineering Services (Pvt) Ltd. (2007), "Feasibility Study of Patrind Hydropower Project", Main Report, Vol -1, DHA, Lahore, Pakistan.
- HEC. (2001), "Technical Reference Manual of HEC-RAS" Version 3.0, US Army Corps of Engineers, USA.
- Chaudhry, M. Hanif. (1993), "Open Channel Flow", Washington state University, Washington, p 246-247.
- Casagrande. A. (1973), "Embankment Dam Engineering" Jhon Wiley and Sons, Inc., USA, p 97-103.
- Tariq, Ata-ur-Rehman, (2006), "Dam and Reservoir Engineering", Class Notes, Center of Excellence in Water Resources Engineering, UET, Lahore, Pakistan, p. 21-22.
- Novak, P, A.I.B. Moffat and C. Nulluri, (1990), "Hydraulic structures" University of Newcastle upon Tyne, Chapman and hall, London, p. 301-302.
- Fell, et al. (1992), "Geotechnical Engineering of Embankment Dams", A.A. Bakema, Rottedam, Netherlands, p 450-455.
- Yanmaz, A. M., (2000), "Overtopping Risk Assessment in River Diversion Facility Design", Canadian Journal of Civil Engineering, Vol. 27, No:2, PP. 319-326.

Evaluation of Small Hydropower Scheme Operating in Chitral, Pakistan; a Case Study of Chitral Hydel Station on Lutkho River

Engr. Javed Zulfiqar^{1*}, Engr. Nazakat Hussain¹

^{1*}Water and Power Development Authority, Lahore, Pakistan.

Abstract: This research presents the optimization with different alternatives of existing Chitral one megawatt (1 MW) hydropower station at Lutkho River through the hydrological analysis. The study involves the estimation of synthetic flows of study area by correlation with having same Climatological and hydrological characteristics, maximum design flood using Log Pearson Type III for various return periods, proposed a permanent concrete weir structure, layout alternate with existing power channel and with extended power channel. In order to estimation of power generation flow duration curve was carried out through derived flows. The analyses revealed that with the permanent concrete weir structure and existing channel and with extended channel the energy can enhance up to 1.8 MW and 5 MW.

Keywords: Hydropower potential, Runoff river, Chitral

Introduction

Nature has been very generous to the Northern Pakistan in its endowments of towering mountain peaks, gigantic glaciers, majestic rivers and splendid green vales and meadows with abundant fruit trees. The steep streams and rivers with abundant flows offer cheap and environmentally friendly power potential to be harnessed in these mountainous areas. Chitral is situated in the extreme Northern part of Pakistan, in Khyber Pakhtun Khua province. The climate of the Chitral city is very cold snowy winter and relatively pleasant summer. Most of the watershed remains covered with snow and glaciers in winter season. The flow in the Lutkho River is mainly due to glacier and snow melting. Chitral valley has a number of potential streams where hydropower potential schemes were identified. A few of them have been planned and are being considered for implementation.

The proposed Chitral weir site has been located on the river Lutkho about 1 km downstream of Chitral village at a latitude of 35° 56' 14" and longitude of 71° 48' 37". The proposed weir site was about 10 km from Chitral town towards North. Lutkho River is a right tributary of Chitral River. Its proposed powerhouse site is located on the right bank of the river Lutkho, about 5 km upstream of Chitral town. The drainage area of the Chitral weir site on the Lutkho River is about 2340 km². The mean elevation of the catchment area is 4009.5 m.a.s.l. The drainage area of Chitral River at Chitral is about 11,400 km². The length of Lutkho River is about 72 km and the

average river gradient is 3.1%. [HPO Publication No. 271, 2009]

The Existing scheme of power generation at Chitral was designed to utilize the portion of flows from Lutkho River. There is no permanent weir for diversion of discharge from Lutkho River to power house is available. Manual dumping of boulders as weir is done in the lean water months and this process is repeated every year and the temporary weir flushed away particularly in the summer session due to high flows in Lutkho river. The main objective of this research is to optimize the hydro power potential of power station at Lutkho River.



Fig. 1 Existing view of temporary stone weir

Hydropower Overview of Chitral Valley

In Chitral and surrounding areas, most of the power generation, transmission and distribution system is being maintained and operated by WAPDA. There is one existing hydel power station 1 MW in addition to power supply from National grid. The Chitral city was connected to national grid through a 33-kV transmission line. The voltage level through long line transmission is low. Either Chitral valley is to be connected with high voltage transmission or medium size power plant is connected to Chitral city to have reliable power supply. In Garam Chashma, hydel power station of 100 kW is being operated and maintained by SHYDO (WAPDA). Another hydel power station of installed capacity 4.2 MW Reshun is in operated by SHYDO to provide electric power to Upper Chitral areas. In lower Chitral, the electric power generation, transmission and distribution system is being operated by SHYDO. A hydel power station of 300 kW installed capacity at Shishi Gol supplies power to Drosh area. Chitral hydel Power Station 1 MW has been in operation since 1975, providing electric power to Chitral town.

Optimization of Chitral Hydropower Station

To exploit the available indigenous resources of Lutkho River, the capacity enhancement of Chitral power station is direly needed. The existing structures would be remodeled for enhanced capacity. Construction of new permanent weir instead of old stone weir and remodeling of power channel may enhance the power generation capacity to meet the growing demand of Chitral city. The topographic features and availability of flows in river allow increasing design discharge by remodeling the hydraulic structures and more power can be generated rather than installed capacity i.e. 1 MW. The enhanced capacity would be exclusively used to meet the growing power demand of Chitral city.

Methodology Adopted

Data Availability & Data Analysis

In order to carry out the proposed study, the relevant data viz. discharge data, climatological data (temperature, precipitation, and humidity), topographic survey, and geological data were collected from Water and Power Development Authority (WAPDA) and processed by using spread sheets where needed. However, the studies were purely theoretical and no experimental work was undertaken. On Lutkho river, discharge observations were performed from 1987-88. So it is necessary to correlate it

with some long term gauging station to prepare a flow series of at least 30 years for reliable estimation of power and energy. The discharge data of the nearby hydrological stations Chitral, having long term record (1964 to 2010) was collected and the synthetic flows have been derived. Ten daily flows at the proposed weir site have been estimated by using different approaches utilizing the available flow data record of station with the similar catchment characteristics. For generation of the temporal distribution of the daily, 10-daily, monthly and annual flows the discharge data of Shah-re-Sham Stream Gauging Station for one year, from June 1987 to June 1988 in combination with Chitral Gauging Station Data from 1964 to 1980 and 1982 to 2010 (46 years) have been used. The annual model used to generate daily flows at weir site and power house sites, as given below and the mean monthly flows is shown in Fig.: 2.

$$Q_{weir} = [0.2526(Q_{chitral})^{0.888}]$$

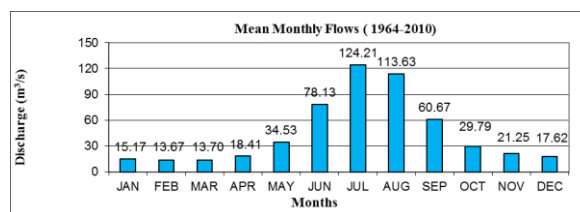


Fig. 2 Mean Monthly Flows of Lutkho River

For the flow study of the weir and powerhouse sites by regional analysis approach, flow data of seven stream gauging stations of the Chitral watershed were selected having similar Climatological and hydrological characteristics. These seven stream gauging stations are Chitral, Reshun Gol, Golen Gol, Shishi Gol, Ojhor Gol, Phander and Shah-Re-Sham (Lutkho River). The graphical relationship between average flows and watershed area is shown Fig. 3. Fig. shows that there is increasing trend in the average flows with the increase in watershed area.

After transforming the daily flow data at the weir site, daily, 10-daily, monthly and annual flows were computed at the weir site. Power and energy have been estimated for discharges of 5.60 m³/s and 15.8 m³/s. Power and energy outputs have been calculated for a period of forty six years using 10 daily flow records.

Estimation of Power and Energy

Power and energy have been estimated for discharges for the design discharge of 4.60 m³/s and 15.8 m³/s. Power and energy outputs have been calculated for a period of forty-six years

using 10 daily flow records. The design capacity is computed with following formula; $P = \frac{g \cdot Q \cdot H}{1000}$ Whereas P is Capacity (MW) estimated from 10 days discharge and corresponding head, Q is the 10 days discharge with maximum value of design discharge Q_d (m^3/s), H is Gross head (m). It is the difference of elevation between operating head and tail water level, is combined efficiencies of turbine, generator, transformer and that of the hydraulic system upstream of powerhouse, g is gravity acceleration = 9.81 m/s^2 . The mean annual energy is estimated on the basis of 10 daily flows using the following formula, $E = \frac{g \cdot Q \cdot H \cdot t}{10^6}$ Whereas E is mean annual energy in GWh/annum, Q is average design discharge (m^3/s), t is time in hours over 10 days. The plant factor which provides the basis for the installed capacity of the project is calculated as follows: $pf = \frac{E}{(P \cdot 8.760)} \cdot 100$ Whereas pf = Plant factor (%), E is mean annual energy (GWh/annum), P is Installed Capacity (MW).

Layout Planning

The various alternatives for the project were studied before the final selection. The final layout was selected based on the technical aspects, the maximum possible head is exploited, the waterways have the shortest possible length and the most suitable structures are selected for prevailing geologic conditions. The topographic survey sheets were used to evaluate a suitable layout and to place the various components of the project. The existing power project was planned and designed with limited capacity channel and without permanent diversion structure about 40 years ago. The topographic conditions from existing intake to powerhouse area allow capacity of power channel and surface powerhouse to be enhanced upto certain limits. The weir axis within 50 m of existing intake has been considered where geological conditions are very good. With weir intake at same area and alternate location of powerhouse, the following two alternate project layouts have been studied.

Alternate I: Project layout with existing channel

Alternate II: Project Layout with extended channel

Alternate I: Project Layout with Existing Channel

The existing channel and power station can be upgraded with permanent weir and by diverting increased flows towards power channel and powerhouse. With weir axis and powerhouse

sites at same locations, an option has been studied to make use existing channel structure. With the construction of new permanent weir, the water level at channel would be raised and discharge capacity increased $4.64 \text{ m}^3/s$ to $5.60 \text{ m}^3/s$, which provide an installed capacity of 1.8 MW. The rise in water level is to be maintained within the limits of all existing hydraulic structures, accordingly the weir height is fixed to 3m high.

Salient Features: Alternate-I

Design capacity (P) = 1.80 MW

Design discharge (Q_{100}) = $5.60 \text{ m}^3/\text{sec}$

Gross head (H) = 37.8 m

Mean annual energy (E) = 15.72 GWh

Plant Factor = 100.0%

Headrace channel length = 3675 m

Energy gradient in channel = 1:1000

Penstock length = 55m

Tailrace length = 30 m

No. and type of units = 2, Francis

Alternate II: Project Layout with Extended Channel

The channel section can be widened to certain limits which the present topographic features of the area allow. The buildings, graveyards, road alignment, river steep slope, weak and hard formation restrict the channel section to certain dimensions. A rectangular concrete channel section 4.5 m wide and 2.4 m high can be constructed and the capacity of canal can be increased to $16.0 \text{ m}^3/s$, which provide an installed capacity of 5 MW.

Salient Features: Alternate-II

Design capacity (P) = 5.0 MW

Design discharge (Q_{75}) = $16.0 \text{ m}^3/\text{sec}$

Gross head (H) = 37.8 m

Mean annual energy (E) = 42.70 GWh

Plant Factor = 97.50%

Headrace channel length = 3675 m

Energy gradient in channel = 1:1000

Velocity in channel = 1.95 m/s

Penstock length = 70 m

Tailrace length = 22 m

No. and type of units = 2, Francis

Advantages of Alternate Layouts

- Alternate-I with power channel can be enhanced to utilize the low flows with same gross head.
- Alternate-I would utilize the same project area as that of existing. Some area would be required to be acquired where realignment of power channel may be required.

- Alternate II provides twice the energy (42.70 GWh) of Alternate I (15.72 GWh)
- The weir height is 3.0 m. The geological conditions for small size structure of weir, headrace channel and powerhouse are very good. These are more favorable for small and surface structures.

Results and Discussion

Design Discharge

A diversion concrete weir structure of 3 m high and 26 m long on the Lutkho River is to be designed that it will divert a flow of 16.0 m³/s to headrace channel. Two units of Frances Turbine for the powerhouse have been proposed, therefore, the design discharge for each unit will be 8.0 m³/s.

Table 1 Summary of Comparison of Alternatives

Alternate	Existing Scenario	Alternate-I (Existing Channel)	Alternate-II (Extended Channel)
Discharge (m ³ /s)	4.64	5.60	16.0
Net Head (m)	35.7	37.8	37.8
Capacity (MW)	1.0	1.8	5.0
Energy (GWh)	8.74	15.72	42.1
Plant factor (%)	100	100	97.0
Weir height (m)	Stone weir	3.0	3.0
Headrace (m)	3675	3675	3675

Flow Duration Curve

Flow duration curves of Lutkho River have been prepared using the *rank-ordered technique* for the years 1964 to 2010 to assess the availability of flows. Flow duration curve based on the generated average daily flow data at the weir site is shown in Fig.: 4. The maximum flow rate is 195 m³/s, minimum, which will remain available throughout the 100% 75% and 50% exceedance time is 9.5 m³/s 16 m³/s and 23.39m³/s respectively.

The flood study is essential for the design of various hydraulic structures at the weir and powerhouse sites including coffer dams and spillways etc, has been carried out. The flood has been estimated at weir and powerhouse sites by using flood frequency methods i.e. Gumbel, Log Pearson (Type-III). Maximum daily flow in a year was converted into instantaneous peak to estimate the flood at weir and powerhouse site. Log Pearson Type III has been adopted for Weir and Powerhouse sites due to best fit distribution of observed data. The flood frequency results for weir site are also shown in tabular form in Table 2 and graphical representation of floods in Fig. 5.

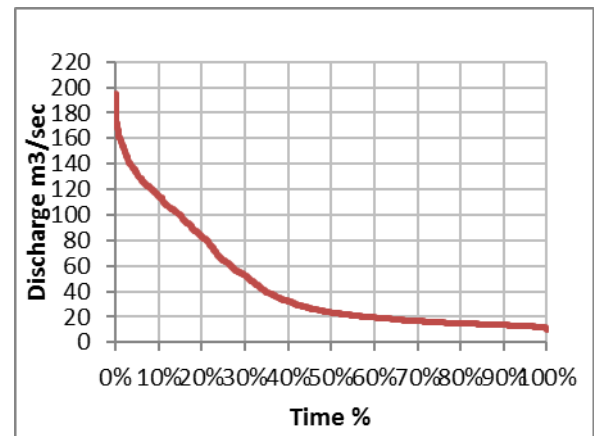


Fig. 4 Flow duration curve at weir site of Lutkho River

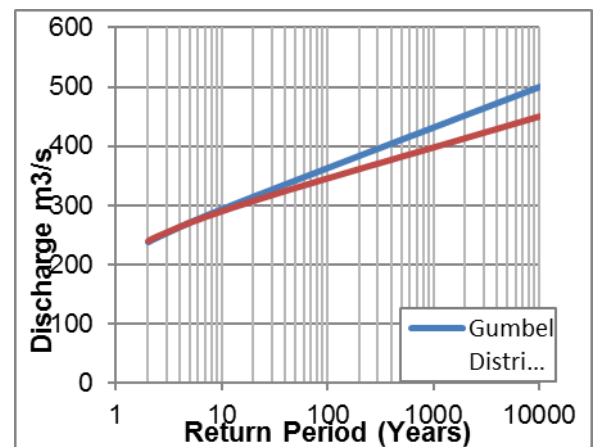


Fig. 5 10,000 years return period floods in the region

Table 2 Floods at proposed weir site by flood frequency analysis

Return Period	Flood (m ³ /sec)	
	Gumbel	Log
2	238	239
2.33	245	245
5	272	270
10	294	290

20	315	307
25	322	313
50	343	329
100	364	345
200	384	361
500	411	382
1000	432	397
10000	500	449

Basic Assumptions in the Calculations

The following basic assumptions have been made in estimating power and energy of the identified schemes.

- The residual water in the Lutkho River during low flow period has been taken as 1.0 m³/s. It is based on sediment flushing requirement and minimum flows required in the river for environmental purpose.
- The variations in the efficiencies of generating units due to change of net heads have not been considered. For design discharge available to powerhouse, an efficiency of 91.0%, 96.0% and 98% have been used for the turbine, generator and transformers, respectively.
- The head loss has been considered as 0.35 m in penstock, 0.10 m at intake and 0.05 m in tailrace. The losses at bend and in draft tube are taken as 0.05 m. The total losses are taken as 0.55 m to estimate net head for turbine. The losses would be less for a discharge less than the design.
- Energy is calculated by multiplying the number of days in a month and 24 hours in a day. For power and energy during peak and

Diversion Weir and Headrace Channel

As per topographic map, the bed level at weir axis is 1531.5 m and Lutkho River flows with mild gradient of about 1 %. To divert the design discharge of 16.0 m³/s into the power channel, a concrete weir of 3.0 m height above the nullah bed has been proposed. A rectangular R.C.C channel has been proposed on the right bank of Lutkho River. The channel would be designed as rectangular R.C.C section with width of 4.5 m and height 2.4 m with free flow condition. The length of headrace channel has been estimated as 3675 m. It has design capacity of 16.0 m³/s and maximum velocity upto 1.95 m/s. The longitudinal slope of channel has been taken as 1:1000.

off-peak hours, the volume of water available for storage and inflow volume in 24 hours is used to calculate the corresponding discharge. The power during peak and off-peak hour is used to calculate the corresponding energy.

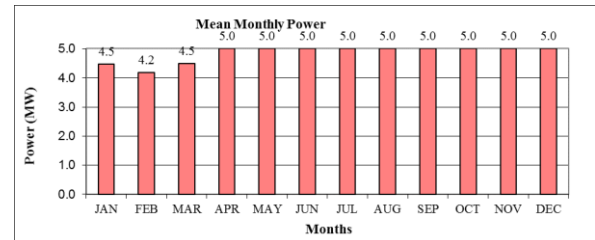


Fig. 6 Mean Monthly Power

The recommended design discharge is 16.0 m³/s, for the net head of 37.2 m the power and energy have been estimated on the basis of 10-day flows for all years from 1964 to 2010, the optimum installed capacity would be 5.0 MW with average mean annual energy of 42.70 GWh. The plant factor has been taken as 97.50%. The firm capacity available 95% time of the year is 4.0 MW. The calculated mean monthly power and annual energy are presented in Fig. 6 and Fig. 7 respectively.

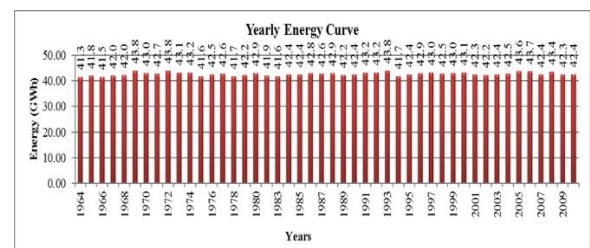


Fig. 7 Mean annually energy

Conclusions

Due to limitation in extension of power channel, the design discharge has been proposed as 16.0 m³/s, available 75% time of the year. The capacity of existing channel section can be improved with lining in its entire length. With construction of diversion weir, some remedial works at hydraulic structure, the capacity can be enhanced to 1.8 MW. This option is not attractive as diversion weir draw additional flows for power channel. The alternate project layout has been considered for optimum utilization of available potential. As power channel has limitation for the design discharge to be conveyed through channel alignment upto powerhouse, therefore capacity has been restricted to 5 MW. Two Horizontal Francis units each of 2.5 MW has been proposed to generate 5.0 MW. As the design flow is available for 75% time of the year and firm capacity is 4.0 MW, therefore the proposed units

would be capable of generating the power round the year. As the project would be developed using the land of existing structures, therefore social and environmental issues have been assessed minimum.

Recommendations

The project area has a history of generating power of 1 MW. The hydrological, topographical and geological condition favors the extension of structure and capacity enhancement for 5 MW, with high plant factor power station to meet the power requirement of remote area. The existing powerhouse structure is old and too small for new units. It has to be dismantled and new building would be constructed at the same place. The remodeling of existing hydraulic structures is essentials as these are about 40 years old. Detailed investigations are required along the power channel to adopt the slop stability measures for the safety of power house also

analysis of sediment carried by the Lutkho River should be carried out as is important for the layout and design of the sand trap.

References

- GTZ-WAPDA. 1999. Layout and Sizing; High Head Hydropower.
- GTZ-WAPDA. 2000. Hydropower in General, High Head and Low Head Hydropower Projects.
- GTZ-WAPDA. 2000. Power Plant Components; High Head Hydropower.
- HEPO-WAPDA. 2009. Reconscience Report of Chitral Hydel Station.
- HEPO-WAPDA. 2011. Updated Feasibility Study Harpo Hydropower Project.
- HEPO-WAPDA. 2012. Updated Feasibility Study Basho Hydropower Project.
- HEPO-WAPDA. 2013. Plans for Development of Hydropower in Pakistan.

Impact of Baglihar Hydroelectric Power Plant on Design Flood of Pakistan

Adnan Majeed^{1*}, Rana Zain Nabi Khan², Neelam Pari¹, Ahsan Naseem¹

¹Civil Engineering Department, University of South Asia, Lahore, Pakistan

²Centre of Excellence in Water Resources Engineering, University of Engineering and Technology, Lahore 54890, Pakistan

*madnan376@gmail.com

Abstract: Water Resource is a live and sensitive issue in Pakistan, both internally between its provinces and externally with India, Pakistan after separation from India the Indus Waters Treaty was signed in 1960 between India and Pakistan but now India is trying to scrap this treaty by constructing Baglihar Hydroelectric Power Plant on Chenab river, that is the allocated river of Pakistan. In this study Flood frequency analysis approach (Gumbel's Distribution) is used to calculate the return periods and decrease in water due to the construction of Baglihar Hydroelectric Plant. Different return periods are calculated at different four gauging stations (Marala, Kahanki, Qadirabad, and Trimmu) at Chenab river. Gumbel's distribution shows that at 1000- year return period Chenab rivers facing huge decrease in flow. At Marala, Khanki, Qadirabad and at Trimmu the percentage reduction are 11.33%, 28.91%, 30.6% and 40% respectively. The average reduction in flows occurs which is almost 27.71 % at Chenab river, which will not only cause energy losses but also serious environmental damage on Pakistan. The percentage reduction in flow at different return periods can be further analyzed by using other flood frequency approaches.

Keywords: Baglihar Hydroelectric Power Plant, Indus water Treaty, Gumbel's Distribution

Introduction

The Indus river system, one of the major systems in the world, comprises the main Indus and its five important tributaries: Jhelum, Chenab, Ravi, Beas and Satluj rivers. Indus river, along with Jhelum and Chenab, are referred to as the 'Western rivers', while the other three tributaries (Ravi, Beas and Satluj) are termed as 'Eastern rivers'. The common features of all of them is that they originate in the Himalayas, pass through Indian territory and, after Indus has received the waters of its five tributaries in Pakistan, it flows through Pakistan provinces of Punjab and Sind and falls in the Arabian Sea, South of Karachi.

The Indus Waters Treaty (IWT) was signed in Karachi on September 19, 1960, by India's Prime Minister Jawaharlal Nehru, Pakistan's President Muhammad Ayub Khan, (Iftikhar, 2011). According to this treaty, Ravi, Beas and Sutlej, which constitute the eastern rivers, are allocated for exclusive use by India before they enter Pakistan. Similarly, Pakistan has exclusive use of the western rivers Jhelum, Chenab, and Indus. (Garg, 1999).

From the rivers flowing in India, India got nearly 33 Million Acre Feet (MAF) from eastern rivers whereas Pakistan got nearly 125 MAF from western rivers. However, India can use the western river waters for irrigation up to 701,00 acres with new water storage capacity not

exceeding 1.25 MAF and use the rivers for run of river hydro power generation with storage not exceeding 1.6 MAF and nominal flood storage capacity of 0.75 MAF. (Raina, 2017). Pakistan has become one of the driest countries in the world because of the recent shortages of water. Pakistan criticizes Indian hydroelectric projects like Ratle, Baglihar on Chenab river and Kishanganga hydroelectric plant on Neelam-Jhelum river which have enabled India either to reduce water flows to Pakistan or to release store waters and cause floods. According to Sahai. M (2006) "The maximum pondage in the operating pool shall not exceed twice the pondage required for firm power as mentioned in IWT. However, the design shall take due account of the requirements of Surcharge storage and of secondary power. Pakistan feels that the planned pondage of 37.7 MCM in Baglihar project is violation of the Treaty provisions. India denies this based on its own calculations. Full Pondage Level is defined in the Treaty as the level corresponding to maximum pondage allowed under it. Pakistan asserts that in the Baglihar design, the space between the maximum water-level and top of the dam is unduly large and would enable India to have a greater storage than full pondage level." In this study, Gumbel's Distribution is used to calculate the peak flows at different return periods and determine the

percentage reduction in flows due to construction of this dam.

Site Description

The Baglihar Dam that is a run-of-the-river power project located on the Chenab River in the Southern Doda district of the Indian occupied state of Jammu and Kashmir. The Chenab river which is of 960 km, a major river of India and Pakistan, forms in the upper Himalayas in the Lahaul and Spiti district of Himachal Pradesh, India, and flows through the Jammu region of Jammu and



Kashmir into the plains of the Punjab, Pakistan.

Fig. 1 Location of Kishanganga and Baglihar Hydroelectric Plants

Data Collection

A 36-years (1980 to 2016) data from different gauging stations is collected from Pakistan Meteorological Department, Lahore. The data includes annual peak discharge of a river at different gauging stations. The gauging stations at Chenab river are Khanki, Trimmu, Qadirabad, and Marala.

Methodology

Flood frequency analysis is a probability model to the sample of annual flood peaks recorded over a period of observation, for a catchment of a given region and period. The model parameters established can then be used to predict the extreme events of large recurrence interval (Pegram and Parak, 2004). Flood frequency results are vital for floodplain management; to protect the public, minimize flood related costs to government and private enterprises, for designing and locating hydraulic structures (Tumbare, 2000).

In this study, Gumbel's frequency analysis method used to estimate the return period at different gauging stations before and after the

construction of dam i.e. Pre-discharges and Post discharges of river, respectively.

Gumbel's Distribution Method

That extreme value distribution was introduced by Gumbel (1941) and commonly known as Gumbel's distribution. Gumbel distribution is a statistical method and It is one of the most widely used probability. The Gumbel distribution is used to observe series of flood peaks, maximum rainfalls, maximum wind speed, etc at different return periods (Subramanya, 2013). According to Gumbel's theory of extreme events, giving the value of the Variate X (peak discharge value) with a return period T is used as

$$X_T = \bar{x} + K \sigma_{n-1} \quad (1)$$

Where in Eq (1)

\bar{x} = Mean value of X

σ_{n-1} = Standard deviation of the sample size N.

K = Frequency factor and expressed as

$$K = \frac{y_T - \bar{Y}_n}{S_n} \quad (2)$$

Where in Eq (2)

$$y_T = \left[\ln \ln \frac{T}{T-1} \right] \quad (3)$$

or y_T can be calculated as

$$y_T = [0.834 + 2.303 \log \log \frac{T}{T-1}] \quad (4)$$

\bar{Y}_n = Reduced mean a function of sample size N

S_n = Reduced standard deviation a function of sample size N

The values of \bar{Y}_n and S_n are to be find in literature given by Gumbel.

Results and Discussions

In Pre-discharges considered those discharges which are on the gauging station before the construction of Baglihar (1980-2004) hydroelectric project whereas in Post- discharges considered those discharges which occur after the construction of Baglihar hydroelectric plant (2005-2016). The Gumbel's distribution is used on both peak flows (Pre and Post discharges). Peak flows determined at four gauging stations at 1000-year return period. The analysis of Gumbel's distribution is shown in below mention graphs Figs. 2 – Fig 5. At Marala gauging station, the average percentage reduction at 1000- year return period is 11.33% as shown in Fig 2. At Khanki gauging station, the average percentage reduction 28.91 % occurs as shown in fig 3. Similar reduction in peak flows can be seen in other gauging stations that are at Qaidrabad and Trimmu. At Qaidrabad and trimmu gauging stations average percentage reduction are 30.6% and 40%, respectively, as shown in fig 4 and fig

5. The overall reduction in flow 27.71 % is observed

Table 1 Summary result of Percentage Reduction on Chenab River due to Baglihar Hydropower Plant

Gauging Station	Marala	Khanki	Qadirabad	Trimmu	Average
Percentage reduction	11.33	28.91	30.6	40	27.71

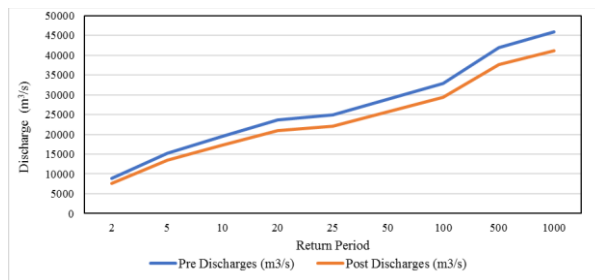


Fig. 2 Gumbel's Distribution at Marala Gauging Station

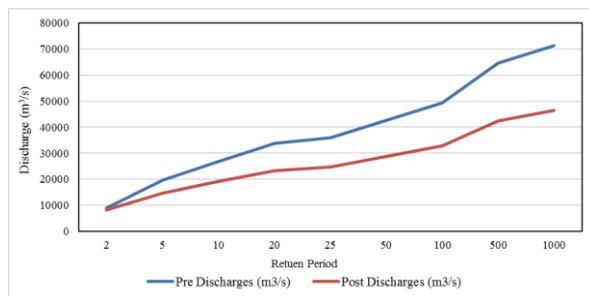


Fig. 3 Gumbel's Distribution at Khanki Gauging Station

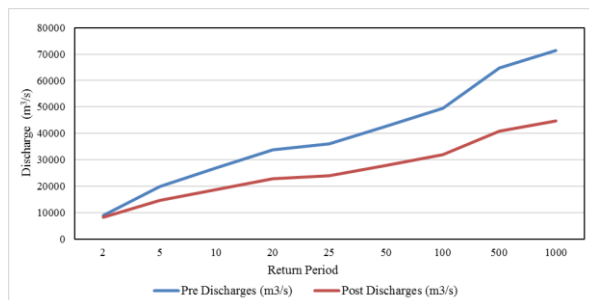


Fig. 4 Gumbel's Distribution at Qadirabad Gauging Station

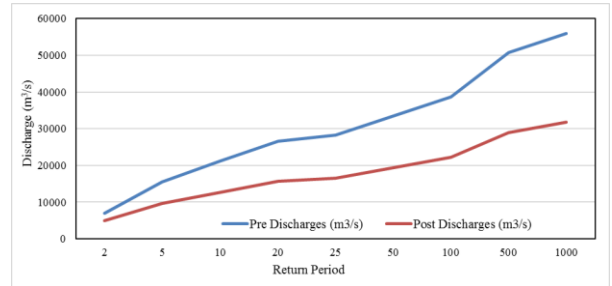


Fig. 5 Gumbel's Distribution at Trimmu Gauging station

Conclusions

Table A, shows the percentage reduction in flow at Chenab river at each gauging station due to Baglihar hydropower plant. There is a significant reduction in post discharges at all gauging stations. The average reduction in flow at Chenab river due to mentioned Indian dam is 27.71% by Gumbel's distribution at 1000- year return period. The results can be verified and compared by using other flood frequency approaches.

Acknowledgement

The authors would like to highly acknowledge Pakistan Metrological Department Lahore, to provide data used in this study.

References

- Garg, S.K (1999). "International and interstate river water disputes".
- Iftikhar, M. (2011). "Tackling the Kishanganga knot. The Nation. Islamabad"
- Raina, A.N (2017) "Geography of Jammu and Kashmir State"
- Sahai, I.M. (2006). "The Baglihar dispute". International Water Power & Dam Construction Pegram, G and Parak, M (2004). "A review of the regional maximum flood and rational formula using geomorphological information".
- Subramanya, K (2013). A book on "Engineering Hydrology" Fourth Edition
- Tumbare, M. J. (2000). "Mitigating floods in Southern Africa". Paper presented at the 1st WARSFA/WaterNet Symposium: Sustainable Use of Water Resources, 1-2 November, Maputo

Risk of Indus Basin Water Transfer in Violation of Indus Basin Treaty

Ahmad Raza^{1*}, Muhammad Waseem¹, Navid Tahir², Ijaz Ahmad¹

^{1*}Centre of Excellence in Water Resources Engineering, University of Engineering and Technology, Lahore 54890, Pakistan

²Department of Irrigation and Drainage, University of Agriculture, Faisalabad 38000, Pakistan
[*engrahmadraza@hotmail.com](mailto:engrahmadraza@hotmail.com)

Abstract: Indus Water Treaty (IWT) was signed in 1960 between Pakistan and India to resolve the water conflict. This study was carried to study threat of unlawful transfer of Western River's water through tunnels. Catchment area of the study area was determined by Arc GIS software. Locations for water diversion were selected considering following criteria: large elevation difference available between source river and recipient river, River have narrow cross section to allow tunnel on steep river section face, and location where river has enough water depth so that the tunnel intake mostly remain under water even during low flow conditions. Cross sections of all possible locations were also determined by Arc GIS software. Tunnel route was marked considering shortest length and largest elevation difference between the source and recipient river and thus tunnel length was determined. Tunnel design was done considering total energy available between source and recipient river, head losses at intake and control gates, friction losses of tunnel surface, tunnel length and exit losses. Tunnel diameter was selected such that tunnel intake remain mostly under water even during low flow conditions. Annual water transfer was estimated from minimum of 141 million cubic meter (MCM) to as much as 2131 MCM from Indus River. Five sites Tso Moriri, Gaik, Nimmo Bazgo, Dah and Batalik on Indus and two sites Jangalwar and Kund Bara on Chenab River are identified as high-risk sites. The Kund Bara tunnel from Chenab River seems to be first adopted due to be shorter length (32.3 Km) and large flow diversion (3532 MCM). Technical capabilities, financial gains and most important socio-political-diplomatic hegemony of India reflect high risk of Indus basin water transfer by India in violation of Indus Water Treaty. There are more than twenty possible locations where unlawful river flow diversion could be made.

Keywords: IWT Indus Water Treaty, Conflict Resolution, Digital Elevation Model (DEM)

Introduction

Pakistan is amongst those countries having shortage of water (Akther, 2010). The major resources of water in Pakistan are rivers, ground water, rainfall and glaciers. The annual average rainfall of Pakistan is less than the 240 mm. Indus River has five main tributaries Sutlej river, Bias River, Ravi river, Jhelum river and Chenab river. Indus river total length is 3,200 kilometres and calculated flow volume is 180 billion cubic meters. The catchment area of the Indus River from the originating point (Himalaya) to the terminating point (Arabian Sea) is 965,120 square kilometers. Indus basin catchment area found in China (Tibet) is 92,160 square kilometers and in Afghanistan 74,240 square kilometers. Catchment area of the basin found in northern areas of Pakistan, Azad Kashmir and other area are 24,3200 square kilometers. Major portion 58% (55,5520 square kilometers) of Indus basin lie in Pakistan.

Indian all run of hydropower project on Indus, Chenab and Jhelum Rivers have serious effect on river flows. Pakistan worries that Indian project can cause flood in the western rivers during wet

seasons and water shortage in the dry seasons. The storage capacities of Indian dams affect the pattern of river flows into Pakistan. India has announced 135 dams on the western rivers which include 24 dams on Indus River, 77 dams on Jhelum River and 34 dams Chenab River. Social media in Pakistan have viewed that India is violating IWT, but India always claimed that all projects are run of river hydropower projects such as Wullar Barrage and other projects constructed within the regularity framework of IWT.

India has started construction big hydropower dams on the Indus river. India point out nine dams on Indus river which will be constructed in future. Three of them are Nimmoo Bazgo, Chtak and Dumkhar big dams explained below. (Haq, 2010). India has completed many dams and many other dams are under construction on Chenab River. Three big dams Salal, Baglihar and Dul Hasti are completed. These three dams are now in operation. India has planned to construct 3 large and 8 small dams and other 24 projects are conduct (Tunnel) type on Chenab River. (Haq, 2010)

India has completed 13 dams on the Jhelum River in which the three major dams are lower Jhelum with 105 MW capacity of power house, Uri dam with 480 MW capacities of power house and Sind phase II with 105 MW capacity of power house. India also point out 74 other projects on Jhelum river which include Gangbal dam with 100 MW capacity of power house, Ujh dam 280 MW, Sonamarg dam 165 MW and Kishanganga 330 MW. (Haq, 2010)

India was spending 200 billion dollars for the construction of water tunnels on Indus River, which ultimately affect the fertility of land (Khalid Mustafa, 2008). India is starting the world 3rd largest dam (Kargal) on Indus river, which will decrease flow of Indus river up to 45 % (News & Views Mohammad Jamil) and other NGO's as Indus Basin Commission Water Pakistan (IBCWP), World Water Council (WWC) pointing out threat of illegal transfer of Indus basin water in violation of Indus basin treaty. However, no specifics are provided by the media and NGO, s about water transfer.

This research would aim to determine the alternative location and route that could be used for un-authorized diversion of river Indus water. So, by determining the routes we can check the tunnel configuration and length of tunnel. Hence, there is need to be vigilant unlawful water transfer of Indus river water which is the major source of water supply of Pakistan. This study is based on the data which was easily available from office files, internet resources and Google Earth images. Flows at different locations were worked on proportionate basis. The low-level accuracy of such data could have affected the study output.

Methodology

India could transfer the water of western rivers (Indus, Jhelum and Chenab rivers) to the eastern rivers (Ravi, Beas and Sutlej Rivers). These un-authorized diversions are possible within territorial boundaries of Jammu and Kashmir. Study area of research is Indus River, but a small portion of Chenab river is also included.

Indus River bed profile was determined by using Google Earth software. Base point was selected at Skardu (35.27° N, 75.25° E). A working map of the whole Indus River and its tributaries was prepared from G.T sheets (25 in number) with the help of CAD. Terrain processing was done by using Arc GIS Tools for catchment extraction. Terrain preprocessing was carried out in a definite sequence for catchment extraction purpose.

Assessment of possible routes and location of the diversion tunnels were located where the diversion could be possible. Twenty locations were selected of which eighteen were on Indus River and two were on Chenab River. Locations were selected by considering following parameters:

- Significant elevation difference between Source River (Indus River or Chenab River) and Recipient River.
- Narrow cross section at diversion site to allow tunnel on steep section face.
- Location where enough water depth so that the tunnel intake (mouth) remain under water and is liable to be not detected due to being covert and unlawful activity.

River Water Depth by Hydraulic Model HEC-RAS

HEC-RAS model was used to determine the depth of water in the cross section of selected locations. Three discharges were estimated on each location by the relationship (Discharge per unit Catchment area). The flow depth of water in each cross section was determined for maximum, minimum, and average discharges.

Under covert operation conditions tunnels can be best way for diverting water from one river system to other. The tunnel is considered to adhere following hydraulic requirements.

- Bottom of the tunnel should be at some slope
- At small discharge the tunnel will perform as open channel flow and at large discharges the tunnel behave like pipe flow
- Minimum Diameter of the tunnel should not less than 5 ft from construction point of view
- Location and design of the tunnel is affected by the Geology (Geology is not considered in this study due to unavailability of geologic details, but a favorable geology is considered).

Typical working sheet showing detail of tunnel design is given in Table 2.1.

Annual Flow Diversion

Following procedure was adopted for the calculation of annual flow diversion from tunnels.

- i. Catchment area of all possible locations were determined from DEM processing through GIS
- ii. Average monthly discharge of 21years of Indus and 14 years of Chenab River was calculated at Skardu and Dhamkund respectively

- iii. Available monthly discharge (Jan to Dec) of all possible locations were calculated on the basis of catchment area
- iv. Water depth at all possible locations during whole year (Jan to Dec) determined with the help of HEC-RAS model.

Table 1 Typical working sheet of tunnel design

Input			
Discharge Q (m ³ /s)	25	n	0.013
Length of Tunnel (m)	56900	u/s Invert level (m)	4497
Water elevation/depth (m)	4527	d/s Invert Level (m)	3833
Assumed dia of tunnel (m)	2.50		
Computation			
Area of tunnel (m ²)	4.91	Gate and valve losses (Kg)	0.19
Velocity of water (m/s)	5.09	Exit losses (Kv)	1
Velocity head (V ² /2g)	1.32	Total head loss (HL)	692.39
Friction losses (fL/D)	523.72	Exit energy head (m)	3835
Entrance losses (Ke)	0.05	U/S energy head (m)	4527
Results			
Water elevation/depth = U/S energy head		4527	

Results and Discussions

The aim of study was to identify the possible locations where the Indus River and Chenab river water could be diverted to Ravi, Beas or Sutlej rivers under the covert operation in violation of Indus basin treaty.

Indus River Bed profile was determined from the Skardu (35.27° N, 75.25° E) to the boundary line of Jammu and Kashmir and China as shown in Fig. 1. Marked river are shown in Fig. 2. From graph it is clear that at Skardu the catchment area is maximum, but the elevation of river is minimum. Catchment area decrease with length at 112,665 km² at Skardu to 10,108 km² near line of control between J&K and China. River bed level increases from 2200 m at Skardu to 4150 m near line of control between J&K and China.

Catchment area of Indus and Chenab River was determined at Skardu and Dhamkund gauging stations by using Arc GIS. The coordinate of Kachura and Dhamkund gauging stations are 35.27 N, 75.25 E and 33.24 N, 75.14 E. Catchment area obtained from Arc GIS are shown in Figs.

Indus River discharge was collected from Kachra gauging station and Chenab River discharge was collected from Dhamkund gauging station. Indus River and Chenab River maximum, average and minimum discharges were based on the historic data. Monthly discharge available from January

to December for each tunnel calculated. Annual volume diverted from tunnels also calculated from the available discharges.

Twenty locations of flow diversion were identified in which eighteen were on Indus River and two were on Chenab River. The diversion sites are given in Table 3.1. The leading tunnels are shown in Fig. 3. Catchment area and discharges (maximum, minimum and average) available at all possible locations were calculated.

Following arrangements were considered to divert flow and minimize the sediment entry to tunnels.

- i. Diversion carried on a steep sloping river face
- ii. No external structures
- iii. Intake constructed as underwater activity
- iv. Flow control gate/valves housed in an underground chamber. Presumed diversion tunnel intake and flow control arrangement are required.
- v. To reduce the bed, load the invert level of tunnels was designed up to 0.5 m from river bed.
- vi. Submerged trash rack will use to eliminate trash load.
- vii. Under water dyke at the upstream of tunnel to ward off sediment load.

viii. During flood in river the tunnel will be closed

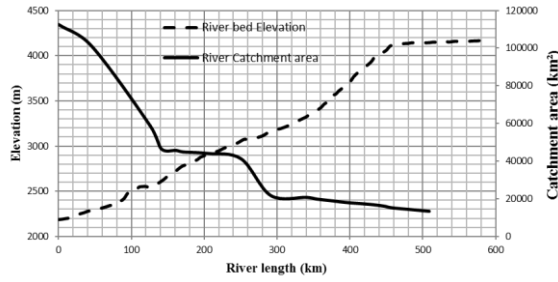


Fig. 1 Indus River Bed Profile



Fig. 2 Indus River catchment area

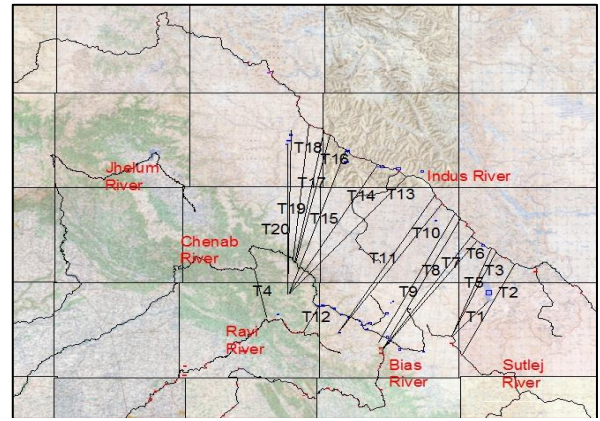


Fig. 3 Twenty possible diversion tunnel sites

Table 2 Detail design of Tunnels (T1-T20)

Location	u/s Elevation (m)	d/s Elevation (m)	Length (km)	Slope (m/m)	Dia (m)	Discharge (m ³ /s)	Annual Volume (MCM)	Q per Length (MCM/km)
T1 Tso Moriri	4527	3833	56.9	0.012	2.5	25	765	13.44
T2 Indus	4127	3633	120	0.004	2.5	15	425	3.54
T3 Indus	4118	3873	106	0.002	3.0	17	522	4.92
T4 Chenab	916.5	629	58.8	0.005	4.5	74	2245	38.18
T5 Indus	4016	3873	109	0.001	3.1	14	417	3.83
T6 Indus	3908	3306	150	0.004	2.7	18	531	3.54
T7 Indus	3775	2250	162	0.009	2.9	32	881	5.44
T8 Indus	3602	2443	170	0.007	2.7	23	657	3.87
T9 Indus	3503	3138	169	0.002	3.0	17	489	2.90
T10 Indus	3389	2513	183	0.005	3.2	30	829	4.53
T11 Indus	3316	2519	188	0.004	3.0	24	639	3.40
T12 Chenab	2450	1357	32.3	0.034	4.2	165	3532	109.3
T13 Indus	3172	2857	170	0.002	2.7	12	375	2.20
T14 Indus	3040	2866	164	0.001	4.5	36	1055	6.44
T15 Indus	2907	2750	165	0.001	3.6	18	540	3.27
T16 Indus	2784	2035	155	0.005	3.0	25	666	4.30

Location	u/s Elevation (m)	d/s Elevation (m)	Length (km)	Slope (m/m)	Dia (m)	Discharge (m ³ /s)	Annual Volume (MCM)	Q per Length (MCM/km)
T17 Indus	2730	1927	158	0.005	4.5	76	2116	13.39
T18 Indus	2590	1867	160	0.005	4.5	73	2131	13.32
T19 Suru	2618	2436	181	0.001	3.1	13	361	1.99
T20 Suru	2786	2585	166	0.001	2.3	6	141	0.88

Risk ranking of tunnels

The other important risk factor is cost, which is reflected by tunnel lengths and diameter. Smaller length tunnels are more viable. Tunnel length varies from 30 to 180 Km. It is clear that the tunnels which have more volume per tunnel length are more viable/attractive route for river water diversion. Considering that minimum 1m extra tunnel radius cutting will be required to accomplish tunnel

lining/stabilizing/smoothing, tunnel total excavation volume is shown in Fig. 6 varies from 0.91 to 5.47 MCM. Considering extraction volumes, tunnel length, and diversion volumes, the most likely activities includes:

Indus River T1, Tso Moriri, T7 Gaik, T14 Nimmo Bazgo, T17 Dah and T18 Batalik
 Chenab River T4 Jangalwar and T12 Kund Bara T12

Kund Bara tunnel from Chenab River seems to adopt due to shorter length (32.3 Km) and large flow diversion (3532 MCM).

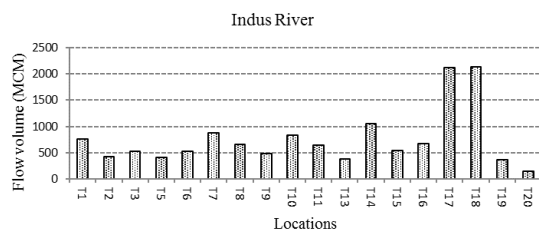


Fig. 4 Flow volume of tunnels

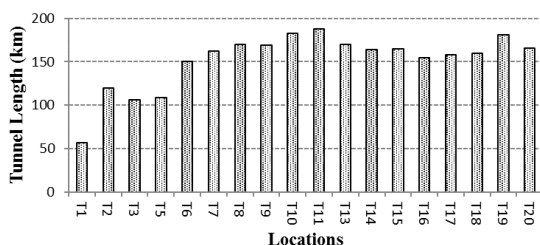


Fig. 5 Possible tunnels lengths at River Indus

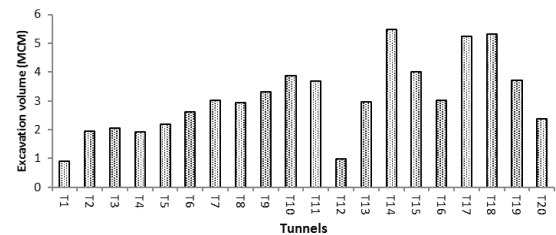


Fig. 6 Excavation volume of tunnels at River Indus

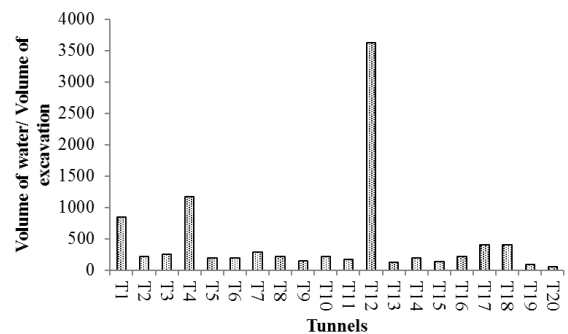


Fig. 7 Volume of water/volume of excavation of tunnels

Conclusions

Technical capabilities, financial gains and most important socio-political-diplomatic hegemony of India reflect high risk of Indus basin water transfer by India in violation of Indus Water Treaty.

India can divert Indus River water at many locations in J&K occupied region and the annual water transfer is estimated from possible locations minimum of 141 MCM to as much as 2131 MCM.

Unusual long tunnel lengths make covert and unlawful water theft/transfer less attractive.

Water transfer by India through tunnels from Indus River is very difficult but cannot be ruled out.

References

Akther,S., (2010). Emerging challenges to Indus waters treaty issues of compliance & transboundary impacts of Indian

- hydroprojects on the western rivers, Journal of the Institute of Regional Studies, Islamabad, Pakistan, V. 28., No.4, Autumn 2010, pp. 3-66
- Abbasi, A., (2012). Indus water treaty between India and Pakistan, Paper of Pakistan Institute of legislative development and transparency, [http://www.pildat.org/publications/publication/FP/IndusWaterTreatybetweenPakistanAndIndia_PakIndiaDialogueIII.pdf]
- Abbasi, A.H., (2009). 'www.defence.defence.pk' The News, Saturday, 14 February, 2009
- Autobee, R., (1996). Colorado-Big Thompson Project, [http://www.usbr.gov/projects/ImageServer?imgName=Doc_1303159857902.pdf]
- Ahmad, F., (2007), Probabilistic flood risk analysis in Chenab Riverine area in Muzaffargarh district. M.Sc Thesis, Center of Excellence in Water Resources Engineering, University of Engineering and Technology, Lahore.
- Ahmad B, Muhammad Shumail Kaleem, Mohsin Jamil Butt, Zakir Hussain Dahri (2010) Hydrological modelling and flood hazard mapping of Nullah Lai, Pakistan Agricultural Research Council (PARC), Islamabad, Pakistan
- Bozdag, A., and Gocmez, G., (2010). Digital elevation model at determining of some basin characteristics: a case study on the cihanbeyli (Konya) basin (balwois 2010 - ohrid, Republic of Macedonia 25, [http://balwois.com/balwois/administration/full_paper/ffp-1492.pdf]
- Bartak, V., (2008). How to extract river networks and catchment boundaries from DEM: a review of digital terrain analysis techniques. Journal of Landscape Studies 2 [<http://fzp.czu.cz/~bartakv/thesis>]
- Ghanbarpour, Shokoufeh Salimi, Mohsen Mohseni Saravi and Mehdi Zarei (2011) Calibration of River Hydraulic Model Combined with GIS Analysis using Ground-Based Observation Data, Research Journal of Applied Sciences, Engineering and Technology 3(5): 456-463, 2011
- Haq, N.U., (2010). Pakistan's water concerns, [<http://ipripak.org/factfiles/ff127.pdf>]
- Hayat, (2012). Indus waters treaty and resolution of water conflicts between two nuclear nations Pakistan and India, [<http://www.feem-web.it/ess/ess12/files/papers/hayat.pdf>]
- Hicks, F.E., and Peacock, T., (2004). Suitability of HEC-RAS for flood forecasting, Canadian Water Resources Journal, V. 30., pp. 159–174 (2005)
- Kiss, R., (1994). Determination of drainage network in digital elevation models, utilities and limitations, Journal of Hungarian Geomathematics Water Resources Research, v.30., p. 1681-1692,
- Latif, Q., (2007), Effect of channel improvement on water levels for Kabul River under flood conditions. M.Sc Thesis, Center of Excellence in Water Resources Engineering, University of Engineering and Technology Lahore.
- Miller, S.N., (2002). Estimating channel morphologic properties from a high resolution DEM, [<http://www.tucson.ars.ag.gov/icrw/proceedings/miller.pdf>]
- Shah, S.J.A., (2011). Indus waters treaty under stress: imperatives of climatic change or political manipulation, Margalla Papers 2011 Special Edition, Vol. 15., Issue I., 2011
- Taylor, T.C., (1975). Tunnel construction and NAWAPA, [<http://www.larouchepac.com/node/17641>]

Subsurface Flow Analysis of Hydraulic Structures using Bligh's Theory, Lane's Weighted Creep Theory and Modern Khosla's Theory

Hasnain Jillani^{*1}, Muhammad Haris Asghar Khan¹, Hammad ur Rehman¹

^{1*}Centre of Excellence in Water Resources Engineering
[*hasnain.civ.01@gmail.com](mailto:hasnain.civ.01@gmail.com)

Abstract: Hydraulic structures on permeable foundation requires special attention towards subsurface flow analysis compared to surface flow as the safety of structure is concerned. The seeping water underneath the foundation endangers the safety of hydraulic structures in two ways. Firstly, it sets up pressure gradient at the toe of structure, if excessive, may cause movement of the bed material with consequent failure of the work. This phenomenon is known as piping. Secondly, uplift pressures are created under the work itself which, if not adequately contained, will burst through it, providing a short path for subsoil flow and leading to total failure of the work. Present study includes the subsurface flow analysis of selected hydraulic structures using Bligh's, Lane's and Khosla's theories. The effect of location and depth of sheet piles on uplift pressures will also be investigated in this study. The preventive measures adopted to control the exit gradient or uplifts will be evaluated and discussed. The results of exit gradient and uplift pressures will be calculated and compared with safe values recommended by the above three researchers.

Keywords: Sub-surface analysis, hydraulic structures, seepage theories

Introduction

Hydraulic structures on permeable foundations are susceptible to seepage beneath the structures. This seepage water undermines the foundation and ultimately results in failure of structure. Hence the hydraulic structures on permeable foundations must be checked against possible pipping and undermining. Sufficient floor length and depth of sheet piles ensures the safety of structure against seepage water. Presently there are three approaches, namely Bligh's, Lane's and Khosla's Theory, to analyze hydraulic structure for subsurface flow. In recent practice, Lane's and Khosla's approaches are frequently adopted because of their reliable results. Subsoil flow threatens the stability of the work in two ways:

1. Sets up pressure gradient at the toe of work, if excessive, may cause movement of the bed with consequent failure of the work. (Piping)
2. Pressures (uplifts) are created under the work itself which, if not adequately contained, will burst through it, providing a short path for subsoil flow and leading to total failure of the work.

There are two major functions for the sheet pile to execute, one being protection of barrage floor against any danger of undermining and second is to increase the creep length in order to make the exit gradient safe. Haigh and Fraser (1941) highlighted the importance of u/s sheet pile as u/s sheet pile may protect the structure from possible

undermining in case of u/s flexible apron failure. The basic purpose of intermediate sheet pile is to protect the main components of barrage i.e. u/s glacis, crest, d/s glacis, piers, bridge, etc. in case of failure of u/s or d/s sheet pile. Singh (2011) stated in his study that the effectiveness of intermediate sheet pile stands nil against reduction in uplift pressures and it only adds to the cost of barrage. Recently Khosla's theory of independent variables is widely used for the safe exit gradient of structures. According to Khosla's exit gradient formula given as $G_E = \frac{H}{d} \frac{1}{\pi\sqrt{\lambda}}$, it's the head and depth of d/s sheet pile that influence the exit gradient value. Although depth of d/s sheet pile is decided by the d/s scour depth, but the value of safe exit gradient is the real governing factor for fixing the depth of d/s sheet pile (Haigh and Fraser, 1941). Shri (1995) engraves that the excessive length of d/s sheet pile may cause the uplifts to increase under the d/s floor while a shorter length reduces the exit gradient, hence a suitable length of d/s sheet pile is provided in order to keep the above problems minimized. During 19th century the value of exit gradient between 1/4 to 1/5 was considered safe against piping and undermining (Kapur, 1941). A lot of investigation were made for local scour in cohesionless soils. However, river banks and beds are often composed of mixture of gravel, sand, silt and clay. The location, extent and geometry of scour hole around bridge piers may

vary extensively in cohesive soils from those in cohesionless soils (Raju et al., 2002).

Scour depth may also vary depending upon the shape of structure to be encountered. Oliveto and Hager (2002) investigate the characteristics of scour holes around cylindrical and square piers and vertical-wall abutments with uniform bed material. Their findings at the end of experimental program were that the maximum scour depths occurred around the centreline of the upstream face of the piers and around the upstream corner of the vertical-wall abutments. It was also concluded that the maximum accretions took place around the rear face of these elements. The location of sheet pile underneath a hydraulic structure effects the seepage through foundation soil. Alsenousi and Mohamed (2008) studied the effect of location and inclination of sheet pile on seepage underneath a structure. According to their findings the exit gradient d/s of hydraulic structure decreases with the increase in sheet pile inclination. If the exit gradient and the seepage behind the hydraulic structure are considered as the major factors in the design of the structures, the optimum location of the sheet pile is at the toe of structure with inclination angle equals to 120° . While if the uplift head is considered as the major factor, the optimum location of the sheet pile is at the heel of the structure with inclination angle equals to 120° . Similarly, Alnealy and Alghazali (2015) use of inclined cut-off towards the upstream side with 45° inclination is beneficial in decreasing the uplift pressure to 40.3%, seepage quantity to 28.5%, as compared with the general case of no cut-off. Also, the use of inclined cut-off towards the downstream side with 120° inclination is beneficial in decreasing value of exist gradient to 5.0% and increasing the safety factor against piping phenomenon to 3.18. It was also concluded that the reduction in uplift pressure, exist gradient and seepage when using double cut-off at U/S with 45° inclination and D/S with 120° inclination is more than that of using double cut-off at the up and downstream at right angle that given decreasing in value of exist gradient to 8.03%, uplift pressure to 42.3%, seepage to 31.15% and increasing the safety factor against piping phenomenon to 2.43.

Al-Saadi et al., (2011) reported that use of downstream cut-off inclined towards the downstream side with angle less than 120° increases the safety factor against the piping phenomenon. It was also concluded that the effect of downstream cut-off inclination angle in reducing uplift pressure head under the hydraulic

structure is very small compared to its effect on exit gradient.

Failure of hydraulic structure by piping is enhance by the enlargement of tunnel, formed underneath the structure, as time passes. In order to estimate the time to downstream flooding i.e. failure of structure one must know the coefficient of erosion. Pipe diameter prior to breaching can also serve as an indicator for the peak flow and consequently time to failure (Bonelli and Benahmed, 2011). Markus et al. (2007) assessed the stability of dams, dykes and levees. Embankment dams and dykes can fail due to three possible failure threats namely external erosion (overtopping), internal erosion and sliding. Internal erosion is more hazardous for hydraulic structures being progressive in nature. To minimize the risk of failure risk management is recommended to understand the internal erosion process.

Hydraulic structures formed on permeable foundation can undergo seepage underneath which will endangers its stability. Subsurface analysis for existing and proposed sections of Panjnad Barrage was carried out using Bligh's approach, Lane's approach and modern Khosla's approach. For the scour calculations, well known Lacey's scour formula was used. The key plan of Panjnad Barrage is shown in Fig. 1.



Fig. 1 Key plan of Panjnad Barrage

Methodology

Hydraulic structures formed on permeable foundation can undergo seepage underneath which will endangers its stability. Subsurface analysis was carried out using Bligh's approach, Lane's approach and modern Khosla's approach. For the scour calculation Lacey's scour formula was used. Different methods employed are discussed as under:

Bligh's Creep Theory

As per Bligh's approach the seeping water follows the bottom contour of structure. The total creep length is calculated as $L = 2(\text{Vertical Length}) + \text{Horizontal Length}$. Head loss per unit length is given as H_L / L , where H_L is the head loss between upstream and downstream, also known as hydraulic gradient. To make structure safe against piping and undermining sufficient creep length should be provided i.e. $L = C.H_L$, where C is Bligh's creep coefficient. Different values of C against different soil types are listed in following Table 1.

Lane's Creep Theory

Extending Bligh's Theory Lane suggested that the vertical creep is more effective in reducing the uplifts as compared with horizontal creep. Hence a weightage factor of 1/3 was suggested for horizontal creep as against 1.0 for vertical creep. Now the total creep length is given as $L = 2(\text{Vertical Length}) + 1/3(\text{Horizontal Length})$. In this case the safe creep length is given as $L_1 = C_1.H_L$, where C_1 is the Lane's creep coefficient. Different values suggested by Lane for C_1 against different soil types are tabulated in following Table 2

Table 1 Bligh's Safe Hydraulic Gradient for Different Types of Soil

Sr. No.	Type of Soil	Value of C	Safe Hydraulic Gradient should be less than
1	Fine micaceous sand	15	1/15
2	Coarse grained sand	12	1/12
3	Sand mixed with boulder and gravel, and for loam soil	5 to 9	1/5 to 1/9
4	Light sand and mud	8	1/8

Table 2 Lane's Safe Hydraulic Gradient for Different Types of Soil

Sr. No.	Type of Soil	Value of C_1	Safe Hydraulic Gradient should be less than
1	Very fine sand or silt	8.5	1/8.5

2	Fine sand	7	1/7
3	Coarse sand	5	1/5
4	Gravel and sand	3 to 3.5	1/3.5 to 1/3
5	Boulders, gravels and sand	2.5 to 3	1/3 to 1/2.5
6	Clayey soils	1.6 to 3	1/3 to 1/1.6

Khosla's Theory

Khosla gave the concept of independent variables. According to Khosla's theory the seepage water doesn't creep along the bottom contour of structure instead it moves in a set of streamlines. Laplacian equation giving the steady seepage in vertical plane is expressed as follow:

$$\frac{d^2\phi}{dx^2} + \frac{d^2\phi}{dz^2} = 0$$

Where ϕ is flow potential and is equal to Kh .
 K = Coefficient of permeability and h = residual head at any point.

Exit Gradient

Khosla defines Exit Gradient as follow:

$$G_E = \frac{H}{d} \frac{1}{\pi\sqrt{\lambda}}$$

Where,

H = Head loss between upstream and downstream

d = Depth of downstream cut-off

$$\lambda = \frac{1 + \sqrt{1 + \alpha^2}}{2}$$

$\alpha = b/d$, b being total floor length

The Exit Gradient computed from above relation must lie within safe limit as given in following Table 3.

Table 3 Khosla's Safe Exit Gradient for Different Types of Soil

Type of Soil	Safe Exit Gradient
Shingle	1/4 to 1/5
Coarse sand	1/5 to 1/6
Fine sand	1/6 to 1/7

To estimate the percentage pressures at various key points of sheet pile one can either make use of developed equations or developed curves. Percentage pressure at key points of downstream sheet pile are estimated as follow:

$$\phi_E = \frac{1}{\pi} \cos^{-1} \left(\frac{\lambda - 2}{\lambda} \right)$$

$$\phi_D = \frac{1}{\pi} \cos^{-1} \left(\frac{\lambda - 1}{\lambda} \right)$$

Where,

$$\lambda = \frac{1 + \sqrt{1 + \alpha^2}}{2}$$

$$\alpha = \frac{b}{d} \text{ (respective)}$$

Percentage pressure at key points of upstream sheet pile are calculated as

$$\phi_{C1} = 100 - \phi_E$$

$$\phi_{D1} = 100 - \phi_D$$

For an intermediate sheet pile, the percentage pressures at key points are estimated by the following relations:

$$\phi_E = \frac{1}{\pi} \cos^{-1} \left(\frac{\lambda_1 - 1}{\lambda} \right)$$

$$\phi_D = \frac{1}{\pi} \cos^{-1} \left(\frac{\lambda_1}{\lambda} \right)$$

$$\phi_C = \frac{1}{\pi} \cos^{-1} \left(\frac{\lambda_1 + 1}{\lambda} \right)$$

Where,

$$\lambda = \frac{\sqrt{1 + \alpha_1^2} + \sqrt{1 + \alpha_2^2}}{2}$$

$$\lambda_1 = \frac{\sqrt{1 + \alpha_1^2} - \sqrt{1 + \alpha_2^2}}{2}$$

$$\alpha_1 = \frac{b_1}{d}$$

$$\alpha_2 = \frac{b_2}{d}$$

b_1 = Length of pucca floor upstream of sheet pile

b_2 = Length of pucca floor downstream of sheet pile

The above calculations are for the line diagram of structure and need corrections for the following three cases:

- Correction for the mutual interference of piles
- Correction for thickness of floor
- Correction for slope of floor

Correction for the mutual interference of piles

The percentage pressure correction due to mutual interference of pile is given by

$$C = 19 \sqrt{\frac{D}{b'}} \left[\frac{d + D}{b} \right]$$

Where, b' = Distance between two pile lines

D = Depth of pile line, the influence of which has to be determined on the neighbouring pile of depth d . D is to be measured below the level at which interference is desired.

d = Depth of pile on which the effect is considered

b = Total floor length

The correction is positive for the points in the rear or back water, and negative for the points forward in the direction of flow.

Correction for thickness of floor

$$C_f = \left(\frac{t_f}{d} \right) (\phi_1 - \phi_2)$$

Where, t_f = Floor thickness

d = Depth of sheet pile

$\phi_1 - \phi_2$ = Difference of uplift pressure between two consecutive key points

The correction is negative for the points in the rear or back water, and positive for the points forward in the direction of flow.

Correction for the slope of floor

Correction for the slope of floor is applicable only to the key points of piles located at the start or end of slope. The correction is estimated by the following relation:

$$C_s = F_s \left(\frac{b_s}{b_1} \right)$$

Where, b_s = Horizontal length of slope

b_1 = Distance between two piles

F_s = Correction factor which depends on the ratio of slope and is given in Table 4

Table 4 Slope Correction Factors

Slope (H : V)	Correction Factor
1:1	11.2
2:1	6.5
3:1	4.5
4:1	3.3
5:1	2.8

6:1	2.5
7:1	2.3
8:1	2.0

The correction is positive for the downward slope and negative for the upward slope following the direction of flow.

Scour Calculations

Scour calculations were performed as per Lacey's Scour Formula which is given as below:

$$R = 0.9 \left(\frac{q^2}{f} \right)^{1/3}$$

Where, q = Discharge per unit width (cusecs/ft)

F = Lacey's silt factor = $1.75\sqrt{D_{50}}$

D₅₀ = Mean particle size (mm)

Results and Discussion

There were mainly four different sections of Panjnad barrage which were analysed, namely Left Pocket, Main Weir, Annexe Weir and Additional Depressed Bays.

Creep results for different barrage sections, as per Bligh's and Lane's Weighted Creep Theory, for existing and remodelled barrage are compared with safe values in Table 5

Exit gradient for different sections of Panjnad Barrage, calculated using Khosla's Exit Gradient approach, are tabulated in following Table 6

The remaining seepage pressure at end of pucca floor, as calculated by equations proposed by Khosla, and required and provided thicknesses for existing and remodelled barrage are tabulated in Table 7 and Table 8 respectively.

Table 5 Creep Analysis Results as per Bligh and Lane Creep Theories

Sr. No.	Description	Existing Barrage		Remodelled Barrage		Safe Bligh's Creep Ratio	Safe Lane's Creep Ratio
		Creep Ratio		Creep Ratio			
		Bligh's Theory	Lane's Theory	Bligh's Theory	Lane's Theory		
1	Left Pocket	16.4	8.5	22.0	13.8	15.0	7.0
2	Main Weir	18.4	10.5	21.8	13.6	15.0	7.0
3	Annexe Weir	14.3	9.1	19.9	12.9	15.0	7.0
4	Additional Bays	18.9	11.9	18.9	11.9	15.0	7.0

Table 6 Exit Gradient Results as per Khosla Theory

Sr. No.	Description	Existing Barrage	Remodelled Barrage	Safe Exit Gradient as per Soil Condition
		Exit Gradient (1/G _E)	Exit Gradient (1/G _E)	
1	Left Pocket	8.03	9.34	6.0
2	Main Weir	8.08	9.34	6.0
3	Annexe Weir	5.41	8.33	6.0
4	Additional Bays	7.92	7.92	6.0

Table 7 Uplift Analysis Results as per Khosla Theory

Existing Barrage				
Sr. No.	Description	Remaining Seepage Pressure	Required Thickness	Provided Thickness
1	Left Pocket	24.90	4.21	2.50
2	Main Weir	23.69	4.01	2.50
3	Annexe Weir	24.36	4.30	4.00

Table 8 Uplift Analysis Results as per Khosla Theory

Remodelled Barrage				
Sr. No.	Description	Remaining Seepage Pressure	Required Thickness	Provided Thickness
1	Left Pocket	26.77	1.42	3.50
2	Main Weir	26.77	1.42	3.50

3	Annexe Weir	29.08	1.27	3.50
4	Additional Depressed Bays	27.06	5.59	6.50
Note: Required thickness with 4-5 ft. water cushion on downstream floor.				

Table 9 Lacey's Scour Results

Sr. No.	Description	Scour Below Bed		Existing Cut-off Depth		Proposed Cut-off Depth	
		U/S	D/S	U/S			U/S
1	Left Pocket (q = 250.82 cusecs/ft)	25.09	32.76	5.00	25.50	22.50	33.50
2	Main Weir (q = 250.82 cusecs/ft)	25.09	32.76	22.00	25.50	22.50	33.50
3	Annexe Weir (q = 250.82 cusecs/ft)	25.09	32.76	22.00	20.00	22.50	32.50
4	Additional Bays (q = 310.58 cusecs/ft)	33.12	35.97	-	-	31.75	35.00

The adequacy of sheet piles was checked on basis of scour calculations. The results of scour as per Lacey's scour formula for existing and rehabilitated conditions are tabulated in Table 9.

Conclusion

The following conclusions are drawn from the present study based on the results discussed above:

- The creep coefficient, as per Bligh's Theory, for annexe weir section falls short from recommended safe value. However, these coefficients are within limit for the existing left pocket and main weir sections.
- The creep coefficients, as per Lane's Weighted Creep Theory, for all existing barrage sections are well above the recommended limiting value of 7.0.
- The required creep length was achieved by sealing the downstream block apron provided with pressure relief holes at regular spacing.
- The creep coefficients are further improved by the remodelling of existing barrage in which the sloping sealed block apron is replaced by the levelled concrete floor with end sill. The creep length for additional depressed bays is well above the requirement.
- Exit gradient calculations for different existing barrage sections are safe as per the site soil condition except for annexe weir where this value is below the limiting safe value of exit gradient. New sheet piles are proposed at end of proposed downstream impervious floor in order to satisfy the exit gradient criteria.
- The required floor thicknesses for the existing sections of barrage (left pocket, main weir and annexe weir) are more

compared with provided or existing thickness. The reason for less provided thickness being sealing of grooves with pressure relief holes in downstream block apron instead of rigid concrete floor. The existing impervious floor thicknesses are satisfied by taking water cushion over stilling basin, however the new concrete floor is provided with thicknesses for severe case of no water cushion. The floor thickness for the additional bays is recommended according to gravity design considerations.

- He provided sheet piles in existing sections of barrage confirms the scour calculations according to Lacey's scour formula with factor of safety being 1.25 and 1.50 for the upstream and downstream respectively. The Lacey's silt factor for the existing barrage sections was adopted as 1.0. However, for the scour calculations of remodelled barrage with additional bays Lacey's silt factor being adopted as 0.85 (as per recent site soil conditions). On the other hand, the factors of safety are same as 1.25 and 1.50 for the upstream and downstream respectively. As per the results of scour calculations a new sheet pile is proposed upstream of left pocket. The depths of proposed sheet piles downstream of left pocket, main weir and annexe weir are fixed in order to satisfy both the scour and exit gradient criteria.

References

- Alnealy, H.K.T., N.O.S. Alghazali (2015), Analysis of Seepage Under Hydraulic Structures Using Slide Program, American Journal of Civil Engineering. Vol. 3, No. 4, pp. 116-124.
- Alsenousi, K.F., G.M. Hasan (2008), Effects of Inclined Cut-offs and Soil Foundation

- Characteristics on Seepage Beneath Hydraulic Structures, Department of Civil Engineering, University of Garyounis, Libya.
- Ansari, S.A., U.C. Kothiyari, K.G.R. Raju (2002), Influence of Cohesion on Scour Around Bridge Piers, Dept. Of Civil Engineering, Aligarh Muslim University, Aligarh, India.
- Bonelli, S., N. Benahmed (2011), Piping Flow Erosion in Water Retaining Structures: Inferring Erosion Rates From Hole Erosion Tests and Quantifying the Failure Time. 8th ICOLD European Club Symposium Dam Safety - Sustainability in a Changing Environment, Sep 2010, Innsbruck, Austria.
- Fraser, F., Haige (1941), The Emerson Barrage, Journal of the Institution of Civil Engineers, Paper No. 5227.
- Kapur, S.N. (1941), River Diversion at Trimmu, I.S.E. Paper No. 229.
- Markus, A., J.J. Fry, G. Matthias, P. Sebastian (2007) Assessment of the Risk of Internal Erosion of Water Retaining Structures: Dams, Dykes and Levees, Intermediate Report of the European Working Group of ICOLD Contributions to the Symposium, Freising, Germany.
- Oliveto G, W.H. Hager (2002), Temporal Variation of Clear-Water Pier and Abutment Scour, Journal of Hydraulics Engineering. 128: 811–820
- Saleh I., K. Al-Saadi, H.T.N. Al-Damarchi, H.C.D. Al-Zrejawi (2011), Optimum Location and Angle of Inclination of Cut-off to Control Exit Gradient and Uplift Pressure Head under Hydraulic Structures, Jordan Journal of Civil Engineering, Volume 5, No. 3
- Shri, N. (1995) Manual on Barrages and Weirs on Permeable Foundation, Central Board of Irrigation and Power, New Delhi, India. Volume 1, Publication No. 179.
- Singh, R.J. (2011), Optimal Hydraulic Structures Profiles Under Uncertain Seepage Head, Motilal Nehru National Institute of Technology, Allahabad-211004, India.

Assessing Hydropower Resilience under Changing Climate: Murum-Bakun Cascade in East Malaysia

Khamaruzaman B. Wan Yusof^{1*}, Mubasher Hussain^{1,2}, Muhammad Raza-ul-Mustafa¹

¹Department of Civil and Environmental Engineering, Universiti Teknologi Petronas, Malaysia

²Hydro Department, Sarawak Energy Berhad, Malaysia

*khamaruzaman.yusof@utp.edu.my

Abstract: This study assessed the climate change impact on the Murum Hydropower Plant (HEP) and Bakun HEP in Sarawak state of Malaysia. Multi-model ensemble of three General Circulation Models (GCMs) from Coupled Model Intercomparison Project Phase 5 (CMIP5) was used to simulate the daily precipitation over the catchment for the period of 2011–2100 under two future scenarios (RCP4.5 and RCP8.5). A hydrological model was developed using Australian Water Balance Model (AWBM) approach; and historical and future river inflows were simulated at Murum Dam and Bakun Dam. Reservoir operation model was developed for the hydropower system to simulate the operation under the historical inflows as well as for the future projected inflows. It was noted that the mean river inflow will improve in the future at both Dams especially under RCP8.5. The similar results were noted while simulating the reservoir operation and it was noted that the annual energy from Murum HEP and Bakun HEP would increase up to 12 % and 7% respectively under RCP8.5 of 2080's.

Keywords: climate resilience, hydrologic modeling, hydropower, reservoir operation, CMIP5

Introduction

When we talk about the renewable energy, hydropower is the major source of renewable energy with relatively lower cost of energy. It integrates well with the other intermittent sources such as solar and wind power to ensure the grid system stability. Currently, hydropower contributes about 16% of the global energy and from 1973 to 2011, the global hydropower production increased by 175 percent [1].

Continuous increase of greenhouse gas emission in the atmosphere, positive radiative forcing and global warming are evidence of anthropogenic influence on the global climate system [2]. During 1951 to 2010, emission of greenhouse gases caused a global surface warming ranging from 0.5 °C to 1.3 °C. It will cause further warming and change the future global climate system [3]. Climate scientists noted that, it would alter the hydrological systems of major river basins as exhibited by [4-10]. In Malaysia, very few studies explored the climate change impact on water resources such as [11-15] and they revealed that there will be notable changes in river inflows during the 21st century.

Stream flow into a reservoir play a vital role for hydroelectric projects as it is the fuel to run the hydroelectric plants. Climate change results in temperature and precipitation change (i.e. intensity and pattern) and it significantly impact on regional hydrological processes [16]. In this

study, we assessed the potential impacts of climate change on the operation of Murum reservoir and Bakun reservoir using General Circulation Models (GCMs) from the Coupled Model Intercomparison Project Phase 5 (CMIP5).

The objectives of this paper were; 1) to project future changes in precipitation over the Rajang River Basin in Sarawak utilizing CMIP5 projections, 2) projection of river inflows to the Murum Reservoir and Bakun Reservoir using the projected future precipitation over the catchment, 3) cascaded reservoir operation modeling to assess the climate change impact on hydropower energy yield from these hydroelectric plants.

Study Area and Data Description

Study Area

Murum HEP

Murum HEP is the recently commissioned hydroelectric plant in the Sarawak state of Malaysia, it is located in upper Rajang River Basin (RRB) and regulates about twenty percent of the Bakun catchment. The project location map is as shown in Fig. 1. The plant generates a maximum output of 944 MW with 4 vertical Francis turbines (each of 236 MW). The project has 141 m high Roller Compacted Concrete (RCC) gravity Dam as shown in Fig. 2. The dam has world tallest stepped spillway structure (54 m wide) with a total discharge capacity of 2160

m³/s. The project has a surface powerhouse connected through 5.5 km long twin tunnels. A catchment of 2750 km² drains into the reservoir to provide water resources to hydroelectric plant. The catchment is covered with the tropical rainforest where precipitation in the form of rainfall drives the water resources system.

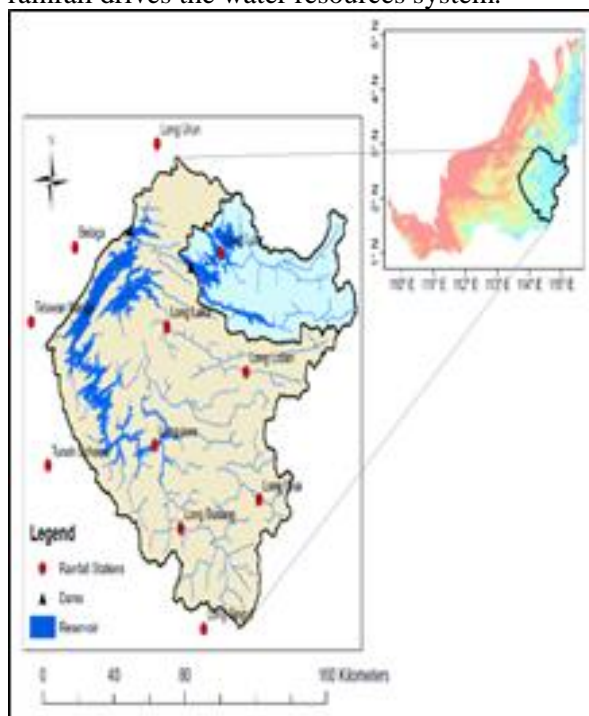


Fig. 1 Location of Bakun HEP and Murum HE Catchments in Sarawak state of Malaysia



Fig. 2 Murum Dam in Sarawak state of Malaysia

Bakun HEP

Bakun HEP is the largest hydroelectric plant in Malaysia with total installed capacity of 2,400 MW. The plant commissioned in 2012 and supply power to the Sarawak state grid. The Bakun Dam is 205 m high concrete face rockfill dam (CFRD) and a side channel gated spillway

with four radial gates to discharge flood water during extreme flood events (as shown in Fig. 3). The Bakun HEP has a surface powerhouse consists of eight Francis turbine each of 300 MW. The Bakun reservoir is the largest fresh water storage reservoir in Malaysia with surface area of about 640 km² masl and storage capacity of 37,521 million m³ at full supply level of 228 masl. A catchment of 14,850 km² drains into the Bakun reservoir to supply inflow to the Bakun HEP.



Fig. 3 Bakun Dam in Sarawak state of Malaysia

Data Description

Daily rainfall record of eleven rainfall stations (as shown in Fig. 1) for the period of 1976–2005 was acquired from Department of Irrigation and Drainage (DID), Sarawak for this study. There were some missing periods in rainfall records at all stations and these were filled using multilevel regression method. For climate change impact assessment, the precipitation ensembles for three GCMs from the CMIP5 have been selected in this study as listed in Table 1. The precipitation time series for the controlled run (1976-2005) and future run (2011-2100) of each GCM were downloaded from Intergovernmental Panel on Climate Change (IPCC) World Data Center for Climate website; http://www.ipcc-data.org/sim/gcm_monthly/AR5/Reference-Archive.html. Only one ensemble member r1i1p1 was used in this study. These three models were declared satisfactory among the others during evaluation over the Rajang River Basin and therefore selected in this study. The mean ensemble of these three selected models (B3MMM) was also developed for the control and future period to assess the climate change impact in this study.

Table 1 Selected GCMs from CMIP5 used in the study

CMIP5 Model	Institute	Modeling Group	Country
ACCESS 1.0	CSIRO-BOM	Commonwealth Scientific and Industrial Research Organization (CSIRO) and Bureau of Meteorology (BOM), Australia	Australia
ACCESS 1.3	CSIRO-BOM	Commonwealth Scientific and Industrial Research Organization (CSIRO) and Bureau of Meteorology (BOM), Australia	Australia
GFDL-ESM2M	NOAAGF DL	Geophysical Fluid Dynamics Laboratory, USA	USA

Methodology

Downscaling future precipitation

A weather generator approach was used to simulate the future precipitation over each selected rainfall station. A weather generator called WeaGETS developed by [17] was used in this study. Third order Markov chain was used for the precipitation occurrence and gamma distribution to generate the precipitation amount for the wet days. The historical daily precipitation for the period of 1976-2005 was used as input to the weather generator to generate the future time series of daily precipitation. The detailed methodology of this method is provided in [17]. The stochastically generated future precipitation at each rainfall station in the catchment was perturbed using the quantile perturbation technique (a change factor technique) employing the controlled (historical) and future runs of mean ensemble of three GCMs under RCP4.5 and RCP8.5. During this study, Climate Perturbation Tool developed by [18] was used for perturbation of daily precipitation at each station.

Hydrological modeling using Aquarius Forecast

A rainfall-runoff model was developed using the Australian Water Balance Model (AWBM) approach. Aquarius Forecast tool was used to develop the hydrologic model for the Bakun catchment. As the Murum HEP lies in the Bakun Dam catchment and control about twenty percent of the Bakun catchment. The river inflows at Bakun Dam are available for the period of 2003 to 2007, therefore a hydrologic model was calibrated at the Bakun Dam and after calibration; the model was run for Murum catchment to simulate the daily inflow at Murum Dam. The meteorological model was established using the Thiessen polygon gauge weight method for precipitation calculation. During the model calibration, the simulated daily inflows were compared (as shown in Fig. 4) with the observed daily inflow using the coefficient of determination (R^2), percent deviation (D), and Nash-Sutcliffe efficiency (E). The model's performance parameters— R^2 , D, and E were calculated using the following equations:

$$R^2 = \frac{\sum((Q_{obs} - \bar{Q}_{obs}) - (Q_{sim} - \bar{Q}_{sim}))^2}{\sqrt{\sum((Q_{obs} - \bar{Q}_{obs})^2 - (Q_{sim} - \bar{Q}_{sim})^2)}} \quad (1)$$

$$D = 100 \times \frac{\sum(Q_{sim}) - (Q_{obs})}{\sum Q_{obs}} \quad (2)$$

$$E = 1 - \frac{\sum(Q_{sim} - Q_{obs})^2}{\sum(Q_{obs} - \bar{Q}_{obs})^2} \quad (3)$$

The value of R^2 close to 1, value of D close to 0% and the value of E close to 1 implies good calibration. During this study, the coefficient of determination (R^2) was noted as 0.68, percent deviation (D) as 0.03 %, and Nash-Sutcliffe efficiency (E) as 0.68. These results were satisfactory and complement well with some previous studies such as [4, 19-22]. All these studies simulated river inflow for the climate change assessment with E ranging from 0.48 to 0.83 and R^2 from 0.63 to 0.84. The performance of hydrological model during calibration is as shown in Fig. 4.

After calibration of the hydrological model, the long term daily inflow were simulated at the Murum Dam and also for the eighty percent of the unregulated catchment of Bakun Dam for the historical period of 1976–2005 as well as for the three future period of 2011–2040 (2020's), 2041–2070 (2050's) and 2071–2100 (2080's). And then the inflow at Bakun Dam were derived from the following equation;

$$Q_{Bakun} = Q_{unregulated} + Q_{regulated\ Murum} \quad (4)$$

where Q_{Bakun} is total inflow at Bakun, $Q_{unregulated}$ is inflow from the unregulated Bakun catchment and $Q_{regulated\ Murum}$ is total outflow from the Murum HEP in the result of reservoir operation.

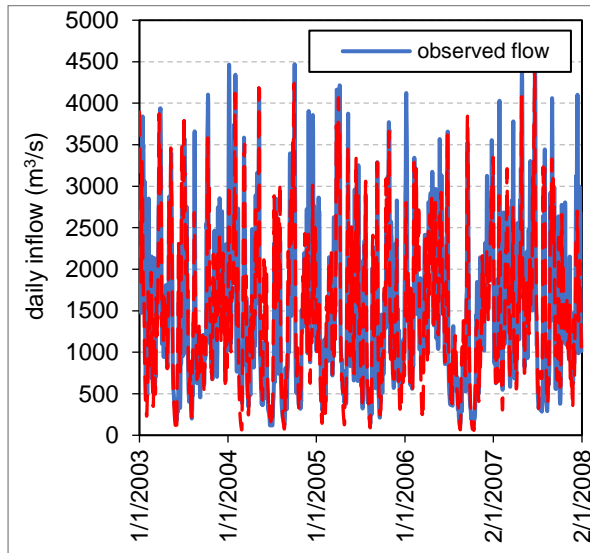


Fig. 4 Observed and simulated inflows at Bakun Dam during the model calibration

Reservoir operation

A reservoir operation model was developed for the Murum reservoir and Bakun reservoir using the HEC-ResSim model. All project features including reservoir storage, surface area, river inflows, evaporation, dam height, spillway discharge rating, station's installed capacity, turbine rated discharge, turbine efficiency, environmental flow requirement etc. were provided in the reservoir operation model. The station dispatch rules were defined for the daily power requirement and additional output to avoid spillway discharge. The reservoir operation was simulated using the historical inflows (1976–2005) and also for the future generated inflows for all of three future periods under the both RCPs.

Table 2 Changes in seasonal availability of water resources at each Dam

	RCP4.5			RCP8.5		
	2020's	2050's	2080's	2020's	2050's	2080's
Murum HEP	1	-1	5	5	4	12
Bakun HEP	1	-1	4	4	4	7

Results and discussion

Projected river inflows under future precipitation scenarios

The future river inflows were simulated under the projected precipitation for both climate scenarios i.e. RCP4.5 and RCP8.5; and were compared with the historical inflows as shown in Table 2. It was noted that the mean inflow at Murum Dam would remain same and increase by 4% during 2020's; decrease by 2% and increase by 3% during 2050's; and increase up to 4% and 11% during 2080's under RCP4.5 and RCP8.5 respectively. It was noted that the mean inflow at Bakun Dam would remain same and increase by 4% during 2020's; decrease by 1% and increase by 3% during 2050's; and increase up to 4% and 11% during 2080's under RCP4.5 and RCP8.5 respectively.

The mean seasonal inflow was also calculated at each hydroelectric plant and their variability in the context of future climate changes were assessed under the both RCPs. It was noted that under RCP4.5, there would be reduction in DJF inflow at Murum HEP and Bakun HEP during 2050's and 2080's. Under RCP8.5 scenario, considerably increase in MAM inflow is noted at Murum HEP and Bakun HEP in future. For the JJA, both HEP would receive increase in JJA inflow in future. The JJA is the period when these catchments yield lowest inflow in result of lowest precipitation over the catchment. It is noted that the lowest flow during JJA would improve in future. MAM is the late North-West monsoon period and receive the average rainfall over the upper RRB, but it is projected that the inflow during this period would also improve in future. But reduction in river inflow in noted during the DJF in the RRB, which indicates that there would be a seasonal shift over the upper RRB in future due to potential climate changes which would result in decrease in inflow during DJF and increase during MAM.

Table 3: Projected changes in future hydropower energy

	RCP4.5			RCP8.5		
	2020's	2050's	2080's	2020's	2050's	2080's
Murum HEP						
Annual	0	-2	4	4	3	11
DJF	3	-9	-9	-1	-3	5
MAM	-4	0	4	10	2	12

JJA	2	4	15	7	15	17
SON	1	-4	6	2	-3	11
Bakun HEP						
Annual	0	-1	4	4	3	11
DJF	2	-7	-8	-1	-1	5
MA						
M	-5	1	2	7	3	10
JJA	2	2	14	7	13	17
SON	-1	-3	5	1	-1	10

Projected changes in hydropower energy

It is noted that the annual energy from Murum HEP would increase by 1% and 5% during 2020's, decrease by 1% and increase by 4% during 2050's and increase by 5% and 12% during 2080's under RCP4.5 and RCP8.5 respectively. Significant increase in annual energy is noted during 2080's under RCP8.5 (as shown in Table 3) due to projected increase in water resources availability under RCP8.5 of 2080's.

For the Bakun HEP, it is also projected that the annual energy would increase by 1% and 4% during 2020's, decrease by 1% and increase by 4% during 2050's and increase by 4% and 7% during 2080's under RCP4.5 and RCP8.5 respectively. Significant increase in annual energy is noted during 2080's under RCP8.5 (as shown in Table 3) due to projected increase in water resources availability under RCP8.5 of 2080's.

Conclusions and Recommendations

While assessing the climate change impact on future precipitation over study area, it was concluded that the annual Precipitation is expected to increase significantly over the river basin under RCP4.5 and RCP8.5. Similar trend is projected for the seasonal precipitation, especially during the March to May, when the increase in precipitation is more robust for both scenarios. As these catchments are projected to receive increase in future precipitation especially for the period of 2080s of RCP4.5 and 2050s and 2080s of RCP8.5, therefore the water resources availability is also increasing during these periods. The projected increase in precipitation under future climate provides water security to the hydroelectric plants. The Murum HEP and Bakun HEP would expect higher increase in hydropower production under RCP8.5 compared to RCP4.5 due to increase in projected inflows under the future climate. The Murum HEP is projected to have 12% and Bakun HEP is

projected to have 7% increases in future energy production under RCP8.5.

The hydrological models are commonly being developed using the current hydrological behavior and catchment characteristics. The model parameters are calibrated with the observed historical inflows. When these models are employed to simulate the future inflows, it is assumed that the catchment characteristics and hydrological behavior of the river will be stationary in future. Even though the Sarawak state of Malaysia is less populated and anthropogenic impacts are comparatively lesser, but the deforestation is being witness in the upper Rajang river basin. These activities would alter the hydrological behavior of these catchments in future and there is a need to investigate the future changes in the catchment characteristics/ land use changes and their impact on river water yield.

Acknowledgment

This study was funded by Sarawak Energy Berhad, Malaysia under a climate change research project. The authors would like to express thanks to Department of Irrigation and Drainage, Sarawak (DID) for providing the relevant observed precipitation data.

References

- [1] M. A. Cole, R. J. R. Elliott, and E. Strobl, "Climate Change, Hydro-Dependency, and the African Dam Boom," *World Development*, vol. 60, pp. 84-98, 2014.
- [2] M. Hassan, P. Du, S. Jia, W. Iqbal, R. Mahmood, and W. Ba, "An Assessment of the South Asian Summer Monsoon Variability for Present and Future Climatologies Using a High Resolution Regional Climate Model (RegCM4.3) under the AR5 Scenarios," *Atmosphere*, vol. 6, pp. 1833-1857, 2015.
- [3] IPCC, "Summary for Policymakers. In: Climate Change 2013: The Physical Science Basis. Contribution of Working Group I to the Fifth Assessment Report of the Intergovernmental Panel on Climate Change [Stocker, T.F., D. Qin, G.-K. Plattner, M. Tignor, S.K. Allen, J. Boschung, A. Nauels, Y. Xia, V. Bex and P.M. Midgley (eds.)],"
Cambridge University Press, Cambridge, United Kingdom and New York, NY, USA., 2013.
- [4] R. Mahmood, S. Jia, and M. Babel, "Potential Impacts of Climate Change on Water Resources in the Kunhar River Basin, Pakistan," *Water*, vol. 8, p. 23, 2016.

- [5] H. G. Hidalgo, J. A. Amador, E. J. Alfaro, and B. Quesada, "Hydrological climate change projections for Central America," *Journal of Hydrology*, vol. 495, pp. 94-112, 2013.
- [6] C. Zhang, B. Zhang, W. Li, and M. Liu, "Response of streamflow to climate change and human activity in Xitiaoxi river basin in China," *Hydrological Processes*, vol. 28, pp. 43-50, 2014.
- [7] S. W. Kienzle, M. W. Nemeth, J. M. Byrne, and R. J. MacDonald, "Simulating the hydrological impacts of climate change in the upper North Saskatchewan River basin, Alberta, Canada," *Journal of Hydrology*, vol. 412-413, pp. 76-89, 2012.
- [8] H. Chang and I.-W. Jung, "Spatial and temporal changes in runoff caused by climate change in a complex large river basin in Oregon," *Journal of Hydrology*, vol. 388, pp. 186-207, 2010.
- [9] M. G. Grillakis, A. G. Koutroulis, and I. K. Tsanis, "Climate change impact on the hydrology of Spencer Creek watershed in Southern Ontario, Canada," *Journal of Hydrology*, vol. 409, pp. 1-19, 2011.
- [10] D. Khadka, M. S. Babel, S. Shrestha, and N. K. Tripathi, "Climate change impact on glacier and snow melt and runoff in Tamakoshi basin in the Hindu Kush Himalayan (HKH) region," *Journal of Hydrology*, vol. 511, pp. 49-60, 2014.
- [11] M. Z. M. Amin, A. J. Shaaban, N. Ohara, M. L. Kavvas, Z. Q. Chen, S. Kure, *et al.*, "Climate change assessment of water resources in Sabah and Sarawak, Malaysia, based on dynamically-downscaled GCM projections using a regional hydroclimate model," *Journal of Hydrologic Engineering*, vol. 21, 2016.
- [12] M. L. Tan, D. L. Ficklin, A. L. Ibrahim, and Z. Yusop, "Impacts and uncertainties of climate change on streamflow of the Johor River Basin, Malaysia using a CMIP5 General Circulation Model ensemble," *Journal of Water and Climate Change*, vol. 5, p. 676, 2014.
- [13] M. R. Mustafa, M. Hussain, and K. W. Yusof, "Climate change impact on water resources of Bakun hydroelectric plant in Sarawak, Malaysia," *Proceedings of the 3rd International Conference on Civil, Offshore and Environmental Engineering*, vol. (ICCOEE 2016, Malaysia, 15-17 Aug 2016), pp. 283-287, 2016.
- [14] M. Hussain, S. Nadya, K. W. Yusof, and M. R. Mustafa, "Potential impact of climate change on inflows to the Batang Ai reservoir, Malaysia," *International Journal on Hydropower & Dams*, vol. 24, pp. 44-48, 2017.
- [15] M. Hussain, K. W. Yusof, M. R. Mustafa, R. Mahmood, and J. Shaofeng, "Projected changes in temperature and precipitation in Sarawak state of Malaysia for selected CMIP5 climate scenarios," *International Journal of Sustainable Development and Planning*, vol. 12, pp. 1299 - 1311, 2017.
- [16] D. Labat, Y. Godd eris, J. L. Probst, and J. L. Guyot, "Evidence for global runoff increase related to climate warming," *Advances in Water Resources*, vol. 27, pp. 631-642, 2004.
- [17] J. Chen, F. P. Brissette, and R. Leconte, "A daily stochastic weather generator for preserving low-frequency of climate variability," *Journal of Hydrology*, vol. 388, pp. 480-490, 2010.
- [18] V. Ntegeka, P. Baguis, E. Roulin, and P. Willems, "Developing tailored climate change scenarios for hydrological impact assessments," *Journal of Hydrology*, vol. 508, pp. 307-321, 2014.
- [19] R. Meenu, S. Rehana, and P. P. Mujumdar, "Assessment of hydrologic impacts of climate change in Tunga-Bhadra river basin, India with HEC-HMS and SDSM," *Hydrological Processes*, vol. 27, pp. 1572-1589, 2013.
- [20] A. K. Verma, M. K. Jha, and R. K. Mahana, "Evaluation of HEC-HMS and WEPP for simulating watershed runoff using remote sensing and geographical information system," *Paddy and Water Environment*, vol. 8, pp. 131-144, 2010.
- [21] G. Yimer, A. Jonoski, and A. V. Griensven, "Hydrological Response of a Catchment to Climate Change in the Upper Beles River Basin, Upper Blue Nile, Ethiopia," *Nile Basin Water Eng. Sci. Mag.*, vol. 2, pp. 49-59, 2009.
- [22] A. Garc a, A. Sainz, J. A. Revilla, C.  lvarez, J. A. Juanes, and A. Puente, "Surface water resources assessment in scarcely gauged basins in the north of Spain," *Journal of Hydrology*, vol. 356, pp. 312-326, 2008.

Rainfall-Runoff Relationship for Small Watershed in Potohar Area

Moien Ahsan^{1*}, Sonia Zafar², Ghulam Nabi¹

¹Centre of Excellence in Water Resources Engineering, University of Engineering and Technology, Lahore 54890, Pakistan

*moienuet@gmail.com

Abstract: Rainfall-Runoff relationship is essential for planning and design of soil and water conservation structures, flood estimation and control. Runoff is a complex interaction between precipitation and landscape. Water is one of the most important resource available and it is controlled by a natural phenomenon of "Hydrological Cycle". Hydrological modeling is a complex phenomenon in which a relationship is created between the input and output parameters. The objective of study is to develop the rainfall runoff relationship for the small watersheds in Potohar regions of Pakistan. In this study the detailed analysis of runoff mechanism was done using Semi distributed approach (TOPMODEL) for three small watersheds (Dharabi, Domeli and Lehri Dam watershed) in Potohar region of Pakistan. The model was simulated for Low, medium and peak flow events to check the applicability of model. TOPMODEL showed satisfactory results for the existing three small dam's watersheds in Potohar area. Comparison of low, medium and peak flows were made between simulated and observed. Model efficiency for Dharabi, Domeli and Lehri dam was 74%, 78 and 79 % respectively. Runoff fraction was determined was 0.73. Rainfall runoff relationship was developed for the Potohar region $y = 12359x + 81183$, $R^2 = 0.844$ in which X =Rainfall (mm), Y =Volume (mm) The outcome of this study is quite helpful for future work in water resources development techniques such as construction of small dams, ponds, soil and water conservation structures for agriculture purposes.

Keywords: Rainfall Runoff Relationship, Runoff Coefficient, Semi-distributed approach

Introduction

Rainfall-Runoff relationship is very important role in Planning, Development and management of water resources. Attempts have been made in the past to determine rainfall-runoff relationship in the for the Potohar area of Punjab, Pakistan catchment. Runoff occurs when parts of the landscape are saturated or impervious. Runoff is a complex interaction between precipitation and landscape factors. There are many factors which effects the peak and volume of flow generated. These may be meteorological and hydrological factors, land use and cover, topography, soil characteristics, etc have been defined for urban, rangeland, and agricultural drainages. There are different techniques which may be used for estimation of peak and volume of flow. There may be Empirical, Rational, Lumped, Distributed and Semi-distributed approaches.

Rainfall-Runoff relationship is essential for design and planning of soil and water conservation structures, flood estimation and control. Mostly empirical approach is used for such purpose, no comprehensive work has been done for estimation of Rainfall-Runoff for Potohar area of Indus basin. The land resources of Potohar area are characterized with fragmented land holdings. An improper selection

of catchment modeling technique causes a lot of variations in the result, which may cause design failure. In order to harvest rainwater, several water resources development schemes such as construction of small dams, mini dams, ponds and soil & water conservation structures should be constructed to store the water for hydropower, agriculture, etc. During this study the detailed analysis of runoff mechanism was done, and the outcome is helpful for water resources development techniques such as construction of small dams, ponds, soil & water conservation structures, and irrigation and agriculture purposes. The purpose of the study is the estimation of runoff by Semi-distributed approach and development of Rainfall-Runoff coefficient for Potohar area in the Punjab, Pakistan. The study was also conducted to establish the guidelines / Rainfall-Runoff relationship for runoff estimation for the soil and water conservation structures.

Haye and Youngs (2005) compared the design characteristics of observed hydrological data of eight small catchments in central Virginia whose area ranges from 2.5 to 52.7 acres. Rational Method was used for estimation of peak discharge. Time of concentration and runoff coefficients were also used in this study.

The temporal changes in spatial distribution of land cover, runoff coefficients, and runoff volume was estimated. A digital elevation model and runoff hydrograph was made for study area which based upon above mentioned data information. From the land cover pattern of the study area it was concluded that with the passage of time urban area increases and vegetation area decreases. Due to this change the runoff volume and peak flow increased. It was concluded that by increasing vegetation in catchment area floods can be reduced Zhan (2005).

Norbiato(2009) has studied 14 catchments whose area ranges from 7.3 to 608.4 km². All the catchments were mountainous and analysis the effect of different factors e.g. flood type, geology, temperature, initial soil moisture conditions and land use on the distribution functions of the event runoff coefficients. Runoff coefficients were determined from hourly rainfall, and runoff data. Five hundred and thirty-five (535) events were from 1989-2004 and these events were analyzed. The results of this study indicate that the correlation between spatial distributions of runoff coefficients with mean annual precipitation is approximately same. Mean annual rainfall well explained the spatial variability in average runoff coefficient value which ranges from 0.40 to 0.48). Runoff coefficients for the micro catchments calculated by using the rainfall runoff relationship (Sepaskhan and Fard; 2010).

Rainfall runoff relationship developed for Prequeno River catchment, located in Brazil was by using two semi-distributed approaches (TOPMODEL and HYCYMODEL). The models were applied series 3360 hourly observed data. The ratio between total runoff and total precipitation was 0.79, 0.81 and 0.74(Chaffe et al; 2008).

Silva et al (2010) concluded that semi-distributed (TOPMODEL) approach seems to more reliable Hydrological approach to estimate the stream flow discharge in large river basins. Monte Carlo simulations were used to find the best set of parameters in terms of Nash-Sutcliffe coefficient. For the two decades runoff is likely to decrease, so a good water management strategy will be necessary as a possible adaptation measure stated by Parinda; 2004.

Description of Study Area Potohar Plateau

The Potohar plateau is located in the south of Islamabad between the River Indus and River Jehlum. It is an open undulating land with

extensive flat areas. The height of Potohar Plateau mainly varies from 300 to 600 meters above sea level. Residual hills such as Kala Chitta and Khairi Murat rise to just over 1000 meters and are the result of resistant rock being left behind the erosion of resistant rock. A large part of Plateau has been dissected and eroded by the action of running water. It presents a varied landscape. This dissected land termed as a badland topography and landscape of ridges, ravines and troughs. The Soan river is the most dominant feature of the region. It forms gullies and alluvial plains, mainly used for agriculture. The Potohar Plateau is rich in minerals like rock salt, gypsum, limestone, coal and oil.

Three small dams (Domeli, Dharabi and Lehri Dam) were selected in the Potohar area to develop the rainfall runoff relationship and for the the estimation of runoff coefficient. TLehri and Domeli are located in the District Jhelum and Dharabi Dam is located in district Chakwal. Catchment area and location of dams is shown given in Table .The Total area of Potohar area is 22,254 km². Elevation of the project area varies between 2365 to 165 m, out of which elevation in approximately 80 % area varies between 1000 to 165 meters as shown in Fig. 4.

Table 1 Catchment Area of Selected Small Dams

Sr No	Name	Catchment area (Sq.km)	District
1	Domli Dam	170	Jhelum
2	Lehri Dam	52	Jhelum
3	Dharabi dam	196	Chakwal



Fig. 4 Study Area

Methods and Materials

The required input data for the selected semi distributed technique (TOPMODEL) has been

used in this research is collected from different organizations. the data required to the rainfall runoff relationship was developed using TOPMODEL. The data required for Semi distributed approaches (TOPMODEL) is Precipitation data of catchment, Stream flow data of catchment, Climatic data, Topographic data, Land cover/ land use data.

TOPMODEL has four basic input files that must be completed to run the model. All these input files are made in notepad program of windows. (a) Catchment data file (b) Hydrological Input data file (c) Topographic Index Map file (d) Text description file.

CROPWAT software is also used to estimate the evapotranspiration of the study area. The evapotranspiration is used in the hydrological input file as an input data.

TOPMODEL Parameters

The basic five parameters for the TOPMODEL are given below.

M; Parameter of the exponential transmissivity function or recession curve. (Units of depth, m)

ln(To); Natural logarithm of the effective transmissivity of the soil when just saturated. A homogeneous soil throughout the catchment is assumed. (Units of m^2/h)

Srmax; Soil profile storage available for transpiration, i.e. an available water capacity. (Units of depth, m)

Srinit; Initial storage deficit in the root zone (an initialisation parameter. (Units of depth, m)

ChVel; Effective surface routing parameter. (Units of m/h)

Model Run and Flow Simulation

TOPMODEL is purely a hydrological model and simulates hydrological affluxes of watershed. The model is run for the three selected dams (Domeli, Lehri and Dharabi) The importance of the current version of is its runoff mechanism. TOPMODEL works on the variable concept of contributing area. Main screen of the TOPMODEL is given in Fig. . The procedure that was adapted to run the model is given below

1. First copy all the input files to the WINDOW'S drive with the path "C:\TmodVB123\projects"
2. Open the TMOD9701 Program then main screen of TOPMODEL will open as shown in Fig. 2 and load the file by selecting the Load Project.

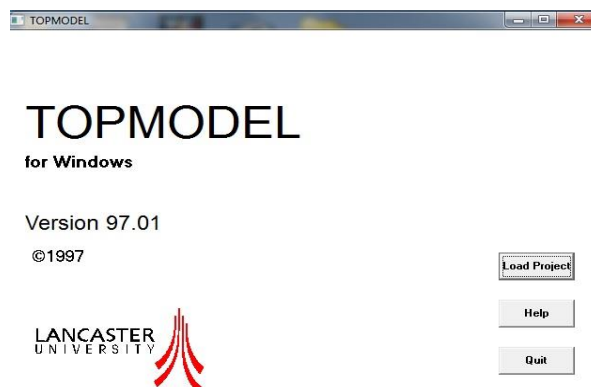


Fig. 2 Main screen of TOPMODEL

3. Give the path of the project files that were previously copied in the WINDOW'S drive as "C:\TmodVB123\projects". The software will automatically detect all the input files and their path will be shown in their respective places.

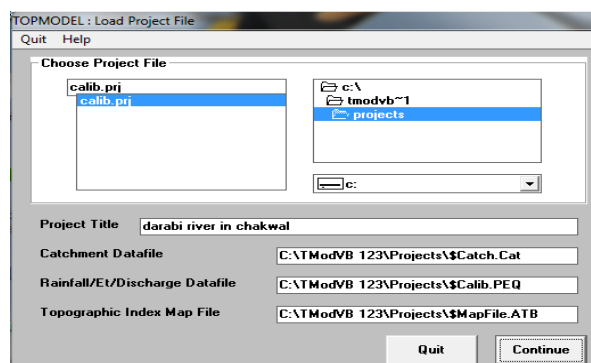


Fig. 3 TOPMODEL Project Loading

4. Press "Continue" button from Fig. and next window will appears as shown in Fig.

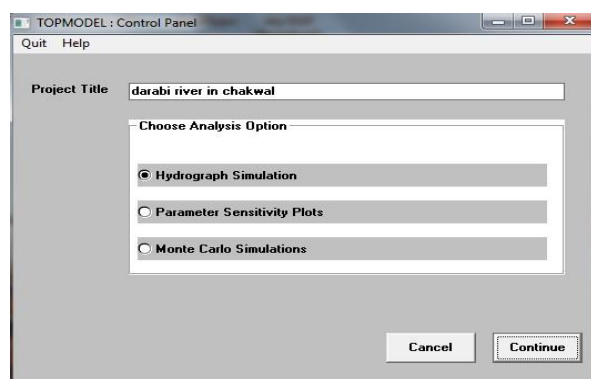


Fig. 4 Control panel screen of TOPMODEL

5. Select "Hydrograph Simulation" option. A new window will open. Select "RUN" from this window. It will give the flow simulation hydrograph for the selected time interval.
6. Model calibration and validation was done for the selected dams watershed.

Evaluation Criteria of TOPMODEL

The evaluation criteria of TOPMODEL are model efficiency and model errors. Model efficiency should be closer to 100% and model errors closer to zero. The minimum acceptable limit for modeling was that minimum modeling efficiency should be greater than 50%. Followings are the TOPMODEL evaluation criteria errors i.e SSE: Sum of squared residuals over all time steps, SLE: Sum of squared log residuals over all time steps, SAE: Sum of absolute errors over all time steps.

Results and Discussions

Semi-distributed (TOPMODEL) has been applied on the three small dams (Domeli, Dharabi and Lahri dam) in the Potohar area of

Punjab, Pakistan and rainfall runoff relationship was developed.

Rainfall runoff relationship for the Dharabi Dam

- 1) The TOPMODEL calibration was a time-consuming process. Hundreds of trails were done for different values of model parameters; finally, that set of parameter values was selected that gave the maximum efficiency with less error. TOPMODEL calibration is shown in Fig. 5 TOPMODEL Calibration, Simulated Vs Observed flow and Rainfall-Dharabi dam
- 2) and efficiency was obtained 74 % which is
- 3) satisfactory.

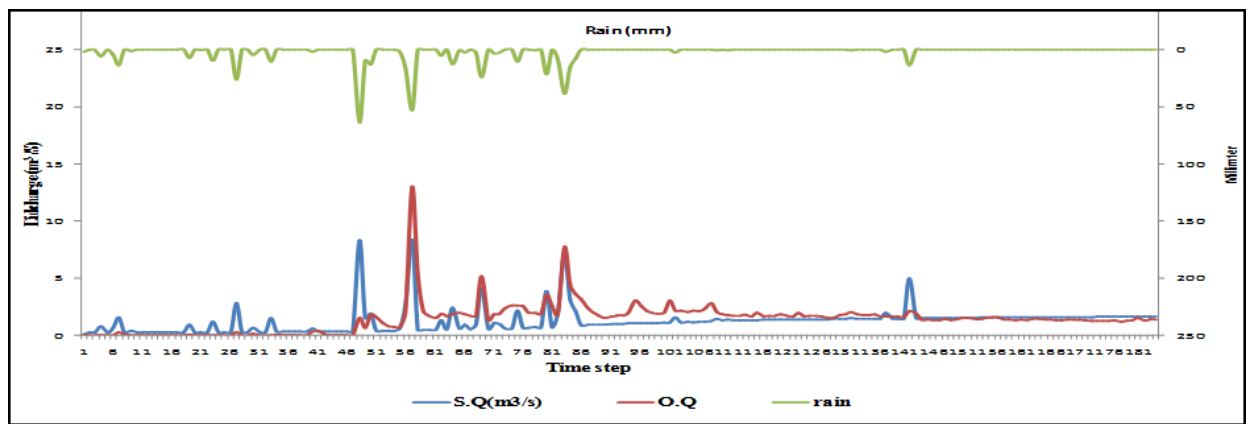


Fig. 5 TOPMODEL Calibration, Simulated Vs Observed flow and Rainfall-Dharabi dam

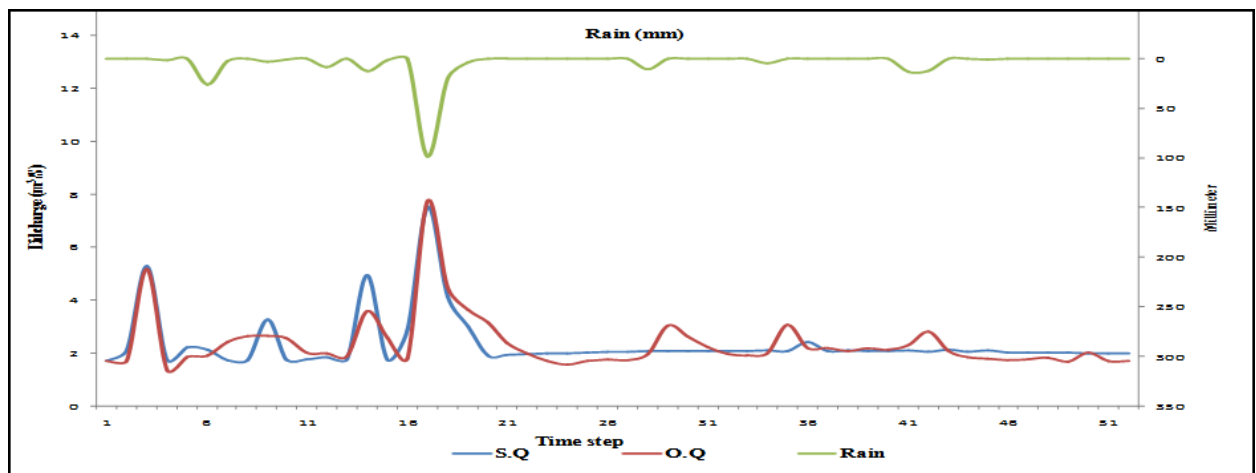


Fig. 6 TOPMODEL validation-Dharabi Dam

TOPMODEL validation was also carried out. The set of parameters showed the maximum matching of the historical and simulated flows. Then the model for these set of parameter values was validated by extending the simulation time for next six months to ensure that the model is capable

for estimating the future flows as well. The graph given below shows the observed and simulated flows for the validated period. Model validation is shown in Fig. .

- 4) Fig. 5 TOPMODEL Calibration, Simulated Vs Observed flow and Rainfall-Dharabi dam

- 5)
- 6) shows that first selected low event having volume 26348 m³ was observed on 5th June 2010 with rainfall 0.40 mm. The volume calculated by TOPMODEL was 23348 m³with percentage difference of 11%. Similarly, for the selected low flow events percentage difference was obtained to be 2, 6, 16 and 5. Hence, it was concluded that the TOPMODEL gave good simulation for low flow events.
- 7) Fig. 5 TOPMODEL Calibration, Simulated Vs Observed flow and Rainfall-Dharabi dam
- 8)
- 9) shows that first selected medium event having volume 130808 m³ was observed on 2nd July 2010 and rainfall was 4.33 mm. The volume calculated by TOPMODEL was only 111260 m³with percentage difference of 15%. Similarly, for the selected medium flow events percentage difference was obtained 10, -4 and 4. Hence, it was concluded TOPMODEL also gave good simulation for medium flow events.
- 10) The first selected high flow event having volume 530778 m³ was observed on 21st August ,2010 and rainfall was 21.47 mm. The volume calculated by TOPMODEL was only 498089 m³with percentage difference of 6%. Similarly, for the selected high flow events percentage difference obtained was 12, 3, 8 and 13. Thus, it was concluded that TOPMODEL also gave good simulation for high flow events.
- 11) It was concluded from the TOPMODEL simulation that this model estimates the low, medium and high flows accurately. For any storage structure peak flow is important. A comparison of observed and simulated flows was made for TOPMODEL. The observed flood peaks for the same year 2010 were compared with the simulated ones. The comparison of different events simulated by TOPMODEL with observed flows and the percentage difference are shown in Table 2.
- 12) Similarly, TOPMODEL was calibrated and validated for the Domeli and Lehri dam.

Table 2 Comparison of Observed flows, TOPMODEL simulated flows and Percentage Errors

Date	Observed(m ³)	Simulated by TOPMODEL	%age difference	Events
6/5/2010	26348	23348	11	Low
5/7/2010	50981	49869	2	
7/20/2010	53999	50999	6	
6/8/2010	61624	51624	16	
12/30/2010	95649	90742	5	
7/2/2010	130808	111260	15	Medium
7/28/2010	230586	201586	10	
6/29/2010	285027	296035	-4	
2/8/2010	335786	320948	4	
8/21/2010	530778	498089	6	High
8/10/2010	565900	498634	12	
8/24/2010	621888	601888	3	
7/20/2010	722166	662166	8	
7/29/2010	2054988	1789669	13	

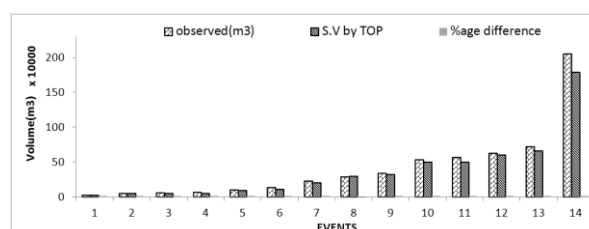


Fig. 5 TOPMODEL simulated, Observed flow and Percentage errors

Determination of rainfall runoff fraction / coefficient

Rainfall runoff fractions were determined for Dharabi, Domeli and Lehri dam watersheds. Runoff fraction was estimated by comparing the simulated and observed runoff of selected events. In order to obtain a single value of runoff fraction for Dharabi, Domeli and Lehri watershed average of runoff fractions of all selected events was taken as 0.72, 0.73 and 0.74, respectively. Runoff fraction for the Potohar area was obtained to be 0.73.

Development of Rainfall runoff relationship

Rainfall-Runoff relationship for runoff estimation for soil and water conservation structures. Rainfall runoff relationship developed for the three dams is shown in

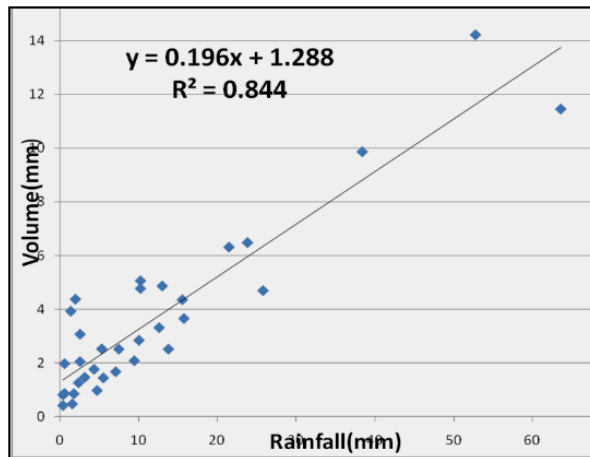


Fig. 6.
 $y=0.196x+1.288, R^2 = 0.844$
 $x= \text{Rainfall}(\text{mm}), y=\text{Runoff}(\text{mm})$

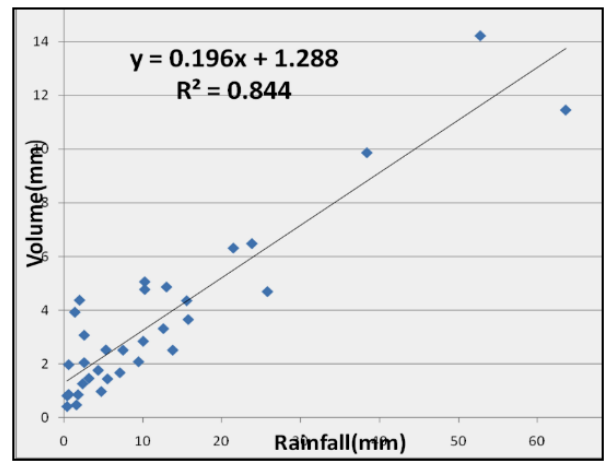


Fig. 6 Rainfall runoff relationship

Conclusions

- According to the formulation of model, it is not suitable for watersheds with long dry season resulting in very low flows. **TOPMODEL** simulates efficiently for low, medium and peaks flows with lesser dry span.
- **TOPMODEL** is more suitable for small watersheds (Dharabi, Domeli Dam and Lehri Dam) as it has shown very good simulation results with less errors.
- Flow simulations by using **TOPMODEL** give efficiency upto 74%.
- Rainfall runoff fraction was obtained to be 0.73. (Appendix C)
- Rainfall runoff relationship was obtained $y = 0.196x + 1.288$
 $R^2 = 0.844, y=\text{Volume (mm)}, x=\text{Rainfall (mm)}$
- Only four (4) years data was available so rainfall runoff Fraction and rainfall runoff relationship can be verified using long time step data.
- As the topography of Dharabi catchment is mountainous so distributed approach by using GIS gridded based data is highly recommended.

Reference

1. Hayes D. C and Young. R. L. 2005. "Comparison of Peak Discharge and Runoff Characteristic Estimates from the Rational Method to Field.
2. Zhan. Y. 2005. "Remote Sensing and GIS in Runoff Coefficient Estimation in Binjiang Basin" Geo science and Remote Sensing Symposium, IGRSS, 05. Proceeding, 2005 IEEE International, volume 6, Page No:4403-4406.

3. Norbiato, D., Borga M., Merz R., Blöschl G., and Carton A. 2009. "Controls on event runoff coefficients in the eastern Italian Alps" *Journal of Hydrology* 375 (2009) 312–325.
4. Sepaskhan A.R and fard S R M. 2010. "Determination of Rainfall-runoff relationship based on soil physical properties for use in microcatchment for water harvesting system design" *Journal of Science and Technology*, 2010, vol 34, issue 4, August 010. Shrazuniversity Iran.
5. Chaffe, P. L. B., Silva. R. V., and Kobiyama. M. 2008. "Rainfall-runoff process analysis of the Pequeno River catchment, Curitiba metropolitan region, Brazil, with two hydrological models" *An Interdisciplinary Journal of Applied Science*, Vol. 3.
6. Silva R V D; Yamashiki Y; Tatsumi K and Takara K. 2010." Distributed TOPMODEL approach for rainfall runoff routing modeling's in large scale basins" Department of environmental Engineering, Kyoto University.
7. Parida B.P(2004) "Forecasting impact of climate change on runoff coefficients in Limpopo basin using Artificial Neural Network". University of Botswana, Gaborone. Welcome to the Second Aiac Workshop, Dakar. Af_42 Research Team Botswana March 24 -27, 2004.

Selection of Best Diversion Facility for the Construction of Kohala Hydropower Dam

Muhammad Yaseen^{1*}, Muhammad Naveed¹, Muhammad Kaleem Sarwar², Muhammad Hassan Rehman², Muhammad Imran Azam³

^{1*}Centre for Integrated Mountain Research, University of the Punjab, Lahore, Pakistan; Email:

²Centre of Excellence in Water Resources Engineering, University of Engineering and Technology, Lahore 54890

³College of Hydraulic and Environmental Engineering, China, Three Gorges University, Yichang 443002, China

*yaseen.cimr@pu.edu.pk

Abstract: Diversion arrangement plays vital role in construction schedule planning and overall safety of the hydropower project in rivers where frequent flash floods and perennial flows of sufficient magnitude can occur. Failure of a diversion scheme results in major damages to the project in terms of manpower, machinery, loss of time and increase in project cost. The main objective of this research work was to study the possible diversion facilities for the construction of Kohala Hydropower Dam and to recommend the best solution for the diversion facility. The project area lies in Muzaffarabad district of Azad Jammu Kashmir (AJK). Different diversion alternatives which applied to this project were diversion through temporary flume and pipe line, diversion through conduits through or under the body of dam, diversion through multiple stages, diversion through impounding of flow behind the dam, diversion through temporary channel through the dam and diversion through tunnel through the abutments. The inflow 4765 m³/s in 100 years return period and 575 m³/s in 30 years return period were selected as the river diversion criteria during the first dry season. By considering the hydrological, topographical and geological conditions of site, provision of diversion tunnel through the abutment with u/s and d/s coffer dams is an optimum solution for the Kohala Hydropower Dam Project. The concrete lined diversion tunnel with 7.5 m diameter on right bank is a better choice. The invert level of the tunnel is at 857m with bell mouth transition at entrance for smooth entry of flow. The crest levels of U/S and two D/S cofferdams were 869m, 859.5m and 856m respectively determined.

Keywords: Hydropower; coffer dam; diversion tunnel; design flood; return period

Introduction

Shortage of energy is becoming an obstacle in economic growth and development of Pakistan. The country has sufficient surface water but unfortunately, Pakistan's energy market investment in hydel-power generation has been caught up in confusion and no significant progress has been achieved so far. The Government is trying to facilitate private investors to promote hydel power generation in the country to meet the ever-increasing demand of electricity in a cost-effective manner. Construction of the hydro-power plant is normally done in the river stream. For creating dry working conditions, the river flow is temporarily diverted by construction of a diversion weir or diversion dam across the main river course. Size and type of the diversion structure depends upon the flood characteristics of the river and topographical conditions at the diversion site. It can be a diversion tunnel if the topography is favorable. A planned diversion

scheme can minimize potential flood damage to the work in progress and overall project completion period. The 10 or 25-year frequency flood is generally selected as the design flood for diversion scheme based on the previous analysis or past experience for sizing the diversion works and risk factor. Thus, diversion scheme need to be capable of diverting the peak flow of selected frequency flood. Any higher flood is liable to overtop the cofferdam leading to its complete failure / destruction along with large damage to the under construction works and delays in project completion. The choice of diversion through cofferdam, diversion channel or diversion tunnel also depend upon the geological conditions of the area, if the geological conditions are not favorable for off channel diversion, part of the main stream/river can also be used as a diversion channel for phased construction. The main objectives of this research work are to study the possible diversion facilities for the construction of Kohala

Hydropower Dam and to recommend the best solution for the diversion facility.

Materials and Methods

Study Area

Selection of best diversion works for Kohala Hydropower project will be carried out through this study. The project area lies in Muzaffarabad district of AJK. The area of interest for the study lies between Chakothi and about three kilometers downstream of Kohala bridge on the Jehlum river between Longitude 73°25' to 73°50' East and Longitude 34°00' to 34°25' North. The bridge is

about 140 Km from Rawalpindi / Islamabad. Muzaffarabad town, capital of AJK (Azad Jammu Kashmir), lies further about 35 km from Kohala Bridge. Chakothi and Kohala villages are situated on upper and lower limbs of the river, respectively. The dam site will be located on the upper limb and power house on the lower limb of Jehlum River. The selected layout of Kohala Hydropower project comprises a concrete dam at Siran, about 18 km long transfer tunnel passing under Mir Fateh and an underground power house near Barsala.

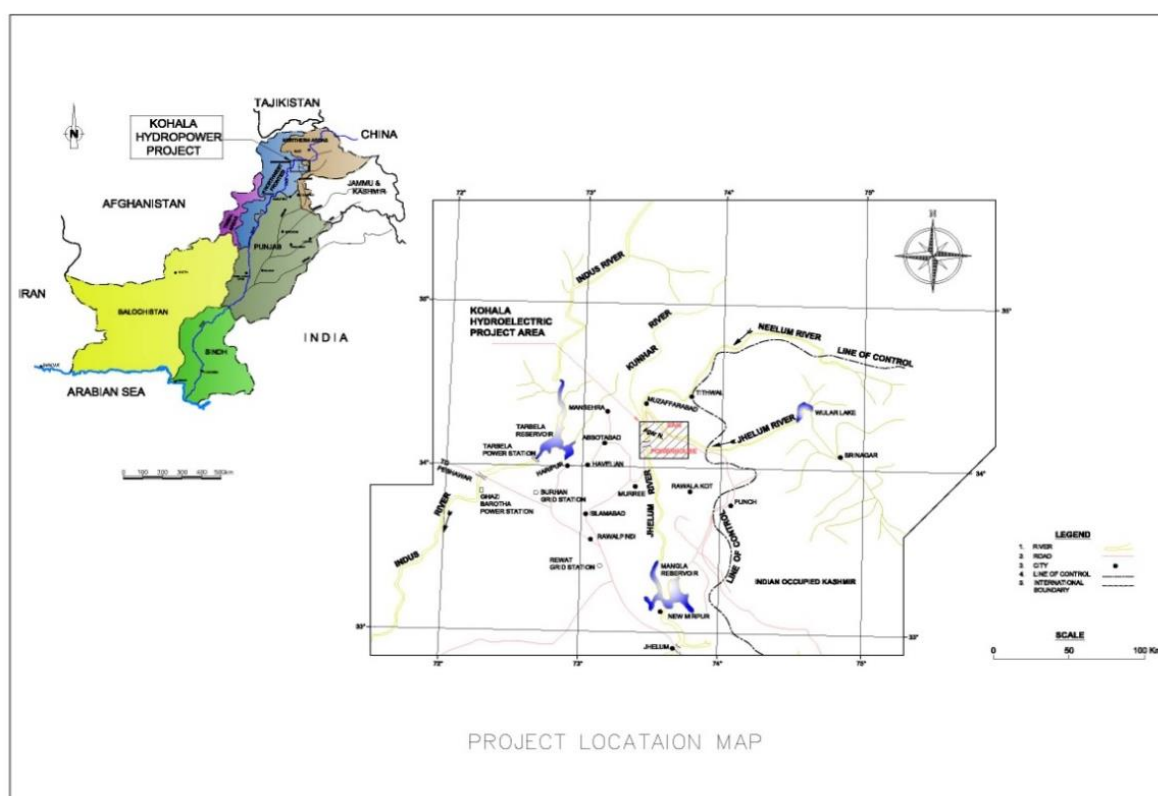


Fig. 1 Project Location Map

The Siran Dam will be designed for a full supply of 900masl creating a reservoir of approximately 14.9 million m³ storage. The minimum draw down level has been taken as 890masl. The live operating storage between full supply level and minimum draw down level is 6million m³. The location of Kohala Hydropower project is shown in Fig. 1.

a. Discharge capacity of Diversion Tunnel

The discharge capacity of diversion tunnel is different in the first dry season and the second monsoon. In river cut and the first dry season, the flow in the tunnel is free discharge. In the second

monsoon, the flow in the tunnel is pressure flow in 100 years return period.

i. Discharge capacity in river cut and first dry season

The discharge capacity in river cut and first dry season can be determined by:

$$Q=Cb(2g)^{0.5}H_e^{1.5}$$

Where:

Q, discharge, m³/s; C, comprehensive discharge coefficient, 0.34; b, width of tunnel, m; g, gravity acceleration, m/s²; H_e, actual head being considered on the invert of tunnel, including velocity of approach head, m

ii. Discharge capacity in second monsoon

The discharge capacity in second monsoon is determined by:

$$Q=C(2gH)^{0.5}$$

Where:

Q, discharge, m³/s; C, comprehensive discharge coefficient; g, gravity acceleration, m/s²; H—head, m

b. Head Losses in the Tunnel

After selection of appropriate diameter head losses through the tunnel are calculated. Following are the different head losses in the tunnel.

- Entry Losses (h_{en})
 - Friction Losses (h_f)
 - Bending Losses (H_b)
 - Exit Losses (h_{ex})
 - Total head losses (H_t)
- $$h_{en} = (1 / c^2 - 1) * (v^2 / 2 g)$$

$$h_f = 29.1 n^2 (L / r^{2/3}) v^2 / 2 g$$

$$H_b = K_b * (v^2 / 2 g)$$

$$h_{ex} = 1.0 * V^2 / 2 g$$

$$H_t = h_{en} + h_f + H_b + h_{ex}$$

RESULTS AND DISCUSSIONS

a. Hydrological Data Analysis

i. Inflow in First Dry Season

The maximum monthly inflows and their return periods in dry season in 35 recorded years are shown in Fig. 2. The dry season is from October to February, a total of 5 months.

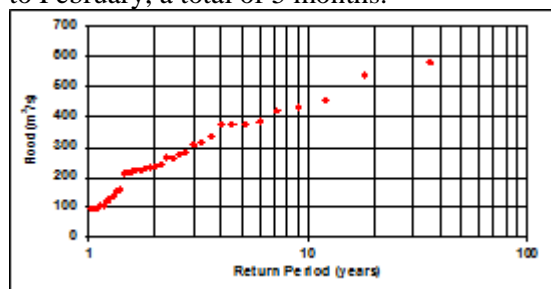


Fig. 2 Flood Flow and Return Period in Dry Season

b. Possible Diversion Facilities for Kohala Hydropower Dam Construction

i. Diversion through Temporary Flume and Pipe Line

The flow may be bypassed by the installation of a temporary flume or pipeline. As the flow is 575 m³/sec with 30 years return period which is so high for flume. For this discharge large cross section and more cost for structure is required

and the topographical limitation does not permit to avail this option.

ii. Diversion through Conduits or Under the Body of Main Dam

The outlet works for an embankment dam often entails the construction of conduit that may be used for diversion during construction of the dam. This method for handling the diversion flows is an economical one, especially if the conduit for the outlet works is large enough to carry the diversion flows. As the topographic data shows that the slope of terrain steep as shown in Fig. 3 and the water carrying channel is narrow where the dam is to be constructed, hence the conduit through or under the body of dam is not recommended.

iii. Diversion through Multiple Stages

The multiple-stage method of diversion over the top of alternate low construction blocks or through diversion conduits in a concrete dam requires shifting of the cofferdam from one side of the river to the other during construction. During the first stage, the flow is restricted to one portion of the stream channel while the dam is constructed to a safe elevation in the remainder of the channel. In the second stage, the cofferdam is shifted, and the stream is carried over low blocks or through diversion conduits in the constructed section of the dam while work proceeds on the unconstructed portion. The dam is then carried to its ultimate height, with diversion finally being made through the spillway, penstock, or permanent outlets. According to the topographic data river section is narrow and slope is steep and also flow is very high which is 575 m³/sec, therefore construction of dam cannot be made in multiple stages. So, this option is unsuitable to divert the peak flow during the construction of dam keeping in view the safety.

iv. Diversion through Impounding of Flow behind the Dam

The flow may be impounded behind the dam during its construction period. Pumps are used, if necessary, to control the water surface. This option is suitable for those dams' areas where flow is small and wider river cross section is available for storage of water during of construction of main dam. As the flow is 575 m³/sec for 30 years return period. So, need a high storage reservoir behind the main dam. The topographic of dam site clearly portray that space is not available to store this large amount of

incoming flow and also cost will be very high to construct this large impounded water body. If we make arrangement for pumping of water, it will further increase the cost. So, this option also not suitable due to topographic, hydrological and economic point of view.



Fig. 3 River view for proposed site of Kohala Hydropower Project.

v. Diversion through Temporary Channel through the Dam

At sites where it may not be economical to provide a tunnel or conduit large enough to pass the diversion design flood, a temporary channel involving a gap through the embankment dam may be used to divert stream flows while the remainder of the embankment is being constructed. This method is adaptable where wider river cross section is available; obviously it cannot be used in narrow canyons. This diversion facility is not possible because of narrow river cross section and high inflow.

vi. Diversion through Tunnel through the Abutments

It is usually not feasible to do a significant amount of foundation work in a narrow canyon until the stream is diverted. In this situation the tunnel may prove the most feasible means for diversion, either for a concrete dam or for an embankment dam. The stream flow is bypassed around the construction area through tunnels in one or both abutments. If tunnel spillways or tunnel outlet works are designed, it usually proves economical to use them in the diversion plan. If the upstream portion of the permanent tunnel is above the river bed elevation, a temporary upstream diversion adit can be provided to affect a stream-level bypass. When there is a river outlet works tunnel, particularly for embankment dams, it is generally used for diversion. Normally the diversion works tunnel is placed at an elevation near river level. When a tower or drop inlet intake is used, a temporary adit upstream of the base of the intake structure is necessary. After diversion, this adit is closed

off by a gate or a bulkhead, and a concrete plug is placed in the intake structure for permanent closure. In addition, gates and second-stage concrete are added in the gate chamber and control structure, where applicable, to complete the outlet works for permanent operation. Temporary diversion tunnels that are not part of a spillway or outlet works can be lined or unlined. The advisability of lining the diversion tunnel is influenced by

- The cost of a lined tunnel compared with that of a larger unlined tunnel of equal carrying capacity;
- The nature of the rock in the tunnel, specifically, whether it can stand unsupported and unprotected during the passage of the diversion flows.
- The permeability of the material through which the tunnel is carried, because it affects the amount of leakage through or around the abutment.

Some means of shutting off the diversion flows must be provided. This can be accomplished through the use of closure devices such as bulk heads, slide gates, or stop logs. Permanent closure of the diversion tunnel is made by placing a concrete plug in the tunnel. Keyways may be excavated into the rock to ensure adequate shear resistance between the plug and the rock or lining. After the plug has been placed and sufficient time has elapsed for concrete shrinkage grout is forced in through previously installed grout connections to the contact between the plug and the surrounding rock to ensure a watertight joint. Keeping in all views of hydrological, topographical, geological and economical concern, this option of providing diversion tunnel through the body of abutment is most suitable for the Kohala Hydropower Dam Project.

c. River Diversion Arrangement for Dam Construction

i. Dam Construction Activity

The headrace tunnel will be 16 km long and its construction will occupy key route, i.e., the total construction schedule will be controlled by construction of headrace tunnel. Thus, the dam construction can be stopped during the first monsoon and resume construction in the second dry season. It will not increase the total time of the project construction schedule. In the end of the second dry season, the dam height can be placed to the elevation higher than 882m based on the rate of concrete placement. The elevation of 882m is the elevation of spillway weir. In the second monsoon, the dam should retain the flood

in the reservoir, prevent the flood from overtopping over its crest and the concrete placement can be continued. The flood will be discharged through diversion tunnel two sluices and spillway.

Diversion Criteria

The diversion criterion is different for the first dry season and the second monsoon. It depends on the dry season, monsoon and concrete placement for dam.

First dry season

If concrete placement can be stopped and the dam is allowed overtopping during the first monsoon, the diverted flood will be small during the first dry season. But, during the first dry season, the flood should not overtop the crest of upstream cofferdam. If there is a flood warning system, even in first monsoon, when flood is smaller than the discharge capacity of diversion tunnel, the concrete placement can be continued.

Second monsoon

In second monsoon, the dam will be placed to certain level, for example, 882m. The dam height is 36m, and overtopping is not allowed. But the flood can pass through the diversion tunnel, sluices and spillway. The flip buckets of all sluices and the downstream surfaces of spillway should be formed in the second dry season, which is not difficult. In this case, the return period of flood control should be raised to 100 years in all year. If the inflow is smaller than the flood of 100 years return period, the concrete placement can continue. In Later monsoon, the flood control will be still the flood of 100 years return period.

Selection of Inflow in First Dry Season for River Diversion

Two main factors will affect the selection of inflow in first dry season: relative lower cost and higher resistance to flood risk. If a smaller return period is selected, the cost of river diversion will be low, but the risk of overtopping upstream cofferdam is higher. The upstream cofferdam built of rockfill is not allowed overtopping during first dry season. From Fig. 2, the maximum inflow in 10, 20 and 30 years return period is separately about 450m³/s, 540m³/s and 575m³/s.

River Cut

The river cut will be performed after monsoon and in early dry season. If it is too early, it will cost more. If it is too late, the duration of concrete placement in the first dry season will be

shortened. In consideration of dam concrete placement, cost of river closure and the ability of contractor for river cut construction, the inflow for river cut can be selected between 100m³/s and 200m³/s. In October, the maximum inflow is 581.50m³/s in 35 years (from 1970 to 2004). In 35 years recorded inflow, there are 71 days of inflow more than 150m³/s from 11th to 20th in October. The probability of daily inflow less than 150m³/s is 93.5%; there are 7 years of inflow more than 150m³/s from 11th to 20th in October. The probability of inflow less than 150m³/s in October yearly is 80%. Based on the above analysis, the inflow of 150m³/s can be selected for river cut. The time of river cut can be arranged from 11th to 20th in October.

d. Hydraulic Calculations for Diversion Tunnel and Crest Elevation of Cofferdams

First Dry Season

The diverting inflow is 575 m³/s in first dry season. One upstream cofferdam and two downstream cofferdams will be built. The calculations are to determine the size of diversion tunnel and the crest elevation of upstream and downstream cofferdams. The calculation also considers that the discharge capacity of diversion tunnel is enough for the first monsoon in order to avoid flood overtopping the main dam.

Optimization of tunnel size

The diverting inflow for the first dry season is 575m³/s. The calculations are carried into comparison among the elevation of inlet invert, dimensions of cross section, velocity in the tunnel, height of upstream cofferdam. The results are given in Table 1.

From Table 1, the higher elevation of inlet invert is, the smaller the section area of the tunnel becomes. But the average flow velocity in the tunnel will increase. Because the diversion tunnel is fully concrete lined, the velocity in the tunnel can be between 15m/s and 18m/s. The flow velocity in the tunnel is not more than 15 m/s. The maximum flow velocity is determined by 4765m³/s in 100 years return period. In this case, 4765m³/s will be discharged through diversion tunnel, sluices and spillway, and the flow velocity in tunnel will not more than 18 m/s. Thus, the option of the elevation of inlet invert at 857m and with 7.5m width is an optimum selection from the point views of economy, height to width and velocity in tunnel. The proportion of height to width should not be too

high, or cost will be higher. In light of the axis of part diversion tunnel parallel to the rock strike or with small angle to the rock strike, the smaller tunnel width will be a better selection.

The tunnel length from the entrance to the exit portal is 320m. The slope of the tunnel is 1.614%. In some area of developed joints and broken rock, shotcrete, rockbolts, meshes and consolidation grouting will be applied. Excavation slopes at tunnel entrance and tailrace channels will be applied with shotcrete, rockbolts and meshes.

Crest elevation of upstream cofferdam

The upstream cofferdam is only for dam construction during the first dry season. It will be flushed away in first monsoon. The crest elevation is 869.00m. During river cut, the two small rockfill cofferdams will be built first. After the river is closed, and the inflow is diverting by diversion tunnel, the clay core can be placed. Based on the inflow of 150 m³/s during river cut, the reservoir level is 858.06m.

Crest elevation of downstream cofferdams

There are two downstream cofferdams. The height of the last downstream cofferdam is determined by the inflow when river is cut. In

section 4.3.4, the flow is 150 m³/s. The levels of cofferdam are given in Table 2.

RCC coffer dam

The height of downstream RCC cofferdam is determined by diverting inflow of 575m³/s. The corresponding downstream water level is 858.70m. By adding 0.80m safety allowance, the crest elevation is 859.50m.

In first monsoon, the upstream cofferdam will be flushed away. The space between Main dam and cofferdam will be no use for dam concrete placement after the first dry season. But Dam construction needs space between dam and cofferdam for delivery of steel bars, forms and other facilities and construction materials. The space between dam and downstream cofferdam can be used for this purpose. Thus, the downstream cofferdam should be an overflow cofferdam constructed with RCC. In order to building RCC cofferdam, a rock fill dam will be built downstream of RCC cofferdam. The last downstream cofferdam is built of rock fill. The crest elevation is 856.00 m. The cofferdam and its gravel foundation will be grouted with spin injection for waterproof. The elevation of river floor is 852m.

Table 1 Hydraulic Calculation for Dimension of Diversion Tunnel

Elevation of Inlet Invert	Tunnel Height	Cofferdam Height	Flow Velocity	Height: Width	Cost
M	m	M	m/s		US\$
Tunnel Width=8.0m					
854	10.4	16.6	9.65	1.30	3487171
855	9.1	16.6	11.42	1.14	3104971
856	8.3	16.6	12.38	1.04	2869771
857	7.7	16.6	14.14	0.96	2693371
Tunnel Width=7.5m					
854	10.95	15.9	9.8	1.46	3663659
855	9.55	15.9	11.54	1.27	3266759
856	8.65	15.9	12.94	1.15	3011609
857	8.05	15.9	14.11	1.08	2841509
Tunnel Width=7m					
854	11.7	15.3	9.65	1.67	3872697
855	10.1	15.3	11.42	1.44	3435897
856	9.1	15.3	12.83	1.53	3162897
857	8.5	15.3	14.02	1.21	3162897

Table 2 crest levels of cofferdam.

Upstream Level	Downstream Level	Crest Elevation of the Last
859.20	854.80	856.00

		Downstream Cofferdam
m	m	m
859.20	854.80	856.00

Second Monsoon

In the second monsoon, the diverting inflow is $4765\text{m}^3/\text{s}$. Before the monsoon comes, the spillway chute should be formed for flood discharge. The weir crest elevation of spillway is 882.00m. The invert elevation of sluices is 862.00m. Added with diversion tunnel, three facilities will jointly discharge flood of $4765\text{m}^3/\text{s}$. By hydraulic calculation, the reservoir level is 885.93m. Based on the analysis of the rate of concrete placement, the spillway chute can be formed before the second monsoon. It is unnecessary to design extra temporary bottom outlet in dam or increase the size of diversion tunnel for diverting flood.

Conclusions

The inflow is $4765\text{ m}^3/\text{s}$ in 100 years return period. It is suggesting that $575\text{ m}^3/\text{s}$ in 30 years return period be selected as the river diversion criteria during the first dry season. Keeping in views the hydrological, topographical and geological conditions, provision of diversion tunnel through the abutment is most suitable for the Kohala Hydropower Dam Project. It is observed that at $575\text{m}^3/\text{sec}$ design flood one tunnels of 7.5 m diameter is required to the river flows during Kohala dam construction. The option of the elevation of inlet invert at 857m

and with 7.5m width is a proper selection from the point views of economy, height to width and velocity in tunnel. The top shape of the entrance is an elliptical curve.

To reduce the losses in diversion tunnel, the concrete lining of appropriate thickness is recommended. As Desilting Chambers are proposed on left bank of river according to Kohala Hydropower Project, Feasibility Study Report. Detail study is recommended after proposing and relocating of desilting chambers for provision of Diversion tunnel on left bank. Detailed engineering geological, hydrological, topographical studies should be carried out for the better design of Diversion Facility for the Kohala hydro Power Project. Detailed Studies should be carried out both in field and laboratory like discontinuity surveying, Drilling and sampling for laboratory testing. Laboratory studies should be performed on core specimens taken from the boreholes, in order to determine physical and mechanical properties of the main

lithotypes. Empirical and numerical methods were used for tunnel design. Single diversion tunnel on the right abutment of dam is recommended for diversion system as it consists of good rock. Detail design of upstream and downstream cofferdams is required for cost estimates of the diversion arrangements.

References

- Benmebarek, N. (2005), "Numerical Studies of Seepage Failure of Sand within a Cofferdam", Biskra University, Biskra, Algeria, p 264-273.
- Casagrande. A. (1973), "Embankment Dam Engineering" Jhon Wiley and Sons, Inc., USA, p 97-103.
- Davis, C.V and Sorensen, K. E. (1993), "Hand Book of Applied Hydraulics", Third Edition, McGraw Hill, New York, p, 14-7
- Fell, et al. (1992), "Geotechnical Engineering of Embankment Dams", A.A. Bakema, Rotterdam, Netherlands, p 450-455.
- Gerodetti, M., (1981), "Model Studies of an Overtopped Rock fill Dam," International Water Power &. Dam Construction, p. 25-31
- Moiseev, S. N., (1975), "Passage of Flows through rock-earth dams during construction", Journal of Engineering, Springer, New York, Vol. 9, No. 1, PP 15-21.
- Neghabat, F and Robert M. Stark, (1972), "A Cofferdam design optimization", Journal of the Mathematical Programming, Springer Berlin, Heidelberg, Vol 3, No. 1, PP. 263-275.
- Novak, P, A.I.B. Moffat and C. Nulluri, (1990), "Hydraulic structures" University of Newcastle upon Tyne, Chapman and hall, London, p. 301-302.
- USBR. (1987), "Design of Small Dams", Water Resources Technical Publication, Third Edition, SSOP, Washington, D.C , p 491-496
- Yanmaz, A. M., (2000), "Overtopping Risk Assessment in River Diversion Facility Design", Canadian Journal of Civil Engineering, Vol. 27, No: 2, PP. 319-326.

Hydropower Optimization Station using PSO and GA Techniques

Ijaz Ahmad¹, Muhammad Zaman^{2,3*}, Shouqi Yuan², Liu Junping², Muhammad Saifullah⁴

¹Center of Excellence in Water Resources Engineering, University of Engineering and Technology, Lahore 54890, Pakistan.

^{2*}Research center of Fluid Machinery Engineering & Technology, Jiangsu University, P.R. China

³Department of Irrigation and Drainage, University of Agriculture, Faisalabad, Pakistan; Email:

⁴Department of Structures & Environmental Engineering, University of Agriculture, Faisalabad, Pakistan

*muhammad.zaman@uaf.edu.pk

Abstract: Optimization of Xin'anjiang hydropower is a complicated problem. This paper tried to get the optimal hydropower generation using two commonly used methods GA and PSO. The model for the optimization is developed and applied to the Xin'anjiang hydropower station. It is observed from the results that for the optimization of the hydropower and for getting maximum benefits, when simple genetic algorithm techniques have applied, it showed some drawbacks such as slow and pre-matures convergence during the process. The results revealed that the particle swarm optimization gave more efficient and optimal results. Findings revealed that PSO technique not only retain the advantages over GA but also showed the high-speed convergence, and search accuracy. We can get more profitability by optimization of the Xin'anjiang hydropower station by the application of this model.

Keywords: PSO, GA, PSO-GA, Optimization, Xin'anjiang, Hydropower generation

Introduction:

Water resources allocation and its appropriate and optimal use is becoming important and challenging for humans due to its shortage and climate change factors. Optimal allocation of water resources is complicated and important for water resources management and this work has become mathematical model based [1]. After the increase of computer performance, some algorithms were developed in 1970 for getting the optimal solution of daily life problems. Different kind of programming approaches (linear, nonlinear and dynamical) were developed and applied for the solution of reservoir operation in the past. [2-7]. Many researchers utilized these methods for the solution of different problems [8-10]. Among of these programming approaches, genetic algorithm is important one, which was developed by Goldberg [11]. Genetic algorithm (GA) is also a global optimization technique used in the optimization of water resources. [12-15]. Another important optimization technique which is called Particle swarm optimization (PSO) were developed by Kennedy and Eberhart (1995) as an optimization technique and it's becoming one of the most important algorithm in optimization problems.[16]. Optimization of Xin'anjiang and Fuchunjiang hydropower stations is a complicated problem. This paper tried to get the optimal hydropower generation using two commonly used

methods GA and PSO. This paper discusses the feasibility and effectiveness of GA and PSO techniques and their comparisons in optimization of these hydropower stations.

Mathematical model for xin'anjiang hydropower scheduling

The mathematical model consists of two-part, objective function and constraints. This model takes water levels of the reservoirs as decision variables represented by H_{jt} in equation 1 and maximizations of the electricity is objective function over the 12 months periods.

The objective function is given below

$$E = \text{Max} = \sum_{j=1}^T \sum_{j=1}^M A_j q_{jt} H_{jt} \Delta t \quad (1)$$

The constraints in the mathematical model are given as below

Water balance equation

$$V_{j,t+1} = V_{jt} + (Q_{\lambda jt} - Q_{jt}) \Delta t \quad (2)$$

Reservoirs discharge limits

$$Q_{jt.min} \leq Q_{jt} \leq Q_{jt.max} \quad (3)$$

Reservoirs storage volume limits

$$V_{jt.min} \leq V_{jt} \leq V_{jt.max} \quad (4)$$

Hydropower station power generation limits

$$N_{jt.min} \leq A_j q_{jt} H_{jt} \leq N_{jt.max} \quad (5)$$

T = total period count within a year, T=12

M = total number of reservoirs

A_j = Power generation coefficient
 E = maximum power generation output from hydropower
 $Q_{\lambda jt}$ = Inflow of reservoir j at time period t , m^3/s
 H_{jt} = Average head of reservoirs j at time period t , m
 $V_{j,t+1}$ = Volume of reservoir j at the end of time period t
 $Q_{jt.min}, Q_{jt.max}$ = minimum and maximum water discharge of reservoir j at time period t , m^3/s
 $V_{jt.min}, V_{jt.max}$ = minimum and maximum volume of reservoir j at time t
 $N_{jt.min}$ = Minimum hydropower generation constraint of reservoir j at time period t
 $N_{jt.max}$ = Installed plant capacity kW

Suppose that inflow has obtained $Q_{\lambda jt}$ and the relation of the water discharges follow equation 2 and if the storage capacity of the reservoir does not satisfy the constraints (3) then there is need to dispose the excessive flow. This will lead towards a complicated and dynamical programming problem.

Optimization techniques

a. Genetic algorithm

Genetic algorithm was developed by Goldberg (1989) Basic difference between GA and other methods are search of optimal results. GA can solve discrete, discontinuous and non-convex problems without differentiations due to search from whole population [11]. In GA search, during each iteration individuals are rated for their effective evaluation and selection, crossover and mutation operator are used to generate new population. The evaluation loop is repeated until desire termination results reached as shown in Fig. 1.

b. Particle swarm optimization

Kennedy and Eberhart (1995) developed particle swarm optimization as a continuous application optimization technique.

It has two parts in first phase particles are randomly distributed within the search space that is called initialization while the second phase is evolutionary phase in which particles change and adjust their position in search of optima by following the most successful particles until the termination. Suppose particles are moving in a D dimensional space with a velocity v . Particles position is represented $k_j = (k_{j1}, k_{j2}, k_{j3}, \dots, k_{jD})$ while the velocity is denoted as $v_i = (v_{i1}, v_{i2}, \dots, v_{iD})$. The velocity and position after $t+1$ time is given as

$$v_i^{t+1} = w * v_i^t + c_1 rand_1 (pbest_i - k_i^t) + c_2 rand_2 (gbest_i - k_i^t) \quad (6)$$

$$k_i^{t+1} = k_i^t + v_i^{t+1}, \quad \text{Where } k_i^{min} < k_i^{t+1} < k_i^{max} \quad (7)$$

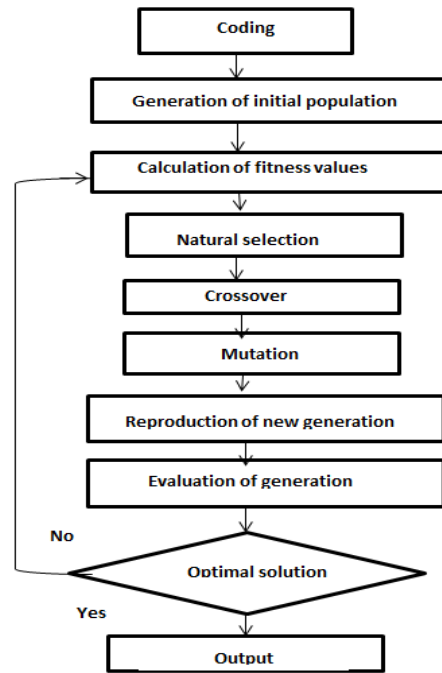


Fig. 1 flowchart of the GA

Where $i = (1, 2, \dots, \text{population size/swarm})$, $t = \text{number of reproduction steps}$, v_i^t : the velocity vector of particle i in the i^{th} reproduction step; w : inertial weight, c_1, c_2 : learning rates, $rand_1, rand_2$: independent random variables from $(0,1)$ uniformly distributed, $pbest_i$ is best solution produced by particle i , $gbest_i$ is the best solution produced by the swarm. Particle swarm optimization is easy and simple for implementation, computationally efficient as compared to other programming techniques. The PSO algorithm is summarized in the following steps

- i. The current position of the k_i and velocity is initialized with $[0, 1]$ random number range.
- ii. Generate initial swarm $k(0)$
- iii. Generate Initial velocity $v(0)$
- iv. Set $t=0$ where t is generation number.
- v. Repeat the procedure
- vi. Compute fitness value of each particle in the swarm
- vii. End the procedure again
- viii. Compute $PBest(i)$ and $GBest$
- ix. Perform PSO operations

- x. Compute $v(t+1)$ from equation 6
- xi. Compute $k(t+1)$ from equation 7
- xii. Perform Elitist mutation
- xiii. Set $t=t+1$
- xiv. Repeat the whole procedure until the termination criteria reached

Case study

The Xin'anjiang and Fuchunjiang hydropower stations are located at the Xin'an River, Zhejiang Province in east China. One hydropower station has installed at Xin'anjiang reservoir which is called Xin'anjiang hydropower station. The Xin'anjiang Hydropower Plant has 9 power generating units with a total installed capacity of 845,000 kW, generating annual output of 1.86 billion kWh. The Xin'anjiang Dam is first 105 meters high reinforced concrete dam in China with 466.5 billion m³ reservoirs capacity. Dam has a maximum flood discharging capability of 14,000m³/s. While Fuchunjiang hydropower station is a run off river plant and its electricity generation is highly variable and dependent at the flow released from Xina'anjinag reservoir and Lan River.

Based on the monthly inflow data of past 48 years from Xin'anjiang and Fuchunjiang reservoirs, model is run and calculates the energy of rainy year, average year and normal years by taking the dead level as the initial water level of scheduling. Genetic algorithm run with different generation value=100,200 and 400 in order to know with which generation value it will give better results. Different parameters used in GA are described here as: population size=200, Cross rate =0.8; mutation rate =0.1; variable dimension =24. Particle swarm optimization performed with randomly initialization and with different generation values=100,200 and 400. Different best parameters found are: $c1=1.4962$; $c2=1.4962$; $w=0.7298$; variable dimension $D=24$; Genetic algorithm and particle swarm optimization techniques have been applied at the mathematical model and the results obtained are given in the table I and II and shown in Fig. 2, 3 and 4. Results revealed that (table II) we can produce more electricity using optimization techniques as compared with conventional method. We can get approximately 33% more

electricity using optimal techniques than conventional methods.

Table 1 Results with different generations

Generation	GA		PSO	
	Energy output (10 ⁸ kWh)	Execution time(s)	Energy output (10 ⁸ kWh)	Execution time(s)
100	41.209	7.086	37.187	1.844
200	41.291	13.504	37.187	2.499
400	41.712	25.175	37.751	3.641

Table 2 Results of different algorithms

Year	Conventional method	GA		PSO	
	Energy output (10 ⁸ kWh)	Energy output (10 ⁸ kWh)	Execution time(s)	Energy output (10 ⁸ kWh)	Execution time(s)
Rainy year	26.413	41.712	25.17	37.751	3.64
Average year	18.614	33.354	25.85	30.125	3.69
Dry year	13.075	25.045	25.64	23.512	3.69
average	19.367	33.369	25.57	30.462	3.67

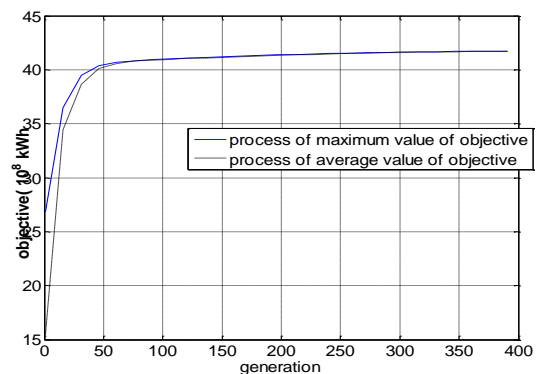


Fig. 2 Electricity generation (a using GA and using PSO) for rainy year of Xin'anjiang and Fuchunjinag

Rainy Years using GA

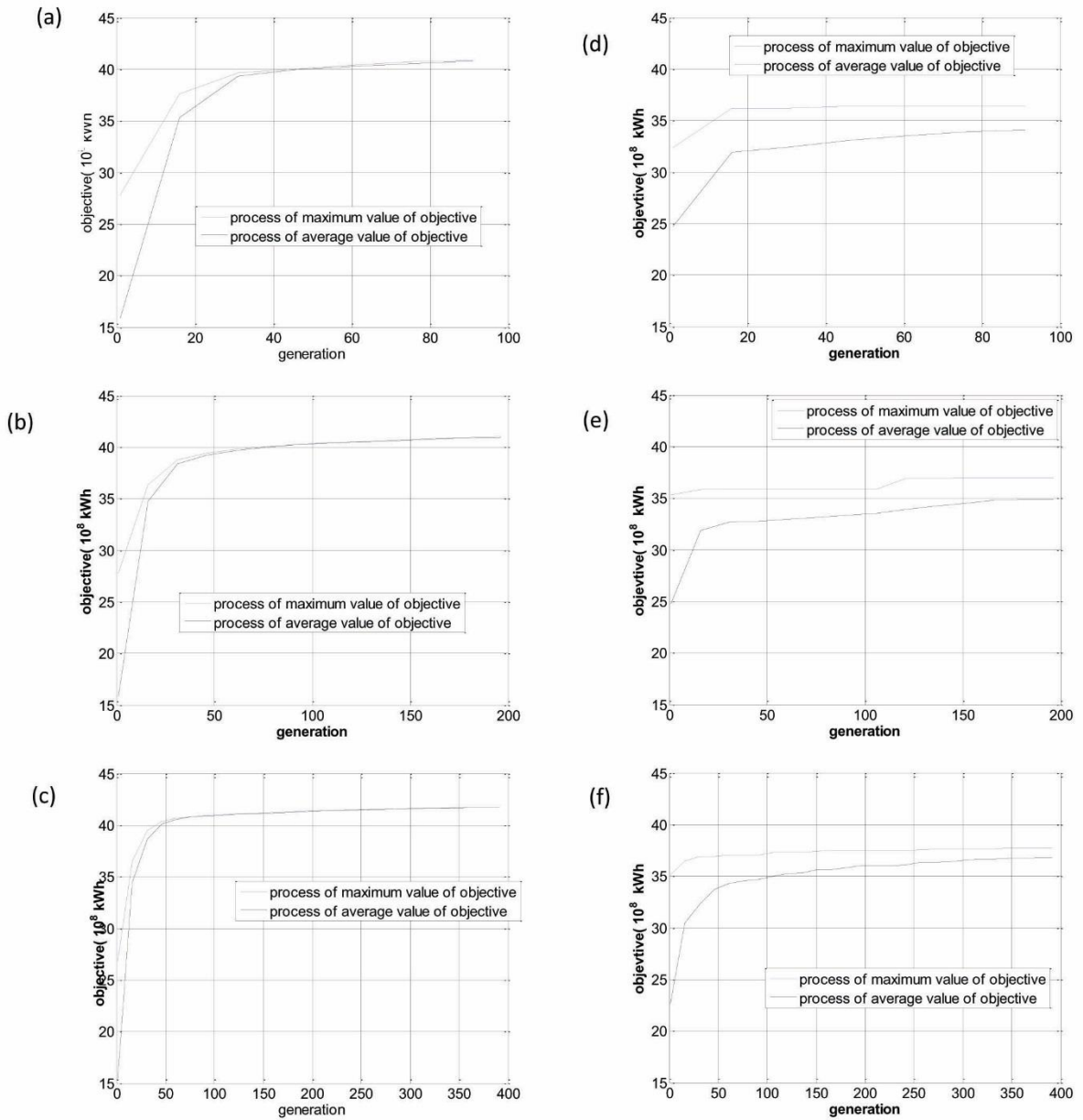


Fig. 3 Monthly total Power generation of Hydropower station with different generation values (a=100, b=200, c=400) using GA and (d=100, e=200, f=400) using PSO for rainy year.

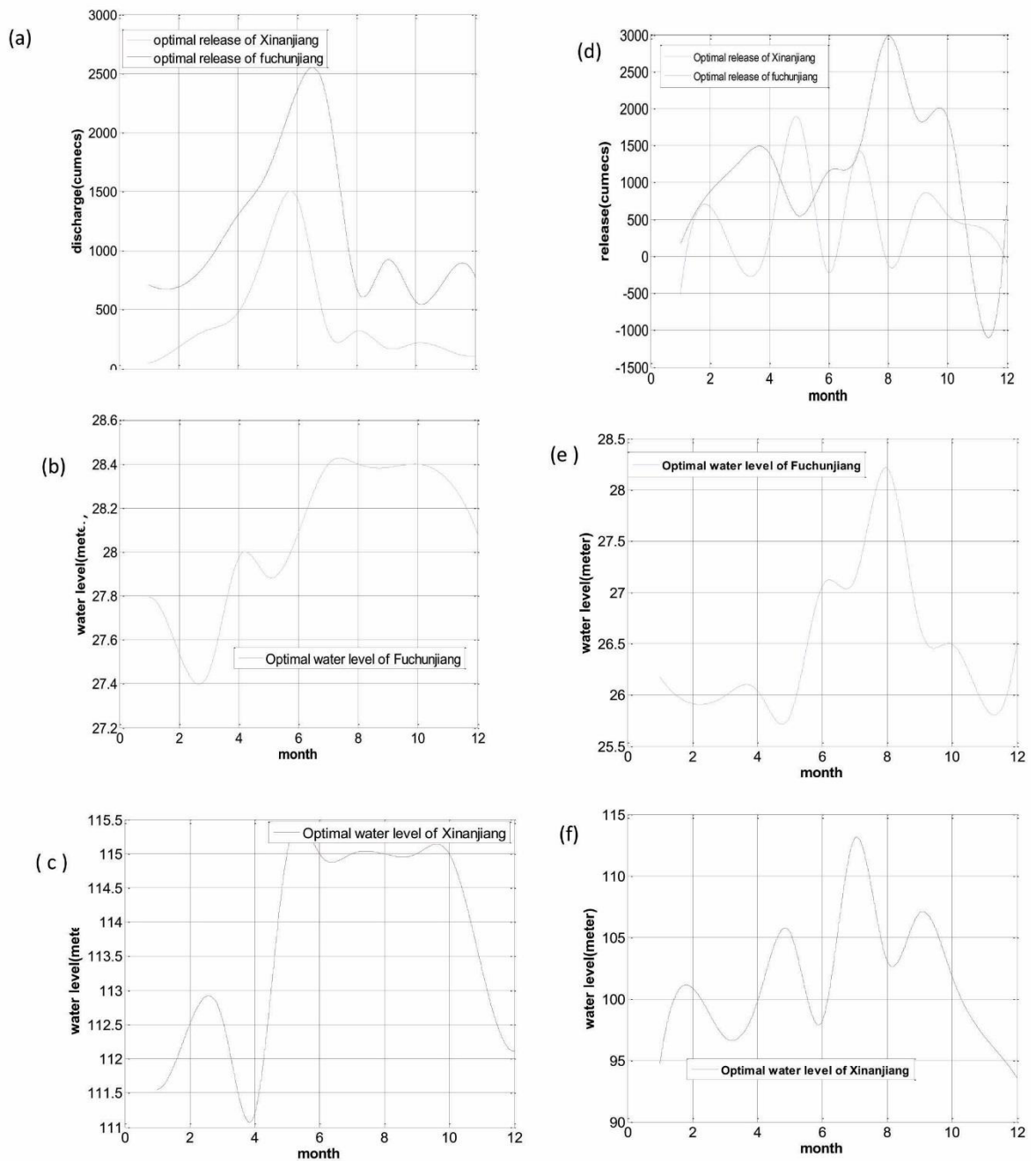


Fig. 4 Monthly water release ((a) using GA and (d) using PSO) and water level ((b, c), using GA and (e, f) using PSO) for rainy year of Xin'anjiang and Fuchunjiang

It has been observed that different generation values gave different value of objective function as shown in Fig. 3. Small generation number give a little less value of objective function (electricity generation) but the time of convergence is little. It can be seen from Fig. 3 and table I that electricity production using GA with different generation rates is more than PSO but the time of convergence of PSO is lesser as compared to GA. Electricity generation (objective function) is also affected due to different discharge rate and water levels as given in table II. It was observed that for different years (rainy, average, dry) electricity production is different. It can be seen that genetic algorithm gives more value of objective function as compared to particle swarm optimization technique but consuming a little more time than PSO.

Results revealed that there is not a big difference in convergence time using two methods, but a significance difference can be seen in electricity production as GA produces more electricity as compared to PSO. Results of the analysis showed that the water level and discharge have an important relationship for the energy output as shown in Fig. 4. Results of the analysis revealed that in order to get the optimal electricity generation, we should manage the discharge and water level of Xin'anjiang and Fuchunjiang reservoirs as shown in Fig. 4. If we supply optimum discharge to the power station by controlling water level of the reservoir as presented in Fig. 4, we can produce optimum electricity; consequently, we can get maximum benefits from this hydropower station.

Conclusion

Optimization of Xin'anjiang and Fuchunjiang hydropower is a complicated problem. This paper tried to get the optimal hydropower generation by building a mathematical model and using Genetic algorithm and particle swarm optimization techniques. Mathematical model for the optimization is developed and applied to the hydropower stations. Results showed that we can get more electricity using optimal methods than conventional methods. It is observed from the results that for the optimization of the hydropower and for getting maximum benefits, when simple genetic algorithm techniques have applied, it gave better objective function value than PSO. Results revealed that when PSO technique have applied at the current mathematical model, it searches objective function with high convergence speed, but value of objective function is less than GA. There is not a significance difference in time of

convergence of both methods but a better value of electricity production has achieved by using GA. The findings reveal that generation value also effect the convergence speed and objective function. For getting the better objective function value we should use high value of generation. Results of the model reveals that by managing our water level and water release equal to optimal water level and water release, we can get maximum electricity. With the application of Genetic algorithm, we can get more benefits in the form of power generation. Results showed that genetic algorithm is a better algorithm for hydropower optimization. However further study is needed with the application of different other techniques and by the combination of different optimization techniques.

References

- Hejazi MI, Cai X (2011) Building more realistic reservoir optimization models using data mining – a case study of Shelbyville reservoir. *Advance Water Resources* 34:701–717. doi:10.1016/j.advwatres.2011.03.001
- Loucks, D. P. , Stedinger, J. R. , and Haith, D. A. (1981). *Water resource systems planning and analysis*, Prentice-Hall, Englewood Cliffs, N.J.
- Yakowitz, S. (1982). "Dynamic programming applications in water resources." *Water Resources Research*. volume, 18 (4), pages 673–696
- Yeh, W. W.-G. (1985). "Reservoir management and operations models: A state-of-the-art review." *Water Resources. Researc.* , volume 21 (12), pages 1797–1818.
- Wurbs, R. A. (1993). "Reservoir-system simulation and optimization models." *Journal of Water Resources Planning and Management*. volume 119 (4) pages 445–472
- Mousavi SJ, Karamouz M, Menhaj MB (2004) Fuzzy-state stochastic dynamic programming for reservoir operation. *Journal of Water Resources Planning and Management*, volume 130(6):pages 460–70.
- Huang WC, Yuan LC (2004)) A drought early warning system on real-time multireservoir operations. *Water Resources Research* 40:W06401. doi:10.1029/2003WR002910
- Ganji A, Khalili D, Karamouz M (2007b) Development of stochastic Nash Game model for reservoir operation I. The symmetric stochastic model with perfect information. *Advances in Water Resources* volume 30(1) pages 528-542.

- Kucukmehmetoglu M (2009) A game theoretic approach to assess the impacts of major investments on Trans boundary water resources: the case of the Euphrates and Tigris. *Water Resources Management* volume 23(15):pages 3069–3099
- Labadie JW (2004) Optimal operation of multi-reservoir systems: state-of the-art review. *Journal of Water Resources planning and Management*, volume 130(2):pages 93–111
- Goldberg DE (1989) *Genetic algorithms in search, optimization and machine learning*. Addison-Wesley, Reading
- Fi-John C, Li C, Li-Chiu C (2005) Optimizing the reservoir operating rule curves by genetic algorithms. *Hydrological Process* volume 19:pages 2277–2289
- Jian-Xia C, Qiang H, Yi-min W (2005) Genetic algorithms for optimal reservoir dispatching. *Water Resources Management* volume 24, pages 321–331
- Hejazi MI, Cai X, Borah D (2008) Calibrating a watershed simulation model involving human interference –an application of multi-objective genetic algorithms. *Journal of Hydro-information* volume 10(1):pages 97–111
- Tung C, Hsu S, Liu C, Li J (2003) Application of the genetic algorithm for optimizing operation rules of the LiYuTan reservoir in Taiwan. *Journal of the American Water Resources Association* volume 39(3) pages 649–57
- Kennedy J, Eberhart R (1995) Particle swarm optimization. *Proc. IEEE Int. Conf. Neural Networks*, Perth, Australia, Dec: 1942–1948

One Dimensional Numerical Simulation of Scour and Deposition in a Channel using Finite Difference Method

Muhammad Zain Bin Riaz^{1*}, Muhammad Masood¹, Rana Zain Nabi Khan¹

^{1*}Centre of Excellence in Water Resources Engineering, University of Engineering and Technology
Lahore, Pakistan
[*zainie38@yahoo.com](mailto:zainie38@yahoo.com)

Abstract: A one-dimensional Saint Venant model is developed for simulating hydraulics and bed changes in irrigation channels. The governing equations are discretized using Finite Difference Method. The Saint-Venant equations describing unsteady flow in open channels and the continuity equation for the conservation of sediment mass are numerically solved. These equations are highly nonlinear and therefore do not have analytical solutions. For this purpose, the MacCormack explicit finite difference scheme is used. The scheme is second order accurate; it is a coupled solution as it is a two-step predictor corrector method. Model gives results in terms of bed level changes, flow depth and discharge provided physical boundaries of the system are valid for simulation time. Model execution and accuracy is very sensitive to time step and stability. Simulations show good accuracy when applied within the limitations of the model. Qualitative trends of results are in good agreement with previous studies.

Keywords: Finite Difference Method, Bed level change, Saint-Venant equations, MacCormack Scheme.

Introduction

Solution of the equations describing gradually varied unsteady flow in open channels is of vital importance in the design of hydraulic structures and water resources system, in the analysis of channel mechanics problems and in the development of channel control works. Many of these problems in rivers and canals involve the transport of sediment by flow and its scour or deposition. Sediment transport phenomena are often time variant, even when the flows are steady. Proper quantification of aggradation and/or degradation and changes in channel form of such channel still has been a subject of considerable research. A systematic study on the aggradation-degradation phenomenon of these channels of Pakistan is, therefore, of utmost importance from the viewpoint of improved planning and design of various water development projects.

A number of experimental studies had been conducted to study the effect of the long term and short-term bed level changes in alluvial channels with different flow conditions. Begin et al. (1981) experimentally studied degradation of alluvial channels in response to lowering of the bed level. Soni et al. (1980) conducted an experiment that covered a wide range of flow and sediment loading conditions. They observed that after a long time, the aggradation in downstream of the section of increased sediment supply was stopped

once the hydraulic conditions became compatible with the increased sediment load. Yen et al. (1989) performed a series of overloading experiments with uniform coarse sediment and found that both the aggradation wave speed and the mean sediment transport velocity increase with the initial equilibrium bed slope and with decreasing loading ratio. Series of experiments were conducted by Yen et al. (1992) to study the reversibility of an alternating aggradation-degradation process. The results show that the recovery rate decreases as standard deviation of sediment gradation increases. Alam (1998) applied MacCormack scheme to the study of aggradation-degradation in alluvial channels. Kassem and Chaudhry (2002) developed a two-dimensional numerical model to predict the time variation of bed deformation in alluvial channel bends. In this model, the depth-averaged unsteady water flow equations along with the sediment continuity equation are solved by using the Beam and Warming alternating direction implicit scheme. Deng and Li (2003) studied the river channel equilibrium profile using one dimensional unsteady flow and sediment transport model. Some of the widely used one dimensional models are MIKE11 (DHI, 2003) and HEC-6 (USACE, 1993) for sediment transport, erosion and deposition in straight channels and rivers.

Current study determines the rate and extent of bed level-changes due to transient conditions of flow and sediment (routing of sediment laden water) by using explicit finite difference method. The continuity and momentum equations along with sediment mass balance equation are solved numerically by finite difference explicit method of MacCormack.

The present work is aimed at investigating more closely with coupled solution through MacCormack, where relatively rapid changes in both fluid and sediment discharge are imposed at the upstream boundary.

Computational Procedures

The simulation method consists of two parts in each time step, i.e., flow computations, and sediment routing. Flow computation is executed first. Then, sediment routing is executed to compute the quantity of channel bed variations. The computational flow chart is shown in Fig.1.

Numerical Simulations

The effective application of a model basically depends on the accurate path to develop the model for a certain problem. The assumptions used in the numerical model development to simplify a phenomenon are sometimes critical to the extent of their validity. Considering all these limitations, a model is developed from the basic equations describing the problem.

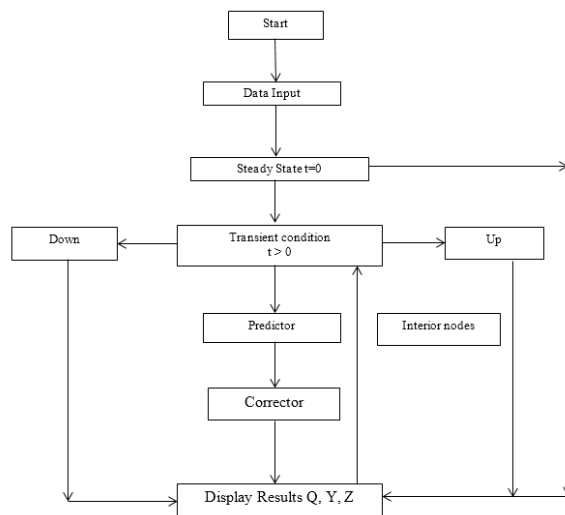


Fig. 1 Computational Flow Chart

Governing equations

The one-dimensional partial differential equations describing unsteady flow in a channel with movable bed (Fig. 2) are given by:

$$1) \text{ Continuity equation for water} \\ \frac{\partial y}{\partial t} + \frac{\partial q}{\partial x} = 0 \quad (1)$$

$$2) \text{ Momentum equation for water} \\ \frac{\partial q}{\partial t} + \frac{\partial}{\partial x} \left(\frac{q^2}{y} + \frac{1}{2} gy^2 \right) + gy \frac{\partial z}{\partial x} + ghs_f = 0 \quad (2)$$

$$3) \text{ Continuity equation for sediment} \\ \frac{\partial}{\partial t} \left[(1 - p)z + \frac{q_s y}{q} \right] + \frac{\partial q_s}{\partial x} = 0 \quad (3)$$

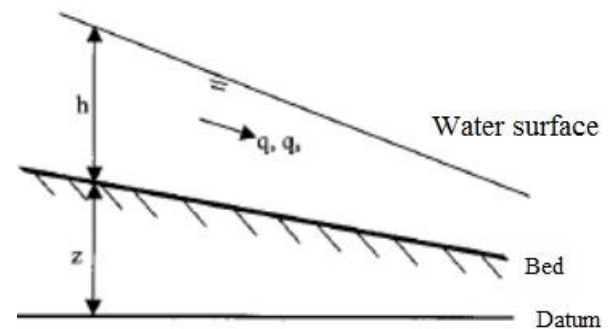


Fig. 2. Definition Sketch of variable

Terms used in these equations are defined as,

- q = Water discharge per unit width
- y = Depth of flow
- z = Bed elevation
- q_s = Unit sediment discharge
- g = Acceleration due to gravity
- S_f = Friction slope
- x = Longitudinal distance along the channel
- t = Time
- p = Porosity of bed layer

The friction slope, S_f is calculated using the Manning equation (SI unit):

$$S_f = \frac{q^2 n^2}{y^{3.333}} \quad (4)$$

Where, n = Manning roughness coefficient.

The sediment discharge is predicted by an empirical function of the flow velocity:

$$q_s = a \left(\frac{q}{y} \right)^b \quad (5)$$

Where, a, b are empirical constants to be adjusted. Values of a, b depend upon sediment properties and channel geometry.

Numerical scheme

The Eq. (1) through Eq. (3) characterizes as nonlinear hyperbolic partial differential equations and closed form solutions of these equations are not conceivable with the exception of rare simplified cases. Therefore, they are solved by numerical schemes. In this model, MacCormack (1969) is used and solved by a finite difference scheme. The MacCormack scheme is a two level predictor-corrector scheme. For one-dimensional flow two possibility of this scheme are conceivable. In one alternate, forward finite differences are used in the predictor part

and backward finite differences are used in the corrector part. In the second alternative, backward finite differences are used in the predictor part and forward finite differences are used in the corrector part. The values of the variables so determined during the predictor part are used during the corrector part. The finite difference approximations for the derivatives of a variable 'f' are as follows:

Predictor step:

$$\frac{\partial f}{\partial t} = \frac{f_i^* - f_i^k}{\Delta t} \quad (6)$$

$$\frac{\partial f}{\partial x} = \frac{f_{i+1}^k - f_i^k}{\Delta x} \quad (7)$$

Where, i= the node in spatial grid, k = the node in time grid, Δx = the distance step and Δt = the time step. An asterisk refers to the predicted values of the variable.

Corrector step:

$$\frac{\partial f}{\partial t} = \frac{f_i^{**} - f_i^*}{\Delta t} \quad (8)$$

$$\frac{\partial f}{\partial x} = \frac{f_i^* - f_{i+1}^*}{\Delta x} \quad (9)$$

Where, the two asterisks denote the value of the variables calculated in the corrector step.

Boundary conditions

The above equations determine the values of h, q, and z at the new time level k+1 at each interior grid points (i = 2,3...N-1). The values at the boundary grid points (i = 1 and N) cannot be calculated by using these equations. Hence, they are calculated by using boundary conditions. For one-dimensional flows, characteristic method gives acceptable results and is employed herein. Two boundary conditions at upstream boundary and one boundary condition at downstream end are required for the proper functioning of the model. In addition to these, initial conditions are needed at every computational grid point. Uniform unit discharge (q_0), uniform flow depth (h_0) and bed levels as calculated from initial bed slope (S_0) were provided as initial conditions, i.e.,

$$\begin{aligned} q(x,0) &= q_0 \\ h(x,0) &= h_0 \\ z(x,0) &= z_0 \quad \text{for } x=0 \end{aligned}$$

The flow depth, h at node 1 was determined by extrapolation from the already calculated values at the interior nodes using the MacCormack scheme. The downstream boundary condition was the constant depth, which was specified by $h(x_n,t) = h_0$ for $t \geq 0$. This was based on the assumption that the channel was long, and the bed transients would not reach the downstream end within the period for which conditions were

computed and that the variation in flow depth would be negligible. The discharge and the bed elevation at the downstream end were determined by extrapolation from the values at the interior nodes.

Model Performance Assessment

The Coding of the model has been checked by comparing it results with the already computed by the implicit model (see Ghumman, 1995) namely, Chen (1974), Chang and Richard (1971), and LUM, (developed by Ghumman, 1994). The results are shown in Fig.. 3. It indicates that the algorithm performs well and the overall agreement is satisfactory.

Channel section is wide rectangular; the length of the reach, L=14 km; bed slope, $S_0 = 0.0003$; and Manning's $n=0.01$.

The value of porosity p was assumed as 0.528 and the sediment load was calculated by using eq. (5) as given below:

$$Q_s = 0.00385 \frac{\left(\frac{Q}{A}\right)^3}{y} Q \quad (10)$$

The inflow hydrograph was defined as a steady flow of 6.2 m^3 per second per unit width. The following equation was described by Chen (1974) for second upstream boundary condition.

$$\Delta A_d(1) = \frac{\Delta t}{2p\Delta x} [Q_{s_2}^{n+1} - Q_{s_1}^{n+1} + Q_{s_2}^n - Q_{s_1}^n] \quad (11)$$

Q_{s_1} is the sediment input discharge at the upstream node, Q_{s_2} is sediment discharge at node 2 calculated by eq. (10), n represent the time step. The initial flow along the reach was assumed to be 6.2 m^3 per second per unit width. The initial depths used are given in the table 1 with upstream and downstream depths 2.15 and 4.0 meters respectively.

Table 1 The initial depths at different nodes (Ghumman, 1994)

Nod e No.	Dept h (m)	Nod e No.	Dept h (m)	Nod e No.	Dept h (m)
1	2.15	6	2.227	11	2.957
2	2.152	7	2.293	12	3.199
3	2.158	8	2.399	13	3.456
4	2.168	9	2.549	14	3.724
5	2.184	10	2.738	15	4.00

An assumed constant water stage was defined. The equation used is;

$$y_n = 4.0 - z_n \quad (12)$$

y_n and z_n are flow depth and total bed elevation change at downstream end of reach since start of simulation, respectively. The sum of y_n and z_n remains constant. Initially z_n at downstream is zero.

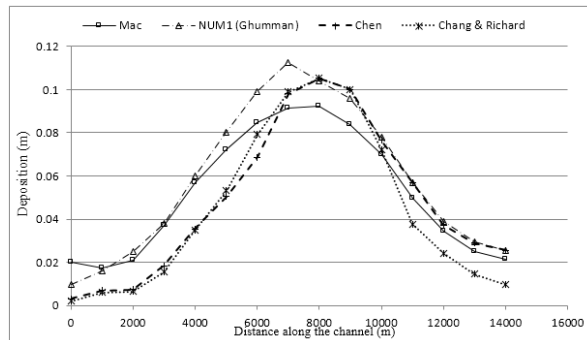


Fig. 3 Bed level changes compared with published solution

Application to CRB Canal

Chashma Right Bank Irrigation Project (CRBIP) is a large irrigation system spread over two provinces (Punjab and North West Frontier Province) of Pakistan. It is the 1st irrigation system in Pakistan, initially conceived as a crop-based supply system, and then followed by the design and construction of its physical infrastructure.

Chashma Right Bank Canal (CRBC) off-takes from Chashma Barrage on right flank of Indus River and runs almost parallel to the river along the highest contour for about 273.5 Km (170 miles). The total command area of the project is 230,675 hectares (570,000 acres) of land on the right flank of River Indus. The canal had been planned to deliver design discharge of 138.3 cumecs (4879 cusecs). The distribution system is about 1,100 Km (700 miles) long and 83 secondary channels irrigate a narrow strip of land between the Chashma Right Bank Canal and Indus River.

The first 38 Km (24 miles) of the canal are unlined with a slope of 1 in 8,000. A flat slope of 1 in 14,000 has been provided in the next 201 Km (125 miles). Last 17.7 Km (11 miles) in the tail reach have a steep slope of 1 in 8,000. The general plan and location map shown in Fig. 4.

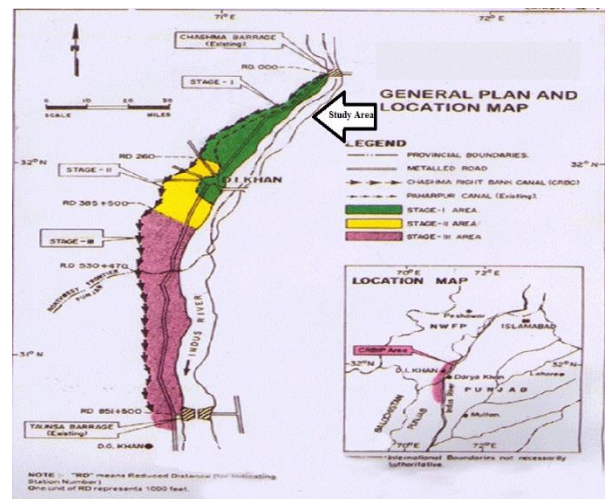


Fig. 4 General Plan and Location Map of CRB Canal

These data, including water stages and channel bed variations, can be used to calibrate and verify the model. Field data from 2000, including geometric cross-sectional data and bed material data, are used as the initial condition. Data from 2000 to 2001 were used to calibrate the model and data from 2002 to 2003 were used for verification.

Parameter Examination

The total simulation time was divided into low sediment flow period and high sediment flow period. May to Sept was high sediment flow period, whereas rest of the period was low sediment flow period. The inflow sediment load was calculated from the measured hydraulic and sediment data for the year 2001. The sediment rating was prepared for the low sediment flow and high sediment flow separately. The outflow sediment rating was used as inflow sediment rating for the next reach and so on.

To avoid an enormous load of calculations, a single representative cross section was chosen. The geometric properties of all the individual sections over the entire reach were averaged for this representative cross-section. The reach length, $L=15$ mile (24 km); bed slope, $S_0=0.000125$; Manning's $n=0.016$

The value of porosity, $p=0.3$; sediment discharge was calculated using eq. (5) in which values of empirical constants were taken as; $\alpha=0.00000006$; $\beta=3.248$; frictional slope was estimated by Manning's formula.

Table 2 The initial values for discharge

No.	Discharge (cfs)	No.	Discharge (cfs)	No.	Discharge (cfs)

1	3443	7	3383	13	3323
2	3433	8	3373	14	3313
3	3423	9	3363	15	3303
4	3413	10	3353	16	3293
5	3403	11	3343	17	3283
6	3393	12	3333		

The initial depths were assumed as normal depth is calculated by Manning's formula using the assumed cross-section as given below.

$$A = (Y - 7.3)/0.000832 \quad (13)$$

$P_w = 2 \cdot y + T$; P_w is wetted perimeter and T

Substituting these terms in the Manning's eq.;

$$Q = \frac{A}{n} \cdot \left(\frac{A}{P_w}\right)^2 \cdot S^{0.5} \quad (14)$$

The downstream boundary was defined by the Manning's equation using a subroutine NDEPTH in the MacCk. Couple Model.

Using table 3 of flow depth satisfies the Manning's equation at initial conditions and thus model runs successfully without facing any complication of instability due to Manning's equation during computations. However, model execution is terminated immature if values of initial flow depths other than table 3 were used.

Table 3 The initial depths at different node

Node No.	Depth (ft)	Node No.	Depth (ft)	Node No.	Depth (ft)
1	6.997	7	7.488	13	8.089
2	7.0343	8	7.5877	14	8.0909
3	7.069	9	7.7615	15	8.1300
4	7.193	10	7.849	16	8.1764
5	7.292	11	7.894	17	8.2125
6	7.390	12	7.982		

For $dx = 1000$ ft.; $dt = c \cdot dt1$; Any increase and decrease of dx and dt have tremendous effect on stability and execution of model. If $c=0.75$, it stops only after 48-time steps and for $c=0.65$ its simulation is completed upto 90 days. Stability problem was overcome by using $c=0.55$ that simulated for more than 198 days and 10841-time steps when ram quota exceeded with the message "Error during write, Disk quota failure" as output file is too large and big. Hence direct display of results was necessary to avoid excess of memory error and for model debugging. However, unnecessary output data could be avoided through managed output file.

The difference between calculated and observed bed level changes is ± 0.82 ft. It is due to the limitations of the model.

The bed profile computed with the model after simulation was compared with the measured bed profile. The computed and measured bed profiles are well matching with each other as shown in Fig. 5.

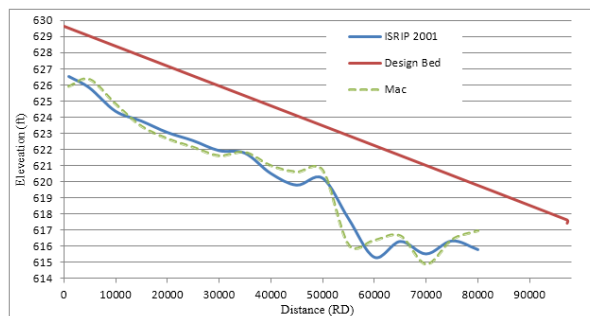


Fig. 5 Observed and Computed bed profile after 325 days simulation

The sediment deposition pattern depends upon the sediment inflow, hydraulic discharge, flow velocity, roughness, bed slope and bed material gradation. The sediment deposition pattern was estimated by plotting the change in bed elevation at different time intervals. The Changes in bed elevation at different time interval are plotted in Fig. 6.

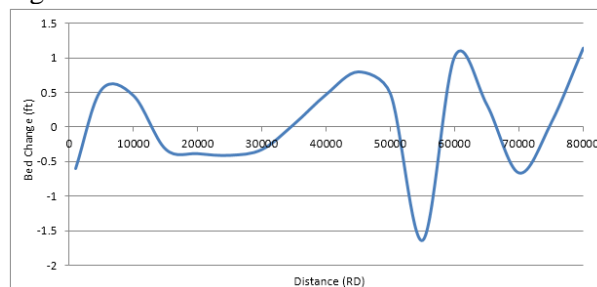


Fig. 6 Bed change after simulation

Verification

Using the parameters determined in the previous analysis, the model is applied to simulate the channel bed evolutions of CRB canal from 2002 to 2003. The total simulation period is 330 days. The comparisons of the observed and computed bed profile and bed change are shown in Fig. 7 and 8 respectively. The overall accuracy is good. The computed and measured bed profiles are well matching with each other as shown in Fig. 7.

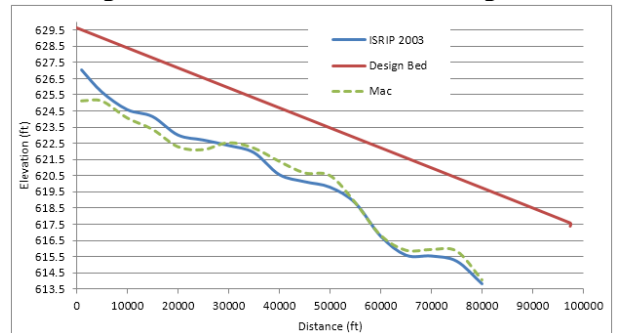


Fig. 7 Observed and Computed bed profile after 330 days simulation

The deposited sediment resulted in raising the bed of the canal at different locations. The graph was plotted for bed changes and it is shown Fig. 8.

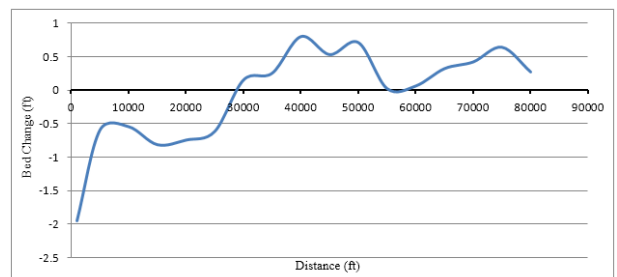


Fig. 8 Sediment deposited and bed changes after 330 days

Running MacCk. Couple Model with this data is humble effort of this study. Generally, set trends of results are fairly responsive but need further minute model calibration and refinement which is expected in future research to make the model a generalized one and viable for sediment as well as for hydraulic routing.

CONCLUSIONS

In this study the change in bed level of channel is studied with application of a one-dimensional mathematical model based on MacCormack scheme. The following conclusions can be made after summarizing the present study:

- 1- Model developed in this study has fairly good qualitative and quantitative accuracy when applied within the limitations of the

- model. However, quantitative estimates may be demoralized sometimes.
- 2- Results and model execution was more stable and prosper for relatively smaller computational time intervals.
 - 3- Employing different equations for similar conditions will yield transport rates that might differ by several orders of magnitude. Therefore, it is difficult to reach at a universal transport equation.
 - 4- The MacCormack scheme can be applied to develop a two-dimensional model to study the two-dimensional problems and also a three-dimensional model to study three-dimensional problem.

References

- Alam, M. (1998) "Application of MacCormack scheme to the study of aggradation degradation in alluvial channels" M.Sc. Engineering thesis work, Department of Water Resources Engineering, BUET, Dhaka.
- Begin, Z.B. (1981) "Development of longitudinal profiles of alluvial channels in response to base level lowering." *Earth Surface Processes and Land Forms*, Vol. 6, No. 1, pp. 46-68.
- Deng, J. and Li, Y. (2003) "A study on the equilibrium profile for the Luoshan-Hankou reach in the middle Yangtze river". *International Journal of Sediment Research*, Vol. 18, No. 2, 2003, pp. 107-114.
- DHI Inc. (2003), 301 South State Street, Newtown, PA, 18940, USA. <http://www.dhisoftware.com/>
- Ghumman, A. R 1994 The development and optimization of numerical model's for the sediment routing in rivers. Ph.D thesis, Queen Mary and Westfield College, University of Landon
- Gill, M.A. (1987) "Nonlinear solution of aggradation and degradation in channels." *Journal of Engineering Mechanics*, IAHR, Vol. 25, No. 5, pp. 537-547.
- Jain, S.C. (1981) "River bed aggradation due to over loading." *Journal of Hydraulic Engineering*, ASCE, Vol. 107 No. HY1, pp. 120-124.
- Kassem, A.A. and Chaudhry, M.H. (2002) "Numerical Modeling of Bed Evolution in Channel Bends". *Journal of Hydraulic Engineering*, ASCE, Volume 128, Issue 5, pp. 507-514. MacCormack, R. (1969). "The effect of viscosity in hypervelocity impact cratering." *Paper 69 354*, American Institute of Aeronautics and Astronautics, Cincinnati, Ohio.
- Soni, J.P.; Garde, R.J.; and Raju, K.G.R. (1980) "Aggradation in streams due to overloading." *Journal of the Hydraulics Division*, ASCE, Vol. 106, No. HY1, pp. 117-132.
- Torres. W.F.J and Jain, S.C. (1984). "Aggradation and Degradation of Alluvial Channel Beds", IIHR Report No. 274, Iowa Institute of Hydraulic Research, University of Iowa.
- Yadav, S.M. and Samtani, B.K. (2008) "Bed Load Equation Evaluation based on Alluvial River Data, India". *KSCE Journal of Civil Engineering*, Volume 12, Number 6, pp. 427-433.
- Yen, C.L; Chang, S.Y.; and Lee, H.Y. (1989). "Recovery of channel bed in aggradation-degradation process" *Proceedings, 23rd congress of IAHR*, Ottawa, Canada, pp. B323-B329
- Yen, C.L; Chang, S.Y.; and Lee, H.Y. (1992). "Aggradation-degradation process in alluvial channels" *Journal of Hydraulic Engineering*, ASCE, Vol. 118, No HY12, pp. 1651-1669.

Risks Involved on Hydropower Projects in Pakistan

Raheel Ahmed Rana^{1*}

^{1*}Centre of Excellence in Water Resources Engineering, University of Engineering and Technology,
Lahore 54890, Pakistan

urrays@gmail.com

Abstract: *Hydroelectric power plant has complex structures and involves large amounts of capital with a long-running construction period. This situation enacts uncertainty factors with considerably high risks. Failure to manage project risks leads to completion time delays and cost overruns. Risk Management (RM) is a logical and systematic process of identifying, analyzing and responding to risks associated with any activity, function or process. The objectives of RM are to increase the probability and impact of positive events and decrease the probability and impact of adverse event. The alternative to risk management is risky management! In the financial world, risk management is the process of identification, analysis and acceptance or mitigation of uncertainty in investment decisions. However, in developing countries like Pakistan, the observance of RM in the construction industry is rare. In Hydropower Sector, such studies are very almost ZILCH as the Hydropower Market is immature in term of indigenous sufficiency. This research is conducted to highlight the main risk factors causing delays of hydropower construction projects subsequently causing the cost over runs, conflicts, Arbitrations and loss to Economy. The research employs risk analysis to obtain feedback from experts participating having experience in Hydropower in Pakistan. The research outcomes are as follows: identifying the risks that can cause delays in the Hydropower construction projects in Pakistan, calculating and classifying the degree of impact of each risk and ranking them along with the comparison of views of different stake holders. The practical significance of this study is to ensure the timely completion of projects, ensuring early risk mitigations techniques that benefits all the stake holder including Investor, Client and Contractor.*

Keywords: Risk Management, Delays in Hydropower Projects.

Introduction

Pakistan's potential from hydro is at least 60,000MW, (according to the Private Power and Infrastructure Board- PPIB) most of this from Khyber-Pakhtunkhwa and Gilgit-Baltistan. But this is where the picture stops looking bright and becomes depressing. The total installed capacity of hydropower in Pakistan is just 6,800 MW as after the construction of the Tarbela Dam, not a single big hydropower project has been carried out during the last 40 years, except Ghazi Barotha. According to the Water and Power Development Authority of Pakistan (WAPDA), two-thirds of the country's electricity is today produced from fossil fuels, and just one-third from hydro.

The biggest hurdle as "assumed generally" may be lack of political will, stability and consensus along with hurdle is finances, considering Pakistan's dwindling ability to attract foreign investors because of the security situation and water dispute with India which constantly crops up. Added predicaments is non-observance and non-provision to investors, the clear pathways from conception to return on investment (ROI) especially in Pakistan being developing

countries. Investors will commit funds toward the development of an energy project in general based upon the project's risks in which the Pakistan is lacking. International Finance Cooperation (IFC of World bank) in its GUIDE TO INVESTOR AND DEVELOPER OF HYDROELECTRIC suggest that Risks can reduce project attractiveness for some lenders; other lenders are willing to accept more risks but for higher yields. But if the project risk profile is too high, project financing may not be feasible. Thus, a well-prepared financial analysis should include a DETAILED RISK ANALYSIS.

But the dilemma does not stop here as the projects that somehow comes from Paper to become reality phase, are also delayed not only in construction phase (construction risks) but also during bidding process for years and years. Private sector analysts say that many of these projects will never see even their ground-breaking.

Very Recent examples are 69 MW Lawi Hydropower (feasibility in 1990, bid for 3 times and still not awarded), 84 MW Matiltan Hydropower (Feasibility studies in 1990, four time re-bid in recent 3 years), Jagaran II (delayed

almost 3 years in bidding process), 34.5 MW harpo (approved from ECNEC, foreign funded, still no sign of bidding process), Neelum Jhelum Hydropwoer (long delays in construction), Dasu Hydropower Project (land acquisition and Chinese contractor issue) Diamer Basha Dam (funding issue) and horrible list continues.

Project Life Cycle

Risk management

PMBOK® Guide (PMI 2004) 2 suggested dividing a project life cycle into four major stages and defined the ‘typical’ project life cycle as: feasibility, planning and design, construction, and turnover and startup. In addition, it is well known that construction activities within the project life cycle are executed under ‘unique’ circumstances and continually face a variety of uncertainties which can result from ‘known’ (the risk events which occur frequently and an inevitable feature of all construction projects), ‘known-unknown’ (the risk events whose occurrence is foreseeable, and their probability of happening is known), and ‘unknown-unknown’ (the risk events whose probabilities of occurrence and effect are not foreseeable, considered moreover, as force-majeure event conditions). In other words, the construction phase deals with many unknown, unexpected, and unpredictable factors (Akintoye, A. S & MacLeod, M. J (1997)), which sometimes put the project at risk. As defined in ISO 31000 4, risk is the effect of uncertainty on objectives ; risk management is the identification, assessment and prioritization of risks followed by the coordinated and economical application of resources to minimize, monitor and control the probability and / or impact of unfortunate events 2 (negative events), or to maximize the realization of opportunities (positive events). Paul Newton, in his book named “ Managing Project risk” 5 suggested that everything that is done in Business contains some Risk. No matter what activity, there is element of risk that must be analyzed and weighed against potential reward. Most of the researchers have claimed that risks in the construction projects can be defined as anything that influences the construction project in the planning phase as well as the execution phase (Akintoye & MacLeod 1997)3. However, few people view risk only as negative indicator. Despite the arguments surrounding risks in the construction project, Zhi, H (1995,’Risk management for overseas construction projects’6, International Journal of Project) Management, stated ‘Risk management

is an important and integral element of project management’. He stated that the success of a project manager was heavily influenced by efficient and effective management of the risk involved. Therefore, systematic risk management needs to be applied in order to manage a project effectively throughout its life cycle.

Risk management steps were also introduced by A Guide to the Project Management Body of Knowledge (PMBOK® Guide-PMI 2004) 2 which stated there were four fundamental steps of risk management: risk identification, risk analysis (qualitative and quantitative), risk response planning, and risk monitoring and control.

Systematic approach to Risk Management

At the first step, risks should be classified into different groups with certain criteria in order to clarify the relationship between them. This step is called risk identification (Zhi 1995) 6. He explained that the background of the identification of risk and the creation of a risk list is dependent upon many factors, such as past experience, personal tendency, and the possession of information. Further, the researchers, Cohen and Palmer (2004) 7, stated there are two common techniques to employ in risk identification: experienced-based risk and brainstorming- based risk assessment.

The second step entails the risk analysis and evaluation of the risks pertaining to risk management. Risk analysis response management may only be performed on identified potential risks.



Fig. 1 Risk Management Process

The third step is to put in place an appropriate method in order to treat the risks. At this step, the project management team should decide and formulate risk treatment strategies or mitigation measures. In short i.e. avoidance, transference, mitigation, and acceptance (PMI 2004).



Fig. 2 Risk treatment

Risk Management Studies on Hydropower Project

The Author has referred few studies that are related to risk management in Hydropower Sector. In order to prevent time delays and cost overruns in hydropower construction in Indonesia (state owned power company of Indonesia like WAPDA here in Pakistan) conducted the study on project risk management in the construction stage of hydropower plant projects. (named: Project Risk Management in Hydropower Plant Projects: a Case Study from the State-owned Electricity Company of Indonesia Author: Weddy, B.S & Hardjomuljad,S.) 8. Similarly, a study in Vietnam was conducted by MAI S.H, WANG J.Q & HONG V.U 9 on Risk evaluation and control of EPC hydropower construction project in Vietnam). This study highlighted the need and importance of RISK Management. Another study on Risk assessment of river-type hydropower plants by using fuzzy logic approach (Kucukali, S, Cankaya University, Department of Civil Engineering, Balgat, 06530 Ankara, Turkey) 10 suggest that that the most concerned risks are site geology and environmental issues.

Proposed Research Orientation

The Author, in this research study, identified the Forty-Four (44) project delay attributes through detailed literature review, brains storming and discussion with Hydropower experts, that were grouped into nine (9) categories keeping in view risk to consultant related, contractor related, design-related, equipment-related, externality - related, labour-related, material-related, owner-related, project-related, engineer-related, contract related and human-behavior related.

Delays Factors in Hydropower Construction

Based on literature reviewed, and interview / discussion with few Hydropower experts following Nine (9) broad Risk categories was clustered in the study that are summarized in the below Fig. 3 and table 1;

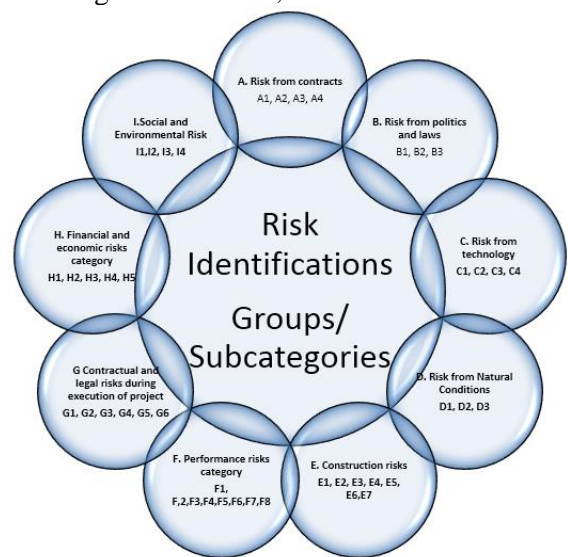


Fig. 3 Risk Groups

Table 1 Risk in Hydropower Project

Risk Category	Risk
A	Risk from contracts
A-1	Unfair contract terms
A-2	uncertain and unclear contract terms
A-3	EPC mode of contract in developing country like Pakistan where expertise level is low
A-4	Second Language contracts with misleading clause (e.g. Chinese companies signing contract in English)
B	Risk from politics and laws
B-1	Relationship among investor, contractor with authority and relevant department
B-2	Political influence / political Change
B-3	Law and regulations from management agencies / Government policies
C	Risk from technology
C-1	Technical Design
C-2	Negative survey data
C-3	Lower expertise level in Developing countries in contractor / consultant

C-4	Electrometrical Equipment's sourcing and performance
D	Risk from Natural Conditions
D-1	Geology of Area (Subsurface condition and subsurface ground water)
D-2	Hydrological risk (lower or excess than expected water causing unusual seasonal variation/ floods)
D-3	safety and security on remote areas
E	Construction risks
E-1	Delayed Site Access
E-2	Availability of plant and equipment at site
E-3	Changes in the work or design at later stage
E-4	Availability of material
E-5	Late drawings and instructions
E-6	Availability of labor
E-7	Lack of local industry experience in Hydropower
F	Performance risks category (construction related)
F-1	Poor Site managements and supervision
F-2	Delays in decision Making
F-3	Accidents / safety
F-4	Rain and flood
F-5	Unsuitable management structure and style of contractor
F-6	Lack of communication / trust / maturity between client, consultant, and contractor
F-7	Defective work
F-8	Lack of Expertise in Hydropower Sector
G	Contractual and legal risks during execution of project
G-1	Insolvency of contractor or owner
G-2	Delayed dispute resolution
G-3	Delayed payment on contract and claims
G-4	Procedural delay from the client specially when LENDER is involved
G-5	EPC mode of contract in Pakistan and lack of EPC expertise in hydro sector
G-6	Chinese EPC contractors (Project taken on low rates then fail to deliver)
H	Financial and economic risks category
H-1	Wrong Costing
H-2	Inflation
H-3	Interest rate
H-4	National and international impact of monetary policies
H-5	Financial capacity of contractors
I	Social and Environmental Risk
I-1	Resettlement and social unrest
I-2	International objection on social environmental or cultural grounds
I-3	Destruction during war
I-4	Environmental risk

Methodology for survey

Questionnaire survey were conducted across hydropower specialist that included consultants, contractors, clients and financial advisor on hydropower projects to gather their views on causes of delay in delivery of hydropower projects.

In this research, only experts from Hydropower industry were selected worked in Pakistan on different hydropower related business in different capacities that include but not limited to project directors, project managers, designers,

owner of contractors worked on hydropower, owner of consultants worked on hydropower, financial advisors, directors of big construction houses, foreigners from china, UK, Iran worked in Pakistan, field specialist, planning engineers, economist, Mechanical specialists, contract specialists etc.

In order to get the realistic and representative results, survey was conducted only through the experts having exposure in Hydropower business. Every risk has to be rated by the

respondent from the scale 1-5 (5 being high risk and 1 as low risk).

Respondents Data:

1. Total respondents = 52

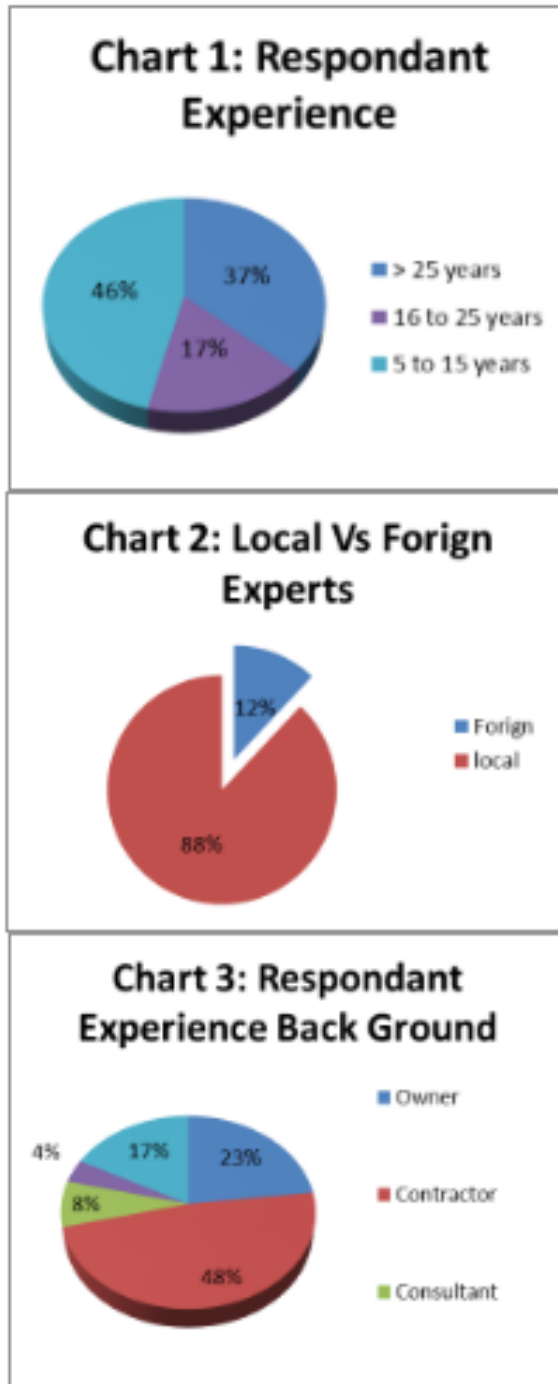


Fig. 4

Data Analysis'

Researched Weddy, B.S & Hardjomuljad,S, 8 used the relative importance index to determine the risk tanks and same process has been adopted here. The contribution of each of the factors to overall delays was examined and the ranking of the attributes in terms of their criticality as perceived by the respondents was done by use of Relative Importance Index (RII) which was computed using equation

$$\text{Relative Important Index (RII)} = \frac{\sum W}{A * N} \quad (0 \leq \text{RII} \leq 1)$$

Where: W – is the weight given to each factor by the respondents and ranges from 1 to 5, (where “1” is “Low Risk” and “5” is “High Risk”);

A – is the highest weight (i.e. 5 in this case) and; N – is the total number of respondents =52 in this case.

Survey Results and Analysis

Ranking of Risk

The Author based on the survey result and calculated Relative Important Index value categorized the risk into extremely Important, Very Important, Important, Less Important and Not important risk. Table 2 shows the Raking of risk based on the RII. The survey results show that there are four risk factors (9.09%) categorized as ‘extremely important’. These four risks namely “Chinese EPC contractors (Project taken on low rates then fail to deliver)”, Wrong Costing, Insolvency of contractor or owner, delayed dispute resolution” are the most “critical” risk. Twenty-Eight risks (63.63%) risks are considered as Very Important (RII = 60 to <80). The average RII score for these Important risks 0.698 so in the “Very Important” Categories group the risks with RII more than the average RII are considered to have significant impact. These risks include form rank 5 to rank 21 in Table 2.

Table 2 Ranking of Risk based on RII

Rankin	Code	Risk	RII	Sco	Relativ
Rank 1	G-6	Chinese EPC contractors (Project taken on low rates		218	2.876
Rank 2	H-1	Wrong Costing		213	2.810
Rank 3	G-1	Insolvency of contractor or owner		209	2.758
Rank 4	G-2	Delayed dispute resolution		208	2.744

Rank 5	F-2	Delays in decision Making	204	2.692
Rank 6	G-5	EPC mode of contract in Pakistan and lack of EPC	203	2.678
Rank 7	F-8	Lack of Expertise in Hydropower Sector	199	2.626
Rank 8	D-1	Geology of Area (Subsurface condition and subsurface	197	2.599
Rank 9	A-1	Unfair contract terms	196	2.586
Rank	G-3	Delayed payment on contract and claims	195	2.573
Rank	A-2	uncertain and unclear contract terms	190	2.507
Rank	C-3	Lower expertise level in Developing countries in	189	2.494
Rank	A-3	EPC mode of contract in developing country like	188	2.481
Rank	F-1	Poor Site managements and supervision	186	2.454
Rank	E-1	Delayed Site Access	185	2.441
Rank	G-4	Procedural delay from the client specially when	184	2.428
Rank	H-5	Financial capacity of contractors	184	2.428
Rank	C-2	Negative survey data	183	2.415
Rank	F-6	Lack of communication / trust / maturity between client,	183	2.415
Rank	E-7	Lack of local industry experience in Hydropower	182	2.401
Rank	I-1	Resettlement and social unrest	182	2.401

The above results depict the pictorial overview regarding the major risk involved in the in-Hydropower project in developing Country like Pakistan. Thus, it may be safely concluded here that Project Management Team must consider these potential risks in Hydropower Projects.

Frequency Analysis on SPSS (Statistical Package for the Social Sciences)

The Author also conducted the frequency analysis of each risk based on count of survey results on SPSS. Frequency table of top ranked risk is shown in table 3 and frequency of rank 2 and ranked 3 risks are depicted in chart 4 to 5 for the 52 respondents of the survey.

Table 3 Frequency Analysis

Rank 1: Chinese EPC contractors (Project taken on low rates then fail to deliver)		Frequency	Percent
	very low risk	1	1.9
	low risk	2	3.8
	Neutral	10	19.2
	high risk	12	23.1
	very high risk	27	51.9
	Total	52	100.0

Ranking of Group

The table 3 show the ranking of group based on Combined RII score of survey results and Group G - Contractual and legal risks during execution of project was ranked number No 1 by the respondents. The author found an interesting fact from the results that in top Ten risks, five risk belongs to Group G that subsequently resulted Group G to be most influenced group to cause issue in Hydropower Projects. The risk

categorized in the group G were the contractual risk during the execution of projects and most of these risks can be foreseen and mitigated with good project management, involving the contractual experts, using the best in practice contract document like FIDIC, timely involving the dispute boards, taking ownership of issues and resolving in good faith.

Table 3 Risk Groups Overall Ranking

Ranking	Group Code	Group Name	Combined Relative Importance Index (RII)
Rank 1	G	Contractual and legal risks during execution of project	0.780
Rank 2	D	Risk from Natural Conditions	0.709
Rank 3	A	Risk from contracts	0.674
Rank 4	F	Performance risks category (construction related)	0.657
Rank 5	C	Risk from technology	0.651
Rank 6	H	Financial and economic risks category	0.644
Rank 7	I	Social and Environmental Risk	0.621
Rank 8	B	Risk from politics and laws	0.621
Rank 9	E	Construction risks	0.603

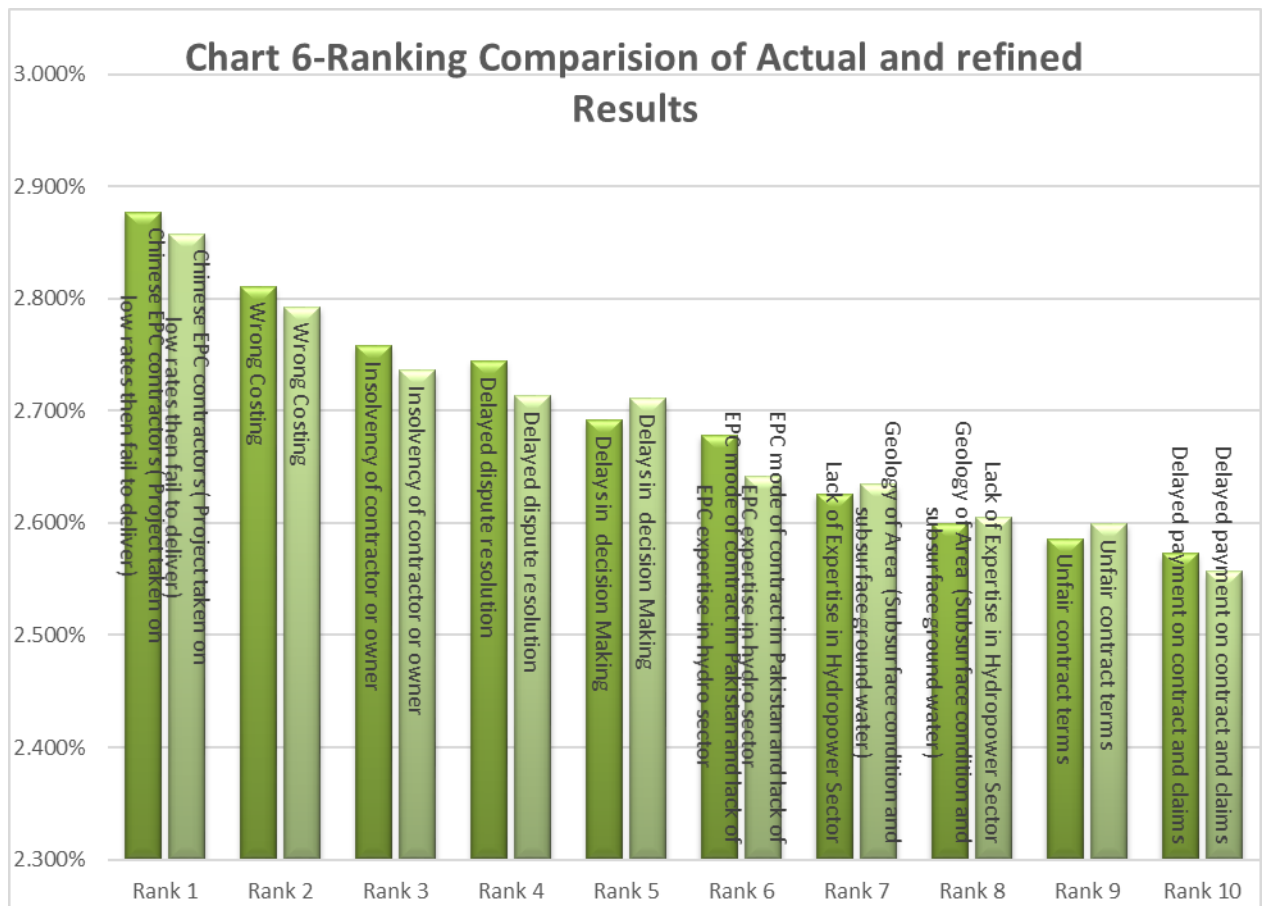
Another stimulating fact is that Ranked 3 group is related to Contracts risks that involve unfair and unclear terms and conditions. One sided contracts terms and unclear/improper contract documents are always the concern for the Contractors and subsequently result in Potential risk for the project.

Weightage Assigned to the Respondents

Though the results were collected from the experts from various trades and back ground in Hydropower Industry, however the Author considered that there may be some kind of biasedness, inconsistency and experience lack in survey result from the respondents. The Author also realized that the same weighted can't be

given to every person as of their experience difference, education differences, exposure difference scope / role differences. So, based on experience, exposure of Hydropower projects, educations and last but not the least experience of Author working with the respondents, weightage to their score is introduced in order to refine the result to ensure authentic and making true representation of issues.

In comparison for actual and refined results, Relative Percentage was introduced to compare the degree and ranking. However, the results show that there is not any substantial upset as first top 10 ranked risk remained the same with up to rank 6 no change in ranking.



Agreement and disagreement between Contractor, Client and TPS

The Author also analyzed the agreement and disagreements in survey results between client, contractor and third-party experts in order to highlight the perspective of different stakeholders. Third party respondents include the experts from consultants, dual experience contractor – client experiences, consultant – client experience, contractor- consultant experience, hydropower financial advisors.

Rank Correlation for risk categories for the three groups of respondents was calculated to establish the level of agreement and disagreement. The author used the rank correlation using spearman coefficient. The Spearman correlation

coefficient, r_s , can take values from +1 to -1. A r_s of +1 indicates a perfect association of ranks, a r_s of zero indicates no association between ranks and a r_s of -1 indicates a perfect negative association of ranks. The closer r_s is to zero, the weaker the association between the ranks.

The formula of r_s for Spearman correlation is

$$r_s = 1 - \frac{6 \sum_{i=1}^n d_i^2}{n^3 - n}$$

where

d_i is the difference between the two ranking
 n is the number of observations.

Table 4 Spearman Correlation (over all result)

Client vs Contractor	0.60
Contractor Vs Third Party	0.84
Client Vs Third Party	0.67

Broadly speaking the Client perspective is different as compared to Contractor and third party, whereas the Contractor and third party experts have more harmony in the views.

Table 5 Ranking Comparison of Client, Contractor and TP

Code	Risk	Client Ranking	Contractor Ranking	Third Party ranking
A-1	Unfair contract terms	26	6	13
A-2	uncertain and unclear contract terms	9	17	8
A-3	EPC mode of contract in developing country like Pakistan where expertise level is low	12	18	9
A-4	Second Language contracts with misleading clause (e.g. Chinese companies signing contract in English	38	43	37
B-1	Relationship among investor, contractor with authority and relevant department	28	26	28
B-2	Political influence / political Change	13	34	24
B-3	Law and regulations from management agencies / Government policies	17	35	33
C-1	Technical Design	35	31	22
C-2	Negative survey data	33	19	4
C-3	Lower expertise level in Developing countries in contractor / consultant	14	11	15
C-4	Electrometrical Equipment sourcing and performance	18	40	36
D-1	Geology of Area (Subsurface condition and subsurface ground water)	15	10	2
D-2	Hydrological risk (lower or excess than expected water causing unusual seasonal variation/ floods)	16	25	16
D-3	safety and security on remote areas	3	27	23
E-1	Delayed Site Access	5	22	18
E-2	Availability of plant and equipment at site	27	38	38
E-3	Changes in the work or design at later stage	31	14	25
E-4	Availability of material	42	42	39
E-5	Late drawings and instructions	29	21	30
E-6	Availability of labor	43	44	43
E-7	Lack of local industry experience in Hydropower	34	15	17
F-1	Poor Site managements and supervision	11	20	14

F-2	Delays in decision Making	6	7	7
F-3	Accidents / safety	41	41	44
F-4	Rain and flood	36	39	42
F-5	Unsuitable management structure and style of contractor	22	23	26
F-6	Lack of communication / trust / maturity between client, consultant, and contractor	7	16	29
F-7	Defective work	19	28	34
F-8	Lack of Expertise in Hydropower Sector	23	3	19
G-1	Insolvency of contractor or owner	8	4	3
G-2	Delayed dispute resolution	10	5	1
G-3	Delayed payment on contract and claims	20	8	11
G-4	Procedural delay from the client specially when LENDER is involved	30	12	20
G-5	EPC mode of contract in Pakistan and lack of EPC expertise in hydro sector	1	9	12
G-6	Chinese EPC contractors (Project taken on low rates then fail to deliver)	2	1	5
H-1	Wrong Costing	4	2	6
H-2	Inflation	32	32	31
H-3	Interest rate	44	36	40
H-4	National and international impact of monetary policies	39	37	32
H-5	Financial capacity of contractors	24	13	21
I-1	Resettlement and social unrest	25	24	10
I-2	International objection on social environmental or cultural grounds	21	33	27
I-3	Destruction during war	40	29	41
I-4	Environmental risk	37	30	35

The detail review of table 4 and 5 epitomizes the concern of contractor, client and consultants etc. and the intensity of their concern, difference and prospective towards various risk. For instance, Client ranked Risk named “EPC mode of contract in Pakistan and lack of EPC expertise in hydro sector” as No 1 but contractor and third-party experts does not agree with the perspective of client. Risk A1 (Unfair contract terms) being ranked 6 by the contractor as one-sided contract is always the concern for contractor and Contractor has to cater these risk at the bidding stage, however, as expectedly the client considers it a less potential risk. The risk like Political and law order (B2 and B3) are the always the concern of client/ developer and ranked high by the client in comparison to contractor and third-party experts. The Risk like technical design and negative survey data is normally responsibility of designer / consultants and subsequently they have ranked them higher than the contractor and client. Delayed site access is one the risk attributed to employer / client risk and their concern is depicted in the survey results. All stakeholder appears to agree on delay Decision Making risk (F-2) risk. Contractor has ranked Lack of Hydropower expertise in Pakistan quite high in compared to the Client and third party. Delayed dispute resolution has been ranked 1 by the Consultants being the neural participants and client side has ranked it No 10. Disputes originates in every project but the lack of ownership form stakeholders and improper contemporary records and delaying tactics results in delayed in dispute resolution and project suffer costs and delays. Delayed payment is one of the main concern of the contractors and ranked higher as compared to client as expectedly. Similar is the case with procedural delay where contractor normally suffer and ranked higher in the results. The risk like Chinese contractor factor and wrong costing brings all stake holder on one page. Wrong costing itself include the lack of expertise, lack of technical staff, not understanding of specification and project requirements / scope from all stake holders etc. Resettlement issue is ranked higher by the Third party that includes consultants but surprisingly the Client has not shown much concern on the issue.

Conclusion

Risk analysis can be undertaken by any party to a construction project, for that part of the project with which they are concerned. There is, however, only one party that can undertake a

comprehensive analysis of the risk, and instigate a reasoned allocation and mitigation strategy, and this is employer or project sponsor. Many contractors, particularly on large projects, undertake a risk assessment as part of tender process, but this will be limited to consideration of the risk within their own scope of work and contractual arraignments and results of the survey second it. Often this will be limited to an analysis of ‘what can go wrong?’ It will rarely consider any of the employer’s risk. The prime mover in this process has to be employer and encompassing all aspects including finance, environmental, construction, operational etc.

In developing countries, the people’s culture standard is low, causing various difficulties; the immigration and resettlement for land withdrawal and handover for the construction contractors are complex, Hydropower equipment for the projects must be imported from abroad with complex procedures, difficult shipment, and slow assembly, dependency on foreign Contractors, lenders involvement, high inflation rates, which affect the purchase of required materials, machines, and equipment, Natural conditions such as climate, hydrology, topography, and geological conditions lead to further complications, lack of expertise like tunnel / surge shaft construction, the sub-contractors construction capacity being poor, the domestic construction technology has low productivity, and is not up to standard, the infrastructure and traffic facilities for transport are poor; machine and equipment transportation encounter many difficulties leading to delays and cost overrun, However, timely risk management on Hydro Power project can minimize / eliminate the effect of aforementioned summarized situation(s) and at the same time can attract the investor and financing agencies and make the project SELLABLE.

References

- 1 International Finance Cooperation (2014) (IFC Of World Bank) “Guide To Investor And Developer Of Hydroelectric” (Page 105).
- 2 Project Management Institute, A Guide to the Project Management Body of Knowledge (PMBOK® Guide), 2014 5th edition, Project Management Institute, Newton Square.
- 3 Akintoye, A. S & MacLeod, M. J (1997), “Risk analysis and management in construction”, International Journal of Project Management, vol. 15, no. 1, pp.31-38.

- 4 ISO31000:2009. (Latest) Risk management - principles and guidelines on implementation. International Organization for Standardization.
- 5 Paul N., 2015 in book named “Managing Project risk”
- 6 Zhi, H (1995), “Risk management for overseas construction projects”, International Journal of Project Management, vol. 13, no. 4, pp. 231-237.
- 7 Cohen, M W & Palmer, G R 2004, 'Project risk identification and management', AACE International Transaction, pp. 13-15. Retrieved September 10, 2006, from ABI/INFORM Global.
- 8 Weddy, B.S & Hardjomuljad,S, 2011 “Project Risk Management in Hydropower Plant Projects: a Case Study from the State-owned Electricity Company of Indonesia.
- 9 MAI S.H, WANG J.Q & HONG V.U Published Online April 2016 “ Study on Risk evaluation and control of EPC hydropower construction project in Vietnam”
- 10 Kucukali,.S , 2011 “Risk assessment of river-type hydropower plants by using fuzzy logic approach” Cankaya University, Department of Civil Engineering, Balgat, 06530 Ankara, Turkey

Analysis of regime behavior of lower Gugera branch canal after rehabilitation/remodeling of the system.

Sajid Mehmood^{*1}, Ghulam Nabi¹

¹Project Management Unit, Punjab Irrigation Department, Lahore, Pakistan

^{*}ddfr.frau@gmail.com

Abstract: Pakistan has one of the world most effective irrigation systems which are comprised of canal network. These canals are mostly unlined and are designed mainly either on Lacey or Kennedy design methods. Irrigation canals essentially off-takes from a river and draw a fair share of silt moving in the river. The sediment is carried either in suspension or along the bed of the canal. The basic criteria of design of irrigation channels are to aim at a velocity which will keep the sediment in suspension without causing silting or scouring, such a velocity is known as non-silting and non-scouring velocity. This is known as minimum stream power concept. Basically, there are two concepts for alluvial channel design. In first concept, the channel design is based on the concept of non-silting and non-scouring approach. Such a channel is known as regime channel. The most common design methods based on this concept are of Kennedy method, Lacey regime and Simon & Albertson regime theory. In the second concept, the design of irrigation channel is based on the properties of boundary material in which the channel is flowing. The most important design method based on this concept is Tractive Force Method.

Keywords: Irrigation, canals, Lacey theory

Introduction

The Lower Gugera Branch Canal Irrigation system lies between the rivers Ravi & Chenab i.e. Rachna Doab. It is bounded by Qadirabad-Balloki (Q.B.) Link Canal on the eastern side while it terminates beyond Trimmun-Sidhnai (T.S.) Link Canal on the western side. The Lower Gugera Branch Canal off-takes from the tail of Upper Gugera Branch canal at Head Buchiana near Jaranwala City as shown in fig 1. Lower Gugera Branch Canal off takes from the Right side and Burala Branch Canal from the front. An Escape channel is also off taking from the left side. The system has been maintained over the years with very limited resources, resulting in backlog of various repair / remodeling works. A large part of the system has already lived over a century of its life and has undergone considerable deterioration. Punjab Irrigation and Drainage Authority (PIDA) decided to rehabilitate the system and remodel/reconstruct various worn out structures. The main object for rehabilitation of the system was to improve conveyance efficiency, reliability and durability of the system as per designed discharges by rehabilitating/remodeling the entire irrigation system, so as to provide irrigation water to the beneficiaries in a more sustainable and equitable manner. The problem of sediment management in off-taking channels became serious after the rehabilitation of the system. The behavior of both the canals in terms of sediment entry is

significantly different from each other. The Lower Gugera Branch Canal had been generally receiving less sediment from the canal head compared to its sediment transporting capacity and is showing scouring trends. However, in contrast, the Burala Branch Canal had been receiving more sediment compared with its transporting capacity and silted up even after five years of its operation. Due to uneven distribution of sediment load in the system the bed of Lower Gugera Branch has scoured up to 2ft in different reaches. Water surface line has been depressed and off taking channel as well as the outlets are suffering badly. The bed of Burala Branch Canal has been deposited and the capacity of the channel has been reduced.

The objectives of study were re-evaluation of the design of the canal system, analysis of the sediment budget of the system and evaluation of sediment carrying capacity of design channel by using different sediment transport functions.

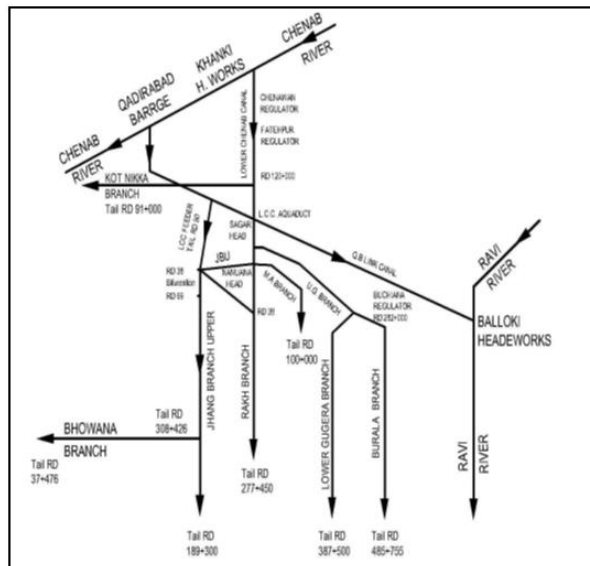


Fig. 1 Line Diagram of Study Area

Understanding of the sediment transport phenomena is inadequate and this makes it very difficult indeed to predict (Sanmuganathan, 1990). Impact of structural intervention on sediment management of large canals is explicated by Shakir et al. (2007) in a case study of Marala Barrage. He concluded that some of the past interventions have a positive effect on silt control entry in the off-taking canals. The analysis of data regarding sediment entry at the head of the canals indicate that the raising of crest of MR Link in the year 2000–2001 has improved the sediment intake in this canal to some extent, but its effect on the UCC is almost negligible. The data regarding sediment entry at the head of the UCC which had a scouring tendency does not show any significant effect of this intervention as was perceived at the implementation stage. However, it is worth mentioning that analysis of data related to cross-sections and L-sections of the head reaches of these canals show a different trend, which makes it difficult to assess the long term and sustainable effect of this intervention on both of the canals. A critical review of data collection process and effective monitoring of the system is compulsory for meaningful analysis and future course of action if the present tendency seems to be changing, the possibility of which does exist.

The analysis was focused on transient bed profiles which are determined, under steady flow conditions, by a decrease of the upstream sediment transport rate. Ankum (1995) defined flow structures as the structures required to keep the irrigation system in the desired state. The purpose of flow control structures is to distribute and to divert the flows to the end users w.r.t the

delivery schedules. The flow control structures are designed at bifurcations for water level regulation, discharge regulation and discharge measurement. Habib (1998) used the SIC model for the hydraulic simulation of CRBC for to predict its design and operation.

Methodology

Three reaches of Lower Gugera Branch Canal have been taken for research (1RD = 1000ft = 304.8m).

1. Reach RD 0+000 to 16+500
2. Reach RD 16+500 to 27+000
3. Reach RD 27+000 to 65+000

The design parameters and actual longitudinal section were collected from respective irrigation divisions. The existing canal cross-sections were also observed at site and the cross-section were also obtained from the consultants of rehabilitation project of Lower Gugera Branch Canal for the data prior to rehabilitation to ascertain the changes in the regime. For suspended sediment/ bed sediment observation the sediment sampler DH-48 sediment sampler and DH-24 sediment sampler has been used for determination of existing sediment load in the flowingwater at the specified sites. Sediment samples were analyzed by International Sediment Research Institute of Pakistan (ISRIP) Water and Power Development Authority (WAPDA) laboratory. The results of samples are used in application of different design procedures and sediment analysis adopted for comparison of different design methods used for the alluvial canal design. The discharge/sediment data of LCC (parent channel of Lower Gugera Branch canal system) at head Khanki has been collected from the irrigation department. Four types of data were collected for this study is geometric data, hydraulic data, sediment data and structural drawing/data.

Daily recorded water discharges released from Khanki Barrage to feed the LCC were used from 2000 to 2013 for hydraulic study. Sediment data was analyzed to construct a sediment rating curve from the suspended sediment inflowing concentration at the head of the LCC canal. A sediment rating curve meant a relationship between sediment load (including both suspended and bed loads) and water discharges. Four design methods i.e. Kennedy, Lacey, Simon & Albertson and Tractive Force was applied to all these selected reaches and calculated canal parameters were plotted against the existing observed cross-sections parameters.

Brief description of these methods is given below,

The Manning Formula: The most frequently used formula for an open channel flow is the

$$V = \frac{1.49}{n} R^{2/3} S^{1/2}$$

Manning formula. The formula is; $V = \frac{1}{n} R^{2/3} S^{1/2}$ or; $Q = \frac{1}{n} A R^{2/3} S^{1/2}$

Kennedy theory:

Kennedy Theory was utilized for a protracted period for the design of canal systems. In Indo-Pak subcontinent some of the initial chief canal systems were based on this theory. $V_c = D^{0.64}$, $V_c = CD^b$. (ft/sec), $V = m * 0.84 D^{0.64}$, where D = depth of channel (ft), Where $m = \frac{V}{V_c}$ = critical velocity

ratio (CVR)

Lacey's theory:

According to Lacey the silt factor 'f' in the regime formula depends upon: Average size of boundary material in the channel and its density;

$$f = 1.76 \sqrt{D_{50}}$$

where 'D50' is the mean particle diameter of silt in mm.

Velocity of flowing water and the hydraulic

$$f = \frac{2.50V^3}{R}$$

mean radius of the channel:
Where V=mean velocity in m/s.

Simons and albertson regime method:

The following equations were fitted to the various straight line graphs plotted in between various parameters:

$$\frac{C^2}{g} = \frac{V^2}{2DS} = K_4 \left(\frac{V_b}{V} \right)^{0.37}$$

Tractive force method

In 1950's investigators established the tractive force technique of stable canal design and that is the solely firmly rational method in practice today. According to tractive force technique when all forces acting on the particle are in equilibrium, there will be no scouring and no silting and the canal will remain stable. Unit

$$\text{tractive force or shear stress} = \tau_0 = \frac{\gamma \cdot A \cdot L \cdot S_0}{P \cdot L} = \gamma \cdot R \cdot S_0$$

Where, R= hydraulic radius. In very wide

channels, $R \approx D$, where 'D' is the normal flow depth. Hence, $\tau_0 = \gamma \cdot D \cdot S_0$,

$$\tau_s = \frac{W_s}{a} \cos \theta \tan \phi \sqrt{1 - \frac{\tan^2 \theta}{\tan^2 \phi}}$$

$$K = \frac{\tau_s}{\tau_l} = \cos \sqrt{1 - \frac{\tan^2 \theta}{\tan^2 \phi}}$$

which may be

$$\text{simplified as, } K = \sqrt{1 - \frac{\sin^2 \theta}{\sin^2 \phi}}$$

$$(\tau_0)_{\max} = 1.5 \gamma R S$$

There are many universal accepted techniques to determine the sediment load entering at the head regulator of the canal. Many techniques have been proposed to access the sediment load entry under a large range of flow conditions and sediment characteristics. In this study sediment transport capacity was calculated by using (Ackers & White (1973), Engelund & Hansen (1967), Van Rijn (1984), Yang (1973), and Brownlie (1981)) formulae. The calculated sediment carrying capacity was compared with sediment load entering in the canal.

i. Ackers and White Method (1973):

The Ackers and White method described the sediment transport in terms of three dimensionless parameters; G_{gr} (transport parameter), D* (grain size sediment parameters), F_{gr} (Mobility parameter).

$$D^* = \left[\frac{(S-1)g}{\rho_2} \right]^{1/3} d_{35}$$

$$F_{gr} = \frac{u_*^n}{\sqrt{g d_{35} (S-1)}} \left[\frac{v}{\sqrt{32 \log \left(\frac{10h}{d_{35}} \right)}} \right]^{1-n}$$

$$G_{gr} = C \left[\frac{F_{gr}}{A} - 1 \right]^m$$

The Ackers and White function to determine the total sediment transport read as:

$$q_s = G_{gr} S d_{35} \left(\frac{v}{u_*} \right)^n$$

Engelund and Hansen Method (1967):

This method is based on an energy approach; they established a relationship between transport and mobility parameters. The Engelund and Hansen function for the total sediment transport is calculated by: Dimensionless transport parameter

$$\phi = \frac{q_s}{\sqrt{(S-1)gd_{50}^3}}$$

$$\text{Dimensionless mobility, } \theta = \frac{U_*^2}{(S-1)gd_{50}}$$

The relationship between those parameters is expressed by:

$$\phi = \frac{0.1\theta^{2.5} C^2}{2g}$$

The total sediment transport is expressed by:

$$q_s = \frac{0.05 V^2}{(S-1)^2 g^{0.5} d_{50} C^3}$$

Yang method (1973):

This method is based on hypothesis that the sediment transport in a flow should be related to the rate of energy dissipation of the flow. The total sediment transport is also expressed in ppm by mass as a function of the unit stream power by:

$$\log c_{t=I+J} \log \left(\frac{V S - V_{cr} S}{w} \right)$$

With the Yang's coefficients represented by:

$$I = 5.435 - 0.286 \log \left(\frac{W_s d_{50}}{\vartheta} \right) - 0.457 \log \left(\frac{U_*}{W_s} \right)$$

And

$$J = 1.799 - 0.409 \log \left(\frac{W_s d_{50}}{\vartheta} \right) - 0.314 \log \left(\frac{U_*}{W_s} \right)$$

The critical velocity for initiation of motion:

$$V_{cr} = 2.05 w_s,$$

The total load transport is calculated by:

$$q_s = 0.001 C_t V h$$

ii. Van Rijn Method (1984a and 1984b):

The total sediment transport by the Van Rijn method is computed by the summation of the bed and suspended load transport

$$q_s = q_b + q_{sus}$$

The bed load transport rate is calculated as:

$$q_b = u_{b\delta} b c_b \text{ Particle, } U_b = 1.5 T 0.6 [(S-1) g d_{50}]^{0.5}$$

Saltation height, $\delta b = 0.3 D 0.7, T 0.5 d_{50}$

Bed load concentration, $C_b = 0.18 C 0 T / D^*$,

Maximum Volumetric concentration $C 0 = 0.65$

With, $D^* = d_{35}$

$$q_b = 0.053 (s-1)^{0.5} g^{0.5} d_{50}^{1.5} D_*^{-0.3} T^{2.1} d_s = [1+0.011] (\sigma_s-1) (T-25) d_{50}$$

$$\beta = 1 + 2 \left(\frac{W_s}{U_*} \right)^2 (4.34)$$

$$\psi = 2.5 + \left(\frac{W_s}{U_*} \right)^{0.8} \left(\frac{C_a}{C_o} \right)^{0.4}$$

Brownlie Method (1981):

Brownlie (1981) defined a method to compute the sediment transport rate, the transport rate (in ppm by weight) is calculated by:

$$q_s = 727.6 c_f (F_g - F_{gr})^{1.978} S^{0.6601} \left(\frac{R}{d_{50}} \right)^{-0.3301}$$

, Cf: Coefficient for the transport rate (Cf = 1 for laboratory conditions and Cf = 1.268 for field conditions).



Fig. 1 Site visit

Results and Discussions

Lower Gugera Branch was designed on Lacey method having a discharge capacity of 2,244 / 2,643 cusecs for Rabi and Kharif respectively

and length of the channel is 387+566 ft off-taking from tail of Upper Gugera Branch. First three reaches RD 0+000 to RD 66+000 were selected for observing cross sections. The existing cross sections were observed at successive 5+000 RDs and the comparison of design versus existing bed profiles as shown in fig 2.

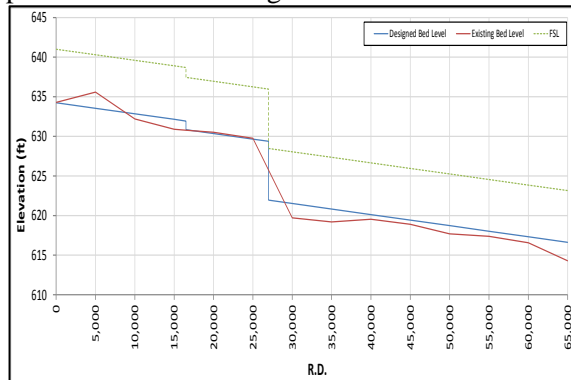


Fig. 2 Comparison of designed and existing bed profile of Lower Gugera Branch Canal

LCC system is the oldest system of Punjab and off-taking from left side of head Khanki having a design discharge of 7,000 cusecs. The daily discharge/sediment data series from the laboratory of head Khanki were collected for the last fourteen years (2000 – 2013). The same data series were analyzed. Yearly and monthly variations in the sediment concentrations entering LCC system with discharge are presented in fig 3 and 4.

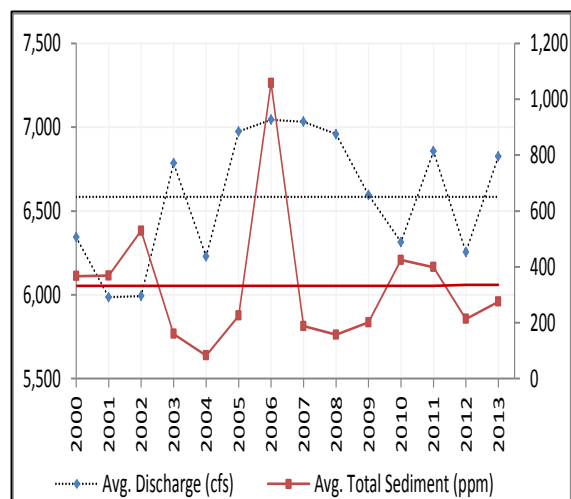


Fig. 3 Annual variations in sediment concentrations versus discharge

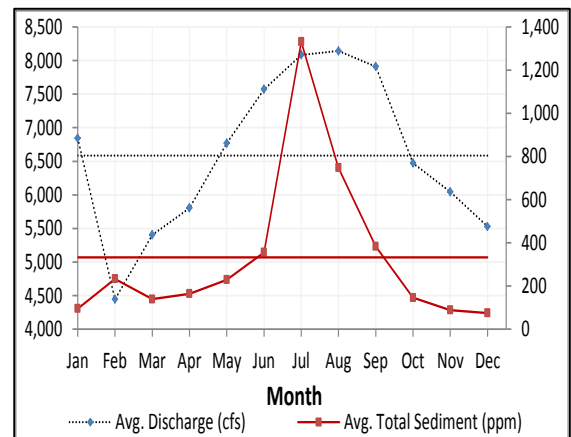


Fig. 4 Long-term monthly variations in sediment concentrations with discharge

During the analysis of collected discharge/sediment data series from 2000-2013, it was found that variation in the sediment load entering LCC system is mainly due to the inflow at head Khanki rather than discharge off-taking in LCC system. The graphical representations of aforesaid phenomena are shown in fig 5 and 6.

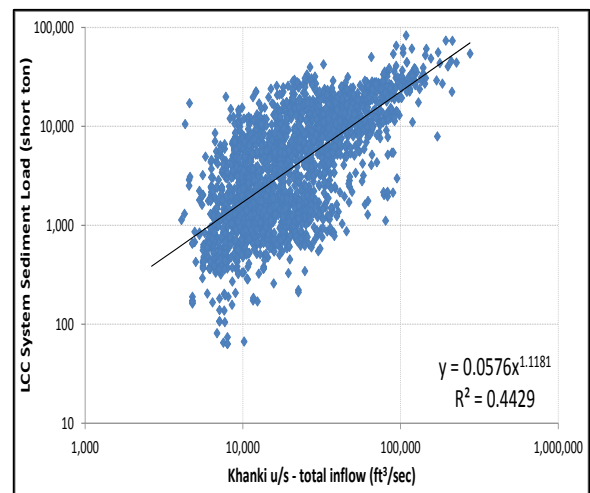


Fig. 5 Suspended sediment rating curve of LCC System versus head Khanki inflows

The existing design parameters of Lower Gugera Branch canal for the selected three reaches are presented below

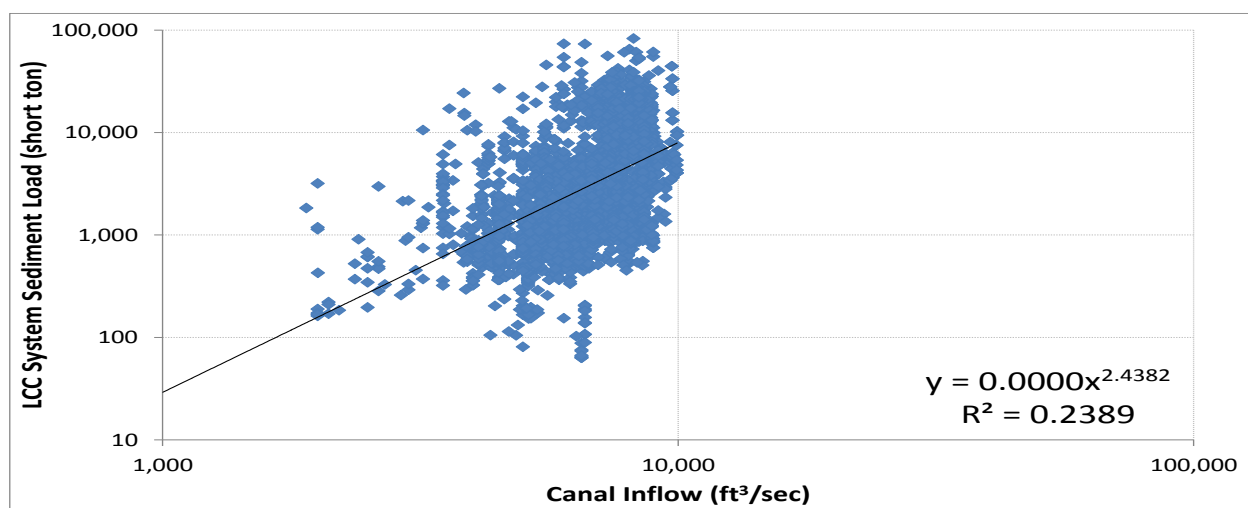


Fig. 6 Suspended sediment rating curve of LCC System versus LCC inflow

Table 1 Existing design data of selected reaches of Lower Gugera Branch Canal

Description	Unit	Reach		
		Reach 1	Reach 2	Reach 3
Start RD	(ft)	0	16+500	27+000
End RD	(ft)	16+500	27+000	65+000
Reach Length	(ft)	16,500	10,500	38,000
Discharge Rabi	(ft ³ /sec)	2,244	2,063	1,992
Discharge Kharif	(ft ³ /sec)	2,643	2,430	2,347
Water Surface Slope	(1/1000)	0.14	0.14	0.14
Manning's n	-	0.021	0.021	0.021
Side Slope (H)	-	0.5	0.5	0.5
Side Slope (V)	-	1	1	1
FSD Rabi	(ft)	6.76	6.6	6.53
FSD Kharif	(ft)	7.47	7.29	7.22
Bed Width	(ft)	115	110	108

Table 2 Re-evaluation of existing design by Tractive Force method

Description	Unit	Reach 1			Reach 2			Reach 3		
		Existing Design	Lacey	Difference	Existing Design	Lacey	Difference	Existing Design	Lacey	Difference
Discharge (Q)	ft ³ /sec	2,643	2,643	0%	2,430	2,430	0%	2,347	2,347	0%
Bed Slope (S _o)	1 in 14	0.00014	0.00014	0%	0.00014	0.00014	0%	0.00014	0.00014	0%
Manning's n	-	0.021	0.021	0%	0.021	0.021	0%	0.021	0.021	0%
Horizontal Slope	-	0.5	1.5	200%	0.5	1.5	200%	0.5	1.5	200%
Vertical Slope	-	1.0	1.0	0%	1.0	1.0	0%	1.0	1.0	0%
Flow Depth (D)	ft	7.5	6.6	-12%	7.3	6.6	-10%	7.2	6.6	-9%

Bed Width (B)	ft	115.0	135.9	18%	110.0	124.8	13%	108.0	120.5	12%
---------------	----	-------	-------	-----	-------	-------	-----	-------	-------	-----

Table 3 Re-evaluation of existing design by Lacey theory

Description	Units	Reach 1			Reach 2			Reach 3		
		Existing Design	Lacey	Difference	Existing Design	Lacey	Difference	Existing Design	Lacey	Difference
Discharge (Q)	ft ³ /sec	2,643	2,643	0%	2,430	2,430	0%	2,347	2,347	0%
Bed Slope (S _o)	1 in 1	0.00014	0.00009	-33%	0.00014	0.00009	-32%	0.00014	0.00010	-32%
Manning's n	-	0.021	0.021	0%	0.021	0.021	0%	0.021	0.021	0%
Horizontal Slope	-	0.5	0.5	0%	0.5	0.5	0%	0.5	0.5	0%
Vertical Slope	-	1.0	1.0	0%	1.0	1.0	0%	1.0	1.0	0%
Flow Depth (D)	ft	7.5	7.9	6%	7.3	7.7	6%	7.2	7.6	6%
Bed Width (B)	ft	115.0	119.5	4%	110.0	114.3	4%	108.0	112.3	4%

Table 4 Re-evaluation of existing design by Simon & Albertson method

Description	Units	Reach 1			Reach 2			Reach 3		
		Existing Design	Simon & Albertson	Difference	Existing Design	Simon & Albertson	Difference	Existing Design	Simon & Albertson	Existing Design
Discharge (Q)	ft ³ /sec	2,643	2,643	0%	2,430	2,430	0%	2,347	2,347	Discharge (Q)
Bed Slope (S _o)	1 in 1	0.00014	0.00006	-56%	0.00014	0.00006	-56%	0.00014	0.00006	Bed Slope (S _o)
Manning's n	-	0.021	0.021	0%	0.021	0.021	0%	0.021	0.021	Manning's n
Horizontal Slope	-	0.5	1.5	200%	0.5	1.5	200%	0.5	1.5	Horizontal Slope
Vertical Slope	-	1.0	1.0	0%	1.0	1.0	0%	1.0	1.0	Vertical Slope
Flow Depth (D)	ft	7.5	9.0	20%	7.3	8.8	20%	7.2	8.7	Flow Depth (D)
Bed Width (B)	ft	115.0	110.6	-4%	110.0	106.0	-4%	108.0	104.1	Bed Width (B)

Table 5 Re-evaluation of existing design by Kennedy theory

Description	Units	Reach 1			Reach 2			Reach 3		
		Existing Design	Simon & Albertson	Difference	Existing Design	Simon & Albertson	Difference	Existing Design	Simon & Albertson	Existing Design
Discharge (Q)	ft ³ /sec	2,643	2,643	0%	2,430	2,430	0%	2,347	2,347	0%
Bed Slope (S _o)	1 in 1	0.00014	0.00014	0%	0.00014	0.00014	0%	0.00014	0.00014	0%

Manning's n	-	0.021	0.021	0%	0.021	0.021	0%	0.021	0.021	0%
Horizontal Slope	-	0.5	0.5	0%	0.5	0.5	0%	0.5	0.5	0%
Vertical Slope	-	1.0	1.0	0%	1.0	1.0	0%	1.0	1.0	0%
Flow Depth (D)	ft	7.5	7.5	0%	7.3	7.3	0%	7.2	7.2	0%
Bed Width (B)	ft	115.0	112.6	-2%	110.0	107.6	-2%	108.0	102.3	-5%

Re-evaluation of existing design parameters of Lower Gugera Branch canal using Kennedy, Lacey, Simon & Albertson and Tractive force methods is presented as follows

To evaluate the sediment load, the sediment data was observed on the following channels at head Buchiana with the coordination of ISRIP (WAPDA), Upper Gugera Branch canal (tail), Burala Branch canal (RD 1+200) and Lower Gugera Branch canal (RD 0+900). Suspended sediment sampler D-49 was used to observe the suspended sediment load. It was found that

average suspended sediment concentrations in Upper Gugera Branch (the parent channel) is 477 ppm, whereas in the off-taking channels of Upper Gugera i.e. Burala Branch and Lower Gugera Branch, are 456 ppm and 400 ppm respectively. The bed material samples were also collected by using BM-54 bed sampler in all three aforesaid channels. Allowable sediment transport capacity of Lower Gugera Branch canal was estimated using different sediment transport functions and the results are presented as follows in table 6.

Table 6 Sediment transport capacity of Lower Gugera Branch Canal estimated by different sediment transport function

Lower Gugera Reach	Design Discharge	Measured Sediment	Allowable Sediment transport capacity (ppm)			
	(ft ³ /sec)	(ppm)	Ackers & White		(ft ³ /sec)	(ppm)
1	2,643	393	1,065	1	2,643	393
2	2,430	406	1,060	2	2,430	406
3	2,347	401	1,054	3	2,347	401

The analysis of existing cross sections of the canal under consideration reaches shows that bed is scoured by more than 1 to 2 ft in selected reaches and the scouring trend increases from head to tail reach. The bed has eroded up to 2 ft at different sites and severe bank erosion is also in progress at the downstream of different fall structures. The analysis of sediment data (2000-2013) at head Khanki shows that maximum sediment concentrations are in the months of July and August which are about 1,350 ppm and 750 ppm on average respectively i.e. in Monsoon. Whereas, the same data shows that there are less sediment concentrations in December which are about 75 ppm. It has been found that relationship between the LCC system's suspended sediment load does not show a good trend with the variation in its discharge. However, when it is plotted against head Khanki's inflow, the relationship shows some good trend which is also

logical because the variation in the approaching sediment load is mainly due to the Chenab river inflow rather than off-taking discharge of LCC system.

The existing canal design has been re-evaluated using different design methods of alluvial channel and the results differ with the existing design in terms of side slope, bed slope, water depth and bed width etc. However, it is important to mention that difference in water depth and bed width is not much significant. The results of suspended/bed material sampling and sediment transport theories show that suspended silt load in LCC System is less than the allowable limits. Furthermore, the distribution of suspended silt at head Buchiana is not equitable which is due to the difference of crest level of the head regulators. The results of different sediment transport functions predict that the sediment concentration carrying by the system is also less

than the permissible limits calculated by these function.

Conclusions

As most of the canal systems in the Punjab are either designed by Lacey or Kennedy, are the modified forms of these method. The existing canal reaches of the selected channel show that bed of channel is scoured up to 2 ft and the sides are also eroded at the downstream of fall structures. The scouring trend is significantly increasing towards the tail and water line has been depressed. Resultantly the off-taking channels and the outlets are suffering badly. The results of suspended sediment samples collected from the selected channels shows that sediment concentration is less than the permissible limits in the LCC System so the System is sediment hungry. Furthermore, the sediment diverting into Lower Gugera Brach canal at head Buchiana is also less which is due to the difference in the crest levels of the off-taking channels. The analysis of bed material samples are mostly composed of bed load depiction in the canal section shows that bed material is composed of coarser silt and fine silt particles in all the reaches. The sediment data at head Khanki clearly reveals that major part of the sediment load entering into the canal consists of finer particles and total sediment concentrations are less than the allowable limits. To balance the

silt load and silt charge water is continuously eroding the canal bed and sides. The results of different sediment predictors also predict that the sediment concentration in the system is not up to the design limits, hence the bed is eroding.

The sediment distribution in the off taking channels is not equitable due to difference in the crest levels, so more silt vanes should be constructed at head of Lower Gugera Branch to balance the load in the off taking channels. The sediment data of Head Khanki reveals that sediment entry into the Lower Chenab Canal is also not up to permissible limits so the functioning of silt excluder and crest of the said channel should be analyzed. The irrigation channel should be designed by considering the sediment concentration in the system and silt carrying capacity should be checked by using the different sediment transport formulae. Due to shortage of water channels runs on rotational regulation pattern which affect the regime conditions and morphology of these canals. Therefore, at any cost channel could not run on less supply. Periodic sediment measurement should be done throughout the year until the canal is in regime. Canal design/operational software should be introduced to facilitate the decision-making authorities.

Impact Analysis of Floods on Fixation of Road Profile Grade Level for Roads in Hilly Terrain

Zafar Iqbal¹, Kaleem Sarwar², Sajid Mahmood³, Muhammad Afzal⁴

¹Research Associate, Centre of Excellence in Water Resources Engineering, University of Engineering and Technology, Lahore, Pakistan

²Assistant Professor, Centre of Excellence in Water Resources Engineering, University of Engineering and Technology, Lahore, Pakistan

³Assistant Professor, Centre of Excellence in Water Resources Engineering, University of Engineering and Technology, Lahore, Pakistan.

⁴Senior Engineer, Water Resources Division, National Engineering Services (Pvt.) Limited, Lahore, Pakistan.

*zafar.24@live.com

Abstract: Flood hazards are the significant threat to the human life as well as their property. Recent example of such destruction is 2010 flash flood. In this study hydrodynamic modeling was performed on Swat River from Kalam to Madyan. Floods for different return periods at Kalam were computed by flood frequency analysis of flow data gauged at Kalam. Floods of lateral tributaries of Swat River downstream of Kalam were computed using HEC-HMS rainfall runoff model with the help of available rainfall data at Kalam and catchment characteristics of the study area. Steady flow simulations were carried out in HEC-RAS and water surface profiles were computed for floods of different return periods. Model geometry was extracted from stereo pairs based Digital Elevation Model (DEM). The computed water surface profiles were processed in HEC-GeoRAS and inundation extents were marked. Finally, the profile of road section was fixed on the basis of water levels computed from hydrodynamic model and inundation extents for 100-year return period flood. The research will be useful for planning and design of bridges, culverts, causeways, river training and flood protection works, channelization of streams and hill torrents to protect the cities and town against floods and road infrastructure especially in hilly areas.

Keywords: Kalam, Madyan, Swat River, Water Surface Profile, Inundation Extents, Profile Grade

Introduction

National Highway N-95 road network starts from Chakdara intersects Mingora, Manglour, Khwazakhela, Madyan, Bahrain and ends at Kalam. This is an important road and connects Islamabad, the capital city to Kalam in Swat Valley. Swat River starts at Kalam from the confluence of Ushu and Utror Rivers. Being adjacent to Swat River this road faced severe flooding in 2010 especially beyond Madyan towards Kalam. Fig. 1 shows the layout plan of the National Highway N-95 [1].

The road section from Madyan to Kalam is approximately 44 Km where Swat River flows through V shape valley lying on the right side of the road whereas; on the left side are the steep hills. This road section was completely washed away by 2010 flood. Every possible way of communication, either transportation or telecommunication, with Kalam was terminated. Bridges and culverts encountered on this road

section were completely destroyed by the flood [1].

The road profile grade level (PGL) of previously built National Highway N-95 was badly affected by the hydrological conditions which needs attention of the authorities to safeguard the important part of the communication.

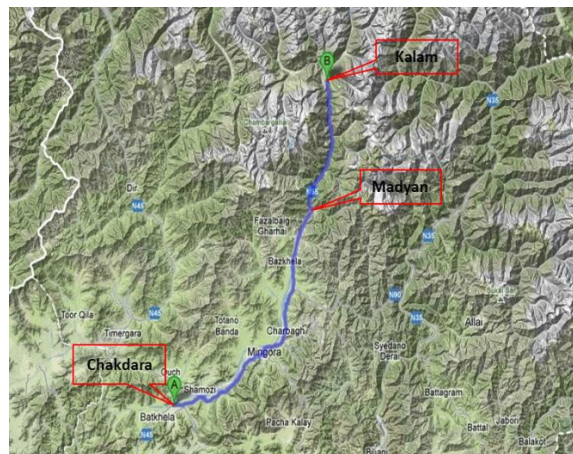


Fig. 1 Layout Plan of National Highway N-95

For the safe passage of flood flows it is pertinent to prepare hydrodynamic model for the study reach which will assist in determining the inundation extents against different return period floods. Thereby i.e. profile grade level (PGL) based on the hydrodynamic model with the provision of certain free board will be designed. Monsoon of the year 2010 brought the worst flooding in past 80 years in the region. Heavy monsoon rainfalls in Khyber Pakhtunkhwa, lower Punjab, Sindh, and Baluchistan regions made the rivers to overflow which devastated the areas from Gilgit - Baltistan to Kotri, the last and biggest barrage on River Indus in Sindh. During flood season of 2010, flows in western rivers were very high and some of the recorded discharge levels were very high than those observed during the past high floods of 1956, 1973, 1976, 1988 and 1992. Therefore, it is unavoidable to redesign / re-section the flood protective bunds according to new water levels obtained during 2010 Flood [2].

HEC-GeoHMS and HEC-HMS rainfall runoff model was applied for Kaha Hill Torrent Watershed Management of D.G.Khan District. HEC-HMS model was used for estimating realistic volume of runoff as a result of rainfall for optimum utilization of water resources and better watershed management [3].

HEC-RAS model was used to identify the flood prone areas in Chiniot District along Chenab River and concluded that HEC-RAS can be efficiently used to simulate the floods. It was suggested that Remote Sensing techniques along with GIS should be involved to get more precise results [4].

Flooding in Nullah Lai in Rawalpindi was studied using GIS and HEC-RAS for estimation of flood extents. GIS model was used to find out the inundation extents and to delineate the variation in topography of the area. It was concluded that HEC-RAS model results are very close to the JICA surveyed results of the inundated area [5].

HEC-RAS model along with GIS and Remote Sensing environment was used for the study of flood in Ping River basin in Thailand. Water levels were generated using HEC-RAS for determination of the inundation extents. HEC-RAS results were verified by remote sensing images. Finally, the model results were used for preparation of hazards maps [6].

A reach of Neka River of Iran was studied for floodplain analysis and delineation of flood extents and water depths using HEC-RAS along

with GIS. Water surface levels were simulated using HEC-RAS. HEC-GeoRAS was used for generation of floodplain maps. It was concluded that HEC-RAS model along with GIS play an important role in determining the flood extent and flood zone mapping [7].

Materials and methods

Hydrological Modeling

Flood frequency analysis at Kalam was carried out using Gumbel Extreme Value Type-I (EVI) and Log Person Type-III. Gumbel Extreme Value Type-I (EVI) is the best fit for the study area as per analytical applications.

Hourly rainfall data was analyzed and intensity duration frequency curves were developed for different durations (i.e. 1hour, 2hour, 3hour, 6hour, 12hour and 24hour) at Kalam rain gauge station using the point rainfall data for each year for representing the rainfall data for decision support of hydrodynamic modeling as shown in Fig. 2.

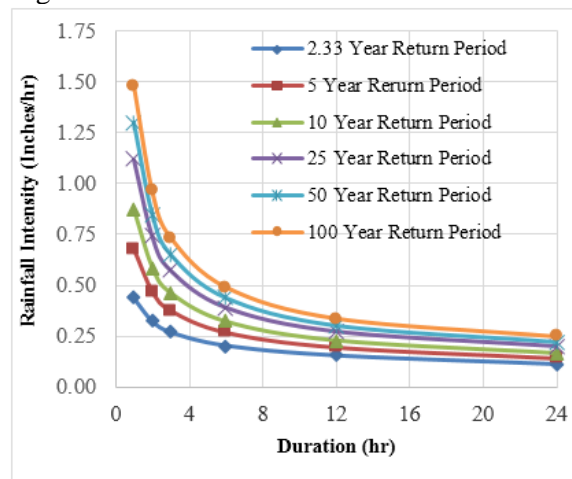


Fig. 2 IDF Curves for Kalam Derived from Recorded Data

Rainfall Runoff Model for Tributaries of Swat River

The Hydrologic Modeling System (HEC-HMS) software was used to simulate the precipitation-runoff processes of Swat River catchment. For this purpose Swat River was divided into thirty sub-catchments. The time of concentration and lag time for each sub catchment was computed separately. The data for computation of time of concentration and delineation of sub catchment areas were extracted by using Shuttle Radar Topographic Mission (SRTM) 90 m Digital Elevation Model (DEM).

Floods for 25, 50 and 100 years for Ushu and Utror Rivers were computed from flood frequency analysis at Kalam using Gumbel Extreme Value Type-I. Floods for lateral

tributaries of Swat for the study reach were computed by HEC-HMS by using respective frequency storms. Only magnitude of rainfall is required, when flood is estimated with SCS distributions in HEC-HMS.

Calibration and Validation of Rainfall Runoff Model

The contribution of rainfall (of about 20%) is very low as compared to snow melt (of about 80%) at Kalam stream gauge station. The results of flood frequency analysis at Kalam were used in HEC-HMS as a constant discharge. HEC-HMS model was actually used to calculate the flow of lateral tributaries of Swat River downstream of Kalam to Madyan (study reach). So, HEC-HMS model was calibrated with Chakdara stream gauging station. The peak discharge on 29 June 2007 was 30,894 cusecs at Chakdara. The curve no 51 was taken at AMC-I condition and adopted for calibration. The specified hyetograph method of metrological model was used. Hourly rainfall data of 28 and 29 June 2007 in all rain gauges selected for calibration was incorporated in the model. The rainfall was assigned to each sub basin by making criteria, which rainfall station is nearest to the sub basin. The peak discharge of 11,270 cusecs at Kalam was taken as constant base flow for the month of June.

The rainfall runoff model was validated with Chakdara stream gauge station also. The peak discharge on 10 October 1987 was 35,600 cusecs at Chakdara. The hourly rainfall data of 9 and 10 October 1987 was incorporated in the model in the same way as discussed above for model calibration. The peak flow of 2150 cusecs was adopted as a constant base flow for the month of October.

Hydrodynamic Modeling

The hydraulic modeling of Swat River was carried out by making use of HEC-RAS which requires various inputs to calculate water surface profiles. These inputs are layout of the river and its tributaries, river cross sections, Manning's roughness for main stream and tributaries and boundary conditions for the selected river reach. Model geometry was generated by making use of HEC-GeoRAS, an extension of Arc GIS. Steady flow data was provided to HEC-RAS and simulations were carried out.

Identification of Study Area and Collection of Stereo Pairs Image

Swat River flows in gorge throughout the length of study area. Area of interest (study reach of Swat River) was marked on Google Earth and Satellite image (0.5m resolution and 5 Km wide strip) was collected from NESPAK. The image was processed using Arc GIS for preparation of DEM. The prepared DEM was calibrated with Ground Control Points (GCPs) collected from the study area. Calibrated DEM on 2 m resolution was used for the extraction of model geometry with the help of HEC-GeoRAS.

Identification of River Reach and Its Tributaries for the Study Reach

As calibrated DEM on 2 m resolution was a limited strip of 5 Km width normal to the Swat River. So, for the identification of river reach and its tributaries falling in area of interest a polygon was marked on Google Earth and imported in Arc GIS along with STRM data as shown in Fig. 3. SRTM data was extracted within the limits of polygon using mask command in Arc GIS. Coordinates of study area was assigned to SRTM data.

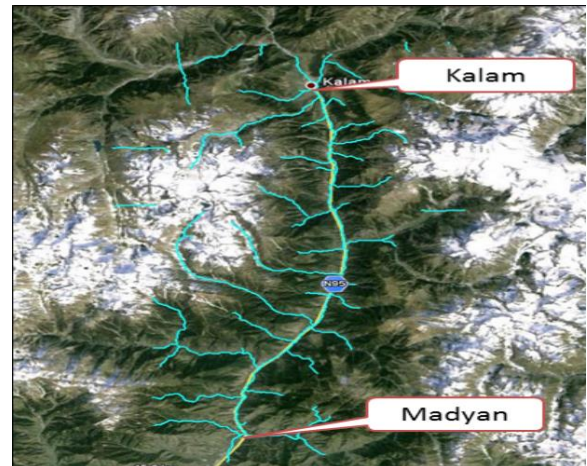


Fig. 3 Identified River Reach and its Tributaries for the Study Area

Extraction of Model Geometry

HEC-GeoRAS was used for the extraction of model geometry in Arc GIS. Different layers were created, exported the cross-sectional data in GIS format and finally imported in HEC-RAS for further processing.

Manning's Roughness

The Manning's roughness for River Swat, its over bank / flood plain was assessed from satellite image and field visit of the study area and adopted as 0.045 for main stream and 0.050 for left and right over banks respectively.

Boundary Conditions for Hydrodynamic Model

U/s boundary conditions were provided as constant discharges (600, 650 & 700 cumecs) for 25, 50 & 100 years return periods respectively at Kalam. Flood peak of 2010 was not recordable as steam gauge at Kalam was washed away. So, flood peak at Kalam was computed from rainfall using rainfall runoff model. This flood peak was used as upstream boundary in HEC-RAS for computation of 2010 flood. The computation of backwater requires known hydraulic conditions at most downstream section of main stream. The representative longitudinal slope in main stream was considered as downstream boundary condition for computation of normal depth for steady flow simulations.

Model Simulation

Steady flow Simulations were carried out using 25, 50 and 100 years peak floods and 2010 flood peak respectively and corresponding water surface profiles were plotted. Flow change locations in model were added for lateral contribution from tributaries. Water levels, depth of flow, average velocity and top width for 25, 50 and 100 year return period flood and 2010 flood at each cross section of Swat River for the study reach were calculated.

Flood Inundation Mapping

Based on simulation results, the estimated 100 year flood levels were used to create inundation map. The layout and top elevations of existing road was compared with simulated flood levels and inundation extents to check its safety against 100 year flood event. Finally the road profile grade level (PGL) was suggested with the provision of certain free board.

Results and discussions

The aim of the analysis is to fix the safe profile of road for the study reach depending upon extents of inundations and water levels.

Flood Frequency Analysis

Flood frequency analysis was carried out at Kalam using Gumbel Extreme Value Type-I (EVI) and Log Pearson Type-III with instantaneous maximum discharge data of each year. The computed discharge values for both the distributions for different return periods are shown in Table-I.

Table 1 Results of Flood Frequency Analysis for Selected Distributions

Return Period (Years)	Calculated Flood Magnitude (Cusecs)	
	Gumbel Extreme Value Type-I	Log-Pearson Type-III
2.33	14,541	15,016
5	16,879	17,113
10	18,782	18,495
25	21,188	19,942
50	22,972	20,853
100	24,744	21,653
200	26,508	22,365
500	28,837	23,201
1,000	30,596	23,767
10,000	36,439	25,338

Table 1 shows that computed flows for different return periods from Log Pearson distribution are slightly on lower side as compared to Gumbel's distribution. Chi square test was applied on both the distributions. The values of chi square test were 5.36 and 3.26 for Gumbel Extreme Value Type-I and Log Pearson Type-III respectively. As computed values for chi square for both the distributions are less than the standard chi square value which is 12.02. So, both the distributions can be used for frequency analysis of the study area. Gumbel Extreme Value Type-I distribution value is close to the standard chi square value. That's why, this distribution is best fit for the study area. Furthermore, Gumbel Extreme Value Type-I distributions are widely used in hydrologic analysis. Storm rainfalls are most commonly modeled by the EVI distribution [8, 9].

Rainfall Frequency Analysis

The rainfall data of day of maximum daily peak for every year was selected. Hourly data of selected storm was analyzed. 1 hour, 2 hour, 3 hour, 6 hour, 12 hour and 24 hour maximum data was calculated from the selected storms and frequency analysis was done using Gumbel Extreme Value Type-I. The results of rainfall frequency analysis for different return periods are shown in Table 2.

Table 2 Results of Rainfall Frequency Analysis for Different Return Periods

Return Period	1hr	2hr	3hr	6hr	12hr	24hr

(Year)	Rainfall Depth (Inches)					
2.33	0.4 4	0.6 5	0.8 1	1.2 1	1.83	2.62
5	0.6 8	0.9 4	1.1 3	1.6 1	2.33	3.36
10	0.8 7	1.1 8	1.3 9	1.9 3	2.74	3.97
25	1.1 2	1.4 8	1.7 2	2.3 4	3.25	4.74
50	1.3 0	1.7 1	1.9 6	2.6 4	3.63	5.32
100	1.4 9	1.9 3	2.2 0	2.9 4	4.01	5.88
200	1.6 7	2.1 5	2.4 4	3.2 4	4.39	6.45
500	1.9 1	2.4 4	2.7 6	3.6 3	4.89	7.20
1,000	2.0 9	2.6 6	3.0 0	3.9 3	5.26	7.76
10,000	2.6 9	3.4 0	3.8 0	4.9 2	6.51	9.63

Table 2 shows the magnitude of rainfall for different return periods. It is clear from the results that the run-off generating rainfall at Kalam is up to 6 hours. Beyond 6 hours there is an appreciable recession in rainfall.

Calibration and Validation of Rainfall Runoff Model

The rainfall runoff model was calibrated with Chakdara stream gauge station. The peak discharge on 29 June 2007 was 30,894 cusecs at Chakdara. The hourly rainfall data of 28 and 29 June 2007 was incorporated in model. The computed peak hydrograph at Chakdara is 32,015 cusecs which is very close to the observed discharge at Chakdara for the same day.

The rainfall runoff model was validated with Chakdara stream gauge station also. The peak discharge on 10 October 1987 was 36,600 cusecs at Chakdara. After incorporating hourly rainfall data of 9 and 10 October 1987, the model gives peak hydrograph at Chakdara as 38,548 cusecs which is very close to the observed flow at Chakdara.

Same procedure for model calibration and validation has been followed for development of design hydrograph of Swat basin [10] and study of Subarnarekha River basin [11].

Flood Computation using Rainfall Runoff Model

Using the results of Table-I and Table-II floods of various return periods was computed by Hydrologic Modeling System software (HEC-HMS). Peak discharges calculated from HEC-

HMS at Madyan are listed in Table-III. Hydrograph of 100-year return period at Madyan is shown in Fig. 4.

Table-III: Peak flows at Madyan from HEC-HMS for 25, 50 and 100 year return periods

Return Period (Year)	Peak Discharge (Cusecs)
25	138,327
50	162,923
100	187,649

Table 3 shows that the difference in computed peak discharges (at most downstream location of the study reach i.e. Madyan) is small (of about 12%) which represents the trend of rainfall and stream flow data at Kalam. Fig. 4 shows a peak hydrograph at Madyan which clearly indicates that discharge contribution from the lateral tributaries is appreciable in the peak of resulting hydrograph.

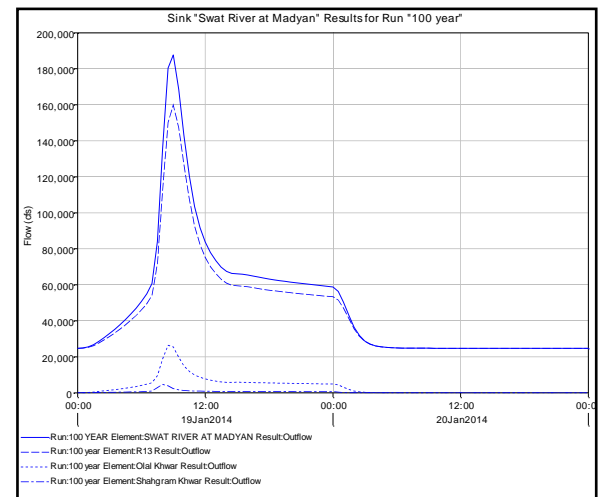


Fig. 4 Hydrograph of 100 Year Return Period Flood at Madyan

Flood Estimation for 2010 Extreme Flood Event

Recorded rainfall of 29 July is 84 mm (3.3 inch) at Kalam, which is 24-hour maximum rainfall. This rainfall was distributed over the entire catchment area of study reach of Swat River. Peak discharge at most d/s location of the study reach i.e. Madyan was estimated as 75,879 cusecs. Hydrograph at Madyan is also presented in Fig. 5.

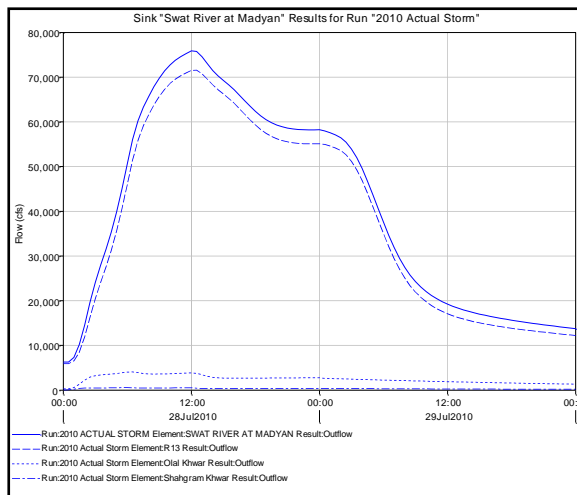


Fig. 5 Hydrograph of Estimated Storm of 2010 at Madyan

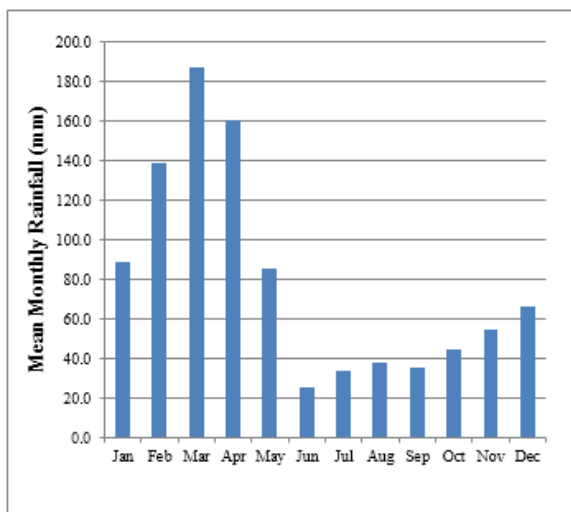


Fig. 6 Mean Monthly Rainfall of Kalam Rain Gauge Station

Monsoon rainfalls at Swat basin are almost nil. In Swat basin rainfall season usually starts in December and prolongs to April/May as shown in Fig. 6. The storm of 2010 which prolonged from 27-30th July 2010 is considered as the highest ever observed rainstorm not only in Swat basin but also in adjoining catchments. Stream flow data was not available beyond 27 July 2010 because stream gauge was washed away due to extremely heavy flows. The rainfall record was also not available beyond 29 July 2010 due to heavy rains in Swat Basin. Recorded rainfall of 29 July is 84 mm (3.31 inch) at Kalam, Annual maximum frequency of this rainfall is 5 years return period while the seasonal frequency (June to September) is 10,000-year return period. 2010 severe flood event occurred in Swat basin due to the Monsoon breaches from Indus to Swat basin. Comparison of annual and seasonal maximum frequency of 2010 rainstorm is shown in Table 4.

Table 4 Comparison of annual and seasonal maximum frequency of 2010 rainstorm

Return Period	Rainfall Depth (Inches)	
(Year)	Annual Max.	Seasonal Max. (June-Sept.)
2.33	2.52	0.80
5	3.31	1.04
10	3.95	1.23
25	4.75	1.47
50	5.35	1.66
100	5.95	1.84
200	6.54	2.02
500	7.32	2.25
1,000	7.91	2.43
10,000	9.88	3.31

Hydrodynamic Modeling

Stereo Pairs based DEM calibrated with ground control points (GCPs) on resolution of 2 m was used for extraction of model geometry. Steady state simulations were carried out with peak discharges of 25, 50 and 100 years return period floods and estimated flood peak of 2010 extreme flood event respectively. Water surface profile and XYZ perspective plot for 100-year return period for part of the study reach are shown in Fig. 7 and Fig. 8.

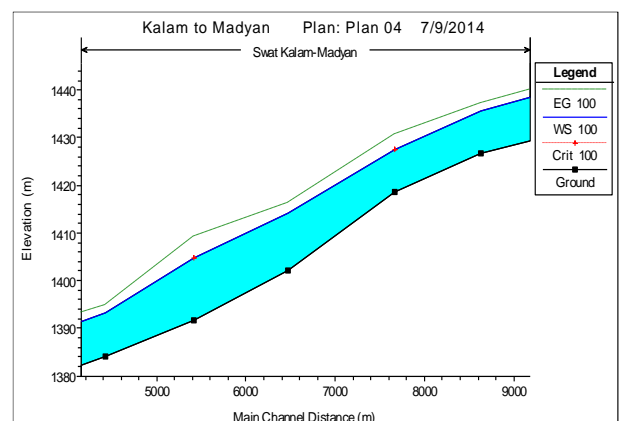


Fig. 7 Water Surface Profile of 100 Year Return Period Flood for Part of the Study Reach

One of the limitations of stereo pairs-based image is that it takes the free water surface as plain ground and cannot take the elevations below the water surface. It gives better results for rivers in gorges as compared to the rivers in plain areas because rivers are very wide in plain areas. Fig. 7 and Fig. 8 clearly shows that the longitudinal

slope of the Swat River is very steep of about 1 in 500. Depth of flow and width of every cross section is very small as compared to the actual depth of cross section i.e. Swat River flows in a gorge throughout the study reach. So, the stereo pairs-based image can safely be applied for the study reach.

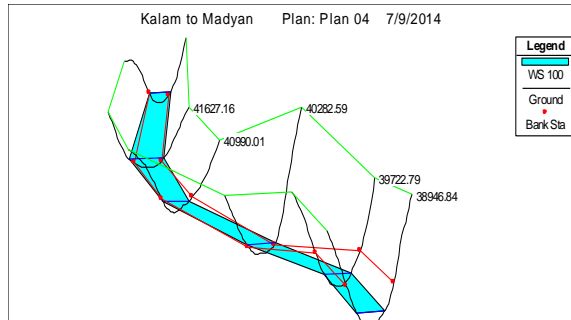


Fig. 8 X-Y-Z Perspective Plot for Part of the Study Reach for 100 Year Return Period Flood

Inundation Mapping

Flood inundation extents were marked by processing HEC-RAS results in HEC-Geo RAS. The inundation extents for 100 years return period flood and existing road imported on Google Earth image is shown in Fig. 9.

Fig. 9 shows the spread of flood waters for the part of modeled stream reach. The difference in computed water levels and inundation extents for different years return period floods (25, 50, 100 and 2010 flood) is of about 5% because Swat River flows in a gorge throughout the study reach. Fig. 9 also shows that the existing road is inundated at most of the locations throughout the study reach. So, there is a dire need to raise the profile of road.



Fig. 9 Inundation Extents and Existing Road for Part of Study Reach

Fixation of Road Profile Grade Level

Profile of road section was fixed on the basis of water levels (water surface profile) computed from hydrodynamic model and inundation extents for 100-year return period flood and shown in Fig 10.

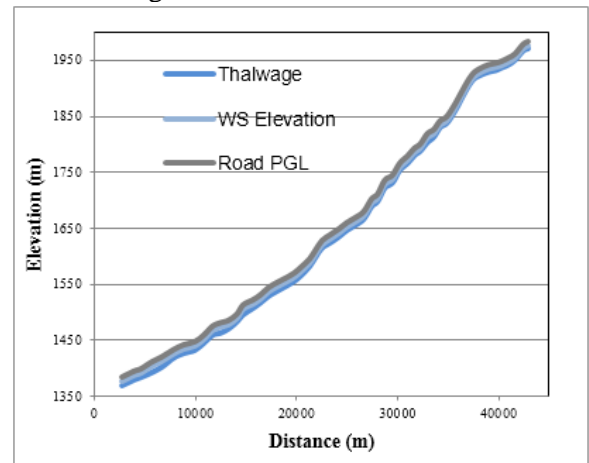


Fig. 10 Safe Profile of the Road for the Study Reach

Fig. 10 shows thalwage of the Swat River, water surface profile and profile grade level of road along the Swat River for the study reach. River thalwage indicates that longitudinal slope of the river is very steep, which is also an indication of very high velocities throughout the study reach. The computed profile of road contains a free board of 1.5 m for further safety of road and its infrastructure.

Conclusions

Recorded rainfall of 29 July 2010 is 84 mm (3.31inch) at Kalam (the rainfall record is not available beyond 29 July due to heavy rains). Annual maximum frequency of this rainfall is 5 years while the seasonal frequency (June to September) is 10,000 years. The severe flood event occurred in Swat basin due to the Monsoon breaches from Indus to Swat basin. The soil was fully saturated prior to the rainfall event due to snow melts and the rainfall was completely converted in to runoff. These were the major causes of such heavy destruction of 2010 flood. The difference in computed water levels for different return periods i.e. 25, 50, 100 and 2010 floods is very small (of about 5%) because Swat River flows in a gorge and the longitudinal slope of the river is very steep (of about 1 in 500) throughout the study reach. The water levels from 100-year return period flood (being the highest at the most downstream location i.e. Madyan) has been selected for design of road profile grade level owing to its importance and

severity of floods. Existing shingle road is not safe due to its low elevation and get inundated at most of the locations. So, there is a dire need to raise the profile of road.

References

- [1] NESPAK. 2013. Study and Detailed Field Survey for Assessment and Mitigation of Potential Flooding Locations on NHA Network. Final Completion Report, May 2013.
- [2] Annual Flood Report. 2010. Office of the Chief Engineer Advisor and Chairman: Federal Flood Commission, Islamabad.
- [3] Abdul Khaliq Hashmi. 2005. Rainfall runoff modeling for Kaha Hill Torrent Watershed Management in D.G.Khan District: M.Sc. Thesis, Center of Excellence in Water Resources Engineering, UET, Lahore.
- [4] Tariq M.A. 2005. Determination and Implementation of Flood Risk Zoning: Employing Physiographic and Hydraulic Parameters for Flood Prone Areas of Chiniot District, M.Sc. Thesis, Center of Excellence in Water Resources Engineering, UET, Lahore.
- [5] Ahmad B, Muhammad Shumail Kaleem, Mohsin Jamil Butt, Zakir Hussain Dahri. 2010. Hydrological modeling and flood hazard mapping of Nullah Lai: Pakistan Agricultural Research Council (PARC), Islamabad, Pakistan.
- [6] Duan Minya, Jixian Zhang, Zhengjun and Aekkapol. 2006. Use of remote sensing and GIS for flood hazard mapping in Chiang Mai province, Northern Thailand: Chinese Academy of Surveying and Mapping, Beijing, China.
- [7] Ghanbarpour, Shokoufeh Salimi, Mohsen Mohseni Saravi and Mehdi Zarei. 2011. Calibration of River Hydraulic Model Combined with GIS Analysis using Ground Based Observation Data: Research Journal of Applied Sciences, Engineering and Technology **3**(5), 2011.
- [8] Chow V.T. 1953. Frequency Analysis of Hydrologic Data with Special Application to Rainfall Intensities, Urbana Ill: University of Illinois Bulletin, **50**(81).
- [9] Tomlinson. A.I. 1980. The Frequency of High Intensity Rainfall in New Zealand, Part I: MWD Technical Publication No.19, Wellington.
- [10] Sulman Maqsood Randhawa. 2012. Development of Design Hyetograph for Flood Estimation in Swat Region: M.Sc. Thesis, Center of Excellence in Water Resources Engineering, UET, Lahore.
- [11] D.Roy, S. Begam, S. Ghosh and S. Jana. 2013. Calibration and Validation of HEC-HMS model for a river basin in Eastern India: ARPN Journal of Engineering and Applied Sciences **8**(1), January 2013.

Hydraulic Performance Assessment of an Orifice Spillways using CFD Modeling

Zohaib Nisar^{1*}, Muhammad Kaleem Sarwar², Ghulam Nabi³

^{1*}Research fellow and corresponding author, Centre of Excellence in Water Resources Engineering, University of Engineering and Technology Lahore, Pakistan

²Assistant Professor, Centre of Excellence in Water Resources Engineering, University of Engineering and Technology Lahore, Pakistan

³Assistant Professor, Centre of Excellence in Water Resources Engineering, University of Engineering and Technology Lahore, Pakistan

* engrzohaibnisar@hotmail.com

Abstract: An orifice spillway is normally gated and is used when substantial discharge capacity is needed at low reservoir levels. Orifice spillways are designed for dual purpose of flood disposal as well as flushing of sediments. Flow passing through the spillway shows the complex turbulent behaviour. To model the effect of turbulence, Reynolds's-averaged Navier-Stokes equations are commonly used which is an expanded form of Navier-Stokes equation. Flow physics becomes more complex in case of orifice spillways due to short lengths of spillway, large variation in reservoir levels, high flow depths and wide range of Froude numbers varying from 3 to 9. In view of this background, present study intends to numerically investigate the hydraulic behaviour of orifice spillway. The objectives of this study include the numerical modeling of complex flows over the orifice spillways, pseudo validation of numerical model results and to assess the flow parameters at different operating conditions. Results showed that model is capable of simulating the orifice spillway flows. Model can measure flow parameters at different operating conditions with an acceptable error of 0.23 to 1.5 %.

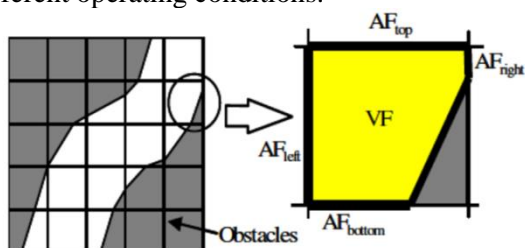
Keywords: Orifice Spillway, Flow Physics, Froude Number, FLOW-3D, Flow Parameters.

Introduction

The large capacity outlets placed below the dam crest and controlled by gates are called orifice or submerged spillway. These outlets are openings in the dam used to drawdown the reservoir level and can also serve to pass density currents. Large bottom openings serve as submerged spillways and their capacity can be used for flushing sediment from the reservoir and disposal of flood [1]. The flow is free surface flow for low reservoir levels and orifice flow for reservoir levels above the orifice opening. The crest profile of most of the orifice spillway is flat ($\alpha < 30^\circ$). Breast walls are provided to hold 60 to 90 m of water heads behind them. Because of narrow river gorges, limited available waterways, and 6 to 8 m thick piers supporting huge breast walls, the discharge intensities range between 100 and 300 m²/sec. The depths of flow are 10 to 12 m leading to low Froude numbers between 3 and 6 [2]. Hydraulic performance of spillways can be checked by physical modelling and numerical modelling. Traditionally, reduced scale physical spillway models are used to study spillway hydraulic performance. But, it has some disadvantages such as scaling effects, time consuming, expensive,

requirement of skilled labour and cannot readily capture behaviour like cavitation and air entrainment effects, which occur in reality [3]. In recent years, numerical modelling is extensively being used to investigate hydraulic performance of spillways. Computational fluid dynamics (CFD) is a numerical method used to solve fluid flow problems. The computational fluid dynamics (CFD) analysis can solve the Navier-Stokes equations in three dimensions and free surface computation in a significantly improved manner. Computational fluid dynamics presents a cost-effective solution that can be employed throughout the entire design process. The use of CFD modelling for spillway application is quite recent [4]. In last decade, many physical model studies have been validated using CFD models. Most of the numerical studies used the CFD code Flow-3D to analyze the spillway flows. Savage and Johnson [5] compared numerically generated discharge rating curves with physical model data and United States Bureau of Reclamation (USBR) calculations. The study found that Flow-3D slightly overestimated the discharges. Gessler [6] model the spillway flows and found 5% difference between CFD and physical model results. Savage

and Johnson [5] did not confirmed application of CFD model for all spillway configurations. Ho and Riddete [3] applied CFD model to evaluate the hydraulic performance of different spillways for increased flood discharges and suggested future work for cavitation, air entrainment, scour modelling, air demand and dynamic interaction. Bhosekar et al. [2] studied the performance of the aerator of orifice spillway by varying the discharge, gate openings and cavity sub-pressures and presented the results with respect to jet length, cavity pressure and air entrainment coefficients in the form of non-dimensional plots and developed equations for jet length and air entrainment coefficient for the orifice spillway aerator. CFD code, Flow-3D was selected for this research study due to its ability to model the free surface flow by using true volume of fluid (true-VOF) method developed by Hirt and Nichols [7] and track the sharp interface between water and air. This code also models the complex geometric region by using fractional area/ volume obstacle representation (FAVOR) technique [8]. This code overlay the mesh on imported non-flow geometry while FAVOR technique is used to determine the void or flow region within each cell as shown in (Fig. 1). With finer grid spacing, high resolution of the non-flow region is achieved. The use of multi block grids enable larger domains to be modelled and use of nested mesh technique enable more flow details to be captured in regions of interest [3]. Flow physics becomes more complex in case of orifice spillway due to short lengths of spillway, large variation in reservoir levels, high flow depths and wide range of Froude numbers varying from 3 to 9. In view of this background, present study intends to numerically investigate the hydraulic behaviour of orifice spillway. The objectives of this study include the numerical modeling of complex flows over the orifice spillways, pseudo validation of numerical model results and to assess the flow parameters at different operating conditions.



VF = Open Volume/Volume of Cell
 AF = Open Area/ Cell Edge Area

Fig. 1 Conceptual diagram of FAVOR method [5]

Mangla Dam Spillway

To study the complex flows behaviour of orifice spillways, CFD modelling of Mangla dam main spillway was carried out by operating the model at different reservoir levels and gate openings. The main spillway of dam consists of two-stage stilling basin and sloping side walls. The head works of the main spillway are 444 feet long. It consists of three monoliths separated by 24 feet wide piers. The head works is followed by parabolic chute and intermediate weir divides the chute into two and creates a stilling basin and water pool at an elevation of 1000 feet [9]. The spillway plan and the longitudinal section is shown in (Fig. 2).

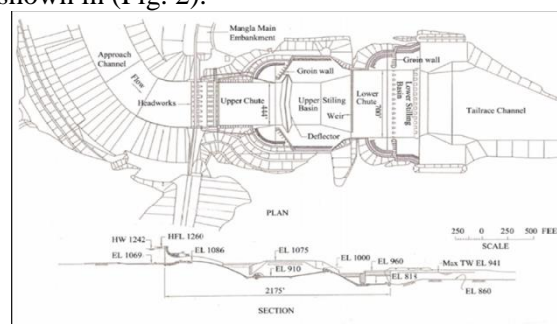


Fig. 2 Plan and Longitudinal section of Mangla Dam Spillway

Material and Method

Data Collection

Data collection for model set up sensitivity analysis and model validation include detail engineering drawings, physical model study results and discharge rating curve. Fig. 3 shows single bay three-dimensional model of Mangla dam spillway up to intermediate weir. This model was imported into CFD model.

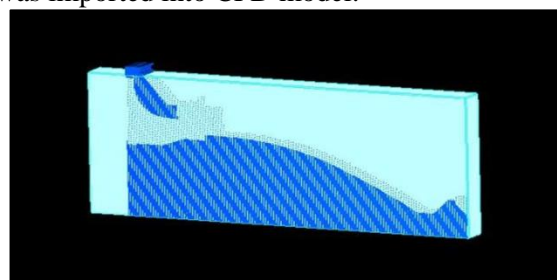


Fig. 3 One Bay of Spillway 3D model

Setting Up of CFD Model

To model Mangla dam spillway, collected drawings were first converted into three dimensional drawings then imported in stereo lithographic (Stl) file extension image. Total four Stl. file images were prepared for different gate openings. These Stl. file images were then imported into CFD code (Flow-3D) for numerical set-up. In next step, meshing of imported Stl. file

images were carried out. The extent of mesh domain on upstream and downstream of structure is defined in such a way that it could show the fluid movement and its impact properly. The boundary conditions applied for this model include, volume flow rate, specified pressure, symmetry, wall and out flow. After specifying boundaries of the model, fluids were added on the upstream and downstream sides of the structure as initial condition. After pre-processing explicit and fluid flow solver option was selected to solve Reynold Average Navier Stokes equation (RANS) which is prime equation used by Flow-3D for simulation.

Sensitivity Analysis

CFD code Flow-3D does not require calibration [10] but it is sensitive to the turbulent models and boundary conditions. Commonly used turbulence models include large eddy simulation, RNG, K- ϵ , RSM and DSM. Code user manual declares that RNG model is robust and most accurate model [11]. So, it was selected for further simulations. Four scenarios of boundary conditions were used for sensitivity analysis as shown in Table 1.

Model Validation

Validation of numerical model is extremely important. Validation process indicates the degree of accuracy of the model. A true validation of model involves the comparing of the model results with those from actual structure [5]. But for this study model validation was carried out by using physical model study result due to the lack of actual performance measurements at prototype.

Table 1 Different Scenario of Boundary Conditions

Scenario 1 X min. Specified Pressure X max. Outflow Y min. Wall Y max. Wall Z min. Wall Z max. Specified Pressure	Scenario 2 X min. Volume Flow Rate X max. Outflow Y min. Wall Y max. Wall Z min. Wall Z max. Specified Pressure
Scenario 3 X min. Volume Flow Rate X max. Specified Pressure Y min. Symmetry Y max. Symmetry Z min. Symmetry Z max. Specified Pressure	Scenario 4 X min. Specified Pressure X max. Specified Pressure Y min. Wall Y max. Wall Z min. Wall Z max. Specified Pressure

Gated Flow Modelling

For sensitivity analysis, gated flow simulations were performed at vertical gate openings of 3.05 m, 6.10 m, 9.14 m and 10.67 m to find out water levels by maintaining reservoir level at 378.54 m and 384 m. Then flow rate was measured for model validation at same operating conditions. Further vertical gated flow simulations were performed to find out the water surface profiles, pressures and velocity at gate opening of 6.10 m and 9.14 m and at reservoir level of 380.07m, 381.59 m and 383.11 m respectively. Initially simulation was performed with 3 m \times 3 m uniform mesh but in order to get more refined results size of mesh was reduced to 1 m. Fig. 4 shows gated flow modelling.



Fig. 4 Flow Simulation at 10.67 m Gate Opening

Results and Discussion

Sensitivity Analysis

Model was run at different operating conditions by applying all set of boundary condition for the sensitivity analysis of the model. The results of sensitivity analysis are discussed below.

Sensitivity Analysis of Model for Boundary Conditions

Model was operated at reservoir level of 378.54 m and 384 m with different gate openings to compare the water levels with physically observed one for all scenarios of boundary conditions. Comparison of results shown in tables 2, 3, 4 and 5 indicate that water levels computed with boundary condition scenario 3 are more close to the physical model results as compared to other scenarios. Hence boundary conditions mentioned under scenario 3 were selected for further simulation.

Model Validation

After sensitivity analysis, model validation was carried out for gated and free flow condition which is discussed as under.

Flow Rate

Discharge passing through spillway was calculated by operating the model at different operating conditions for validation of model. A comparison between CFD model discharge and physically observed one at various gate openings and reservoir level is shown in Table 6.

Comparison shows that percentage difference is in the range of 0.43% to 0.63% which is quite acceptable. Similarly, percentage error at free flow condition is within 0.40 % as shown in Table 7 Which indicates that model has successfully validated for Mangla dam spillway.

Table 2 Numerical and Physical Model Results for Scenario 1 of Boundary Condition

Sr. NO	Reservoir Level (m)	Avg. Physically Observed Water Level (m)				Avg. Numerically Calculated Water Level (m)				Avg. % Difference
		G/O 3.05 m	G/O 6.10 m	G/O 9.14 m	G/O 10.67 m	G/O 3.05 m	G/O 6.10 m	G/O 9.14 m	G/O 10.67 m	
1	378.54	324.15	324.59	325.37	327.13	321.97	322.49	323.25	324.77	0.67
2	384	-	-	-	327.17	-	-	-	324.46	0.83

Table 3: Numerical and Physical Model Results for Scenario 2 of Boundary Condition

Sr. NO	Reservoir Level (m)	Avg. Physically Observed Water Level (m)				Avg. Numerically Calculated Water Level (m)				Avg. % Difference
		G/O 3.05 m	G/O 6.10 m	G/O 9.14 m	G/O 10.67 m	G/O 3.05 m	G/O 6.10 m	G/O 9.14 m	G/O 10.67 m	
1	378.54	324.30	324.59	325.37	327.13	320.42	321.24	322.90	324.10	0.98
2	384	-	-	-	327.17	-	-	-	324.26	0.89

Table 4: Numerical and Physical Model Results for Scenario 3 of Boundary Condition

Sr. NO	Reservoir Level (m)	Avg. Physically Observed Water Level (m)				Avg. Numerically Calculated Water Level (m)				Avg. % Difference
		G/O 3.05 m	G/O 6.10 m	G/O 9.14 m	G/O 10.67 m	G/O 3.05 m	G/O 6.10 m	G/O 9.14 m	G/O 10.67 m	
1	378.54	324.15	324.59	325.37	327.13	322.57	322.93	323.67	324.74	0.56
2	384	-	-	-	327.17	-	-	-	325.36	0.55

Table 5: Numerical and Physical Model Results for Scenario 4 of Boundary Condition

Sr. NO	Reservoir Level (m)	Avg. Physically Observed Water Level (m)				Avg. Numerically Calculated Water Level (m)				Avg. % Difference
		G/O 3.05 m	G/O 6.10 m	G/O 9.14 m	G/O 10.67 m	G/O 3.05 m	G/O 6.10 m	G/O 9.14 m	G/O 10.67 m	
1	378.54	324.30	324.59	325.37	327.13	319.03	320.93	322.75	323.91	1.13
2	384	-	-	-	327.17	-	-	-	324.45	0.83

Table 6: Comparison of results between CFD model and Physical Model (Gated Flow)

Sr. NO	Reservoir Level (m)	Physical Model Discharge (Cumec)			CFD Model Discharge (Cumec)			Avg.% Difference
		G/O 3.05 m	G/O 6.10 m	G/O 9.14 m	G/O 3.05 m	G/O 6.10 m	G/O 9.14 m	
1	378.54	523.45	1044.09	1657.88	523.88	1058.58	1628.96	0.43 %
2	384	555.92	1117.22	1790.38	556.49	1117.93	1810.91	0.63%

Table 7: Comparison of results between Physical and CFD Model (Free Flow)

Sr. No	Reservoir Level (m)	Discharge (Cumec)		Avg. % Difference
		Observed	CFD	
1	378.54	2077.91	2069.81	0.39
2	384	2222.43	2227.48	0.23

Water Surface Profiles

On successful validation of model, water surface profile at different vertical gate openings were computed at reservoir level of 380.07 m, 381.59 m and 383.11 m as shown in (Fig.s 5, 6 and 7). Flow surface profiles are important to ensure that flood water is not interfering with other structures such as bridges at crest or raised gates or overtopping the chute walls. The fluctuation in water surface is negligible along the chute but show slight fluctuation due to variation of discharge beyond 150 m at all operating conditions. Further, continuous drop in water surface level is noted in all cases. Fluctuations in water surface levels are negligible and it is not interfering the bridge at crest or raised gates or overtopping the chute walls throughout the length of spillway chute.

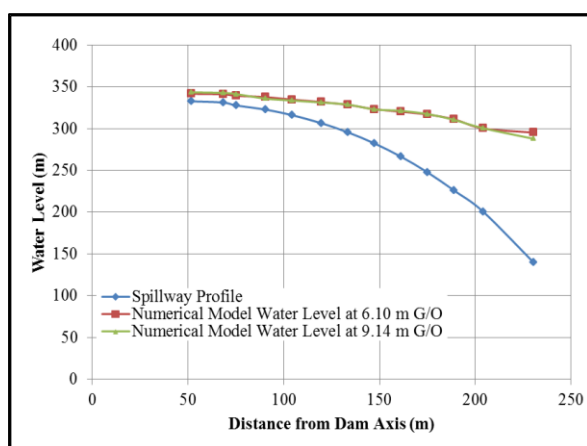


Fig. 5 Water Level for Gated Flow at 380.07 m of Reservoir Level

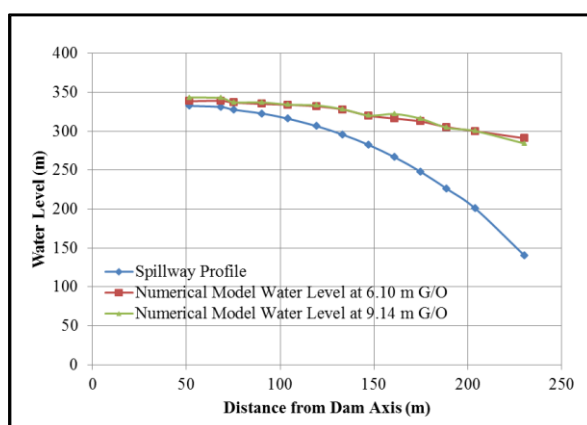


Fig. 6 Water Level for Gated Flow at 381.59 m of Reservoir Level

Pressure Distribution

The computations of pressure along spillway chute are used to examine the potential for cavitation damage due to excessive sub atmospheric pressure. Pressure distribution for

gated operation of the model at reservoir level of 380.07 m, 381.59 m and 383.11 m are shown in Fig.s 8, 9 and Fig. 10 respectively. Significant, pressure variation is observed due to variation in flow depth and velocity between 50 m to 125 m length of the chute from dam axis at large gate opening and at all reservoir levels. Further, pressure remained high up to 175 m distance at large gate opening (9.14 m) in all cases. Beyond 175 m, little higher-pressure values than large gate opening are noted at 6.10 m against all reservoir levels. At all operating conditions, gradual increasing trend in pressure value is observed due to high flow depth from 175 m to the end of the chute. Generally, pressure remained positive throughout the length of spillway chute which shows that Mangla dam spillway chute is safe against the cavitation damages.

Velocity

Velocity indicates the potential for erosion damage downstream of the spillway. The erosion assessment depends on the accurate prediction of flow velocity. CFD modelling can reliably predict the velocities provided the model is properly prepared. Velocity profile for gated operation of the model at different operating condition is shown in Fig.s 11, 12 and 13 respectively. Fig.s shows that velocity values are increasing with distance but near the entry point of stilling basin, velocity values drops abruptly due to increase of water depth. Near the crest of spillway, flow velocity is in the range of 10 to 15 m/sec but when water moves further downward it attains maximum value of 30 m/sec on all operating conditions. So, velocity varies from 10 m/sec to 30 m/sec along the chute of Mangla dam spillway. Water depth increases due to the presence of small height weir at end of spillway chute which reduces the velocity 10 m/sec. The existence of two stage stilling basin at spillway site will further reduced this velocity value which will ultimately reduce the potential for the downstream bed erosion.

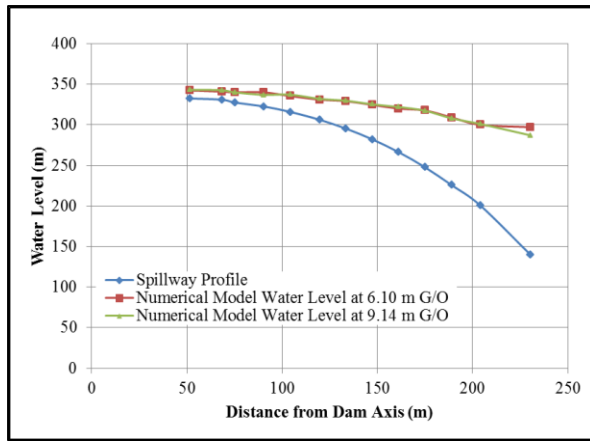


Fig. 7 Water Level for Gated Flow at 383.11 m of Reservoir Level

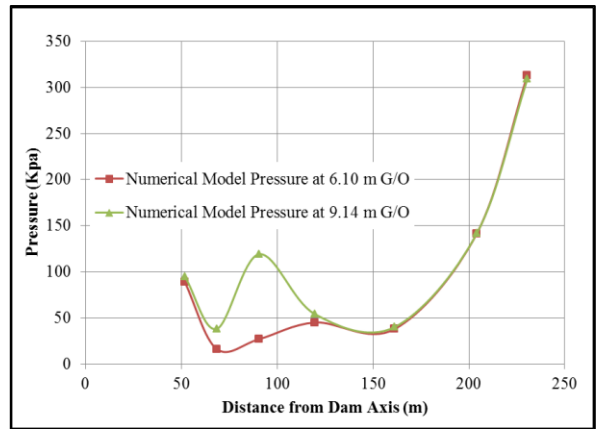


Fig. 10 Pressure Distribution at Reservoir Level of 383.11 m

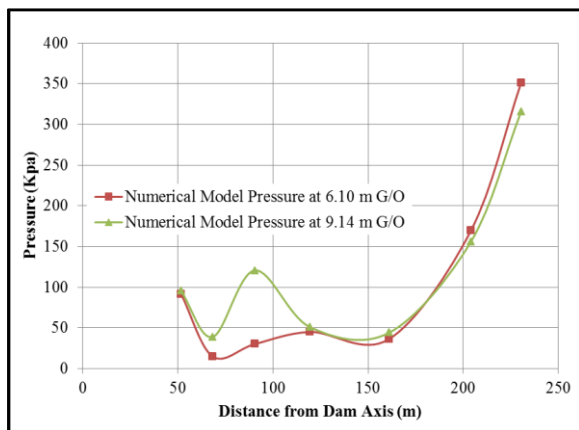


Fig. 8 Pressure Distribution at Reservoir Level of 380.07 m

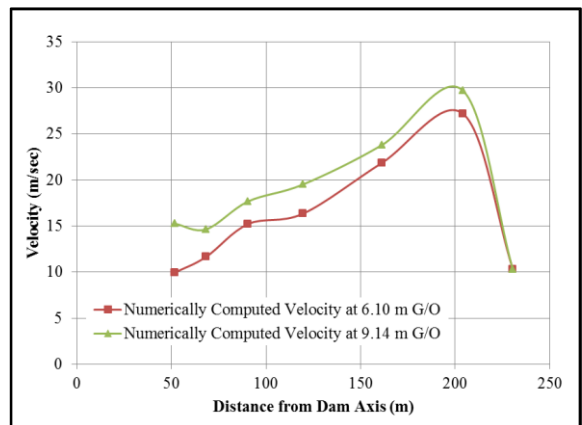


Fig. 11 Velocity Profile at 380.07 m of Reservoir Level

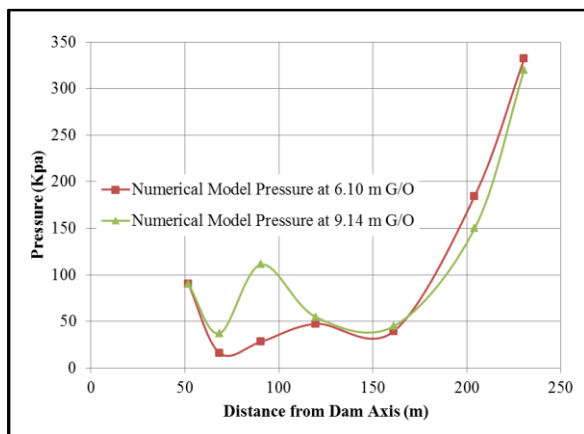


Fig. 9 Pressure Distribution at Reservoir Level of 381.59 m

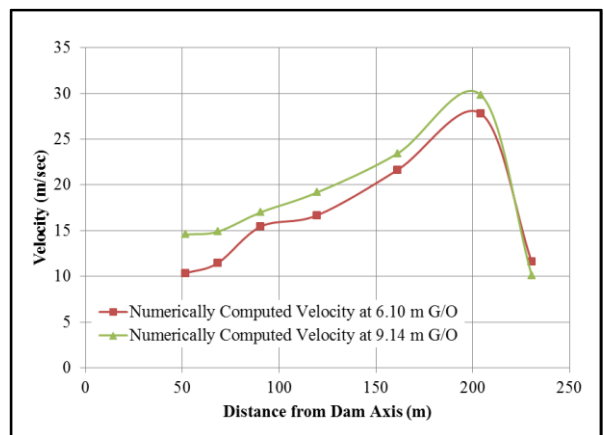


Fig. 12 Velocity Profile at 381.59 m of Reservoir Level

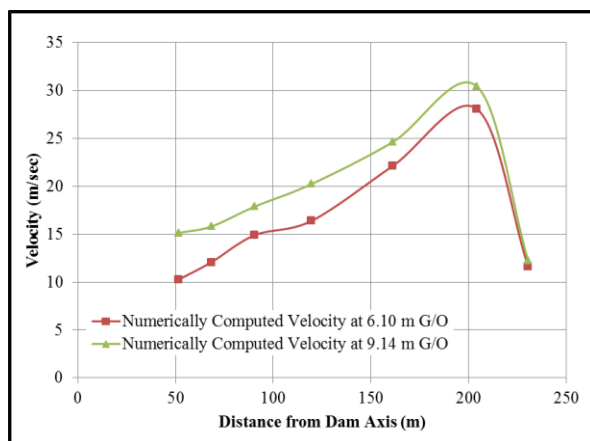


Fig. 13 Velocity Profile at 383.11 m of Reservoir Level

Conclusion and Recommendations

Computational Fluid Dynamics (CFD) model of Mangla dam spillway was operated by varying the reservoir levels and gate openings. Model computed the pressures at different gate openings and reservoir levels. The computed pressures were found in range of 10 KPa to 350 KPa at all opening conditions. Pressures over the chute remain positive which indicates no danger of cavitation. Variation in velocity over the profile was noted between 10 m/sec to 30 m/sec which reduce to 10 m/sec near the entry point of stilling basin. Flow depth computed near gate slot was 6.02 m which raise to 48.81 m at the end of chute. The maximum mean level of water surface computed at a distance of 51.72 m from dam axis was 343.24 m which is well below top level of the chute wall 376.10 m indicating the no danger of overtopping.

Model computed the discharge both for vertical gated and free flow (vertical full gate opening) conditions. For gated flow conditions, maximum flow passed through single bay of spillway was 1810.91 m³/sec while at full vertical gate opening, it was 2227.48 m³/sec which confirms the design discharge capacity 3173.04 m³/sec at maximum flood level of 384 m. Computed flow parameters with low percentage error difference in comparison with observed one confirms that model is able to assess the flow behaviour successfully. Simulations of flows with nested mesh technique, other turbulence model, and numerical options are required especially for the smaller gate openings. Moreover, air entrainment effect on flow parameters is also required to be model for refinement of results. Modelling of flows in stilling basin of spillway is recommended for analysis of flow behaviour and to check the potential for erosion damage.

Acknowledgements

The author (Zohaib Nisar) would extremely like to thank Engr. Kaleem Sarwar (Assistant Professor) for their guidance, help in this research and writing this research paper. Author also would like to thank Dr. Ghulam Nabi (Assistant Professor) and Center of Excellence in Water Resources Engineering, University of Engineering & Technology, Lahore, Pakistan for doing research and completion of my specialization in Water Resources Engineering.

References

- [1] Novak, P, A.I.B, Moffat, C. Nalluri and R. Narayanan, Hydraulic Structures, Taylor & Francis Co. 4th Edition, ISBN 0-203-96463-2, 2007.
- [2] Bhosekar, V.V, V. Jothiprakash and P.B, Deolalikar, Orifice Spillway Aerator: Hydraulic Design, Journal of Hydraulic Engineering, Vol. 138, No. 6, pp: 563-572, 2012.
- [3] Ho, D. K.H. and K.M, Riddette, Application of computational fluid dynamics to evaluate hydraulic performance of spillway in Australia, Australia Journal of Civil Engineering, Vol. 6, No.1, pp: 81-104, 2010.
- [4] Chanel, P.G and J.C, Doering, Assessment of spillway modelling using computational fluid dynamics, Canadian Journal of Civil Engineering, pp: 1481-1485, 2008.
- [5] Savage, B.M. and M.C, Johnson, Flow over ogee spillway: Physical and Numerical Model Case Study, Journal of Hydraulic Engineering, Vol. 127, No. 8, pp: 640-649, 2001.
- [6] Gessler, D, CFD Modelling of Spillway performance, Proceedings of world Water and Environmental Resources Congress 2005, American Society of Civil Engineer, Anchorage, Alaska, 2005.
- [7] Hirt, C.W and Nichols, B.D, Volume of fluid method for dynamic of free boundaries, Journal of Computational Physics, Vol. 39, pp. 201-225, 1981.
- [8] Hirt, C.W. and Sicilian, J.M, A Porosity technique for the definition of obstacles in rectangular cell mesh, Proceedings of 4th international conference of ship dynamic, National Academy of Science, Washington D.C, 1985.
- [9] WAPDA Model Study Cell, IRI, Hydraulic Model Studies for Mangla dam Raising Project, Final Technical Report, Hydraulic Research Station, Nandipur, 2004.

- [10] USBR, Folsom Dam Joint Federal Project, Existing spillway modeling, Discharge Capacity Studies, California, USA, 2009.
- [11] Flow Science, Inc., Flow-3D user manuals, Version 9.2. Flow Science, Inc., Santa Fe, N.M, 2007.

CFD = Computational Fluid Dynamics
RNG = Re-normalized Group Model
RANG = Reynold Average Navier Stokes Equation
Stl. = Stereo lithographic
G/O = Gate Opening
Cumec = Cubic meter per second (m³/sec)

Appendix – notation

Following symbols used in this paper:



Conference

AT A GLANCE














ISBN: 978-969-8670-06-01



Centre of Excellence on Water Resources
Engineering
UET, G.T. Rd, Lahore- Pakistan. 54890
Tel: +92 42 99250257
Fax: +92-42-99250259
Email: cewre@cewre.edu.pk
www.cewre.edu.pk

For orders, please contact:
Conference Organizing Committee
Tel: +92 42 99250257
Email: cewre.media@gmail.com

 Printed on recycled paper.

© 2017 Centre of Excellence on Water Resources Engineering,
UET Lahore-Pakistan.

All rights reserved. Published 2018.
Printed in the Pakistan.

